Informatics Control Measurement
in Economy and Environment Protection

3/2022

Informatyka Automatyka Pomiary

www.e-IAPGOS.pl

w gospodarce i ochronie środowiska

ISSN 2083-0157

Kwartalnik Naukowo-Techniczny

fot. arch. SSU

**Sumy State University
(Sumy, Ukraine)**

3/2022

lipiec – wrzesień

Wydanie pod redakcją naukową
prof. dr hab. inż. Waldemara Wójcika

INFORMATYKA AUTOMATYKA POMIARY
W GOSPODARCE i OCHRONIE ŚRODOWISKA
Informatics Control Measurement in Economy and Environment Protection

p-ISSN 2083-0157, e-ISSN 2391-6761, www.e-iapgos.pl

EDITORIAL OFFICE
REDAKCJA

Redakcja czasopisma
Informatyka, Automatyka, Pomiary w Gospodarce i Ochronie Środowiska
Katedra Elektroniki i Technik Informacyjnych
Politechnika Lubelska
ul. Nadbystrzycka 38A, 20-618 Lublin
tel. +48 81 53 84 309,
fax: +48 81 53 84 312
iapgos@pollub.pl
www.e-iapgos.pl
iapgos.pollub.pl
ph.pollub.pl/index.php/iapgos

PUBLISHER
WYDAWCA

Politechnika Lubelska
ul. Nadbystrzycka 38D
20-618 Lublin
tel. +48 81 53 84 100
www.pollub.pl
ph.pollub.pl

PRINTING HOUSE – DRUKARNIA

Agencja Reklamowa TOP
https://www.agencjatop.pl

nakład: 100 egzemplarzy

OTHER INFORMATION – INNE INFORMACJE

Czasopismo jest indeksowane w bazach:

DOAJ	doaj.org
BazTech	baztech.icm.edu.pl
IC Journals Master List	www.journals.indexcopernicus.com
Google Scholar	scholar.google.pl
POL-index	pbn.nauka.gov.pl
Sherpa RoMEO	www.sherpa.ac.uk
OAJI	oaji.net
SCOPUS	www.scopus.com

Czasopismo *Informatyka, Automatyka, Pomiary w Gospodarce i Ochronie Środowiska* zostało objęte finansowaniem przez Ministerstwo Nauki i Szkolnictwa Wyższego w ramach programu *Wsparcie dla czasopism naukowych* w latach 2019-2020.

Czasopismo znajduje się w wykazie czasopism naukowych opublikowanym w Komunikacie Ministra Edukacji i Nauki z dnia 1 grudnia 2021 r., Unikatowy Identyfikator Czasopisma: 200167 – z przypisaną liczbą punktów przyznawanych za publikację artykułu równą 20.

Zasady publikowania artykułów, przygotowania tekstów, zasady etyczne, procedura recenzowania, wykazy recenzentów oraz pełne teksty artykułów dostępne są na stronie internetowej czasopisma:

www.e-iapgos.pl

W celu zwiększenia oddziaływania czasopisma w środowisku naukowym redakcja zaleca:

- w artykułach publikowanych w IAPGOS cytować artykuły z renomowanych czasopism międzynarodowych (szczególnie indeksowanych w bazach Web of Science oraz Scopus) używając oficjalnych skrótów nazw czasopism,
- w artykułach publikowanych w innych czasopismach (zwłaszcza indeksowanych w bazach Web of Science oraz Scopus) cytować prace publikowane w IAPGOS – zwłaszcza posługując się numerami DOI, np.:
  Kluszczyński K. *Modelowanie – umiejętność czy sztuka?* Informatyka, Automatyka, Pomiary w Gospodarce i Ochronie Środowiska – IAPGOS, 1/2016, 4–15, https://doi.org/10.5604/20830157.1193833.

CONTENTS – SPIS TREŚCI

1. **Jan Kubicki, Krzysztof Kopczyński, Jarosław Młyńczak**
Absorption characteristics of thermal radiation for carbon dioxide
Charakterystyka absorpcji promieniowania cieplnego dla dwutlenku węgla 4

2. **Vitaly Pochernyaev, Nataliia Syvkova, Mariia Mahomedova**
Switch-filter on a rectangular waveguide partially filled by dielectric
Przełącznik-filtr na falowodzie prostokątnym częściowo wypełnionym dielektrykiem 8

3. **Jakub Kisała, Andrzej Kociubiński, Karolina Czarnacka, Mateusz Gęca**
Giant magnetoresistance observed in thin film NiFe/Cu/NiFe structures
Zjawisko gigantycznego magnetooporu obserwowane w cienkich strukturach NiFe/Cu/NiFe 12

4. **Sergiy Tymchuk, Oleksiy Piskarev, Oleksandr Miroshnyk, Serhii Halko, Taras Shchur**
Expansion of the area of practical application of the PLC control system with parallel architecture
Rozszerzenie obszaru praktycznego zastosowania systemu sterowania PLC o architekturę równoległą 16

5. **Vasyl V. Kukharchuk, Waldemar Wójcik, Sergii V. Pavlov, Samoil Sh. Katsyv, Volodymyr S. Holodiuk, Oleksandr Reyda, Ainur Kozbakova, Gaukhar Borankulova**
Features of the angular speed dynamic measurements with the use of an encoder
Cechy pomiarów dynamicznych prędkości kątowej z wykorzystaniem enkodera 20

6. **Bogdan Palchevskiy, Lyubov Krestyanpol**
Application of predictive maintenance in the packaging production
Zastosowanie predykcyjnej diagnostyki w produkcji opakowań 27

7. **Andrii Perekrest, Vladimir Chenchevoi, Olga Chencheva, Alexandr Kovalenko, Mykhailo Kushch-Zhyrko, Aliya Kalizhanova, Yedilkhan Amirgaliyev**
Prediction model of public houses' heating systems: a comparison of support vector machine method and random forest method
Model prognozowania systemów grzewczych budynków użyteczności publicznej: porównanie metody support vector machine i random forest 34

8. **Petr Lezhniuk, Viacheslav Komar, Iryna Hunko, Daniyar Jarykbassov, Dinara Tussupzhanova, Bakhyt Yeraliyeva, Nazbek Katayev**
Natural-simulation model of photovoltaic station generation in process of electricity balancing in electrical power system
Naturalny model symulacyjny generacji stacji fotowoltaicznej w procesie bilansowania energii elektrycznej w systemie elektroenergetycznym 40

9. **Anzhelika Stakhova**
Application for vibration diagnostics
Aplikacja do diagnostyki wibracyjnej 46

10. **Magdalena Michalska-Ciekańska**
Deep neural networks for skin lesions diagnostics
Głębokie sieci neuronowe dla diagnostyki zmian skórnych 50

11. **Roman Obertyukh, Andrii Slabkyi, Leonid Polishchuk, Oleksandr Povstianoi, Saule Kumargazhanova, Maxatbek Satymbekov**
Dynamic and mathematical models of the hydroimpulsive vibro-cutting device with a pressure pulse generator bult into the ring spring
Modele dynamiczne i matematyczne hydraulicznego urządzenia impulsowego do cięcia wibracyjnego z generatorem impulsów wbudowanym w sprężynę pierścieniową 54

12. **Liudmyla Shkilniak, Waldemar Wójcik, Sergii Pavlov, Oleg Vlasenko, Tetiana Kanishyna, Irina Khomyuk, Oleh Bezverkhyi, Sofia Dembitska, Orken Mamyrbayev, Aigul Iskakova**
Expert fuzzy systems for evaluation of intensity of reactive edema of soft tissues in patients with diabetes
Eksperckie systemy rozmyte do oceny intensywności reaktywnego obrzęku tkanek miękkich u pacjentów z cukrzycą 59

13. **Oleksii M. Shushura, Liudmyla A. Asieieva, Oleksiy L. Nedashkivskiy, Yevhen V. Havrylko, Yevheniia O. Moroz, Saule S. Smailova, Magzhan Sarsembayev**
Simulation of information security risks of availability of project documents based on fuzzy logic
Symulacja zagrożeń bezpieczeństwa informacji w zakresie dostępności dokumentów projektowych w oparciu o logikę rozmytą 64

14. **Nataliia Geseleva, Ganna Proniuk, Olexander Romanyuk, Olga Akimova, Tetiana Troianovska-Korobeynikova, Liudmyla Savytska, Saule Rakhmetullina, Nurbapa Mekebayev**
Management of the workplaces by the facilities of operations research
Zarządzanie miejscem pracy za pomocą badań operacyjnych 69

15. **Ivan V. Zayukov, Iryna M. Kobylianska, Oleksandr V. Kobylianskyi, Sofia V. Dembitska**
Modeling of labor potential of Ukraine: formation of knowledge base
Modelowanie potencjału siły roboczej Ukrainy: budowanie bazy wiedzy 74

http://doi.org/10.35784/iapgos.2998

received: 08.06.2022 | revised: 02.08.2022 | accepted: 15.09.2022 | available online: 30.09.2022

ABSORPTION CHARACTERISTICS OF THERMAL RADIATION FOR CARBON DIOXIDE

Jan Kubicki, Krzysztof Kopczyński, Jarosław Młyńczak
Military University of Technology, Institute of Optoelectronics, Warsaw, Poland

***Abstract**. The article presents graphs of absorption of thermal radiation as a function of the mass of absorbing carbon dioxide per unit of illuminated area. Experimental research was preceded by an analysis of a simplified model of radiation absorption, paying attention to the phenomenon of saturation. The results of the experimental research were compared with the theoretical ones and the discrepancies were interpreted. Based on the conclusions, suggestions were made regarding the impact of further CO_2 emissions on climate change.*

Keywords: absorption characteristics, saturation of absorption, thermal radiation, Schwarzschild's equation

CHARAKTERYSTYKA ABSORPCJI PROMIENIOWANIA CIEPLNEGO DLA DWUTLENKU WĘGLA

***Streszczenie**. W artykule przedstawiono wykresy absorpcji promieniowania cieplnego w funkcji masy absorbującego dwutlenku węgla na jednostkę oświetlanej powierzchni. Badania eksperymentalne poprzedzono analizą uproszczonego modelu absorpcji promieniowania, zwracając uwagę na zjawisko nasycenia. Wyniki badań eksperymentalnych porównano z teoretycznymi, a rozbieżności zinterpretowano. Na podstawie wniosków sformułowano sugestie dotyczące wpływu dalszej emisji CO2 na zmiany klimatyczne.*

Keywords: charakterystyka absorbcji, nasycenie absorbcji, promieniowanie cieplne, równanie Schwarzschilda

Introduction

The physical and chemical properties of carbon dioxide are well-known, and due to its frequent occurrence in chemical and biological processes, it is one of the most popular gases. In recent years, due to the coincidence of its absorption spectrum with a part of the thermal spectrum of the Earth's surface, carbon dioxide has gained much popularity as "a harmful gas, wreaking havoc on the climate and thus threatening the inhabitants of the planet". The absorption of thermal radiation in CO_2 has been given a lot of attention, among others, in such works as [7–10]. These works provide a valuable contribution to understanding the phenomenon of radiation absorption in the Earth's atmosphere, but they do not directly provide arguments for the apocalyptic vision related to CO_2 emissions. Such a vision is based on direct observation of nature, which shows that the rise of CO_2 concentration is accompanied by the rise of the temperature of the Earth's atmosphere. Apparently, it makes sense and therefore it is easily accepted by society. However, the fact that event A accompanies event B does not necessarily imply that the former is the cause of the latter. The events may be independent or vice versa, the second event may be the cause of the first. Therefore, it is worth getting acquainted with the results of the work [3], where, on the basis of the measurement results across the globe, it was shown that the cyclic peaks of temperature increase precede in time the corresponding peaks of CO_2 concentration. It follows unequivocally that it is not the increase in CO_2 concentration that causes the temperature increase, but conversely, the increase in temperature most likely causes the release of CO_2 from the oceans, leading to an increase in its concentration.

Another argument adopted by the society is the calculation results for the used computer models. However, as shown, among others, in [4], a relatively large number of input data should be used for these models. Of course, these data can only be obtained from the results of measurements carried out simultaneously at a very large number of measurement points around the globe and at different altitudes. One should also pay attention to the high dynamics of processes in the atmosphere. Moreover, it should be noted that the use of averaged quantities for nonlinear dependencies, such as the average temperature using the Stefan-Boltzmann law, can generate very large errors. So it seems that it is only possible to estimate the upper or lower limit of the possible value of the absorption of the Earth's thermal radiation in atmospheric carbon dioxide. The difference between these limits can be very large. In practice, it can be reduced by experimentally verifying the results of computer calculations at every stage of their implementation. Therefore, the experiment described in articles [5] and [6] was carried out, where it was shown that thermal radiation from the hot surface of the Moon, after passing through the Earth's atmosphere, is not absorbed in carbon dioxide. Thus, it was shown that for this radiation there is a complete saturation of the process. This may suggest that it may be similar in the case of the Earth's thermal radiation.

Therefore, in the present work, the research focused on the phenomenon of saturation of the absorption process of thermal radiation in a mixture of carbon dioxide and air.

1. A simplified description of the process of resonance absorption of radiation in gases

Illuminating a solution of an absorbing substance by a collimated beam of monochromatic radiation, one can obtain a decrease in the intensity of this radiation according to the Lambert-Beer's law:

$$I = I_0 e^{-\alpha \cdot l \cdot C} \tag{1}$$

where:
I_0 – intensity of radiation penetrating the sample,
I – intensity of radiation after passing through the sample,
α – mass absorption coefficient [m^2 kg^{-1}],
l – thickness of the layer [m],
C – mass concentration [kg m^{-3}].

Absorption defined as the ratio of the energy of the absorbed radiation to the energy of the incident radiation at a given time can be described by the formula:

$$A = \frac{I_0 - I}{I_0} = 1 - e^{-\alpha \cdot l \cdot C} \tag{2}$$

By introducing a new quantity called the absorbing mass per unit area defined as $m = l \cdot C$, equation (2) takes the form:

$$A = 1 - e^{-\alpha \cdot m} \tag{3}$$

The graph of this function is shown in figure 1.

It can be seen that with the increase of m, the absorption will asymptotically approach the value 1 and for a sufficiently large value, we can assume that we are dealing with saturation.

It should be noted, however, that the absorbing substance not only absorbs the radiation but also emits it. However, while for monochromatic radiation, the resonance absorption occurs for a strictly defined wavelength (within the line width), then spontaneous emission is the result of all possible transitions and a small share for the wavelength corresponding to the absorbed radiation is neglected in the Lambert-Beer description. The situation is different with the absorption of thermal radiation. In this case, both absorption and emission take place for all possible transitions.

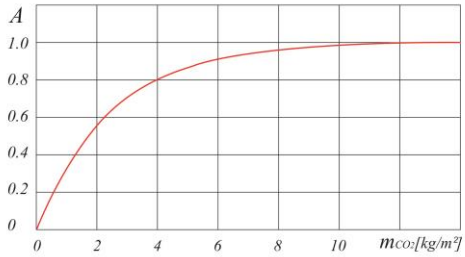

Fig. 1. Illustrative diagram of monochromatic radiation absorption as a function of the absorbing mass for α = 0.4 m²/kg

Moreover, especially with low-temperature radiation sources, its intensity is relatively low. Thus, the thermal radiation emitted by the absorbing gas cannot then be neglected. The situation is further complicated by the fact that with a relatively large number of oscillatory-rotational lines and their overlapping at higher extinction values, the normalized line shape function $g(\nu)$ describing the frequency-dependent interaction of radiation with molecules becomes very complex. This phenomenon has been thoroughly analysed in [1]. It shows that the absorption of thermal radiation A in a gas is a corresponding function of the mass m of the absorbing substance and the pressure p of the gas in which this substance is dissolved. An arbitrary parameter A_0 related to the bandwidth was introduced and the absorption notation for $A \leq A_0$ was adopted in the form:

$$A = cm^d p^k \tag{4}$$

While for $A > A_0$

$$A = C + Dln(m) + Kln(p) \tag{5}$$

All quantities A_0, c, d, k, C, D i K are assumed to be empirically fitted quantities.

It should be noted, however, that the function *A(m)*, written by the formula (5) as a logarithmic function, is an increasing function for any large value of the argument *m*. Meanwhile, the absorption *A*, according to the definition, cannot exceed the value of 1. This clearly shows that formula (5) can describe the phenomenon relatively correctly only for a limited value of *m*.

The propagation of the Earth's thermal radiation in the atmosphere for various concentrations of CO_2 at a constant concentration of water vapor, as well as ozone and methane was described in the study cited in the introduction [2]. Performing the calculations for the adopted computer model, the author obtained the graph of the absorption of this radiation as a function of CO_2 concentration in the atmosphere presented in Fig. 2.

Taking into account that in a cylinder with a unit cross-sectional area (1m²) and a height from the Earth's surface to the stratosphere, there is an air mass $m_{pow.} \cong 10^4$ kg, the mass of CO_2 in this cylinder can be determined for a given concentration according to the formula:

$$m_{CO_2}[kg/m^2] = m_{pow.}[kg/m^2] \cdot \frac{M_{CO_2}}{M_{pow}} \cdot \frac{C_{CO_2}[ppm]}{10^6} = 10^4 kg/m^2 \cdot \frac{44}{29} \cdot 10^{-6} \cdot C_{CO_2}[ppm] = 1{,}52 \cdot 10^{-2} kg/m^2 \cdot C_{CO_2}[ppm]$$

where:

M_{CO_2} – molar mass of carbon dioxide,

M_{pow} – molar mass of air,

$C_{CO_2}[ppm]$ – carbon dioxide concentration in the air.

Hence for the Earth's atmosphere:

$$C_{CO_2}[ppm] = 65{,}8 \cdot m_{CO_2}\,[kg/m^2].$$

Taking these dependencies into account, the graph in figure 2 can be replaced with the graph shown in figure 3. It can be seen that also this time the absorption function of A in the presented CO_2 mass range is increasing, especially for the value corresponding to the current CO_2 concentration in the atmosphere ~ 400 ppm ($m_{CO2} \approx 6$ kg/m²) and the saturation should be expected only for higher m_{CO2} values. It should be noted, however, that these are the results of theoretical work with input data, the reliability of which may be questioned.

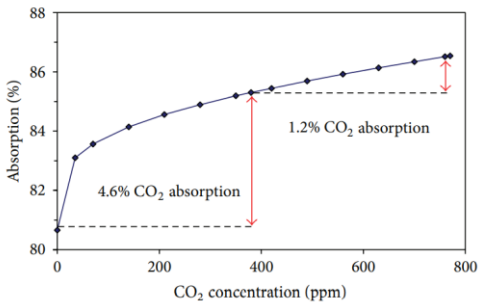

Fig. 2. Graph of the absorption of the Earth's thermal radiation as a function of CO_2 concentration in the atmosphere [2]

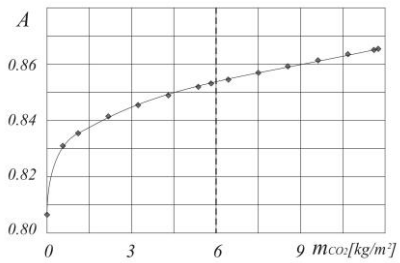

Fig. 3. Graph of the absorption of the Earth's thermal radiation as a function of the mass of CO_2 in the atmosphere per 1 m² of surface; the dashed line represents the mass of CO_2 for a concentration of 400 ppm

It should be noted, however, that these are the results of theoretical work with input data, the reliability of which may be questioned. Meanwhile, as mentioned in the introduction in [4] and [5], it has been experimentally demonstrated that there is a complete saturation of the process of absorption of thermal radiation from the moon in carbon dioxide in the Earth's atmosphere. Therefore, let us try to carry out the considerations once again, using the well-known Schwarzschild equation used, among others, in [6]:

$$\frac{dI_\lambda}{d\tau} = -I_\lambda + B_\lambda(T) \tag{6}$$

where: $d\tau = k_\lambda \rho ds$, τ – optical thickness measured rectilinearly (with neglecting refraction in the atmosphere), k_λ – mass absorption coefficient, ρ – density of the absorption medium, *s* – propagation path, $B_\lambda(T)$ – Kirchhoff-Planck's function.

Taking into account that the optical thickness is proportional to the mass of the absorbing substance *m* and assuming a constant temperature of the gas (omitting e.g. its heating by the absorption of radiation) after integration by frequency and neglecting the fact of widening of the oscillatory-rotational lines for large values of the absorbing mass, equation (6) can be written in the form:

$$\frac{dI}{dm} = -\alpha I + E \tag{7}$$

where α and E are constants.

The solution to equation (7) has the form:

$$I = \left(I_0 - \frac{E}{\alpha}\right) e^{-\alpha m} + \frac{E}{\alpha} \tag{8}$$

where I_0 is the intensity of the incident radiation.

Using equation (2), one can write:

$$A = \frac{I_0 - I}{I_0} = 1 - \left(1 - \frac{E}{\alpha I_0}\right) e^{-\kappa m} - \frac{E}{\alpha I_0} = \left(1 - \frac{E}{\alpha I_0}\right) - \left(1 - \frac{E}{\alpha I_0}\right) e^{-\alpha m} \tag{9}$$

By introducing the designation:

$$1 - \frac{E}{\alpha I_0} = \psi \tag{10}$$

formula (9) will take the form:

$$A = \psi(1 - e^{-\alpha m}) \tag{11}$$

Formula (11) is similar to formula (3) and shows that, analogically to monochromatic radiation, the absorption of thermal radiation have to saturate, reaching the value of ψ for a sufficiently large value of the absorbing mass *m*.

Of course, the presented considerations require experimental verification.

2. Experimental work

The aim of the experimental work was to measure the characteristics of the absorption of thermal radiation as a function of the mass of carbon dioxide absorbing this radiation. The scheme of the experiment is shown in figure 4.

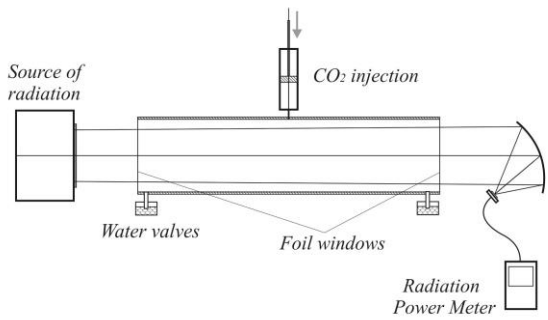

Fig. 4. Schematic diagram of a laboratory system for measuring the absorption of thermal radiation in carbon dioxide

It uses a source of thermal radiation analogous to that described in [5], introducing a graphite emissive surface applied to a copper plate adjacent to the flat surface of a glass vessel with heated oil. The absorption cuvette was made in the form of a horizontal PVC pipe, 1 m long and 150 mm in diameter, closed with removable windows made of polyethylene foil. A small closable opening was provided in the centre of the cuvette for introducing a defined volume of carbon dioxide. At the ends of the cuvette, there were two hoses with the ends immersed in water, constituting check valves, through which a part of the previous gas mixture was ejected from the cuvette, with a volume equal to the volume of introduced carbon dioxide. At the bottom of the cuvette there were two loosely connected panels with a thin rod led outside the cuvette through a suitable sealed passage. As a result, by pulling the rod out and inserting it, it was possible to mix the introduced portion of carbon dioxide with the previous mixture in the cuvette by the movements of the panels. Small portions of CO_2 were injected with a medical syringe, while larger portions were introduced using a graduated vessel filled with carbon dioxide closed with a water jacket at the bottom, which pushed the gas through the tap at the top into the cuvette. One hundred percent concentration of CO_2 in the cuvette was obtained by passing carbon dioxide from the vessel through it for 20 minutes, using a gas mixing device, and checking in the meantime whether the absorption increased further.

Table 1. Absorption of thermal radiation in carbon dioxide

T=78.6ºC			T=109.5ºC		
Measurement	m [kg/m^2]	A	Measurement	m [kg/m^2]	A
1	0	0	1	0	0
2	0.00561	0.0177	2	0.00561	0.0031
3	0.01101	0.0402	3	0.01101	0.0171
4	0.02202	0.0524	4	0.02202	0.0303
5	0.03303	0.0595	5	0.03303	0.0454
6	0.06213	0.0749	6	0.06213	0.055
7	0.09081	0.0848	7	0.09081	0.0676
8	0.11907	0.0853	8	0.13548	0.0761
9	0.16311	0.1014	9	0.17912	0.0863
10	0.20613	0.1046	10	0.22192	0.0913
11	0.24831	0.1083	11	0.26369	0.0903
12	0.28945	0.1117	12	2.078	0.12
13	2.078	0.13			

The tests were carried out for two temperatures of the radiation source: 78.6°C and 109.5°C, reading the radiation power on the meter. Using the formula (1) and taking I_0 as the radiation power for zero CO_2 concentration, the values of radiation absorption were calculated. The results are presented in table 1. On their basis, the graphs shown in Fig. 5 were made.

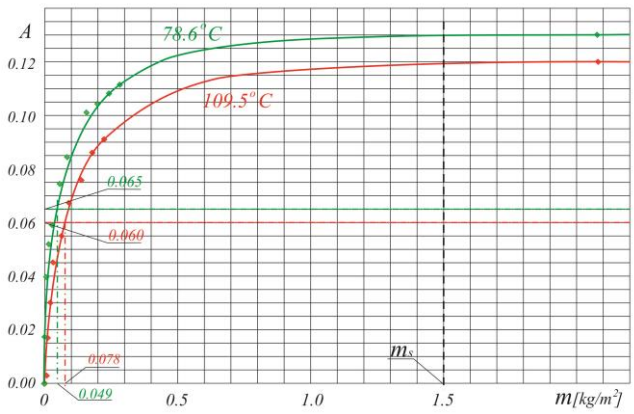

Fig. 5. Graph of absorption of thermal radiation as a function of absorbing mass of CO_2 for the source temperature of 78.6°C and 109.5°C, respectively

On the basis of the obtained graphs, it can be concluded that for the mass of carbon dioxide m_s = 1.5 kg/m^2, we are very close to the full saturation of absorption A_s, which for the source temperature of 78.6ºC corresponds to the absorption A_s = 0.13, while for the temperature of 109.5ºC A_s = 0.12. From the obtained graphs it is also possible to read the values of CO_2 mass for which the absorption value is equal to half of the maximum absorption. These readings show that for the source temperature of 78.6ºC $m_{1/2}$ = 0.049, while for 109.5ºC $m_{1/2}$ = 0.078. By introducing these values into the formula (11), for the temperature of 78.6ºC one can determine α_1 = 0.13, κ_1 = 14.1 m^2/kg and for the temperature of 109.5ºC α_2 = 0.12, κ_2 = 8,9 m^2/kg.

After inserting these values back into formula (11), the graphs were obtained, which are shown in the form of dashed lines in Fig. 6.

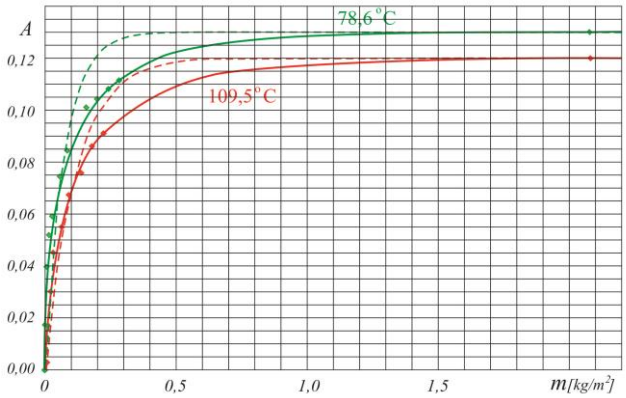

Fig. 6. Thermal radiation absorption charts: solid lines –experimental curves; dashed lines – curves made on the basis of formula (11)

The obtained graphs show that the actual saturation process is "slower" than the saturation process resulting from formula (11). However, as can be seen, the saturation process itself occurs and cannot be questioned.

3. Relating the results of experimental research to the Earth's atmosphere

As already mentioned in the first chapter, in the Earth's atmosphere in a cylinder with a diameter of 1 m^2 and an altitude from sea level to the stratosphere, there is a mass of carbon dioxide equal to:

$$m_{CO_2}[kg] = 1.52 \cdot 10^{-2} kg \cdot C_{CO_2}[ppm]$$

At a CO_2 concentration of 400 ppm, we get the value of the absorbing mass of carbon dioxide ~ 6 kg/m^2. Therefore, in Fig. 7, in order to better illustrate the phenomenon, the graph in Fig. 5 has been extended to this mass value.

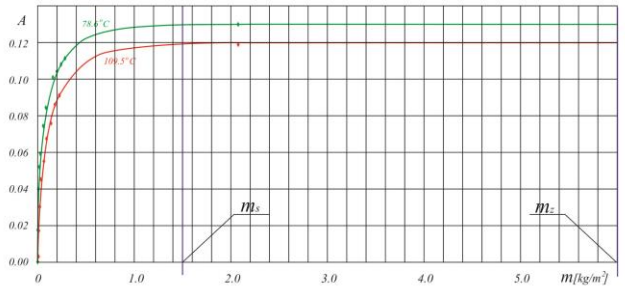

Fig. 7. Graph of absorption of thermal radiation in carbon dioxide, taking into account the mass of saturation m_s and the mass of CO_2 in the Earth's atmosphere m_z

It can be seen that practically with the mass of carbon dioxide of about 1.5 kg/m^2, the process of absorption of thermal radiation goes into saturation with a tendency to "faster" saturation at lower temperatures of the radiation source. So, for the current concentration of 400 ppm for which the mass of CO_2 in the atmosphere is ~ 6 kg/m^2, the limit is for times exceeded. Thus, it can be presumed that the carbon dioxide additionally emitted into the atmosphere does not absorb thermal radiation and thus is not a greenhouse gas.

4. Conclusions

The presented experimental work should be continued. Among other things, it would be necessary to carry out tests for a radiation source with a temperature close to the temperature of the Earth's surface and to measure the absorption of thermal radiation in a mixture of CO_2 with air for various temperatures and pressures. The obtained measurement results could then be used for appropriate computer models so that the final results could be compared with those adopted by the IPCC (Intergovernmental Panel on Climate Change).

Some of the works cited in the introduction and in chapter 1 and the results of the presented experiment, clearly suggest that there can be the saturation of the absorption of the Earth's thermal radiation in atmospheric carbon dioxide. If this was the case, the carbon dioxide additionally emitted into the atmosphere would not have to be the greenhouse gas. Therefore, taking into account the extremely high costs incurred as a result of reducing CO_2 emissions, more attention should be paid to the described experimental studies. However, hard coal and crude oil are valuable raw materials for the chemical industry, and burning them to produce energy is a sheer waste. The degradation of the natural environment is also associated with the extraction of coal. In addition, the often used old "soot" furnaces and primitive internal combustion engines emit a lot of harmful gases and dust. Therefore, it would be good to switch to energy from renewable sources and from nuclear reactors. However, when promoting climate projects, unproven hypotheses treated as a reliable source of information should not be used. It should be emphasized once again that the fact that two phenomena occur simultaneously does not imply that one is the cause of the other. All conditions and results of scientific research should be taken into account, especially the results of experimental work which are both a source of input data and a confirmation of the performed calculations.

References

[1] Goody R. M., Yung Y. L.: Atmospheric Radiation: Theoretical Basis. Oxford University Press, New York 1989, 178–183.

[2] Harde H.: Radiation and Heat Transfer in the Atmosphere: A Comprehensive Approach on a Molecular Basis. International Journal of Atmospheric Sciences 2013, 503727 [http://doi.org/10.1155/2013/503727].

[3] Humlum O. et al.: The phase relation between atmospheric carbon dioxide and global temperature. Global and Planetary Change 100, 2013, 51–69 [http://doi.org/10.1016/j.gloplacha.2012.08.008].

[4] Kubicki J., Kopczyński K., Młyńczak J.: Saturation of the absorption of thermal radiation by atmospheric carbon dioxide. IAPGOŚ 10(1), 2020, 77–81 [http://doi.org/10.35784/iapgos.826].

[5] Kubicki J., Kopczyński K., Młyńczak J.: Wpływ wzrostu stężenia CO2 w atmosferze na proces absorpcji promieniowania termicznego, Biuletyn WAT 69(3), 2020, 15-34 [http://doi.org/10.5604/01.3001.0014.8870].

[6] Markowicz K.: Procesy radiacyjne w atmosferze – Materiały do wykładu. Instytut Geofizyki, Wydział Fizyki, Uniwersytet Warszawski [https://www.igf.fuw.edu.pl/m/documents/28/c7/28c7b491-658c-475a-9c03-fbb50707c9de/wykladradiacja.pdf].

[7] Meserole C. A. et al.: CO_2 Absorption of IR Radiated by the Earth. Journal of Chemical Education 74(3), 1997, 316 [http://pubs.acs.org/doi/10.1021/ed074p316].

[8] Peng-Sheng W. et al.: Absorption coefficient of carbon dioxide across atmospheric troposphere layer. Heliyon 4, 2018, e00785 [http://doi.org/10.1016/j.heliyon.2018.e00785].

[9] Régalia L. et al.: Laboratory measurements and calculations of line shape parameters of the H2O–CO2 collision system. Journal of Quantitative Spectroscopy and Radiative Transfer 231(7), 2019, 126–135.

[10] Smirnov B. M.: Greenhouse effect in the atmosphere. Europhys. Lett. 114(2), 2016, 24005 [https://iopscience.iop.org/article/10.1209/0295-5075/114/24005].

Ph.D. Eng. Jan Kubicki
e-mail: jan.kubicki@wat.edu.pl

Ph.D. Eng. Jan Kubicki is a graduate of the Faculty of Technical Physics of the Military University of Technology. Currently works at the Institute of Optoelectronics of the Military University of Technology. He is the author or co-author of several dozen scientific publications in the field of laser physics, high power laser systems, laser spectroscopy, the interaction of laser radiation with matter and the use of pulsed electric discharges to modify metal surfaces. Author or co-author of technological studies and patents on the use of high-power laser pulses, pulsed electrical discharges in gases and liquids, and issues related to remote detection of alcohol vapors. Currently, he deals with remote detection of vapors and gases in open and closed spaces.

http://orcid.org/0000-0002-5191-7850

D.Sc. Eng. Krzysztof Kopczyński
e-mail: krzysztof.kopczynski@wat.edu.pl

D.Sc. Eng. Krzysztof Kopczyński is the director of the Institute of Optoelectronics of the Military University of Technology. In addition to managing the Institute, he is involved in research and teaching. He managed many domestic and foreign projects as part of KBN, NCBR, EU and EDA. Currently, he conducts research related to opto-electronic systems in the field of security and defense. He has won many gold medals and awards at the International Innovation Exhibitions in Moscow, Geneva and Brussels, as well as diplomas of the Minister of Science. He is the author of over 100 publications in Polish and foreign scientific journals. Member of SPIE International Society for Optics and Photonics, OSA Optical Society of America and EOS European Optical Society.

http://orcid.org/0000-0002-3319-3940

D.Sc. Eng. Jarosław Młyńczak
e-mail: jaroslaw.mlynczak@wat.edu.pl

D.Sc. Eng. Jarosław Młyńczak is a university professor at the Institute of Optoelectronics of the Military University of Technology. He published dozens of articles in peer-reviewed scientific journals and many papers and communications at national and international conferences. He is also a co-author of several patents. He received several awards at international and national exhibitions of inventions SIIF, IWIS, IENA, BRUSSELS INNOVA. Currently, he is a Head of Accredited Research Laboratory of IOE WAT and conducts research in the fields of laser safety, new active laser media, passive q-switches, optoelectronic detection of chemical and biological agents as well as remote alcohol detection.

http://orcid.org/0000-0002-0823-9302

http://doi.org/10.35784/iapgos.3052

received: 22.08.2022 | revised: 21.09.2022 | accepted: 15.09.2022 | available online: 30.09.2022

SWITCH-FILTER ON A RECTANGULAR WAVEGUIDE PARTIALLY FILLED BY DIELECTRIC

Vitaly Pochernyaev[1], Nataliia Syvkova[1], Mariia Mahomedova[2]

[1]State University of Intellectual Technologies and Communications, Faculty Telecommunications and Radioengineering, Odesa, Ukraine, [2]Kyiv Professional College of Communications, Faculty of Information and Communication Systems and Information Protection, Kyiv, Ukraine

Abstract. *At article investigates a broadband switch for microwave technology, antenna-feeder paths of which are implemented on a rectangular waveguide partially filled by dielectric. Modern means of communication of the microwave range can operate for transmission through two independent antenna channels, each of which includes its own microwave transmitter. It is also provided the operation of one microwave transmitter for two antennas. The transmission of high-power signals requires the implementation devices based on rectangular waveguide partially filled by dielectric. The active element is an open nonlinear structure included in a dielectric plate which located in a rectangular waveguide. The electrodynamic problem is solved by the method of eigenfunctions. In this article, the transfer coefficient and plotted the graphs of the dependence of the electrical length of the waveguide segment with the open nonlinear structure on the value of the reactive conductivity of the inductive loop at fixed reactive conductivity of the open nonlinear structure is determine. The results of this article can be used in the development of broadband switches for mobile digital combined troposcatter-radio relay stations with space-diversity transmission, antenna-feeder paths of which are implemented on the rectangular waveguide partially filled by dielectric. The article developed a filter on waveguide tees partially filled by dielectric. A design based on an H-tee on a rectangular waveguide partially filled by dielectric is proposed. The equivalent circuit of the H-tee is based on the equivalent circuit in the longitudinal slot in the narrow wall of the waveguide. Such a gap interrupts the lines of the transverse surface current of the main wave of a rectangular waveguide partially filled by dielectric. Numerical results are obtained for transformation ratios.*

Keywords: rectangular waveguide partially filled by dielectric, switch, filter, open nonlinear structure

PRZEŁĄCZNIK-FILTR NA FALOWODZIE PROSTOKĄTNYM CZĘŚCIOWO WYPEŁNIONYM DIELEKTRYKIEM

Streszczenie. *W artykule zbadano szerokopasmowy przełącznik dla techniki mikrofalowej, którego tory antenowo-podajnikowe są realizowane na falowodzie prostokątnym częściowo wypełnionym dielektrykiem. Nowoczesne urządzenia do komunikacji mikrofalowej mogą pracować na dwóch niezależnych kanałach antenowych, z których każdy zawiera własny nadajnik mikrofalowy. Możliwa jest również praca jednego nadajnika mikrofalowego na dwóch antenach. Transmisja sygnałów dużej mocy wymaga realizacji urządzeń opartych na falowodzie prostokątnym częściowo wypełnionym dielektrykiem. Elementem aktywnym jest otwarta struktura nieliniowa zawarta w płytce dielektrycznej, która znajduje się w prostokątnym falowodzie. Problem elektrodynamiczny jest rozwiązywany metodą funkcji własnych. W artykule wyznaczono współczynnik transmisji oraz wykreślono wykresy zależności długości elektrycznej segmentu falowodu o otwartej strukturze nieliniowej od wartości reaktancji obwodu indukcyjnego przy ustalonej reaktancji otwartej struktury nieliniowej. Wyniki artykułu mogą być wykorzystane przy opracowywaniu szerokopasmowych przełączników ruchomych cyfrowych kombinowanych stacji przekaźnikowych troposferycznych z separacją przestrzenną, których tory antenowo-podajnikowe realizowane są na falowodzie prostokątnym częściowo wypełnionym dielektrykiem. W artykule opracowano filtr na trójnikach falowodowych częściowo wypełnionych dielektrykiem. Zaproponowano konstrukcję opartą na trójniku typu H na falowodzie prostokątnym częściowo wypełnionym dielektrykiem. Obwód równoważny trójkąta H jest oparty na obwodzie równoważnym w szczelinie podłużnej w wąskiej ściance falowodu. Szczelina taka przerywa poprzeczne linie prądu powierzchniowego fali fundamentalnej w falowodzie prostokątnym częściowo wypełnionym dielektrykiem. Otrzymano wyniki numeryczne dla współczynników transformacji.*

Słowa kluczowe: prostokątny falowód częściowo wypełniony dielektrykiem, przełącznik, filtr, otwarta struktura nieliniowa

Introduction

Combined radio engineering systems are one of the trends in the development of microwave technology [1-4, 8, 9]. In article [7], a mobile digital tropospheric radio relay station is analyzed, which includes two microwave transmitters. This station can transmit on two independent antenna channels, each of which includes its own microwave transmitter. It is possible to operate one microwave transmitter on two antennas; the second microwave transmitter is on standby. Different modes of operation of the microwave transmission path are equipped with two on-off microwave switches [7]. The requirement to ensure broadband operation of the microwave transmission path can be met by implementing the path on a rectangular waveguide partially filled by dielectric (RWPFD). In this case, it is necessary to implement two-position microwave switches also on RWPFD.

The aim of the work is to develop a broadband microwave switch on the RWPFD and a trap filter on the RWPFD.

1. Microwave switch on RWPFD

The microwave switch incorporates a packageless diode, which is included in a dielectric plate in the form of an open nonlinear structure (ONS). The inclusion of ONS can be both parallel and serial.

With the serial connection of the ONS in the RWPFD, a wide bandwidth can be obtained, but the capacitance of the ONS should be minimal. Parallel connection of ONS allows to provide a higher level of switching power than with series connection. It should be noted that it is the implementation of the switch on the RWPFD that provides a wider operating frequency band and a higher dielectric strength [6]. In addition, it is possible to expand the operating frequency band if the parallel connection of the ONS in the RWPFD is carried out together with a loop that compensates for the capacitance of the ONS.

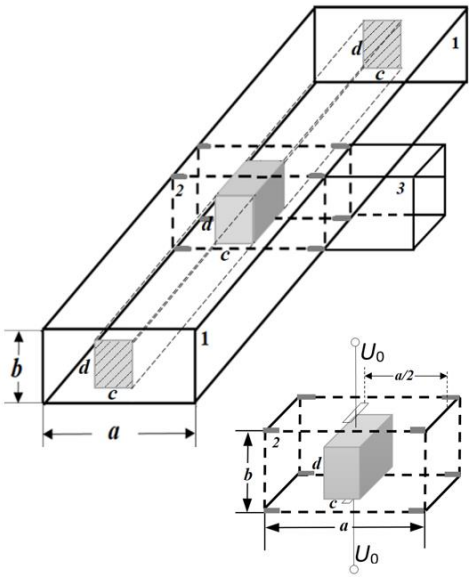

Fig. 1. The design of the switch on RWPFD with a compensating loop

On Fig. 1 shows the design of the switch on the RWPFD with a compensating loop. This RWPFD is a rectangular waveguide with dimensions $a \times b$, in which a dielectric plate with dimensions $c \times d$ is located, which does not affect the walls of the waveguide and has a relative permittivity ε_r. A ONS of the same geometric dimensions is included in the dielectric plate. Waveguide 1 is a RWPFD, waveguide 2 is a RWPFD with ONS, waveguide 3 is a hollow rectangular waveguide.

The ONS is controlled through a non-radiating longitudinal slot in the wide wall of the RWPFD. The value of the resistance of the ONS is a few ohms in the presence of a control voltage and thousands of ohms in its absence. To compensate for the capacitance of the ONS, which should be as small as possible, a compensating inductive loop is turned on in the form of a segment of a hollow rectangular waveguide from the side of the narrow wall of the main waveguide. Such an inclusion is an *H*-connection of waveguides.

On Fig. 2 shows the equivalent circuit of the plane-transverse joint of the RWPFD with the ONS, the plane-transverse joint of the ONS with the RWPFD and a parallel-connected compensating loop. On Fig. 2 shows the normalized reactive conductivity jb_c of the plane-transverse junction of the RWPFD with ONS and the ONS with RWPFD, the transformation coefficients N_0 for the main quasi-H_{10} wave and the normalized reactive conductivity $-jb_L$ of the compensating inductive loop.

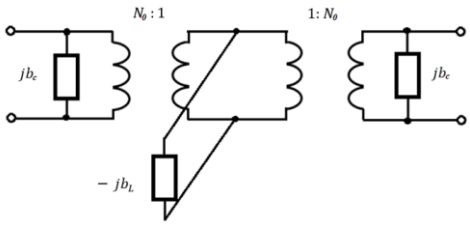

Fig. 2. Equivalent circuit of the plane-transverse joint of the RWPFD with ONS, the plane-transverse joint of the ONS with RWPFD and a parallel-connected compensating loop

"Collapsing" the circuit shown on Fig. 2 through the recalculation of the transformation ratios N_0, we obtain an equivalent circuit with parallel normalized conductivity jb_Σ and normalized reactive conductivity $-jb_L$ of the compensating inductive loop (Fig. 3).

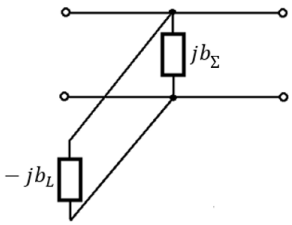

Fig. 3. Equivalent circuit with parallel normalized conductivity jb_Σ and normalized reactive conductivity $-jb_L$ of a compensating inductive loop

Calculation of the normalized reactive conductivities was carried out according to the following formulas:

$$b_c = \frac{1}{N_0^2}\sum_{k=1}^{\infty} N_k^2 y_k \tag{1}$$

$$b_\Sigma = \frac{2b_c}{N_0^2 y_0} \tag{2}$$

$$N_0 = \int_S \bar{\mathcal{E}}_{h_{10}} \bar{\mathcal{E}}_H \, dS$$

$$N_k = \int_S \bar{\mathcal{E}}_{h_{10}} \bar{\mathcal{E}}_k \, dS$$

$$\bar{\mathcal{E}}_{h_{10}} = \sqrt{128/ab\left(64+q^2+p^2+q^2p^2\right)}\,\frac{1}{k_{h_{10}}} * \mathcal{F} \tag{3}$$

$$\mathcal{F} = \left\{\left[\left(\frac{\pi}{a}\right)\sin\frac{\pi x}{a} - \left(\frac{p\pi}{2a}\right)\sin\frac{\pi x}{a}\cos\frac{2\pi y}{b} - \left(\frac{3q\pi}{ba}\right) * \right.\right.$$
$$* \sin\frac{3\pi x}{a}\sin\frac{\pi x}{a}\cos\frac{2\pi y}{b} - \left(\frac{3q\pi}{ba}\right)\sin\frac{3\pi x}{a} +$$
$$\left. + \left(\frac{3qp\pi}{16a}\right)\sin\frac{3\pi x}{a}\cos\frac{2\pi y}{b}\right]\bar{y}^0 + \left[\left(\frac{p\pi}{b}\right)\cos\frac{\pi x}{a} * \right.$$
$$\left.\left. * \sin\frac{2\pi y}{b} - \left(\frac{2qp\pi}{8b}\right)\cos\frac{3\pi x}{a}\sin\frac{2\pi y}{b}\right]\bar{x}^0\right\}$$

$$\bar{\mathcal{E}}_H = \sqrt{128/ab\left(64+q^2+p^2+q^2p^2\right)}\,\frac{1}{k_H} * \mathcal{F} \tag{4}$$

$$k_H^2 = k_0^2\left(\varepsilon_{ef}\left(1+\alpha\bar{\mathcal{E}}_{10}^2\right)\right) - \gamma_{10}^2$$

where $\bar{\mathcal{E}}_k$ – transverse electric eigenfunction of higher types of quasi-H_{30} and quasi-H_{50} waves RWPFD [6]; $\bar{\mathcal{E}}_{10}$ – transverse electric eigenfunction of a hollow rectangular waveguide [6]; k_0, γ_{10} – the wavenumber of a hollow rectangular waveguide and the longitudinal wavenumber of the RWPFD respectively [6]; ε_{ef} – effective permittivity [6]; y_0, y_k – the normalized conductivity of the main quasi-H_{10} wave and the normalized conductivity of higher types of quasi-H_{30} and quasi-H_{50} waves RWPFD, respectively [6].

As a local field, in the first approximation, we take into account the quasi-H_{30} and quasi-H_{50} waves:

$$\bar{\mathcal{E}}_{h30} = \sqrt{128/ab\left(64+q^2+p^2+q^2p^2\right)} * \frac{1}{k_{h30}} * \mathcal{J} \tag{5}$$

$$\mathcal{J} = \left\{\left[\frac{p\pi}{b}\cos\frac{3\pi x}{a}\sin\frac{2\pi y}{b} - \frac{qp\pi}{16b}\left(\cos\frac{5\pi x}{a} - 2\cos\frac{\pi x}{a}\right) * \right.\right.$$
$$\left. * \sin\frac{2\pi y}{b}\right]\bar{x}^0 + \left[\frac{3\pi}{a}\sin\frac{3\pi x}{a} - \frac{3p\pi}{2a}\sin\frac{3\pi x}{a}\cos\frac{2\pi y}{b} - \right.$$
$$- \frac{q\pi}{8a}\left(\frac{5}{2}\sin\frac{5\pi x}{a} - \sin\frac{\pi x}{a}\right) +$$
$$\left.\left. + \frac{qp\pi}{16a}\left(\frac{5}{2}\sin\frac{5\pi x}{a} - \sin\frac{\pi x}{a}\right)\cos\frac{2\pi y}{b}\right]\bar{y}^0\right\}$$

$$\bar{\mathcal{E}}_{h_{50}} = \sqrt{128/ab\left(64+q^2+p^2+q^2p^2\right)} * \frac{1}{k_{h_{50}}} * K \tag{6}$$

$$K = \left[\left(\frac{p\pi}{b}\right)\cos\frac{5\pi x}{a}\sin\frac{2\pi y}{b} - \left(\frac{qp\pi}{8b}\right)K_1\sin\frac{2\pi y}{b}\right]\bar{x}^0 +$$
$$+ \left[\left(\frac{5\pi}{a}\right)\sin\frac{5\pi x}{a} + \left(\frac{qp\pi}{16a}\right)K_2\cos\frac{2\pi y}{b} - \right.$$
$$\left. - \frac{qp\pi}{8a}K_2 - \left(\frac{5p\pi}{2a}\sin\frac{5\pi}{a} - \cos\frac{2\pi y}{b}\right)\right]\bar{y}^0$$

$$K_1 = \frac{1}{3}\cos\frac{7\pi x}{a} - \frac{1}{2}\cos\frac{3\pi x}{a}$$

$$K_2 = \frac{7}{3}\sin\frac{7\pi x}{a} - \frac{3}{2}\sin\frac{3\pi x}{a}$$

Note that the dielectric plate, in contrast to the ONS, which is an isotropic nonlinear dielectric from ε_d, is an isotropic linear dielectric with ε_r. Even with the passage of current through the ONS, the nonlinear process will proceed in a weak electromagnetic field. Therefore, the dependence of the electrical induction on the electrical intensity will be linear in the working range of changes in the magnitude of the electrical intensity. In accordance with [5], this is a local linearization of the above dependence. Taking into account that the electromagnetic field will also change slightly in the local hollow area of the RWPFD,

located in the immediate vicinity of the ONS ($\mathscr{L} << \Lambda_{h_{10}}$, where $\mathscr{L}$ is the maximum size of the ONS, $\Lambda_{h_{10}}$ is the length of the main quasi-H_{10} wave of the RWPFD), the expression for the relative electric ONS permeability will have following:

$$\varepsilon_{\mathrm{d}} = \left(1 + \alpha \bar{\mathcal{E}}_{10}^{2}\right) \tag{7}$$

where α – coefficient of nonlinearity, depending on the material of the ONS [5].

The transmission coefficient T_{11} for the circuit in Fig. 3 has the following form:

$$T_{11} = 1 + \frac{1}{2}\left[jb_{\Sigma}\Delta f - jb_{L} ctg\left(\theta \Delta f\right)\right] \tag{8}$$

where b_{Σ}, b_L – normalized reactive conductivities of the RWPFD with ONS and inductive loop respectively, $\Delta f = f / f_o$ – frequency range, θ electrical length of the inductive loop. At the resonant frequency $T_{11} = 1$, then we have:

$$\theta = arcctg \frac{b_{\Sigma}}{b_{L}} \tag{9}$$

On Fig. 4 shows the dependence of the value of θ on the value of b_L at fixed b_{Σ}: curve 1 is plotted at $b_{\Sigma} = 0.5$, curve 2 – at $b_{\Sigma} = 1$ These graphs can be used when calculating switches in transmission modes (de-energized ONS).

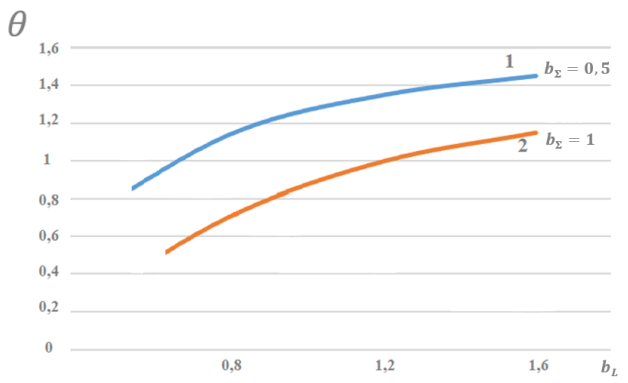

Fig. 4. Dependence of the value of θ on the value of b_L at fixed b_{Σ}

2. Filter on RWPFD

If a diaphragm is added to the design of Fig. 1 at the junction of the loop with the main waveguide and the loop is short-circuited with a short-circuiting plate.

The design of the filter on the *H*-tee is shown in Fig. 5.

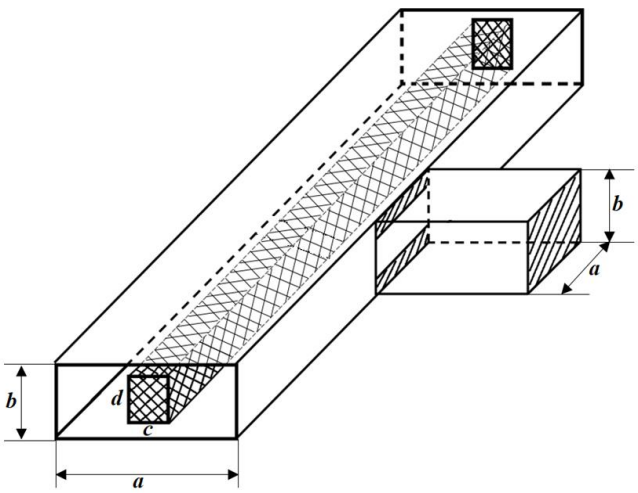

Fig. 5. Filter design on H-tee

The equivalent circuit of the filter on the *H*-tee is shown in Fig. 6.

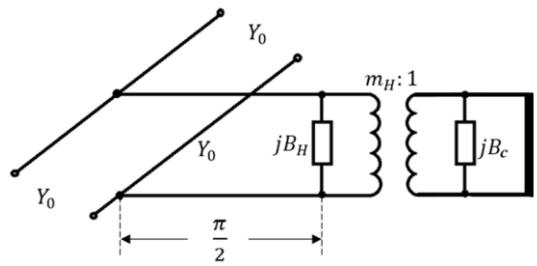

Fig. 6. Equivalent circuit for connecting the main waveguide with a side waveguide in an H-tee with a piston

When an electromagnetic wave falls from the *H*-arm of the tee, the electric fields in the side arms at equal distances from the joint are in phase, and the magnetic fields are in antiphase. The equivalent circuit of the *H*-tee is based on the equivalent circuit of the longitudinal slot in the narrow wall of the waveguide. Such a slit interrupts the lines of the transverse surface current of the main quasi-H_{10} wave of the RWPFD. The reaction of local fields in the vicinity of the slot is displayed by reactive conductivity jB_H and the conversion of the field amplitude at the slot to the amplitude of the propagating wave is shown by switching on an ideal transformer with a transformation coefficient m_H .

In order for the circuit to be valid under any load, including short circuit, the metallization of the slot must turn the waveguide into a regular one. This can be achieved by turning on a quarter-wave section of the transmission line having an electrical length of $\pi/2$ at all frequencies. The short-circuited quarter-wave transmission line does not affect the passage of the wave in the main waveguide.

Conductivity B_C is determined as follows:

$$B_C = \sum_k n_k Y_k$$

$$n_k = \int_S \bar{\mathcal{E}}_{h_{10}} \bar{\mathcal{E}}_k dS \tag{10}$$

The expressions for the transformation coefficients and reactive conductivities are as follows:

$$m_H = \int_S \bar{\mathfrak{I}}_H \bar{\mathcal{E}}_{h_{10}} dS$$

$$B_H = -\sum_k Y_k \left[\left(k_k^2 + \gamma_k^2\right) / \gamma_k^2\right] \int_S \bar{\mathfrak{I}}_H \bar{\mathcal{E}}_k dS$$

where k_k – transverse wavenumbers of higher wave types RWPFD, γ_k – longitudinal wavenumbers of higher wave types RWPFD [6]. The coordinate function $\bar{\mathfrak{I}}_H$ [7] approximating the field distribution at the hole has the following form:

$$\bar{\mathfrak{I}}_H = \sqrt{128 / \left(64 + q^2\right)}\ Ce_1\left(x, q\right) \bar{z}^0$$

where Ce_1 – even Mathieu function of the first kind, q – fill parameter of RWPFD.

Also note that in a frequency-tunable filter, the side arm is a segment of a hollow rectangular waveguide, as shown in Fig. 5. In a filter that does not tune in frequency, the side arm is RWPFD.

Tables 1 show the values of the transformation coefficient m_H for formule (11) depending on the value of $\frac{2a}{\Lambda}$.

Table 1. Dependence of the transformation coefficients on the normalized value

m_H	1.7	1.5	1.3	0.91	0.75	0.69	0.61	0.53
$\frac{2a}{\Lambda}$	0.7	0.8	0.9	1.1	1.2	1.3	1.4	1.5

3. Conclusions

In conclusion, we note that the developed broadband switch on the RWPFD can be used for microwave transmission paths of mobile digital troposcatter stations, mobile space communication stations and mobile digital combined troposcatter-radiorelay stations, which include two microwave transmitters. The prospects for the use of such broadband switches are significantly increased due to the introduction of space-diversity transmission into microwave technology. Once again, we note that the broadband bandwidth of the device was achieved not only due to design features, but also due to the implementation of the design on the RWPFD.

The inclusion of an open-frame semiconductor diode in the form of an ONS allows the device to function as a two-position switch: in the presence of a control current, the resistance of the ONS is units Ohm, in the absence – thousands Ohms. Such a switch on RWPFD provides two-position switching of high transmitting power in a wide frequency band. The high dielectric strength of the RWPFD was investigated in [6].

When implementing a filter on rectangular waveguides with dimensions of 40×20 mm^2 with a dielectric plate with $\varepsilon_r = 4$, it is possible to ensure the operation of the mobile digital troposcatter radio relay station radio relay component in two frequency ranges 3.8...4.2 GHz + 5.925...6.425 GHz [10, 11] with one antenna-feeder path. This filter provides a blockband of 4.2...5.925 GHz.

References

[1] Li C., Chen X., Liu X.: Cognitive tropospheric scatter communication. IEEE Trans. Veh. Technol 67(2), 2018, 1482–1491.
[2] Luis B., Wietgrefe H.: Geographical Analysis of Highly Deployable Troposcatter Systems Performance. IEEE Military communications conference MILCOM, 2013, 661–667.
[3] Luis B., Wietgrefe H.: Highly-deployable troposcatter systems in support of NATO expeditionary operations. Military communications conference MILCOM, 2011, 2042–2049.
[4] Luis B.: Tactical troposcatter applications in challenging climate zones. Military communications conference MILCOM, 2012, 1–6.
[5] Nikolskiy V. V., Nikolskaya T. I.: Elektrodinamika i rasprostraneniye radiovoln. URSS, Moscow 2011.
[6] Pochernyaev V. N., Cibizov K. N.: Teoriya slozhnikh volnovodov. Naukoviy svit, Kyiv 2003.
[7] Pochernyaev V. N., Povhlib V. S.: Mobile digital microwave radio station of dual purpose. Proc. of the O.S. Popov ONAT 2, 2014, 76–82.
[8] Prokis Dzh.: Cifrovaya svyaz. Radio i svyaz', Moscow 2000.
[9] Volkov L. I., Nemirovskij M. S., Shinakov Y. S.: Sistemy cifrovoj radiosvyazi-Eko-Trend, Moscow 2005.
[10] Recommendations ITU-R F.385.
[11] Recommendations ITU-R F.386.

Prof. Vitaly Pochernyaev
e-mail: vpochernyaev@gmail.com

Doctor of Technical Sciences, professor, member of the Institute of Electrical and Electronics Engineers, professor at the State University of Intelligent Technologies and Communications. Author of more than 200 publications, including 3 monographs, 2 textbooks, 12 patents for inventions. Research interests: applied electrodynamics, radiophysics, telecommunications and radioengineering, microwave theory and technology.

http://orcid.org/0000-0001-7130-8668

M.Sc. Nataliia Syvkova
e-mail: natsivonat@gmail.com

Ph.D. student, Senior Lecturer State University of Intelligent Technologies and Communications. Author of more than 30 publications, including 1 textbook and 4 patents for inventions. Research interests: telecommunications and radioengineering, microwave theory and technology.

http://orcid.org/0000-0002-4934-4109

M.Sc. Mariia Mahomedova
e-mail: kkz.praktika@ukr.net

Ph.D. student at the State University of Telecommunications. Lecturer at the Kyiv Professional College of Communications. Author of more than 10 publications. Research interests: telecommunications and radioengineering, microwave theory and technology.

http://orcid.org/0000-0003-1936-5555

http://doi.org/10.35784/iapgos.2884

received: 20.02.2022 | revised: 08.07.2022 | accepted: 15.09.2022 | available online: 30.09.2022

GIANT MAGNETORESISTANCE OBSERVED IN THIN FILM NiFe/Cu/NiFe STRUCTURES

Jakub Kisała[1], Andrzej Kociubiński[1], Karolina Czarnacka[2], Mateusz Gęca[1]

[1]Lublin University of Technology, Faculty of Electrical Engineering and Computer Science, Department of Electronics and Information Technology, Lublin, Poland,
[2]University of Live Science of Lublin, Faculty of Production Engineering, Department of Technology Fundamentals, Lublin, Poland

Abstract. *In this paper, the technology for fabricating NiFe/Cu/NiFe layered structures by magnetron sputtering is presented. Two series of samples were fabricated on a glass substrate with a layered structure, where the individual layers were 30 nm NiFe, 5 nm Cu, and finally NiFe with a thickness of 30 nm. The series differed in the type of technology mask used. A constant magnetic field was applied to the substrate during the sputtering of the ferromagnetic layers. Measurements of the DC resistance of the obtained structures in the constant magnetic field of neodymium magnet packs with a constant magnetic field of about 0.5 T magnetic induction have been carried out. Comparison of the two series allows us to conclude the greater validity of using masks in the form of kapton tape. The obtained results seem to confirm the occurrence of phenomena referred to as the giant magnetoresistance effect.*

Keywords: magnetoresistance, sputtering, thin films, static magnetic field

ZJAWISKO GIGANTYCZNEGO MAGNETOOPORU OBSERWOWANE W CIENKICH STRUKTURACH NiFe/Cu/NiFe

Streszczenie. *W pracy przedstawiono technologię produkcji struktur warstwowych NiFe/Cu/NiFe metodą rozpylania magnetronowego. Wykonane zostały dwie serie próbek na szklanym podłożu o strukturze warstwowej, gdzie poszczególne warstwy stanowiły 30 nm NiFe, 5 nm Cu oraz ostatecznie NiFe o grubości 30 nm. Serie różniły się rodzajem zastosowanej maski technologicznej. Podczas napylania warstw ferromagnetycznych do podłoża przyłożone zostało stałe pole magnetyczne. Przeprowadzone zostały pomiary rezystancji stałoprądowej otrzymanych struktur w stałym polu magnetycznym okładów magnesów neodymowych o stałym polu magnetycznym o wartości indukcji magnetycznej około 0,5 T. Porównanie obu serii pozwala stwierdzić większą zasadność stosowania masek w postaci taśmy kaptonowej. Otrzymane wyniki zdają się potwierdzać występowanie zjawisk określanych jako efekt gigantycznego magnetooporu.*

Słowa kluczowe: magnetorezystancja, napylanie, cienkie warstwy, statyczne pole magnetyczne

Introduction

Sensors for physical measurements are key components of almost all electronic devices. The purpose of using them is to collect information about the environment in order to process it and put it to a specific use. Sensors for specific physical quantities can be based on completely different physical phenomena. By discovering new physical relationships and effects, new sensors can be designed and existing ones improved to increase their signal processing capabilities, e.g., by increasing their range or sensitivity. This also applies to magnetic field sensors. Currently, the best known sensors for magnetic field measurements are those based on the Hall effect. In 1856 Lord Kelvin observed resistance changes in ferromagnetic metals (iron and nickel) when an external magnetic field was applied. The group of effects, that includes the phenomenon observed by Kelvin, are called magnetoresistive phenomena [19].

Giant magnetoresistance (GMR) is a phenomenon observed in FM/NM/FM structures, where FM stands for ferromagnetic material and NM for nonmagnetic material. This phenomenon, which is part of the magnetoresistance family, is characterized by a change in the resistance of the structure in the external magnetic field [4, 9, 20]. The value of resistance of GMR structures depends on the direction of magnetization of adjacent ferromagnetic layers separated by a non-magnetic layer. The scattering of an electron moving through the structure depends on the correspondence of its spin and the direction of magnetization of the ferromagnetic layer [8]. The compatibility of the spin direction and the magnetization direction of the ferromagnetic layer results in less frequent scattering of the electron in the ferromagnetic layer as well as at the FM/NM interface than in the case of opposite directions of these vectors. Both of these configurations are shown in figure 1.

If the alternating ferromagnetic layers have the same direction of magnetization, the electron with conformal spin will be scattered less frequently, while the motion of the electron with opposite spin will be disrupted much more frequently [8]. The apparent result of this behavior is a decrease in the resistance of the structure relative to the configuration in which the alternating ferromagnetic layers have opposite resultant magnetization vectors [13]. These two states, referred to as parallel and antiparallel configurations, are shown in figure 1.

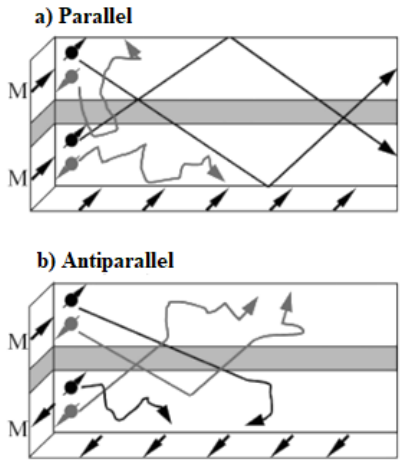

Fig. 1. Parallel (a) and antiparallel (b) configuration of FM/NM/FM structure exhibiting giant magnetoresistance phenomenon [3]

The thicknesses of the layers of structures exhibiting the giant magnetoresistance phenomenon are on the order of nanometers [16]. Such small sizes are crucial for the occurrence of this effect. The adequate thickness of the non-magnetic layer is particularly important; as its thickness decreases, an increase in the GMR effect is observed [2, 17]. For non-magnetic layer thicknesses on the order of a few nanometers, an oscillatory dependence of the exchange interaction is observed translating into an oscillatory nature of the phenomenon [10].

There are various realizations of structures exhibiting the phenomenon of giant magnetoresistance [20]. Additional layers and their thicknesses can significantly improve the desired magnetoresistance properties of a given sample. The basic one is the FM/NM/FM structure. It serves as the simplest possible explanation of the main mechanisms of the Giant Magnetoresistance phenomenon. These include multilayer FM/NM/FM structure, spin valve, pseudo spin valve, and granular alloys [5, 18]. Due to the current stage of development, only the basic FM/NM/FM designs are produced at this time.

The aim of this study was to develop a fabrication technology for NiFe/Ti/NiFe MEMS structures and to perform DC resistance measurements under a strong magnetic field. As part of the presented work, two series of structures differing in the type of technological mask used were fabricated.

1. Magnetron sputtering

There are several ways of obtaining thin film-structures. They differ in the purity and homogeneity of the obtained layers, in the time required for the process, in the possibilities of sputtering different types of materials, and in the cost of the necessary equipment and the process itself [1, 6]. Structures exhibiting the phenomenon of giant magnetoresistance do not require technological processes requiring high temperatures, i.e. diffusion or implantation, to be produced, as compared to semiconductor components. Production of GMR structures, which can already serve as sensors of e.g. magnetic field strength, is relatively simple; just a few lithographic processes are enough to obtain a functional device [7]. A frequently used method is sputtering, which provides uniform coverage and high sample purity [15].

Magnetron sputtering is a type of ion sputtering. Ionized particles of noble gas, for example, argon, thanks to the high voltage applied in a high vacuum chamber, are bombarding the target, which is the source of the material. Bombarding causes the material particles to be knocked out and deposited on the desired substrate. The magnetron sputtering chamber is shown in.

Magnetron sputtering is characteristic of using an additional magnetic field under the target in the form of permanent magnets or electromagnets. The magnetic field at the source of the material causes the trapping of electrons above the surface of the target leading to an increase in ion density. This increases the efficiency of the entire sputtering process. Metallic materials, like ferromagnetic and non-magnetic layers in GMR structures, can be sputtered using the DC power supply of the magnetron [21].

The Kurt J. Lesker® NANO 36 sputtering system, which is at the disposal of the Department of Electronics and Information Technology of the Lublin University of Technology, was used to produce thin films.

2. Technology of thin-film GMR structures

Microscope slides were used as substrates for the structures. In the case of the first series, enclosures made by 3D printing were used as a technological mask. In the second series, kapton tape was used as a technological mask; the process sequence used is shown in figure 2.

The sputtering processes take place in a high vacuum chamber. Each individual process requires a change of target and re-adjustment of the sputtering chamber to the appropriate pressure level. The thickness of the resulting layer is monitored during the process, making it easy to adjust the sputtering length to the desired layer thickness. Permalloy NiFe was used as ferromagnetic material, while copper Cu was used as non-magnetic material [14]. A permanent magnetic field of neodymium magnets was applied along the long edge of each sample during the sputtering of ferromagnetic layers near the substrate [11, 22]. This procedure was intended to induce easy axis magnetization of these layers [12].

The sputtering process parameters for both series are shown in Table 1. All technological processes take place under a vacuum of 10^{-7} Torr.

The final dimensions of the structure are 20 mm × 2 mm and 65 nm of thickness. Using graphite glue, copper wires are attached to both edges of the structure. An additional plastic housing protects the sample from mechanical damage and makes it easier to carry out measurements (Fig. 3).

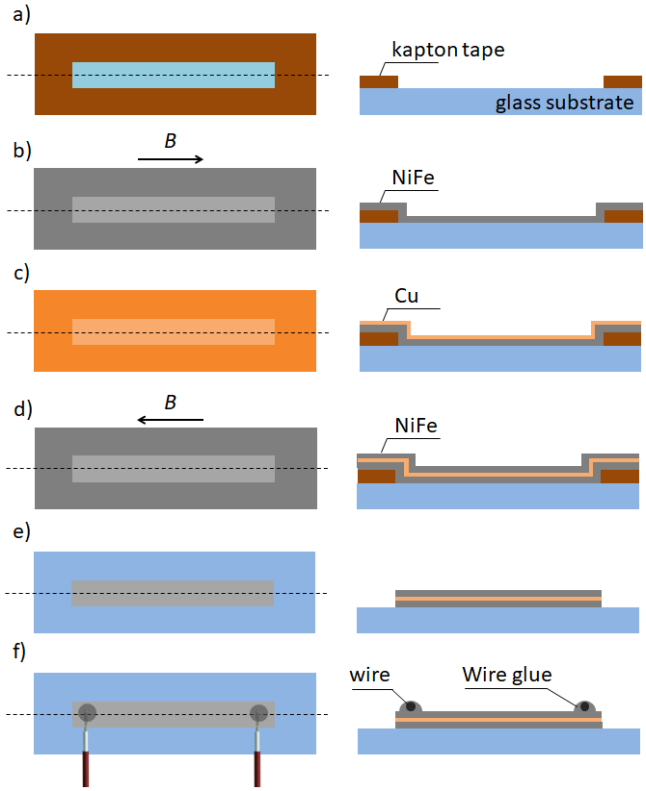

Fig. 2. Structure process sequence: (a) use of kapton tape as a technological mask, (b) deposition of a 30 nm NiFe layer in the presence of an magnetic field, (c) deposition of the 5 nm Cu layer, (d) deposition of a second 30 nm NiFe layer in the presence of an magnetic field, (e) removal of the kapton tape, (f) final structure

Table 1. Processes parameters

Lp.	Layer material and thickness	Plasma power Density [W/sq^2]	Argon flow rate [sccm]	Deposition time [min]
Series 1	NiFe (30 nm)	75	50	15
	Cu (5 nm)	50	40	3
	NiFe (30 nm)	75	50	15
Series 2	NiFe (30 nm)	90	85	15
	Cu (5 nm)	90	50	3,5
	NiFe (30 nm)	65	85	18

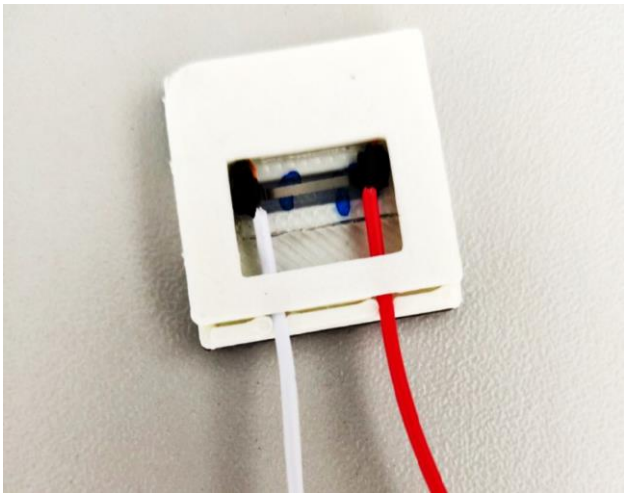

Fig. 3. Final structure in plastic protection

3. Experiment methodology and results

Samples of both series were measured for two-wire DC resistivity. These measurements were carried out using two strong neodymium magnets whose magnetic field induction was about 0.5 T, a KeySight 34410A multimeter cooperating with LabVIEW software, and a PC unit. These measurements consisted of alternating resistance measurements of the structure outside the magnetic field and in the magnetic field of the neodymium magnets. One hundred measurements were made alternately for each state. The longer edge of the sample is parallel to the external magnetic field lines of the neodymium magnets. Resistance measurement results for one of the samples of both series are shown in figure 4 and figure 5, respectively.

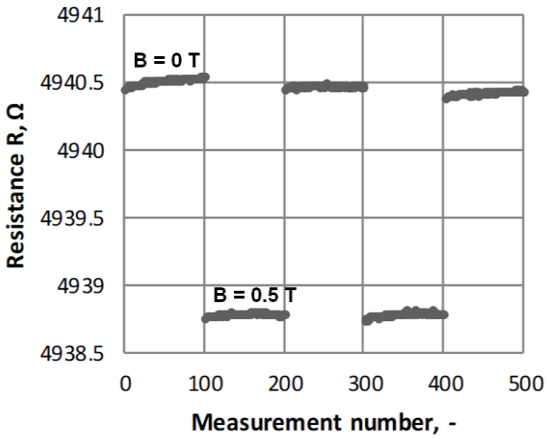

Fig. 4. Sample from the first series, NiFe(30)/Cu(5)/NiFe(30); plastic technology mask

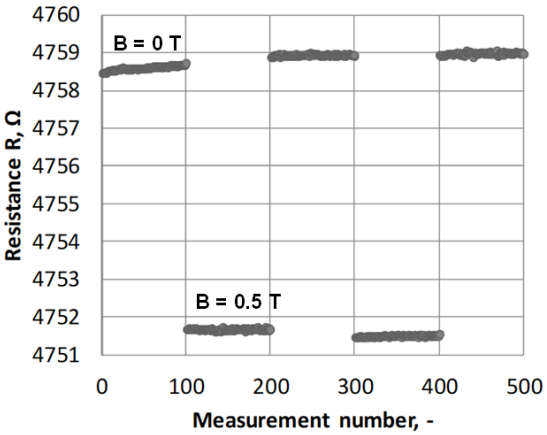

Fig. 5. Sample from the second series, NiFe(30)/Cu(5)/NiFe(30); technology mask made of kapton tape

The first one hundred measurements are made in the presence of a zero magnetic field induction. The measured resistance is therefore the resistance of the structure under the default conditions. Another hundred measurements were taken 5 seconds later when the tested structure was already between the plates of neodymium magnets. From both figures, it is possible to notice a decrease in the DC resistance of structure under the influence of a strong external magnetic field. In the case of the first series structure, this difference is about 1.7 ohm, while for the second – over 7 ohm. For the first sample, the decrease of the resistance in relation to the initial resistance is about 0.3‰ and for the second sample – about 1.6‰. In each of the states, with no magnetic field and strong magnetic field, the consecutive measurements do not seem to differ much from each other.

4. Summary

The performed measurements of the two-wire DC resistance of NiFe/Cu/NiFe thin structures in an external magnetic field seem to confirm the occurrence of the giant magnetoresistance phenomenon in them. In the case of the structures of both series, an apparent change in the sample resistance in a strong magnetic field is noticeable.

For the second series structure, the resistance difference between the two abdicated states is more than 7 ohms. The resistance changes of sample one are much smaller. It is suspected that this is due to the types of technology masks used. While the kapton tape adheres tightly to the substrate surface and marks the exact boundary of the sample, the 3D printing enclosures used are not certain to maintain sufficient contiguity. The applied method of mounting substrates in the created enclosures gives the possibility of uneven deposition of sputtered materials at the boundaries of the structure. This can result in unforeseen phenomena due to inhomogeneities in layer thickness and possible contacts between ferromagnetic layers. The boundaries of the fabricated structures under the naked eye appeared to have no clear boundary. It is possible that the use of uncertain plastic material in the sputtering chamber during the magnetron sputtering process affects the purity of the resulting films. Concerns arising from the previous use of additional enclosures as a process mask in the magnetron sputtering process result in the abandonment of the intention to use them in this role in future research. 3D enclosures as technological masks are not used because they require more effort and, as the present results indicate, their use does not result in the desired results. The use of kapton tape in this role on a larger scale of production in comparison to the photolithography method used also seems to be ineffective and is not used. This method can be used when making single runs of structures.

The measurement methodology was to observe the magnitude of resistance changes of the structures in a sufficiently strong magnetic field. It is impossible to obtain a complete characterization of the resistance changes as a function of the magnetic field induction in this way. We also do not know the saturation induction field of the structures in question, above which values the resistance changes are not observed.

The method used to fabricate thin-film structures exhibiting giant magnetoresistance appears to be correct. The developed technological sequence allows to obtain a series of samples exhibiting resistance changes in an external magnetic field. On the basis of the obtained results, it can be concluded that at the present stage the application of the kapton tape as a technological mask is satisfactory.

Acknowledgments

This research was co-funded by the Polish Minister of Education and Science from the state budget under the program "Student research clubs create innovation" (SKN/SP/495923/2021) and the funds for the activities of young scientists of the University of Life Sciences in Lublin TKT/MN-1/IMECH/21.

References

[1] Bakonyi I., Péter L.: Electrodeposited multilayer films with giant magnetoresistance (GMR): Progress and problems. Progress in Materials Science 55, 2010, 107–245 [http://doi.org/10.1016/j.pmatsci.2009.07.001].
[2] Baraduc C., Chshiev M., Dieny B.: Spintronic Phenomena: Giant Magnetoresistance, Tunnel Magnetoresistance and Spin Transfer Torque, Smart Sensors. Measurement and Instrumentation 6, 2013, 1–30 [http://doi.org/10.1007/978-3-642-37172-1_1].
[3] Barnaś J.: Spin w elektronice. Materiały XXXVI Zjazdu Fizyków Polskich, Toruń, 2001, 78–84.

[4] Czarnacka K., Kisała J., Kociubiński A., Gęca M.: Technology and measurements of three-layer NiFeCuMo/Ti/NiFeCuMo structures exhibiting the giant magnetoresistance phenomenon. Journal of Vacuum Science & Technology B 40, 2022, 012806 [http://doi.org/10.1116/6.0001488].
[5] Diao Z. et al.: Half-metal CPP GMR sensor for magnetic recording. Journal of Magnetism and Magnetic Materials 356, 2014, 73–81 [http://doi.org/10.1016/j.jmmm.2013.12.050].
[6] Dixit G. et al.: Structural and magnetic behaviour of NiFe2O4 thin film grown by pulsed laser deposition. Indian Journal of Pure & Applied Physics (IJPAP) 48(4), 2010, 287–291.
[7] Fermon C.: Micro- and Nanofabrication Techniques. Spin Electronics, Lecture Notes in Physics 569/2000, 379–395.
[8] Ennen I., Kappe D., Rempel T., Glenske C., Hütten A.: Giant Magnetoresistance: Basic concepts, microstructure, magnetic interactions and applications. Sensors 16, 2016, s16060904 [http://doi.org/10.3390/s16060904].
[9] Inoue J.: GMR, TMR and BMR. Nanomagnetism and Spintronics 2009, 15–92 [http://doi.org/10.1016/B978-0-444-53114-8.00002-9].
[10] Johnson A.: Spin Valve Systems for Angle Sensor Applications. Technische Universität Darmstadt, 2004.
[11] Kisała J.: Wpływ dodatkowego pola magnetycznego podczas napylania magnetronowego na efekt GMR w strukturach cienkowarstwowych. Przegląd Elektrotechniczny 1, 2022, 194–197 [http://doi.org/10.15199/48.2022.01.42].
[12] Kurenkov A. S., Babaytsev G. V., Chechenin, N. G.: An origin of asymmetry of giant magnetoresistance loops in spin valves. Journal of Magnetism and Magnetic Materials 470, 2019, 147–150 [http://doi.org/10.1016/j.jmmm.2017.10.036].
[13] Kuru H., Kockar H., Alper M.: Giant magnetoresistance (GMR) behavior of electrodeposited NiFe/Cu multilayers: Dependence of non-magnetic and magnetic layer thicknesses. Journal of Magnetism and Magnetic Materials 444, 2017, 132–139 [http://doi.org/10.1016/j.jmmm.2017.08.019].
[14] Leitao D. C., Amaral J. P., Cardoso S., Reig C.: Microfabrication Techniques, Smart Sensors. Measurement and Instrumentation 6, 2013, 31–46 [http://doi.org/10.1007/978-3-642-37172-1_2].
[15] Motomura Y., Tatsumi T., Urai H., Aoyama M.: Soft Magnetic Properties and Heat Stability for Fe/NiFe Superlattices. IEEE Transactions on Magnetics, 26(5), 1990, 2327–2331 [http://doi.org/10.1109/20.104714].
[16] Stobiecki T.: Urządzenia elektroniki spinowej. Wydawnictwo AGH, Kraków 2012.
[17] Szewczyk A., Wiśniewski A., Puźniak R., Szymczak H.: Magnetyzm i nadprzewodnictwo. PWN, Warszawa 2012.
[18] Reig C., Cubells-Beltrán, M. D., Muñoz, D. R.: Magnetic field sensors based on Giant Magnetoresistance (GMR) technology: Applications in electrical current sensing. Sensors 9/2009, 7919–7942 [http://doi.org/10.3390/s91007919].
[19] Thomson W.: On the Electro-Dynamic Qualities of Metals:—Effects of Magnetization on the Electric Conductivity of Nickel and of Iron. Proceedings of the Royal Society 8, 1857, 546–550 [http://doi.org/10.1098/rspl.1856.0144].
[20] Tsymbal E. T., Pettifor D. G.: Perspectives of Giant Magnetoresistance. Solid State Physics 56/2001, 113–237 [http://doi.org/10.1016/S0081-1947(01)80019-9].
[21] Waite M. M., Chester W., Glocker D.: Sputtering Sources. Society of Vacuum Coaters 2010, 42–50.
[22] Wu Y. P., Han G. C., Kong L. B.: Microstructure and microwave permeability of FeCo thin films with Co underlayer. Journal of Magnetism and Magnetic Materials 322, 2010, 3223–3226 [http://doi.org/10.1016/j.jmmm.2010.06.032].

M.Sc. Eng. Jakub Kisała
e-mail: j.kisala@pollub.pl

Ph.D. student at the Lublin University of Technology in the discipline automation, electronics and electrical engineering. The current work focuses on magnetoresistance phenomena in thin film structures.

http://orcid.org/0000-0002-4898-3670

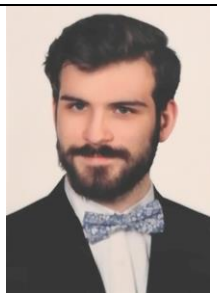

Ph.D. Eng. Andrzej Kociubiński
e-mail: akociub@semiconductor.pl

He received the M.Sc. and Ph.D. degrees in electronic engineering from Warsaw University of Technology, Poland. In 2007 he joined the Lublin University of Technology (Poland), where he was involved in research on semiconductor technology. His research interest is concentrated on semiconductor devices and technology. His recent activities are related to microsystems for biomedical applications.

http://orcid.org/0000-0002-0377-8243

M.Sc. Eng. Karolina Czarnacka
e-mail: karolina.czarnacka@up.lublin.pl

An employee as an assistant in the Department of Fundamentals of Technology at the University of Life Sciences in Lublin. Ph.D. student at the Lublin University of Technology in the discipline of Electrical Engineering.

http://orcid.org/0000-0003-1434-734X

M.Sc. Eng. Mateusz Gęca
e-mail: mati.geca@gmail.com

An employee in the Department of Electronics and Information Technology, Lublin University of Technology. He received the M.Sc. degree in mechatronics from LUT. Research area concerns diagnostics and characterization of semiconductor devices.

http://orcid.org/0000-0002-0519-7389

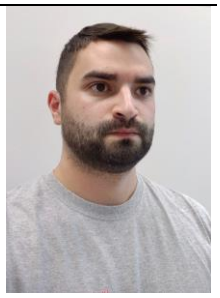

http://doi.org/10.35784/iapgos.2983

received: 30.05.2022 | revised: 22.08.2022 | accepted: 15.09.2022 | available online: 30.09.2022

EXPANSION OF THE AREA OF PRACTICAL APPLICATION OF THE PLC CONTROL SYSTEM WITH PARALLEL ARCHITECTURE

Sergiy Tymchuk[1], Oleksiy Piskarev[1], Oleksandr Miroshnyk[2], Serhii Halko[3], Taras Shchur[4]

[1]State Biotechnological University, Faculty of Energy, Digital and Computer Technologies, Department of Automation and Computer Integrated Technologies, Kharkiv, Ukraine, [2]State Biotechnological University, Faculty of Energy, Digital and Computer Technologies, Department of Electricity Supply and Energy Management, Kharkiv Ukraine, [3]Dmytro Motornyi Tavria State Agrotechnological University, Department of Information Technologies of Design named after V. M. Naidysh, Melitopol, Ukraine, [4]Lviv National Environmental University, Dubliany, Ukraine

***Abstract**. The analysis of architecture is carried out and offers concerning expansion of a area of practical application of PLC of parallel action are offered. The proposed methodology for constructing a logical control automaton of parallel action, the developed models, algorithm and structures represent a theoretical platform for the practical implementation of information technology for parallel logical control of railway automation objects.*

Keywords: programmable logic controllers, parallel architecture, software control system

ROZSZERZENIE OBSZARU PRAKTYCZNEGO ZASTOSOWANIA SYSTEMU STEROWANIA PLC O ARCHITEKTURĘ RÓWNOLEGŁĄ

***Streszczenie**. Przeprowadzono analizę architektury i zaproponowano rozszerzenie obszaru praktycznego zastosowania PLC o działaniu równoległym. Zaproponowano metodologię budowy logicznego automatu sterującego o działaniu równoległym, opracowano modele, algorytm i struktury, które stanowią teoretyczną platformę dla praktycznej implementacji technologii informatycznych do równoległego logicznego sterowania obiektami automatyki kolejowej.*

Słowa kluczowe: programowalne sterowniki logiczne, architektura równoległa, programowy system sterowania

Introduction

One of the effective directions of scientific and technological progress in the automation of objects is the development and application of the latest information technologies using microprocessor programmable logic controllers (PLC) and modern tools [3].

The practical application of these technologies has revealed not only their unconditional advantages in comparison with those used previously, but also significant drawbacks, the main of which is the sequential principle of processing the flow of commands and data, as a result of which both the speed of logical control of objects and the probability of failures become significantly dependent on both the number of monitored sensors and controlled mechanisms, as well as the length of the control program (the number of processor cycles expended), as a result of which microprocessor PLCs, which have sufficiently high reliability indicators, often do not provide the necessary level of information processing reliability when controlling automation objects and therefore for direct control of actuators are used very limitedly [11].

In recent years, for the reliable and efficient implementation of the functions of logical control of automation objects, the active use of information technologies based on the use of programmable logic integrated circuits (FPGA) has begun, in which the capabilities and advantages of regular microelectronic structures are fully implemented and can be effectively used.

The widespread use of programmable logic controllers (PLCs) in industrial production has had a significant impact on reducing costs and improving the quality of products.

Logic controllers have dozens of inputs/outputs for connecting sensors and actuators, but there are models that support more than a hundred inputs/outputs. Controllers implement the simplest typical functions of information processing, blocking, regulation and software and logic control. Many have one or more physical ports for transmitting information to other automation systems.

Some types of PLCs are highly reliable, durable and fast. They provide various options for complete current diagnostics of faults with their localization to a separate board, backup of individual components and the device as a whole [2, 4].

1. Analysis of recent research and publications

Massive practical application of PLCs revealed not only their unconditional advantages over other controls, but also significant shortcomings, the main of which is the consistent principle of information processing, which leads to a certain contradiction between the fantastic speed of modern hardware (clock speed is already tens of GHz) and short length of machine words.

It turns out that the speed of maintenance of controlled inputs of the controller significantly depends on their number. In addition, microprocessor-based PLCs often do not provide the required level of reliability and reliability of data processing due to the large number of sequentially executed commands in the management of critical applications (in nuclear power, rail and metro, aircraft) and therefore for direct control. units and installations in the specified branches are used extremely limited [5, 6, 10].

The aim of the article is increasing the speed and reliability of the implementation of the functions of logical control of automation objects by developing models and information technology for parallel logical control.

2. Basic research materials

In [1, 3] the structure of an asynchronous programmable automaton is described (Fig. 1), which is the basic structure of matrix parallel logic controllers for different functional purposes.

The principles of construction of an asynchronous programmable automaton controlled by the flow of input states and its structure were used in the development of methods of structural construction and actual structural organization of matrix PLCs with parallel architecture (PPLK) as functionally complete control devices [7–9].

A significant number of variants of structural organization of specialized and universal models of PPLK for different purposes have been developed.

The principle of operation of the considered control automaton is as follows. Let at the *i*-th moment of time from the matrix |MC| the row vector of control commands {ci1, ci2, …, cim} is read. This row vector is checked for a match with those programmed in the matrix |ME| prohibited combinations of control commands, and in the presence of such a match, the function ε takes the value of logical "1", which leads to the prohibition of issuing the vector of control commands to the output of the automaton.

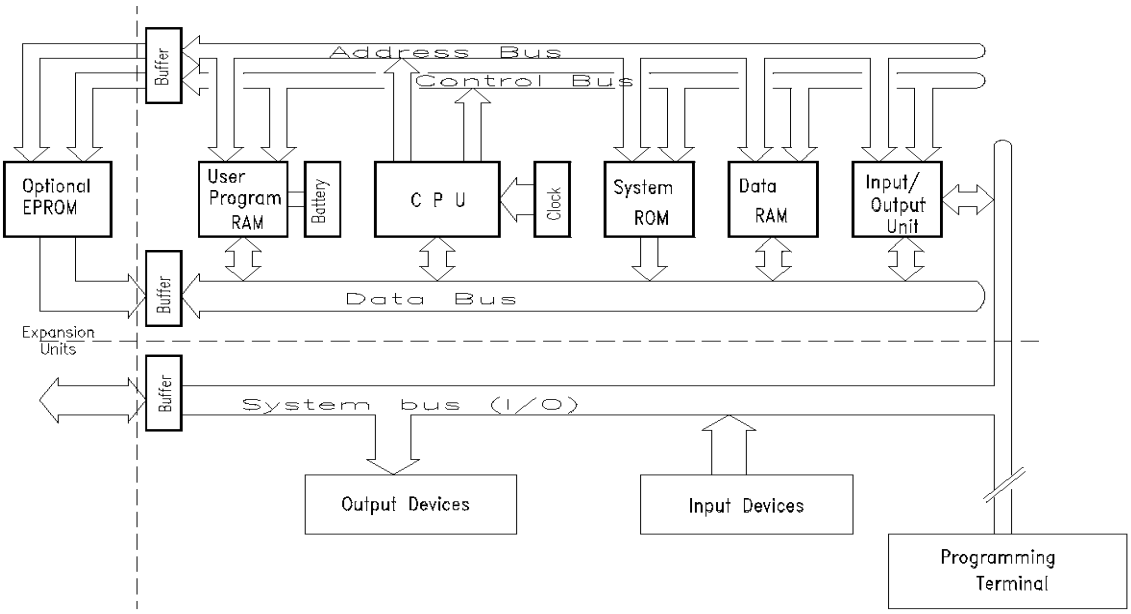

Fig. 1. The structure of the asynchronous programmable machine

If the function ε=0, the vector {ci1, ci2, …, cim} generates commands for controlling the actuators {ci1', ci2', …, cim'}, under the influence of which the state of the controlled object changes, resulting in the inputs of the automaton the vector {ai1, ai2, … , aik} is formed, which in parallel for all components k is compared for logical equivalence with the vector programmed on the given line of the program by the row of the matrix |MA| = {Ai1, Ai2, … , Aik}, i.e. In this case, the logical operation "AND" or the logical operation "OR" is performed according to the value of the attribute Fp.

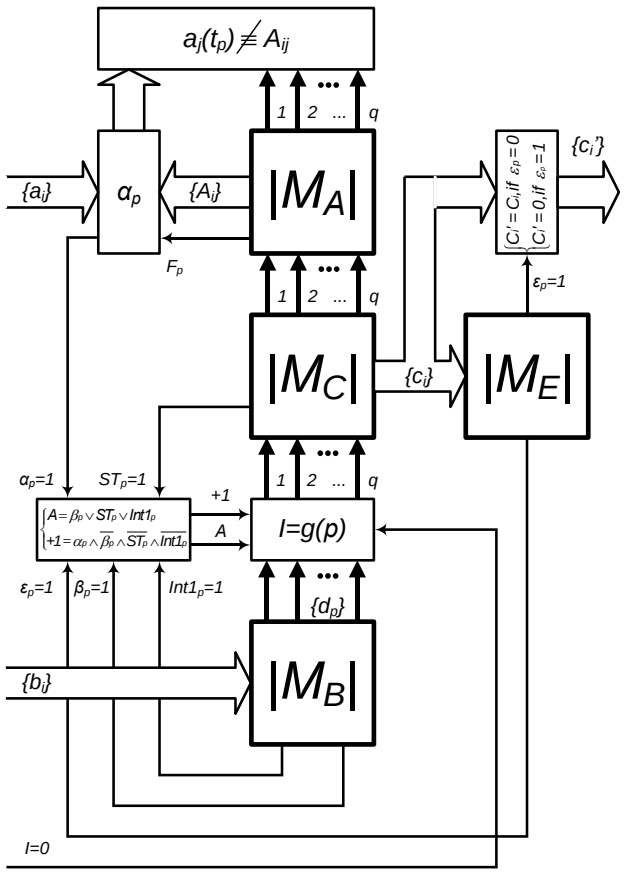

Fig. 2. The structure of the logical control automaton parallel action

Similarly, a comparison is made for equivalence of the vector of actual states of the external environment (vector of conditions) {bi1, bi2, … , biu} with the programmed values of the matrix vectors |MB| = {Bx1, Bx2, … , Bxu}, where the index x ranges from 1 to n, (i.e. the entire matrix |MB| is analyzed simultaneously), thus, the logical function βp.

The block that performs the functions of logical control is described by the following system of equations, which is a generalization of equations

$$\begin{cases} A = \beta_p \vee ST_p \vee Int1_p \\ +1 = \alpha_p \wedge \overline{\beta_p} \wedge \overline{ST_p} \wedge \overline{Int1_p} \end{cases} \quad (1)$$

Depending on the truth of the logical functions αp and βp, as well as the values of the signs STp and Int1p, the step function of the algorithm I = g(p) takes the value "+1", which means the transition to the next step of processing the current subroutine, or the value "A", which means a conditional jump to the first line of the subroutine whose address is written in the matrix |MB|.

The described automaton can be considered as a kind of universal control device, since it can be used to implement sequential, situational control algorithms (in which the entire cyclogram consists of elementary (in one line) subcycles, the sequence of processing of which is determined only by the situation that has developed in the external environment in *i*-th moment of time) and situationally sequential as well (in which the start of processing the *f*-th subcycle is determined by the situation prevailing in the environment and at the control object at the *i*-th moment of time, and the elements of the subcycle are processed sequentially). Depending on the implemented type of algorithm, all or part of the automaton structure elements are used. So, for example, when implementing unbranched sequential algorithms, a truncated version of the structure (without |MB|) can be used.

To improve the quality of diagnosis, it is proposed to equip the PLC with a classical architecture with a FPGA-based operation control device (PCF). The electrical block diagram of the software control system using SCS is shown in Fig. 3. This system consists of two logic controllers (PLC) - working and diagnosing. The first is needed to process the input signals, solve logical equations specified by the program, and submit signals to the controlled object. The second must respond to combinations of input (or output) signals that are prohibited or may result in process equipment accidents or accidents. FPGA – parallel action controller can be used as a diagnostic device.

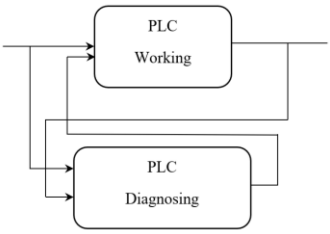

Fig. 3. Electrical block diagram of the software control system using SCS

In Fig. 4 shows a block diagram of the algorithm of the SCS PLC. First, the "Automatic" mode is started, the presence of the "Automatic" mode is checked. If it is enabled – the program proceeds to compare the combinations of input and output signals of the main PLC with the wrong and dangerous combinations. When either incoming or outgoing signals match with false ones, alarm routines are triggered. After the subroutines are run, the program returns to the beginning and the algorithm is run again.

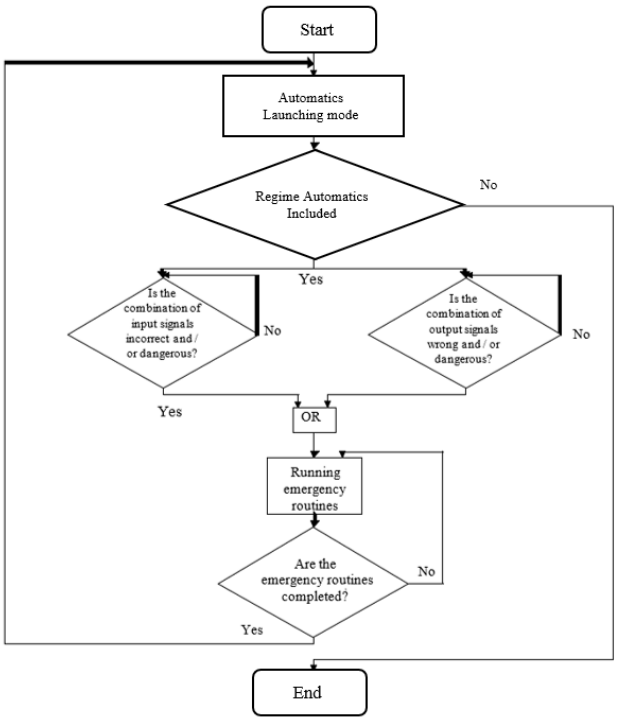

Fig. 4. Block diagram of the algorithm of the SCS PLC

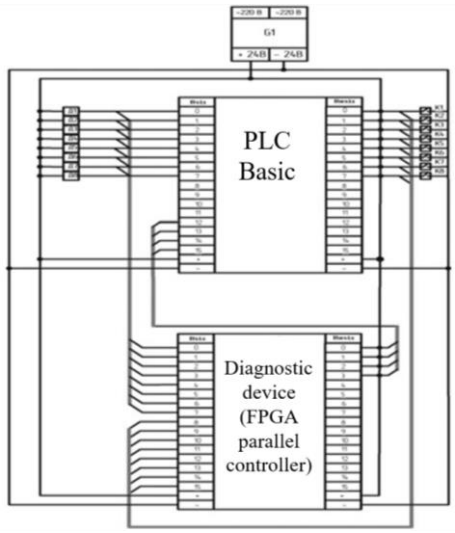

Fig. 5. Schematic electrical diagram of the software control system using SCS

The scheme of the electrical principle of the software control system with the use of SCS PLC is shown in Fig. 5. The software control system consists of a PLC of the main TWIDO TWD LCAA 16 DRF from Schneider Electric, a PLC of the diagnostician (FPGA-parallel controller) and a 220/24 V power supply. and inputs 12–15 – signals from outputs 0–3 of the diagnostic PLC. Signals from sensors D1-D8 are fed to inputs 0–7 of the diagnosing PLC, and signals from outputs 0–7 of the main PLC are fed to inputs 8–15, which are compared with emergency combinations for matches.

3. Conclusions

Knowledge of the general theoretical principles for constructing highly efficient computing and control devices based on homogeneous microelectronic structures, the emergence of modern FPGAs and their adaptability to programming using languages oriented to parallel logical data processing creates objective prerequisites for developing a fundamentally new approach to the structural organization of logical control automata. expressed parallel action and creation on this basis of information technology for parallel logical control of automation objects.

A combined solution using FPGA-based operation control device is proposed, which allows to expand the area of practical application of PLCs with parallel architecture. The proposed methodology for constructing a logical control automaton of parallel action, the developed models, algorithm and structures represent a theoretical platform for the practical implementation of information technology for parallel logical control of railway automation objects.

The prospect of further research is the development of a language, automated technology and tools for programming algorithms for parallel logical control of automation objects.

References

[1] Badretdinov I. et al.: Mathematical modeling and study of the grain cleaning machine sieve frame operation. INMATEH-Agric. Eng. 60, 2020, 19–28.

[2] Bazaluk O. et al.: Energy Saving in Electromechanical Grain Cleaning Systems. Appl. Sci. 12, 2022, 1418.

[3] Furman I. O., Piskarev O. M., Staroverov R. M.: Analysis of promising technologies for automation of grain cleaning and sorting processes. Bulletin of the Kharkiv National Technical University of Agriculture. Problems of energy supply and energy saving in the agro-industrial complex of Ukraine 37(2), 2005, 143–146.

[4] Furman I. O., Radchenko S. S.: Principles of construction and industrial implementation of ASKTP of elevator complexes of grain storage. Visnyk of Kharkiv National Technical University of Agriculture. named Petro Vasylenko. Problems of energy supply and energy saving in the agro-industrial complex of Ukraine 165, 2015, 79–80.

[5] Giyevskiy A. M. et al.: Substantiation of basic scheme of grain cleaning machine for preparation of agricultural crops seeds. IOP Conf. Ser. Mater. Sci. Eng. 327, 2018, 042035.

[6] Halko S., Suprun O., Miroshnyk O.: Influence of temperature on energy performance indicators of hybrid solar panels using cylindrical cogeneration photovoltaic modules. IEEE 2nd KhPI Week on Advanced Technology, KhPIWeek2021, 2021, 132–136.

[7] Havrylenko Y. et al.: Representation of a monotone curve by a contour with regular change in curvature. Entropy 23, 2021, 923.

[8] Mudarisov S. G., Badretdinov I. D.: Numerical implementation of a mathematical model of the technological process of the diametric fan in a rotating coordinate system. News Int. Acad. Agr. Educ. 17, 2013, 79–83.

[9] Mudarisov S. G., Badretdinov I. D.: Substantiation of the parameters of the diametrical fan based on a mathematical model of the process of its operation. International Scientific-Practical Conference in the Framework of the XXIII International Specialized Exhibition AgroComplex-2013, 2013, 363–367.

[10] Piskarev O. M., Staroverov R. M.: Application of microprocessor control system in non-traditional scheme of grain cleaning and sorting. Bulletin of the Kharkiv National Technical University of Agriculture. Problems of energy supply and energy saving in the agro-industrial complex of Ukraine 27(2), 2004, 163–166.

[11] Tabor S. et al.:. Mathematical simulation of separating work tool technological process. E3S Web Conf. 132, 2015, 01025.

D.Sc. Sergiy Tymchuk
e-mail: stym@i.ua

Sergiy Tymchuk received the Doctor of Technical Sciences degree from the National Technical University "Kharkiv Politechnic Institute", Kharkiv, Ukraine, all in electrical power engineering. He is the author of three books, more than 200 articles, and more than 10 inventions. His research interests include the Smart Grid, renewable energy, quality of electrical energy, losses of electrical energy, overhead power lines monitoring, power system automation.

http://orcid.org/0000-0002-8600-4234

Ph.D. Oleksiy Piskarev
e-mail: post@3g.ua

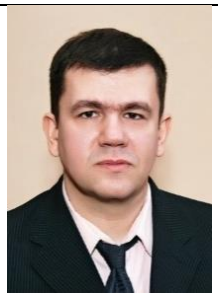

Piskarev, Oleksiy received the M.Sc. degree from the National Technical University "Kharkiv Politechnic Institute", Kharkiv, Ukraine, and the Candidate of Technical Sciences degree from the National Technical University "Kharkiv Politechnic Institute", Kharkiv, Ukraine, all in electrical power engineering. He is the author of three books, more than 50 articles, and more than 5 inventions. His research interests include the Smart Grid, renewable energy, quality of electrical energy, losses of electrical energy, overhead power lines monitoring, power system automation.

http://orcid.org/0000-0002-6980-984X

D.Sc. Oleksandr Miroshnyk
e-mail: omiroshnyk@ukr.net

Oleksandr Miroshnyk received the M.Sc. degree from the Kharkiv State Technical University of Agriculture, Kharkiv, Ukraine, in 2004, and the Doctor of Technical Sciences degree from the National Technical University "Kharkiv Politechnic Institute", Kharkiv, Ukraine, in 2016, all in electrical power engineering. He is the author of three books, more than 200 articles, and more than 30 inventions. His research interests include the Smart Grid, renewable energy, quality of electrical energy, losses of electrical energy, overhead power lines monitoring, power system automation.

http://orcid.org/0000-0002-6144-7573

Ph.D. Serhii Halko
e-mail: galkosv@gmail.com

Serhii Halko graduated from Melitopol Institute of Mechanical Engineers of Agriculture, Ukraine, in 1994, and was qualified as an Electrical Engineer. He received his Ph.D. in Electric Engineering (power stations, systems and networks) from the Donetsk National Technical University, Ukraine, in 2003. Presently, he is an Assistant Professor of Dmytro Motornyi Tavria State Agrotechnological University and Educational Scientific Institute of General University Training, Melitopol, Ukraine. He is the author of more than 100 scientific publications, 10 inventions, and two monographs. His research interests are related to research in the field of renewable and alternative energy.

http://orcid.org/0000-0001-7991-0311

Ph.D. Taras Shchur
e-mail: shchurtg@gmail.com

Taras Shchur received the M.Sc. degree from the Kharkiv State Technical University of Agriculture, Kharkiv, Ukraine, in 2004, candidate of technical sciences Kharkiv Petro Vasylenko National Technical University of Agriculture in 2010.
He is the author of one book, more than 60 articles. His research losses of electrical energy, overhead power lines monitoring, power system automation.

http://orcid.org/0000-0003-0205-032X

http://doi.org/10.35784/iapgos.3035

received: 19.07.2022 | revised: 31.08.2022 | accepted: 15.09.2022 | available online: 30.09.2022

FEATURES OF THE ANGULAR SPEED DYNAMIC MEASUREMENTS WITH THE USE OF AN ENCODER

Vasyl V. Kukharchuk[1], Waldemar Wójcik[2], Sergii V. Pavlov[1], Samoil Sh. Katsyv[1], Volodymyr S. Holodiuk[1], Oleksandr Reyda[1], Ainur Kozbakova[3], Gaukhar Borankulova[4]

[1]Vinnytsia National Technical University, Vinnytsia, Ukraine, [2]Lublin University of Technology, Lublin, Poland, [3]Almaty Technological University, Institute of Information and Computational Technologies MES CS RK, Almaty, Kazakhstan, [4]Taraz Regional University M. Kh. Dulaty, Taraz, Kazakhstan

Abstract. *Based on the most significant features of the angular velocity dynamic measurements selected by the authors, the main phases of measuring information transformation were established, which allowed to obtain new mathematical models in the form of transformation function, equations for estimating quantization errors, analytical dependences for measuring range that are initial for modeling physical processes occurring in such digital measuring channels with microprocessor control. The process of converting an analog quantity into a binary code is analytically described, an equation for estimating the absolute and relative quantization error is obtained and a measurement range is established, which provides a normalized value of relative quantization error for angular velocity measuring channels with encoder. For the first time, the equation of sampling error was obtained, and it was proved that the limiting factor of the angular velocity measurements upper limit is not only the normalized value of quantization error, as previously thought, but also the value of sampling frequency f_D. Therefore, to expand the measurement range (by increasing the upper limit of measurement), it is proposed not only to increase the speed of analog-to-digital conversion hardware, but also to reduce the execution time of software drivers for transmitting measurement information to RAM of microprocessor system. For this purpose, the analytical dependences of estimating the upper limit of measurement based on the value of the sampling step for different modes of measurement information transmission are obtained. The practical implementation of the software mode measurement information transmission is characterized by a minimum of hardware costs and maximum execution time of the software driver, which explains its low speed, and therefore provides a minimum value of the upper limit measurement. In the interrupt mode, the upper limit value of the angular velocity measurement is higher than in the program mode due to the reduction of the software driver's execution time (t_{Fl} = 0). The maximum value of the angular velocity measurements upper limit can be achieved using the measurement information transmission in the mode of direct access to memory (DMA) by providing maximum speed in this mode (t_{Fl} = 0, t_{DR} = 0). In addition, the application of the results obtained in the work allows at the design stage (during physical and mathematical modeling) to assess the basic metrological characteristics of the measuring channel, aimed at reducing the development time and debugging of hardware, software, and standardization of their metrological characteristics.*

Keywords: angular velocity, encoder, quantization, sampling, angular velocity measuring channel, transformation function

CECHY POMIARÓW DYNAMICZNYCH PRĘDKOŚCI KĄTOWEJ Z WYKORZYSTANIEM ENKODERA

Streszczenie. *Na podstawie najistotniejszych cech dynamicznych pomiarów prędkości kątowej ustalono główne fazy transformacji informacji pomiarowej, co pozwoliło na uzyskanie nowych modeli matematycznych w postaci funkcji transformacji, równań do szacowania błędów kwantyzacji, analitycznych zależności dla zakresu pomiarów, które są podstawą do modelowania procesów fizycznych zachodzących w takich cyfrowych kanałach pomiarowych ze sterowaniem mikroprocesorowym. analitycznie opisano proces konwersji wartości analogowej na kod binarny Po raz pierwszy otrzymano równanie błędu próbkowania i udowodniono, że czynnikiem ograniczającym górną granicę pomiarów prędkości kątowej jest nie tylko znormalizowana wartość błędu kwantyzacji, jak sądzono wcześniej, ale także wartość częstotliwości próbkowania f_D. Dlatego w celu rozszerzenia zakresu pomiarowego (poprzez zwiększenie górnej granicy pomiaru) proponuje się nie tylko zwiększenie szybkości działania sprzętu do konwersji analogowo-cyfrowej, ale również skrócenie czasu wykonania sterowników programowych do transmisji informacji pomiarowej do pamięci RAM systemu mikroprocesorowego. w tym celu uzyskano analityczne zależności górnej granicy pomiaru od wartości kroku próbkowania dla różnych trybów transmisji informacji pomiarowej. W trybie przerwania górna wartość graniczna pomiaru prędkości kątowej jest wyższa niż w trybie programu ze względu na skrócenie czasu wykonania sterownika programowego (t_{Fl} = 0). Maksymalną wartość górnej granicy pomiaru prędkości kątowej można uzyskać przesyłając informacje pomiarowe w trybie bezpośredniego dostępu do pamięci (DMA) zapewniając maksymalną prędkość w tym trybie (t_{Fl} = 0, t_{DR} = 0). Ponadto zastosowanie uzyskanych w pracy wyników pozwala na etapie projektowania (podczas modelowania fizycznego i matematycznego) na ocenę głównych cech metrologicznych kanału pomiarowego, co ma na celu skrócenie czasu rozwoju i debugowania sprzętu, oprogramowania oraz standaryzacji ich cech metrologicznych.*

Słowa kluczowe: prędkość kątowa, enkoder, kwantyzacja, próbkowanie, kanał pomiaru prędkości kątowej, funkcja konwersji

Introduction

During the rotation of a rigid body [1, 6] around its axis, the angle of rotation φ is a function of time

$$\varphi = f(t).$$

This equation is also called the equation of rotation, which is the basis for the experimental study of such parameters of rotational motion as angular velocity $\omega(t) = \frac{d\varphi}{dt}$, angular acceleration $\xi(t) = \frac{d\omega}{dt} = \frac{d^2\varphi}{dt^2}$ and dynamic moment $\mathrm{M}_D = J\frac{d\omega}{dt} = J\frac{d^2\varphi}{dt^2}$.

The vast majority of the rotational motion of mechanisms is described by the terms "angular velocity" or "frequency of rotation", the essence of which is different. We give the definition of these parameters of angular displacements corresponding to the international system of units of measurement [3].

Angular velocity is a physical quantity that is described by the first derivative of the angle of rotation φ for the time t, rad/s:

$$\omega(t) = \frac{d\varphi}{dt}.$$

Rotation frequency n is a physical quantity determined by the ratio of the number of revolutions N_O per rotation time, rpm:

$$n = \frac{N_o}{t}.$$

It is easy to see that the term "rotation speed n" used corresponds exactly to the physical quantity "rotation frequency". The basic equations for measuring rotation speed and rotation frequency are also the same.

The above also indicates that the speed, as well as the speed, are not synonymous with angular velocity. In physical terms, these are different physical quantities that are not proportional to each other. Equality

$$\omega = 2\pi n$$

valid only for uniform rotation.

Based on this, we note the first feature – the angular velocity is related to dynamic measurements, because at each time its instantaneous value is known, and the rotation frequency (rotation speed) to static, because the measurement result in this case characterizes the average speed per full revolution.

Angular velocity refers to non-electric quantities, which are measured by converting a non-electric quantity into an electric one using a primary measuring transducer (sensor). The presence of this measuring transformation determines the second feature of the measurement of angular velocity ω.

Encoders are now preferred for dynamic angular displacement transducers in dynamic angular velocity measurements. They perform the conversion of angular displacement into a sequence of electrical signals, the frequency of which contains information about the value and direction of the informative parameter.

Such transducers are used to measure angular velocity, speed and other physical quantities functionally related to it. The transformation equation for rotational motion sensors, which are based on the construction of angular displacement transducers – encoders, are shown in table 1.

Table 1. Transformation equation of angular displacement sensors

Measured physical quantity	Measurement units	Transformation equation
Rotation angle	deg	$\varphi_x = i\frac{360}{z}$, φ_x – rotation angle, i – current number of output pulses ($i \in 0\ldots z$), z – number of pulses per full revolution ($z \in 10^3\ldots10^6$)
	rad	$\varphi_x = i\frac{2\pi}{z}$
Rotation frequency	rpm	$f_x = \frac{n_x Z}{60}$, n_x – rotation speed, f_x – frequency of output rectangular pulses
Angular speed	rad/s	$f_x = \frac{\omega_x Z}{2\pi}$, ω_x – angular speed

The advantages of such sensors are: wide measuring range (from 10^3 to 10^6 rpm), simplicity of design, low load on the object of measurement due to the low moment of inertia of the moving part of the sensor, high noise immunity, almost unlimited service life. For dynamic measurements, their high resolution is extremely important, which is determined by the Z – the number of pulses per full revolution ($Z \in 10^3\ldots10^6$).

Based on the above, it becomes obvious the usage of digital tachometers by the vast majority of developers, which generalized block diagram for dynamic measurements of angular velocity, is shown in Fig. 1.

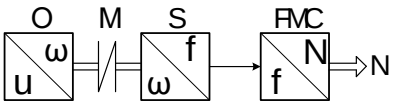

Fig. 1. Generalized block diagram of dynamic measurements ω_x: O – measuring object, u – supply voltage, ω – rotation frequency, angular speed, S – sensor, encoder, f – output pulse frequency, FMC – frequency measuring channel, N – the number of pulses at the output of the measuring channel

The third feature of dynamic measurements of angular velocity is the implementation of the measuring channel of the frequency of instantaneous values, which is based on the indirect method of frequency conversion f_x in parallel binary code N. In such measuring channels, the quantization of the period T_X, which is formed at the direct output of the counting trigger T, is carried out by the periods T_0 of the sample frequency f_0. As a result of such comparison of the measured T_X and sample T_0 of physical sizes receive numerical values of N angular velocity through the period – in even or not even periods. At dynamic measurements of angular velocity, it is necessary to have its numerical values in each period of frequency f_x at the output of the encoder, which in the literature is called frequency measurement in the "adjacent intervals". This is especially true for compatible measurements, the results of which are functional dependencies$\omega_x(t), \xi_x(t), M_D(t), M_D(\omega)$.

Such block diagrams are known and widely used by developers of information and measurement technologies [10]. Mathematical models that adequately describe the various transformation phases of information in angular velocity measurement channels remain unexplored here. The lack of such theoretical results is a scientific and applied problem, the solution of which will allow at the stage of development and design of hardware and software to model such basic metrological characteristics of the measuring channel as the transformation function, quantization and sampling errors, measurement range, aggregates will provide new knowledge in the field of metrological support of angular velocity dynamic measurements.

The aim of the work is to obtain mathematical models, which are a transformation function of the angular velocity measuring channel, the quantization equation and sampling errors, analytical dependences for estimating the measurement range in the form of lower and upper limits of measurement and speed [7].

1. Measuring channel of instantaneous angular velocity

The characteristic features of the structural diagram of the angular velocity measuring channel (Fig. 2) include the following:

1. Quantization of periods T_x by periods T_0 of exemplary frequency f_0 carried out in the logic circuit "AND" from the direct T or inverse $\overline{T}$ outputs of the counting trigger T, which is also called the period selection device [6].
2. The presence of a binary counter CT2, which counts the number of N sample periods T_0, which quantize the periods T_x or $\overline{T_x}$, formed, respectively, on the direct or inverse outputs of the counting trigger T;
3. The presence of a programmable interface for transmitting binary codes of the number of pulses N from the outputs of the binary counter CT2 in the ACC accumulator of the microprocessor system MPS, the main components of which are the CPU microprocessor, RAM and ROM constant memory.

The beginning of the measurement is the signal 1/0 – start/stop to the measurement object from the CPU microprocessor of the MPS microprocessor system through the parallel programmable PPI interface. The sensor shaft connected by a coupling to the shaft of the measuring object begins to rotate. The encoder (sensor) converts the angular velocity into a sequence of electrical signals, the frequency of which is determined [8, 9]

$$f_x = \frac{\omega Z}{2\pi} \tag{1}$$

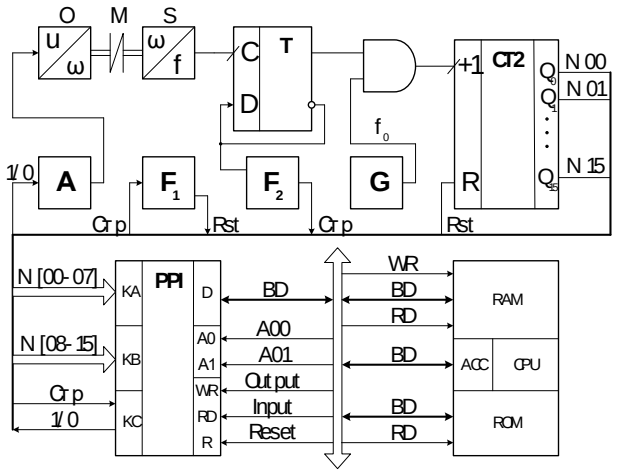

Fig. 2. Block diagram of the measuring channel of the angular velocity: T – trigger (period selection device); F_1, F_2 – shapers; A – measuring object adapter; G – sample generator f_0; CT2 – binary counter; PPI – parallel programmable interface; microprocessor system MPS, consisting of a CPU microprocessor and its dedicated ACC accumulator, RAM and non-volatile ROM. T_X – direct trigger output T; Res– zero setting of the binary counter triggers CT2; Cmp – signals for recording 2 bytes of information from the outputs N00, N01…N15 of binary counter CT2 in the buffer ports of the channels KA i KB interface PPI; BD – data bus; A00, A01 – lest significant bits of the address bus; Out – signal for writing information to the PPI; Input – a signal to read information from the PPI; Reset – zero signal of all interface ports PPI; WR – information recording signal в RAM; RD – information reading signal from RAM (ROM); 1/0 – start/stop of the measuring object

Rectangular output signals of the encoder with frequency f_x arrive at the C–input of the counting trigger T, at the direct output of which the period T_x of the encoders output frequency f_x is formed (Fig. 3).

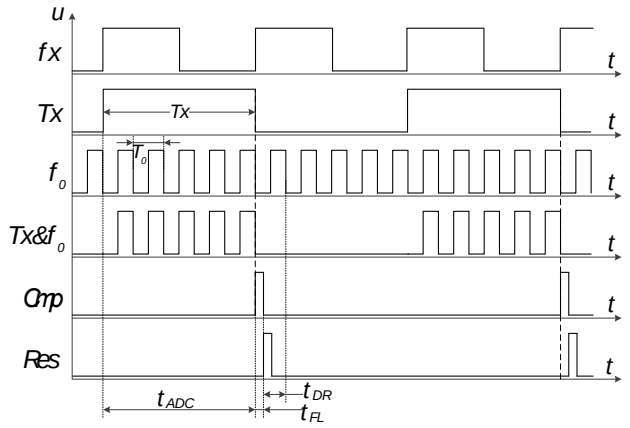

Fig. 3. Timing diagrams of the measuring channel

In the scheme of logical "AND" quantization takes place by comparing the measured physical quantity T_x with the sample T_0. As a result of such comparison the equations of transformation of the measuring channel of frequency of the instantaneous values giving the following function of transformation receive [2, 11]

$$N = \frac{T_x}{T_0} = T_x \cdot f_0 = \frac{f_x}{f_0} \tag{2}$$

To obtain the conversion function of the angular velocity measuring channel in instantaneous values, we substitute in the equation (2) the value of f_x from the equation (1), which uniquely connects the input value of the angular velocity ω with the output value of the rectangular pulse frequency

$$N = \frac{2\pi \cdot f_0}{\omega z} \tag{3}$$

The number of pulses N passing through the open "AND" gate is counted by the binary counter CT2. The obtained equation (3) shows that the static characteristic of such a measuring channel is nonlinear (Fig. 4).

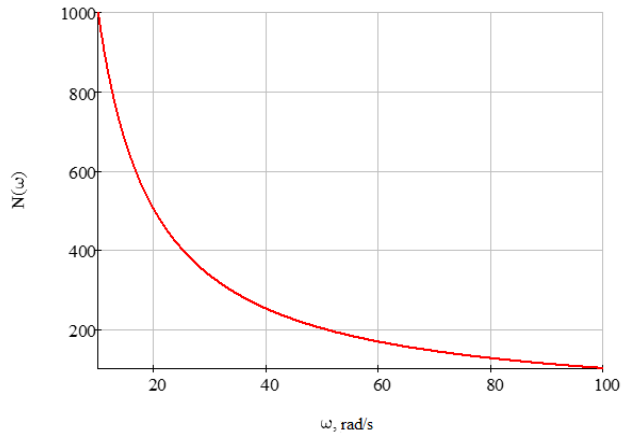

Fig. 4. Static characteristic: z = 628; f_0= 10^6 Hz; $\omega \in 10 \cdots 100$ rad/s

The process of counting the periods T_0, coming to the input of the binary counter CT2, continues until the end of the period T_X. At the moment when the level of logic "1" quickly turns into the level of logic "0" (decline of the T_X) shaper F_1 at its output forms a short rectangular pulse Cтр, according to which the number of pulses N given in binary code N00…N15 from the outputs of the binary counter CT2 are written to the buffer ports of the parallel interface PPI. At the same time the signal Cтр sets to a single state the flag of readiness (Flag) which signals the accumulator ACC of the microprocessor CPU on completion of measurements and start of transmission of measurement information temporarily stored in the buffer ports KA and KB of the PPI. Upon completion of the signal Cтр (on its trailing edge) the shaper F_2 at its output generates a short pulse Res, which on the R–inputs resets all the triggers of the binary counter CT2, and thus "prepares" it for the next cycle of measurements [1, 4, 5].

The process of transmitting the measurements information N00… N15 from the parallel interface to the microprocessor accumulator is controlled by an assembly program, the algorithm of which is as follows:

1. Begin.
2. Initialization of software of the measuring channel, as a result of which it is established:
   - The initial ADR address of the RAM buffer, in which the results of direct measurements of the T_X period will be recorded;
   - Organization of a software meter, which sets the number [i] of frequency measurements
3. Initialization of measuring channel's hardware:

3.1. Software setting of PPI operation mode channels:
   - channel KA[00-07] is programmed to mode "1" – synchronous input of the least byte of information from digital N [00-07] outputs of binary counter CT2 compatible with gating discharge channel KC04;
   - channel KB[08-15] is programmed to the mode "0" – a simple input of the high byte of information from the digital N [08-15] outputs of binary counter CT2;
   - KC [04] – the gate of the KA channel, which uses the signal Cтр from the output of the shaper F1;
   - bit KC [00] to mode "0" – asynchronous output of the control signal of the measurement object;
   - KS [00] – software signal generation (1/0) for adapter A of the measurement object.
4. The next step is a software survey of the presence of a flag in the KC [04] bit. If KC [04] = "0", then the polling of the flag continues (conditional transition) until (looping) until the process of measuring the frequency in this period is completed KC [04] = "1". The subroutine of waiting for the flag presence will be called Flag, and the time of its execution will be marked t_{FL}.
5. After the appearance of the flag in the bit KC [04] = "1" first step is the reading of the low-order byte N [00… 07] from the buffer register (port) of the programmable PPI interface to the ACC accumulator of the MPS microprocessor system and then store it in RAM, and then leading byte N [08… 15].
6. Increases (increments) by one $ADR := ADR + 1$ RAM buffer address to store the next bytes of measured information.
7. Decreases (decrements) by one $i := i - 1$ the value of the measurement counter.
8. The contents of the measurement counter are checked to zero $i = 0$ If $i = 0$, then the measurement process ends. The conditional transition to the p.10 and to the operator "End" is carried out.
9. If $i \neq 0$, the driver program makes a conditional transition to the p.4 of this algorithm. The subroutine for the transfer of information from the parallel interface to the accumulator is called the Driver, and the time of its execution is denoted t_{DR}.
10. From equation (3) indirectly determine the array of numerical instantaneous values of the measured angular velocity

$$\omega = \frac{2\pi \cdot f_0}{Nz} \tag{4}$$

11. End.

This mode of information exchange between the external device (CT2) and the ACC accumulator of the microprocessor system is called – software mode.

2. Metrological characteristics of the measuring channel

As a result of replacing the analog value ω, which has an infinite number of values, with a continuous quantized value with a limited number of values in the form of a binary code N [00… 15], there is an absolute quantization error [11]

$$\Delta_K = \frac{1}{2}h = \frac{1}{2}T_0 \quad (5)$$

A more universal characteristic of accuracy is the relative quantization error

$$\delta_K = \frac{1}{N}100\% \quad (6)$$

Substituting the value of N in (6) from (3), we obtain the equation for estimating the relative quantization error

$$\delta_K = \frac{\omega \cdot z \cdot 100\%}{2\pi f_0} \quad (7)$$

Graphical representation of the relative quantization error dependence in the changing range of the measured value is shown in Fig. 5.

Analysis of the quantization error equation (7) and the results of its modeling, shown in Fig.5, show that the resolution z of the encoder and the value of the sample frequency f_0 are ways to reduce it.

Since the dependence of the relative quantization error on the change of the measured angular velocity is linear, it can be concluded that the normalized value δ_{KH} quantization error [7, 10] restricts the upper limit of measurement

$$\delta_{KH} = \frac{\omega_{max} \cdot z \cdot 100\%}{2\pi f_0} \quad (8)$$

From (8) we obtain the dependence for estimating the upper limit of the angular velocity measurement

$$\omega_{max} = \frac{2\pi f_0 \delta_{KH}}{z \cdot 100\%} \quad (9)$$

The dependence of the upper ω_{max} measurement limit on the normalized value of the relative error δ_{KH} is shown in Fig. 6.

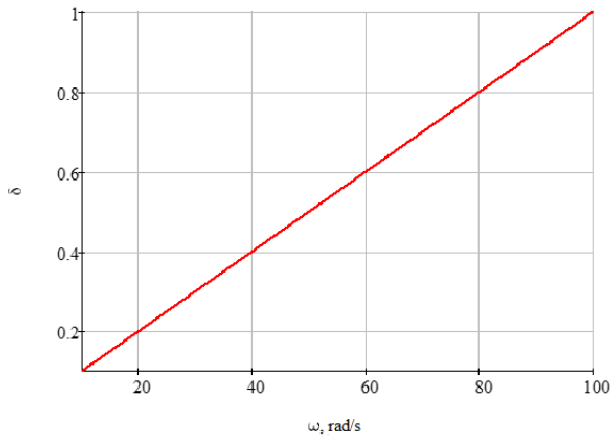

Fig. 5. Relative quantization error: z = 628; f_0= 10^6 Hz; ω ∈ 10 ··· 100 rad/s

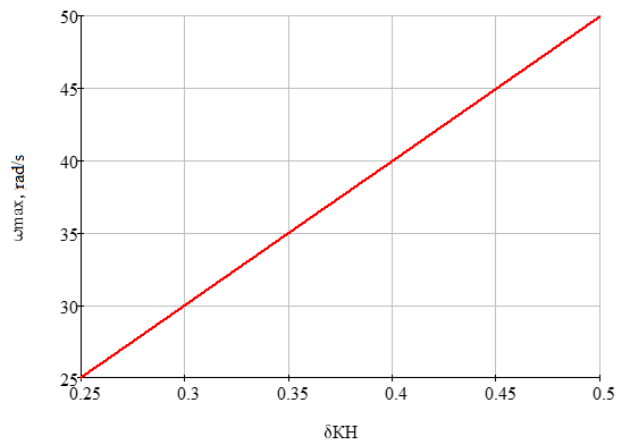

Fig. 6. Dependence of the upper ω_{max} measurement limit on the normalized value of the relative error δ_{KH}

The lower limit of angular velocity measurement is limited [7, 10] by the maximum capacity of the binary counter CT2

$$N_{max} = 2^n \quad (10)$$

where n is the bit rate of the binary counter CT2.

Taking into account (10), rewrite the transformation equation (3) and present it as follows:

$$N_{max} = 2^n = \frac{2\pi \cdot f_0}{\omega_{min} \cdot z} \quad (11)$$

From (11) we obtain the dependence for estimating the lower limit of the digital tachometer of instantaneous values

$$\omega_{min} = \frac{2\pi \cdot f_0}{2^n \cdot z} \quad (12)$$

The dependence of the lower limit of measurement ω_{min} on the bit rate n of the binary counter CT2 is shown in Fig. 7.

Therefore, in the range of change of angular velocity from the lower ω_{min} to the upper limit ω_{max} it is converted into binary code with a relative quantization error not exceeding the normalized value δ_{KH}.

As a result of such replacement of the analog value ω having an infinite number of values in the set range (from ω_{min} to ω_{max}), a limited number of its instantaneous values in the specified time intervals T_D there is a sampling error [10]

$$\Delta_D = \frac{1}{2}T_D \cdot \frac{d\omega}{dt} \quad (13)$$

In (13) T_D the sampling step, which for the measuring channel (Fig. 2) according to the time diagrams (Fig. 4) is defined as:

$$T_D = t_{ADC} + t_{FL} + t_{DR} \quad (14)$$

t_{ADC} – the duration of the analog-to-digital conversion, which is equal to the measured period

$$t_{ADC} = T_X \quad (15)$$

t_{FL} – time spent executing the Flag waiting subroutine,
t_{DR} – time to run the Driver software subroutine.

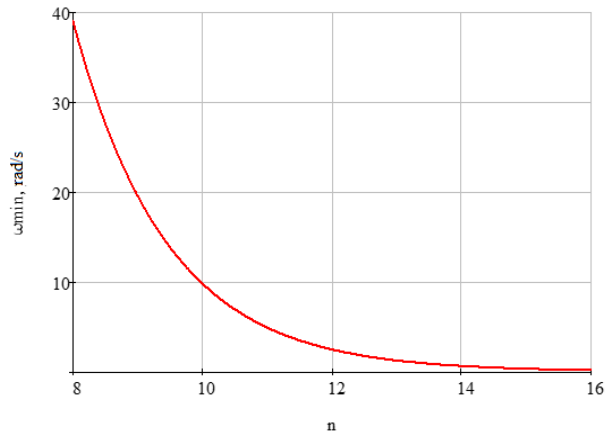

Fig. 7. Dependence of the lower limit of measurement ω_{min} on the bit rate n of the binary counter CT2

Determining the time [7, 10] of sampling the sum of time components for analog-to-digital conversion by hardware of the measuring channel circuit and time for execution of software drivers by software instruments of transmitting measuring information to the microprocessor system accumulator and its RAM is another feature of dynamic angular velocity measurement.

The maximum time required to execute the commands of the assembly subroutines Flag and Driver is estimated [11] by their initial listings.

$$t_{FL} = T_T \sum_{i=1}^{n} P_i \quad (16)$$

$$t_{DR} = T_T \sum_{j=1}^{m} P_j \quad (17)$$

where T_T – the period of the clock frequency f_T of the microprocessor CPU;
i – the number of commands in the Assembly subroutine Flag;
j – the number of commands in the Assembly subroutine Driver;
P_i, P_j – number of cycles in one command.

Taking into account (14) the sampling frequency of the angular velocity measuring channel is defined as:

$$f_D = \frac{1}{T_D} = \frac{1}{T_X + t_{FL} + t_{DR}} \tag{18}$$

We present the transformation equation of the encoder (1) as follows:

$$f_D = \frac{\omega_{max} \cdot z}{2\pi} \tag{19}$$

and we get the inequality

$$\omega_{max} \leq \frac{f_D \cdot 2\pi}{z} \tag{20}$$

which shows that the limiting factor of the upper limit of the angular velocity measurement is not only the normalized value of the quantization error δ_{KH} but also the value of the sampling rate f_D.

Rewrite (20) in a form convenient for further analysis of the upper limit of measurement [6, 11]

$$\omega_{max} \leq \frac{2\pi}{z \cdot (T_X + t_{FL} + t_{DR})} \tag{21}$$

Different modes are used for the I/O process: software, interrupt and capture (direct memory access).

The structural scheme (Fig. 2), time diagrams (Fig. 4) and the algorithm of the angular velocity measuring channel considered above belong to the program mode of operation, which is carried out under the control of the assembler subroutines Flag and Driver. The practical implementation of this mode of transmission is characterized by a minimum of hardware costs, which explains its low speed. This statement is well explained by the analysis (21) of the expression in parentheses in the denominator. Here are all the components that explain the maximum value of the sampling step

$$T_D = t_{ADC} + t_{Fl} + t_{DR} \Rightarrow max$$

and as a consequence, the lowest data transfer rate, which limits the upper limit of angular velocity measurement ω_{max}.

Unlike software, the interrupt mode is initiated by an external device (in our case, CT2). If you use the signal Cтр as an "Interrupt Request", the microprocessor system MPS under the control of Driver software proceeds to transfer N [00..15] data from the digital outputs of the binary counter CT2 to the ACC accumulator of the CPU microprocessor. Therefore, the value of the sampling step is less at time t_{Fl} than in program mode and is determined accordingly

$$T_D = t_{ADC} + t_{DR}$$

Therefore, in the interrupt mode, the value of the upper limit of the angular velocity measurement

$$\omega_{max} \leq \frac{2\pi}{z \cdot (T_X + t_{DR})}$$

higher than in software mode.

In the "capture" mode, the transfer of information from the digital outputs of the binary counter CT2 to the CPU accumulator is carried out directly into the RAM memory of the microprocessor system MPS under the control of the controller direct access to memory.

3. Practical results

The algorithm of data transfer in the DMA mode is implemented using the scheme shown in Fig. 8. This measuring channel is implemented according to the frequency measurement scheme in the "adjacent intervals". And the last feature of dynamic measurements of angular velocity is the frequency measurement from the output of the encoder in the "adjacent intervals", and the measurement information transfer from the digital outputs to the accumulator in DMA mode.

The algorithm of the angular velocity measuring channel operation in the DMA mode is as follows:

1. Set the initial ADR address of the RAM memory by the software, which will store the binary code N [00-15] from the digital outputs in its cell CT2;
2. Software to install CT counter number of bytes to be transferred from digital outputs of CT2 counters to MPS RAM;
3. The external device (from the output of the logic gate "OR") sends to the DMA controller signal “DMA Request”, which enters the CPU through the bus BC;
4. At this signal, the microprocessor responds with a signal to confirm direct memory access CDMA, puts its buses BA and BD in the third state and confirms its readiness to exchange information under the control of the controller direct access to DMA memory. This signal is the beginning of data transfer to the RAM.
5. The DMA controller sets the specified ADR address on the BA address bus;
6. An odd byte (T_X) from the digital outputs N [00-15] of the binary counter is fed to the BD data bus by the DMA controller. CT2.
7. The DMA controller generates an WR record of an odd byte of information in the RAM cell at the selected address.
8. The DMA controller automatically increments the initial ADR address by: (+1): = ADR + 1, thereby generating the address of the next cell to store the even ($\overline{T}_x$) byte of the measurement results array.
9. Decreases by (-1) the value of the LT byte counter: = LT-1. The current count of exchange bytes is performed.
10. When the value of the byte counter is zero LT: = 0, the DMA process ends, the DMA controller gives the CPU processor a signal End of DMA.
11. At the end of the DMA signal, the processor converts its BA address bus and the BD data bus to the active state and the PDP controller bus to the third state and proceeds to the execution of the interrupted DMA program.
12. If the value of the counter is not equal to zero, the controller proceeds to the transmission of the next byte of information (according to p.5 of this algorithm).

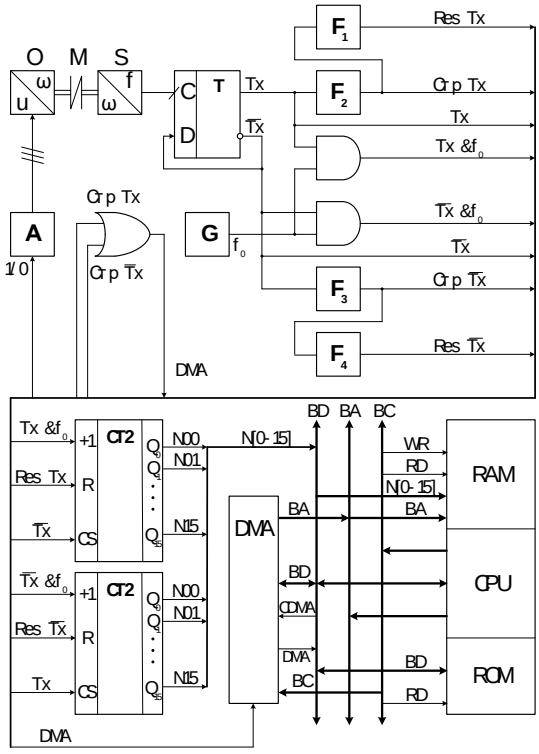

Fig. 8. Direct access to memory mode

In the DMA mode, the transmission of measurement information N [00… 15] from the digital outputs of the binary counter CT2 is carried out by hardware. Therefore, in this mode there are no time costs for execution of Flag and Driver subroutines (t_{FL} = 0, t_{DR} = 0). Therefore, in the DMA mode, the value of the upper limit of the angular velocity measurement is maximum

$$\omega_{max} \leq \frac{2\pi}{z \cdot T_X}$$

To increase the upper limit of measurement, it is necessary to propose adaptive algorithms for changing the resolution of the z encoder.

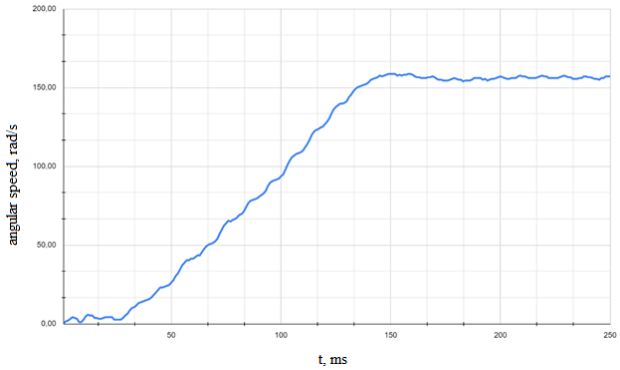

Fig. 9. The results of the experiment

Experimental studies were based on a prototype consisting of the object of measurement – three-phase asynchronous motor UAD-34 with a nominal speed of 1500 rpm, coupling shaft membrane type, encoder LIR-250A (z = 1500 marks per revolution) and debug board based on dual-core 32-bit microcontroller (MCU) TMS320F28379D, containing 1 MB of flash memory, 128 KB of RAM. This MK provides 12 32-bit general-purpose timers as well as 12 16-bit ADC channels, which is sufficient for this kind of dynamic measurements. The transient process for this object of measurement is shown in Fig. 9.

4. Conclusions

For the first time, the most significant features of angular velocity dynamic measurements, the numerical value of which is given in binary code, are highlighted in the paper. The main phases of measuring information transformation are established, which allowed to obtain new mathematical models in the form of transformation function, equations for estimating quantization errors, analytical dependences for determining the measuring range, which are the starting point for modelling physical processes in such digital measuring instruments.

Applying the methods of experimental computer science of reproduction, comparison and calculation on the example of indirect conversion of angular velocity into binary code for the first time analytically described the process of conversion of analog value ω_x into binary code N, the equation for estimating the absolute and relative quantization error is obtained and the measurement range is set, which provides the normalized value of the relative quantization error for angular velocity measuring channels with encoders.

The sampling error equation was obtained for the first time and it was proved that the limiting factor of the upper limit of angular velocity measurement is not only the normalized quantization error value δ_{KH}, as previously thought, but also the sampling frequency value f_D. Therefore, to expand the measurement range (by increasing the upper limit of measurement ω_{max}) it is proposed not only to increase the speed of analog-to-digital conversion hardware, but also to reduce the execution time of software drivers for transmitting measurement information to microprocessor memory. In this regard, the analytical dependences for estimating the upper limit of measurement for different modes of information transmission: software, interrupt, capture.

The practical implementation of the software mode of transmission of measurement information is characterized by a minimum of hardware costs and maximum execution time of the software driver, which explains its low speed, and therefore provides a minimum value of the upper limit of measurement ω_{max}. In the interrupt mode, the value of the upper limit of the angular velocity measurement is higher than in the program mode due to the reduction of the execution time of the software driver (t_{FL} = 0). The maximum value of the upper limit of the angular velocity measurement can be obtained using the transmission of measuring information in the DMA mode by providing the maximum speed in this mode (t_{FL} = 0, t_{DR} = 0).

In addition, the application of the results obtained in the work allows at the design stage (during physical and mathematical modeling) to assess the basic metrological characteristics of the measuring channel ω_x, which aims to reduce the development and commissioning of hardware and software and standardization of their metrological characteristics.

References

[1] Azarov A. D. et al.: Class of numerical systems for pipe-line bit sequential development of multiple optoelectronic data streams. Proc. SPIE 4425, 2001, 406–409.
[2] Azarov O. D. et al.: Static and dynamic characteristics of the self-calibrating multibit ADC analog components. Proc. SPIE 8698, 2012, 86980N.
[3] DSTU 2681-94. Metrology. Terms and definitions. Kyiv: State Standard of Ukraine, 1994.
[4] Kolobrodov V. G. et al.: Physical and mathematical model of the digital coherent optical spectrum analyzer. Optica Applicata 47(2), 2017, 273–282.
[5] Kolobrodov V. G. et al.: The diffraction limit of an optical spectrum analyzer. Proc. SPIE 9809, 2015, 98090F.
[6] Kukharchuk V. V. et al.: Discrete wavelet transformation in spectral analysis of vibration processes at hydropower units. Przegląd Elektrotechniczny 93(5), 2017, 65–68.
[7] Kukharchuk V. V. et al.: Information Conversion in Measuring Channels with Optoelectronic Sensors. Sensors 22(271), 2022 [http://doi.org/10.3390/s22010271].
[8] Kukharchuk V. V. et al.: Method of magneto-elastic control of mechanic rigidity in assemblies of hydropower units. Proc. SPIE 10445, 2017, 104456A.
[9] Kukharchuk V. V. et al.: Noncontact method of temperature measurement based on the phenomenon of the luminophor temperature decreasing. Proc. SPIE 10031, 2016, 100312F.
[10] Kukharchuk V. V. et al.: Torque measuring channels: dynamic and static metrological characteristics. Informatyka, Automatyka, Pomiary w Gospodarce i Ochronie Środowiska 3, 2020, 82–85.
[11] Kvyetnyy R. et al.: Modification of fractal coding algorithm by a combination of modern technologies and parallel computations. Proc. SPIE 9816, 2015, 98161R.
[12] Murzenko O., et al.: Application of a combined approach for predicting a peptide-protein binding affinity using regulatory regression methods with advance reduction of features. 10th IEEE International Conference on Intelligent Data Acquisition and Advanced Computing Systems: Technology and Applications IDAACS 2019, 1, 8924244, 431–435.
[13] Ornatsky P. P.: Automatic measurements and instruments. Higher School, Kiev 1980.
[14] Ornatsky P. P.: Theoretical foundations of information and measurement technology. Higher school, Kiev 1983.
[15] Osadchuk A. et al.: Pressure transducer of the on the basis of reactive properties of transistor structure with negative resistance. Proc. SPIE 9816, 2015, 98161C.
[16] Ostafiev V. A. et al.: Laser diffraction method of surface roughness measurement. Journal of Materials Processing Technology 63(1–3), 1997, 871–874.
[17] Podzharenko V. O., Kukharchuk V. V.: Measurement and Computer Measurement Technology: A Tutorial. UMKVO, Kiev 1991.
[18] Sena L. A.: Units of physical quantities and their dimensions. Nauka, Moscow 1977.
[19] Trishch R. et al.: Methodology for multi-criteria assessment of working conditions as an object of qualimetry. Engineering Management in Production and Services 13(2), 2021, 107– 141.
[20] Trishch R. et al.: Qualimetric method of assessing risks of low quality products. MM Science Journal 2021, 4769–4774.
[21] Tymchik G. S. et al.: Diagnosis abnormalities of limb movement in disorders of the nervous system. Proc. SPIE 104453, 2017, 104453S.
[22] Tymchik G. S. et al.: Distortion of geometric elements in the transition from the imaginary to the real coordinate system of technological equipment. Proc. SPIE 10808, 2018, 108085C.
[23] Vedmitskyi Y. G. et al.: New non-system physical quantities for vibration monitoring of transient processes at hydropower facilities, integral vibratory accelerations. Przegląd Elektrotechniczny 95(3), 2017, 69–72.
[24] Volodarsky E. T. et al.: Metrological support of measurements and control: A textbook. VSTU, Vinnytsia 2001.

D.Sc. Vasyl Kukharchuk
e-mail: BKuch@ukr.net

Doctor of science, Professor of the Department of Computerized Electromechanical Systems and Complexes, Vinnytsia National Technical University. Research interests: development of new methods of experimental computer science, microprocessor tools and computerized systems for measurements and control of electromechanical energy converters, mathematical, algorithmic, and metrological support for them.

http://orcid.org/0000-0001-9920-2726

Prof. Waldemar Wójcik
e-mail: waldemar.wojcik@pollub.pl

He is profesor of the Department of Electronics and Information Technology, former long-time dean of the Faculty of Electrical Engineering and Computer Science at Lublin University of Technology. Doctor Honoris Causa of five universities in Ukraine and Kazakhstan.
In his research he mainly deals with process control, optoelectronics, digital data analysis and also heat processes or solid state physics. In total, he has published 56 books, over 400 papers, and authored several patents

http://orcid.org/0000-0002-6473-9627

Prof. Sergii Pavlov
e-mail: psv@vntu.edu.ua

Academician of International Applied Radioelectronic Science Academy, Professor of Biomedical Engineering and Optic-Electronic Systems Department, Vinnytsia National Technical University. Scientific direction – biomedical information optoelectronic and laser technologies for diagnostics and physiotherapy influence.
Deals with issues of improving the distribution of optical radiation theory in biological objects, particularly through the use of electro-optical systems, and the development of intelligent biomedical optoelectronic diagnostic systems and standardized methods for reliably determining the main hemodynamic cardiovascular system of comprehensive into account scattering effects.

http://orcid.org/0000-0002-0051-5560

Ph.D. Samoil Katsyv
e-mail: katsyvsam@ukr.net

Candidate of Technical Sciences, Associate Professor of the Department of Computerized Electromechanical Systems and Complexes of Vinnytsia National Technical University.
Research interests: development of the axiomatics of weak operations in the theory of fuzzy sets and their application, application of non-standard analysis methods in theoretical electrical engineering, application of methods of the wavelet transformation theory in diagnosing and predicting the development of defects in hydraulic units.

http://orcid.org/0000-0003-1375-5229

M.Sc. Volodymyr Holodiuk
e-mail: vgolodyk@gmail.com

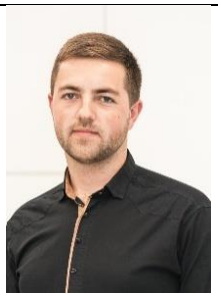

Postgraduate student of the Department of Computerized Electromechanical Systems and Complexes of Vinnytsia National Technical University. Research interests: Power electronics, measurements in power converters and modern power systems.

http://orcid.org/0000-0002-2449-5488

Ph.D. Oleksandr Reyda
e-mail: alexreyda@gmail.com

Candidate of Technical Sciences, Associate Professor of the Software Department of Vinnytsia National Technical University.
Research interests: image and signal processing, hardware and software engineering, developing of optoelectronic system, analysis of images and 3D (Lidar) data

http://orcid.org/0000-0001-8231-6268

Ph.D. Ainur Kozbakova
e-mail: ainur79@mail.ru

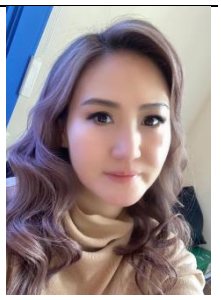

Ph.D, Associate Professor Almaty Technological University, Institute of Information and Computational Technologies of the Ministry of Education and Science CS of the Republic of Kazakhstan. Research interests: mathematical modeling of discrete systems, evacuation tasks, operations research, technology design of complex systems.

http://orcid.org/0000-0002-5213-4882

Ph.D. Gaukhar Borankulova
e-mail: b.gau@mail.ru

Candidate of Technical Sciences, Associate Professor, Head of Chair Department of „Information systems", Taraz Regional University M. Kh. Dulaty.
Research area: information systems, big data.

http://orcid.org/0000-0001-5701-8074

http://doi.org/10.35784/iapgos.3051

received: 18.08.2022 | revised: 06.09.2022 | accepted: 15.09.2022 | available online: 30.09.2022

APPLICATION OF PREDICTIVE MAINTENANCE IN THE PACKAGING PRODUCTION

Bogdan Palchevskiy[1], Lyubov Krestyanpol[2]

[1]Lutsk National Technical University, Faculty of Computer and Information Technologies, Lutsk, Ukraine, [2]Lesya Ukrainka Eastern European National University, Faculty of Foreign Linguistics, Lutsk, Ukraine

Abstract. *To solve the problem of predictive maintenance for packaging manufacturing, we propose a hybrid model that optimizes the maintenance plan. The model is based on monitoring the state of many components of a multi-position automatic packaging machine and makes it possible to predict their future malfunctions and estimate the remaining service life of the equipment. The effectiveness of the proposed solution is demonstrated with the help of a real industrial multi-position machine for the automatic production of film bags and packaging of paste in them. The methodology is based on the analysis of diagnostic information using an expert system.*

Keywords: technological equipment, expert system, monitoring, diagnostics, intelligent control system

ZASTOSOWANIE PREDYKCYJNEJ DIAGNOSTYKI W PRODUKCJI OPAKOWAŃ

Streszczenie. *Aby rozwiązać problem predykcyjnego utrzymania ruchu w produkcji opakowań, proponujemy hybrydowy model optymalizujący plan utrzymania ruchu. Model ten opiera się na monitorowaniu stanu wielu komponentów wielostanowiskowej automatycznej maszyny pakującej i umożliwia przewidywanie ich przyszłych awarii oraz szacowanie pozostałego czasu eksploatacji urządzenia. Skuteczność proponowanego rozwiązania została zademonstrowana na przykładzie rzeczywistej przemysłowej maszyny wielostanowiskowej do automatycznej produkcji torebek foliowych i pakowania w nie pasty. Metodyka opiera się na analizie informacji diagnostycznych z wykorzystaniem systemu eksperckiego.*

Słowa kluczowe: aparatura technologiczna, system ekspertowy, monitoring, diagnostyka, inteligentny system sterowania

Introduction

The change in the technical condition, which is automatically determined by the system, is caused by the appearance and development of defects in parts, nodes and systems of technological equipment [10]. Diagnosis during the operation of technological machines and their maintenance has its own characteristics. Diagnostic methods are divided into two groups:

1. Organoleptic (subjective) methods performed with the help of the performer's sense organs by side effects or using simple technical means, as well as on the basis of expert assessments. Experienced mechanics quickly determine up to 70% of equipment malfunctions and failures using organoleptic methods and the simplest tests.
2. Instrumental (objective) methods, when the measurement of the technical condition parameters is carried out by technical means.

Organoleptic methods allow you to identify by ear the places and nature of abnormal knocks, noise, equipment interruptions, a drop in engine power, its difficulty starting, as well as malfunctions in mechanical gears (rattle, noise). On inspection, you can also establish the places of leakage of oil, water and other technological liquids, the beating of rotating parts, the tension of chain gears, and a decrease in machine performance. When touched, the places and degree of abnormal heating, beating, vibration of parts are established, the viscosity of liquids is changed, and clutch failure, gas leakage and other media, short circuit wiring are determined by smell.

Instrumental methods by the nature of measuring parameters are divided into direct and indirect.

Direct measurement methods are based on direct measurements of the parameters of the technical condition of the equipment. They include kinematic measurements of the relative position and movement of parts (control of gaps in connections, in bearings, deflection of belt and chain gears, resizing of parts due to wear, radial, end and angular displacements of shafts of mechanisms, their inconsistency and non-parallelity), capillary control methods for detecting defects in the structure of parts and assemblies using liquids – penetrants that have a high ability to wet and penetrate through defects (kerosene, paints, or phosphors), ultrasonic search for surface defects, based on the phenomenon of ultrasound waves reflection from an insurmountable obstacle for it (for example, the transition of metal – air).

Indirect measurement methods are based on measuring the values of physical quantities characterizing the technical condition of mechanisms, systems and assemblies of machines (pressure, pressure drop, temperature, temperature difference in the working body of the system, gas consumption, electricity, oil, vibration parameters of the machine components, acceleration during run-up of parts, etc.). They include energy and thermal methods, vibroacoustic (registration of elastic vibrations parameters that occur in mechanisms when parts collide during operation) and pneumohydraulic (time of decrease in air pressure at specified limits of pressure change; relative leakage; absolute leakage) diagnostic methods.

To carry out diagnostics to obtain a complete picture of the state of technological equipment, it is advisable to combine the experience of specialists – experts who will allow to form for the ES a list of production rules based on organoleptic control methods, and the results of current direct and indirect measurements of the machine state during its operation. The creation of an ES for predictive maintenance of equipment in production conditions is carried out in stages.

- At the first stage, data display and the equipment status monitoring is ensured, to do it sensors, actuators, controllers are installed on industrial equipment (in the most important places of equipment). As a result, it becomes possible to collect information. When processing a huge array of unstructured data coming from sensors, filtering and adequate interpretation becomes a priority. Therefore, the creation of a program for information processing is of particular importance.
- The second stage is the creation of algorithms and subroutines based on an understanding of how changing parameters affects the operation of equipment. Here it is necessary to determine the limiting values of the operational parameters, upon reaching which it is necessary to perform certain operations of technological maintenance of equipment. In addition, when creating algorithms, one should consider the availability of organoleptic control data and their relationship with the parameters of the state of the equipment, determined by the results of the analysis of expert responses.

1. Statement of the problem

The aim of the study is to improve the process of diagnosing technological equipment, which allows to increase production efficiency by reducing equipment downtime during repair, to

reduce production costs by reducing repair costs and restoring equipment. The system of monitoring and diagnosis should provide a combination of the results of organoleptic and instrumental methods for diagnosis and their analysis. To do this, the equipment management system includes an expert system (ES). The system of monitoring and diagnostics using the ES should detect deviations in the early stages of changes in the technical condition and at the same time indicate also the ranked contribution of each technical means to the change in the general technical condition of the equipment. This is achieved by comparing the current state of the equipment with the reference (obtained during modeling), which allows you to choose the direction of searching for sources of emerging problems, as well as to implement predictive maintenance.

In general, most research focuses on the application and optimization of predictive models (mainly public and dedicated manufacturing datasets), but does not consider decision support such as optimization of maintenance planning using predictive models combined with the use of expert systems.

However, in this case, it is necessary to create fundamental approaches to the construction of algorithms for the joint work of organoleptic and instrumental methods for diagnosis and methods for forming the functional structure of the ES software part for a specific type of technological equipment, which is the purpose of this work.

In our work, the model is based on a hybrid approach, that is, the data of the statistical analysis of malfunctions and failures of packaging production equipment components are studied, on the basis of which the selection of sensors characterizing the state of the machine is carried out, and based on various combinations of data on the operation of the machine and its state, an expert system is built allows you to determine the status of the machine and create a schedule for its maintenance.

Such a maintenance system is able to predict its future condition and determine the necessary maintenance measures, based on the current state of the equipment. In this case, the probability of unplanned equipment failure will be minimized.

2. Literature review

Technical equipment is expensive, and its performance can have a huge impact on the production chain. Essentially, any unexpected equipment failure can lead to unintended downtime and costs for the entire production line. Over time, the condition and performance of production machines deteriorates. This eventually causes the machine to fail or malfunction if no maintenance measures are taken [1, 10]. The maintenance can be done in a variety of ways, from conventional approaches such as emergency, preventive, to predictive approaches. The emergency approach is used in the event of a failure that is costly and unpredictable. The preventive approach relies on expert knowledge, that is, on the actual model of system degradation [10]. The predictive approach focuses on maintenance based on the actual state of the equipment. For this, various data obtained from sensors are used.

Many researchers believe that the optimal strategy for maintenance and repair of technological equipment is to perform it according to the actual condition of the equipment using technical diagnostic methods. Existing predictive maintenance research usually focuses on either a predictive model without considering maintenance decisions or maintenance optimization based on known system degradation models [10].

The complexity of machinery involved in modern packaging production has grown rapidly. Thus, it is important to use an effective strategy that coordinates the prediction and detection of malfunctions in the operation of the equipment, and allows the formation of a maintenance schedule to optimize its operation. Consequently, any maintenance activity to be performed in such complex systems must consider not only the individual component, but also the relationships between the various machine components. This creates several problems for the design and implementation of predictive maintenance, namely in data collection, data processing and their interaction with the maintenance process [8].

Predicting the remaining useful life (RUL) of process equipment is a key component. Model-based methods rely solely on the degradation model of the physical structure to a predictive state of equipment performance. Therefore, they are ineffective for equipment with a complex structure, for example, for multi-position technological machines [17]. Methods used for forecasting models include autoregressive integrated moving average (ARIMA) models [14, 20].

The research community has investigated various aspects of maintenance. In the case of traditional maintenance, single-component systems were mainly investigated. Different existing maintenance policies for both single-unit and multi-unit systems are compared here [19]. These approaches mostly consider a single machine or component without paying attention to related machines or components. Thus, the aspect of maintenance of a multicomponent system becomes the focus of various works [3]. In this context, machine equipment with more than one component was considered, for which the main criteria for optimizing technical maintenance of technological equipment were considered, which included the structure of the equipment [18].

However, the requirements of advanced forecasting make traditional data-driven methods impossible for the processing of structurally complex technological machines [11]. To overcome this, a combination of various data on its working and operational parameters of technological equipment is used, which allows for a more accurate assessment of its actual condition. However, all this requires the creation of a principled approach to the construction of algorithms for the joint work of organoleptic and instrumental diagnostic methods for equipment with a complex structure.

Predictive maintenance includes two key components: predictive analytics and equipment maintenance planning.

To analyze data describing the condition of technological equipment, a number of authors used expert systems (ES) for diagnosing complex mechanical systems [9, 12], CNC machines [4], engines [5], and weapons [2]. In order to solve typical problems in the manufacturing process of copper phosphor ball, an expert diagnostic system based on failure tree analysis was built by merging the theory of failure trees and ES. The fault tree model of unqualified quality of production of copper phosphor ball and malfunction of the hydraulic system is highlighted [21]. According to the results of the analysis of numerous works, we note that a good help for diagnosing the technical condition of the equipment in different conditions of its operation can be the determination of zones of fuzzy condition of the equipment [5, 10]. These zones are defined by fixed variables such as "vibration level", "noise level", "heat level", etc., which correlate with terms such as "maintenance required", "faulty condition", "element replacement required", etc. In addition, for each specific type of equipment, the expert himself must set the limiting level of these variables. This is where the ES begins to play the main role.

All ES for the diagnosis of technological equipment in one way or another perform the following generalized functions [2, 4, 5, 9, 12]:

- Determination of the general condition of the equipment.
- Determining the period of occurrence of a malfunction or failure, changes in the state of equipment according to a trend or by an increase in diagnostic parameters.
- Constant monitoring and diagnostics of the condition of the equipment during the entire period of use of the equipment while saving its maintainability.

Packaging manufacturing systems are complex systems of closely interconnected machines and devices that interact and cooperate to achieve common goals. Consequently, any maintenance activity to be performed in such complex systems must consider not only the individual component, but also the dependencies of the various machine components involved.

The main problem that arises when using ES to diagnose technological equipment is the need to combine production rules in one functional software structure based on the results of organoleptic control of the equipment and due to the results obtained by instrumental control methods. Next, it is necessary to form recommendations for forecasting the future state of technological equipment and choosing the type of its maintenance.

The general process of predictive maintenance includes stages.

The first stage is the collection of data for predictive maintenance, which is critical for effective maintenance operations.

The second stage of predictive maintenance is data processing and forecasting. Collected data from facilities or resources is processed to reduce the significant impact on the production chain in the event of their failure. The second step provides a framework to support maintenance decisions.

The third stage in the process is service decision support. This step covers the general aspect of maintenance by helping the operator, in the maintenance engineer, to act on an event that triggers a specific maintenance task.

3. Researches methodology

3.1. The sequence of designing the functional structure of software for diagnosing technological equipment

The process of creating an EC diagnostic system for analyzing the reliability of technological equipment includes the following steps.

1. At the first stage, the decomposition of technological equipment into technological blocks is carried out. All elements included in its composition are determined and potential malfunctions of each element and possible diagnostic signs are identified.
2. The parameters that the information system will control in real time are determined. All parameters can be divided into groups according to the degree of significance:
a) technological parameters controlled by the SAC;
b) direct and indirect parameters of the equipment state, including those related to organoleptic control, a change in the values of which can lead to deviation of the process from the norm or failure.
3. Norms for quantitative parameters are determined considering normative documents (technological regulations, instructions of the manufacturing plant, expert opinion, etc.), as well as expert knowledge. For each malfunction, the possible causes that cause it are revealed. Each fault corresponds to one or more ways to fix it.
4. The nature of the links between diagnostic parameters and malfunctions is determined. For this, cause-and-effect diagrams are built for each failure and malfunction
5. Simplification of the process of building a diagnostic strategy can be achieved using the fault tree analysis (FTA) method, which contributes to a thorough analysis of the causes of failures of technical systems and the development of measures most effective for their elimination [6, 7]. FTA is used to imagine how the functions of technological equipment, its components (mechanisms, nodes, parts) interact with the control system and its software. When analyzing the occurrence of a failure, the failure tree consists of sequences and combinations of violations and malfunctions, which means it is a multi-level graphological structure of causal relationships obtained as a result of tracking dangerous situations in reverse order, in order to identify possible causes of their occurrence (Fig. 1).
When analyzing a fault tree, the contribution of specific processes and their combinations to the occurrence of a failure is determined.
6. A list of possible faulty states of the equipment is formed.
7. Possible dangerous modes on technological equipment associated with violation of normal operating conditions or failure of individual nodes or parts, as a rule, are known in advance. Automatic control devices perceive controlled technological values (temperature, pressure, etc.) and other diagnostic parameters, when reaching the maximum allowable values, a signal is sent. For such situations, a separate rule of this type is created: "If Parameter i = Critical, then Situation = Failure", where "Parameter i" corresponds to a dangerous value. Based on the results of an expert survey, an assessment of the situation in each case is determined according to the rules. Rules are formed and determine the most likely causes of malfunctions and how to eliminate them. The method of expert assessments for each rule created earlier determines one or more reasons.
8. As a result of the research, a software functional structure that consists of the production is developed. The production system is based on the rules and works cyclically. In each product cycle, the rules from the knowledge base are viewed by the rules interpreter in a certain order. If there is a rule, the condition of which, when compared, coincided with some facts from the working memory, then the rule is activated, and its conclusion is added to the working memory. Then the cycle repeats. The choice of ES strategy for decision-making determines the sequence of application of rules for a multi-stage process.

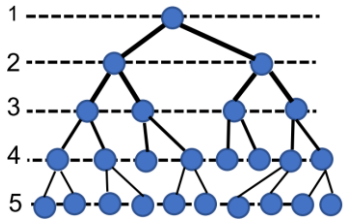

Fig. 1. Conditional scheme of building a tree of faults and malfunctions: 1 – equipment failure, 2 – failures of mechanisms, 3 – failures of components and parts, 4 – events causing failure, 5 – types of impacts

3.2. Methods

The change in the technical state caused by the initiation and development of defects in parts and nodes is determined by the diagnostic system, which allows analyzing various options for complete and partial failures, the operation of devices considering their operating modes, the influence of both the environment and different degrees of wear of parts. The complexity of using logical analysis methods to solve a diagnostic problem (Ishikawa diagram, decision tree, fault tree) is due to the lack of strict formal procedures for their implementation, that sometimes makes it possible to attribute this stage more to heuristics than to science. For analyzing the reliability of technological equipment it is promising to use digital twins that is, virtual prototypes reflecting how a particular technological equipment should work, under the condition that its components – parts, nodes, mechanisms – are fully functional. By comparing the current state of the equipment with a virtual sample, it is possible to identify current and predict future malfunctions and act proactively, eliminating problems before they lead to failure. The digital model can be simplistically represented as a multidimensional surface in the space of operational parameters [12]. For the practical implementation of this approach, it is necessary to form an integral indicator of the technical state of equipment **Y** and establish a functional relationship between it and the set of selected diagnostic parameters specified by vector **X**:

$$Y=F(X) \tag{1}$$

Here, the indicator of the technical condition is understood as a quantitative parameter characterizing the performance of the equipment. The change in this parameter is indicated in the diagram, where it is possible to predict its exit "beyond the permissible limits" in real time using interpolation. This allows you to predict the failure of equipment [14].

4. Experiments and results

4.1. Object of study

As an example, the sources of loss of efficiency for a multi-position automatic machine (MPAM) for packing pastes in doy-pack bags were studied (see Fig. 2b) [15].

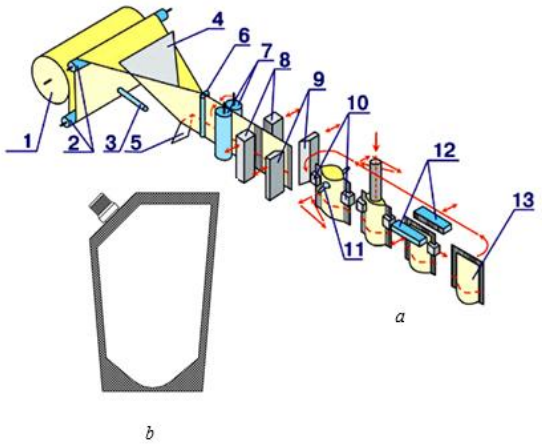

Fig. 2. Technological scheme of packing paste in "doy-pack" bags (a) and a doypack package with cork (b): 1 – laminate roll, 2 – laminate unwinding, 3 – perforator, 4 – pipe forming, 5 – photo sensor, 6,7 – rolls, 8 – longitudinal welding, 9 – cutting, 10 – opening of the package, the 11 cork welding mechanism, 12 – sealing of the package (for packs with a cork, between the cutting mechanism 9 and the mechanism for opening the package 10, the mechanism for cutting off the corner of the pack 9-a, the cork feeding mechanism 9-b and are not shown)

To do this it was considered and recorded in databse of simpl MPAM for the period of time its operation in the real Manufacturing conditions during one year. MPAM performs the following technological transitions: unwinding the laminate from a roll, forming a pipe of it, longitudinal welding of sidewalls to form a package, cutting it off, cutting the corner of the package and welding the cork into it, filling the package and sealing it by welding (Fig. 2a). The results of the study for the MPAM reliability were obtained based on data collection on the duration of its operating state in working conditions and in states of downtime for various reasons.

For data collection and their subsequent analysis, a complex machine is divided into autonomous units. The structure of the MPAM is shown in figure 3.

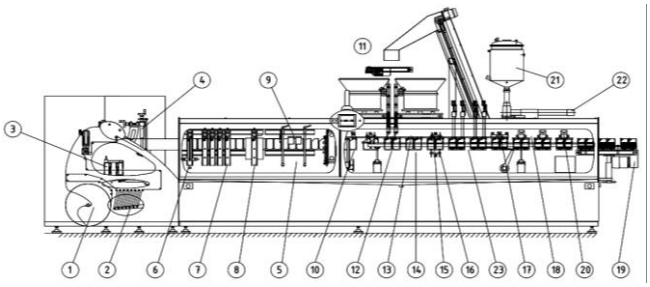

Fig. 3. Multi-position automatic machine (MPAM) for packaging of pastes in "doy-pack" type packs: 1 – laminate roll, 2 – laminate unwinding, 3 – perforator, 4 – forming triangle, 5 – guides, 6 – bottom soldering iron with drive, 7 – mechanism of vertical welding, , 8 – cooling mechanism, 9 – angular stamps, 10 – cutting mechanism (scissor), 11 – cork feeding mechanism, 12 – cork soldering irons, 13 – upper stretcher with tweezers, 14 – lower stretcher with tweezers, 15 – upper suction cups, 16 – lower suction cups, 17 – pack stretching mechanism, 18 – horizontal soldering irons, 19 – conveyor, 20 – cooling mechanism, 21 – tank with product, 22 – dispenser drive, 23 – dispensers (4 pieces) with drive

To analyze the reliability of MPAM as a complex technological equipment, we will limit ourselves to the analysis of the most probable failures only. The duration of downtime in the functioning of MPAM in real production conditions during the year are shown in figure 4.

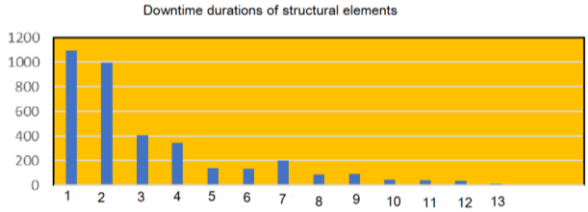

Fig. 4. Ranking of downtime durations of structural elements of MPAM: 1 – broaching mechanism, 2 – cork feeding mechanism, 3 – the cork feeding and inserting mechanism, 4 – cap soldering mechanism, 5 – soldering iron mechanism, 6 – dispenser with nozzle, 7 – cooling mechanism, 8 – vacuum pump, 9 – thermo sensor, 10 – photo sensor, 11 – vibrobunker with a controller, 12 – printer, 13 – scissor mechanism

From the conducted analysis and ranking of downtimes of MPAM structural elements, it follows that the most frequent failures are typical for the mechanisms of stretching the laminate, welding the cork, forming the package and dosing the product [13, 15].

In general, the situation at MPAM depends on a set of factors that are quantified or evaluated qualitatively. To obtain information about the flow state of the technological equipment, it is advisable to install temperature control sensors in the main working areas of the machine, to control the force of moving the laminate per step, the resistance force to the movement of the dispenser piston, a sensor for controlling the viscosity and temperature of the paste, a sensor for electricity consumption, a sensor for the consumption of compressed air, vibration level sensor during machine operation. Next it is necessary to set their normalized values and develop an algorithm for monitoring the interaction of their deviations.

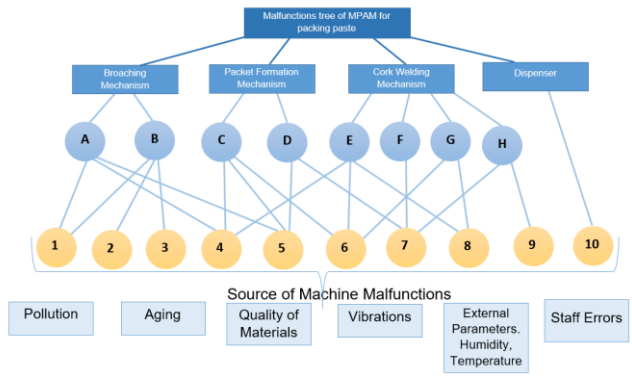

Fig. 5. Malfunctions tree of MPAM for packing paste: Components of the machine that failed: A – stretcher, B – tweezers, C – soldering iron of the package seam, D – package opening mechanism, E – cork soldering iron, F – cork gripping mechanism, G – cork feeding mechanism, H – vibrotank. Machine malfunctions: 1 – laminante tightening, 2 – stretching of the package, 3 – sagging of the package, 4 – burning of the package laminate, 5 – pouring the product, 6 – deformation of the package, 7 – non-installation of the cork, 8 – poor installation of the cork, 9 – jamming of the cork, 10 – dose deviation in the package

In packaging manufacturing, various data are collected during operation. This collected data typically includes data about events, conditions, and transactions. Operational data can include data about a specific process, while event data can collect data about machinery, what has happened to it and what maintenance has been applied to it. Condition data may include the collection of general condition data, i.e. health, and machine condition measurements. In addition, with various sensors such as accelerometers and rain sensors, various signal data such as vibration, temperature, pressure, humidity and climate can be acquired as part of an overall data collection, i.e. events or conditions. In addition to receiving a variety of data from production equipment, tools and systems.

Technological parameters for assessing the state of MPAM, obtained by instrumental control of its state, are given in table 1.

Table 1. Designation of machine condition evaluation parameters

No	Parameter	Characteristics of the parameter
1	t_1	Laminate temperature
2	t_2	corc soldering iron temperature
3	t_3	package soldering iron temperature
4	t_4	paste temperature
5	p_1	laminate pulling force
6	P_2	cork feeding force
7	p_3	paste injection force
8	c	laminate elasticity
9	μ	paste viscosity
10	V	machine vibration level
11	S	noise level at work
12	W	air humidity
13	P	user power of the electric drive
14	Q	consumption of compressed air during operation

The results of a survey of MPAM operators and debuggers, as well as the results of studying and analyzing the relationships between the technological parameters and malfunctions (Fig. 5) were used to form a sequence of production rules in the ES. Information on the identification of components close to failure was obtained by creating an algorithm for the analysis of monitoring results carried out by the ES.

In the data collection process for predictive maintenance, data is usually collected from several sources. In the pre-processing stage, the collected data is cleaned, prepared and formatted as needed to create specific predictive models or general analytical functions [16].

In real conditions, when it is impossible to calculate theoretically the real values of the controlled technological equipment parameters considering its technical condition, it is necessary to provide for the conduct of an educational experiment to obtain reference numerical estimates of the controlled parameters. At the training stage the components of the ES database and knowledge base are filled with reference estimates of the values of parameters and rules that correspond to the specifics of the machine's operation. The reference values of the controlled equipment parameters obtained during the training experiments are used in the future during the operation of the control system and diagnostics of the technological system to ensure its maximum productivity without loss of product quality.

4.2. Results and discussion

Table 2 shows the rules for assessing the state of MPAM, which are used to design the functional structure of ES software. We mark the excess of the specified value of the parameter (see designation in table 1), obtained by the instrumental method, as "+", and its low value as "-".

The procedure for designing the software functional structure for diagnosing a malfunction "Poor/non installation of the cork" is taken as an example from point 7 of table 2 and is illustrated by the following scheme (Fig. 6).

Table 2. Rules for assessing the state of MPAM

No	Evaluation results	Machine malfunctions	Mark in Fig. 5	Reason	Mark in Fig. 7
1	$+t_1$, $-p_1$, -c, +V, +W, +P	laminage tightenning	3	Breakage of the spring of clamped tweezers	4
2	$+t_1$, $+p_1$, -c, +V, +Q	package stretching	5	Incorrect stretcher adjustment	12
3	$+t_1$, $-p_1$, -c, +V, -Q	package sagging	6	Breakage of the clamping tweezers spring	13
				Incorrect stretcher adjustment	14
4	$+t_3$, $+t_2$, $-p_1$, +P	buming the laminate of the package	7	Incorrect temperature adjustment of the package soldering iron	15
				Incorrect temperature adjustment of the cork soldering iron	16
5	$+t_4$, $+p_3$, - μ, -Q	pouring the product	8	Incorrect adjustment of the dispenser	17
				Incorrect adjustment of the paste temperature	18
6	$+t_1$, $+t_2$, $-p_1$, $+p_2$, +V, -Q	deformation of the package	9	Incorrect temperature adjustment of the package soldering iron	19
				Incorrect temperature adjustment of the cork soldering iron	20
				Incorrect stretcher adjustment	21
				Increased laminate temperature	22
7	$+t_1$, t_2, t_3, $-p_2$, +V, -Q	poor/non installation of the cork	10	Incorrect adjustment of the cork feed force	23
				Exceeded temperature of cork soldering irons and laminate	24
				Incorrect adjustment of the vibrotank	25
				Increased temperature and vibrations in the machine	26
8	$\pm t_4$, $-p_3$, ±μ, -Q, ±W	dose deviation in the package	11	Incorrect regulation of paste temperature and vascosity	27
				Dispenser drive effort	28
				Air humidity	29
				Non-compliance with the specified air pressure in the system	30

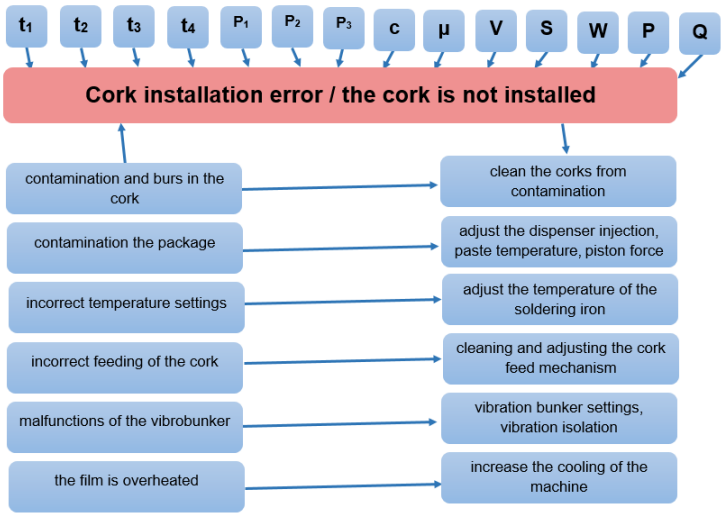

Fig. 6. The scheme of connections when there is the malfunction "Poor/non installation of the cork": temperature (t_1 – laminate, t_2 – cork soldering iron, t_3 – pack soldering iron, t_4 – paste), force (p_1 – laminate pulling, p_2 – cork feeding, p_3 – paste injection), c – laminate elasticity, μ – paste viscosity, V – machine vibration level, S – machine noise level, W – humidity, P – used power of the electric drive, Q – consumption of compressed air during operation

The development of ES for diagnosing MPAM malfunctions was carried out in CLIPS software environment. CLIPS combines 3 programming paradigms: logical, procedural and object-oriented. Clips also provides 3 main formats for presenting information: facts, global variables, and objects. The task of the developed ES is to find the reasons for the breakdown of BPMA mechanisms based on already known defects and malfunctions. Accordingly, using the example of a malfunction "Poor/non installation of the cork", it is possible to determine the reasons for its occurrence: incorrect adjustment of the cork feed force, excessive temperature of the cork or laminate soldering irons, incorrect adjustment of the vibrotank, increased temperature and vibrations in the machine The main task of the developed EC is to identify a malfunction, check the technological parameters, and, as a result, identify the reason of the breakdown. The obtained causes of the malfunction make it possible to select the necessary troubleshooting measures.

The algorithm of work of the EC, which specifies the sequence of application of the developed production rules, is presented in Fig. 7.

Figure 7 shows the ES algorithm, where each circle with a dotted line indicates the index of the question (production rule), and the circle with a solid line indicates the answers that the system displays.

Product rule 1 – the question: "Are there any malfunctions?". The answer "No" goes to the mark 2, which shows the final action – the answer: "The machine is in good working order." The answer "Yes" goes to the production rule with index 3, where a new question is asked: "Is there is laminate tightening malfunction?". The answer "Yes" goes to the choice of the malfunction reason 4 – "Breakage of the spring of clamped tweezers." The answer "No" goes to index 5 which indicates the next malfunction, etc.

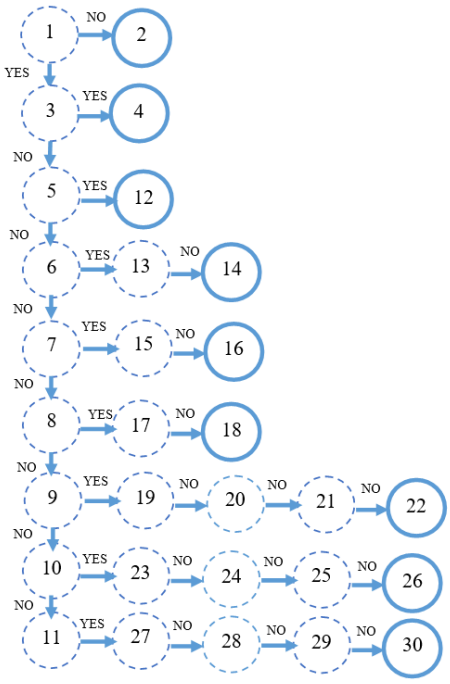

Fig. 7. Algorithm of ES work

The formation of a knowledge base involves entering the questions, in accordance with which the reason of the breakdown is determined, as well as the knowledge that characterizes the malfunctions. The knowledge base also includes additional questions that will be displayed to the user.

In CLIPS, the knowledge base is described as an array of facts of the following form:

```
(deftemplate rule
(multislot if)
(multislot then))
(deffacts knowledge-base
(goal is machine malfunctions)
(legalanswers are yes no)
(rule (if malfunctions is yes) (then type.malfunctions is select))
(rule (if malfunctions is no) (then machine is work))
(question malfunctions is "Is machine malfunctions ?")
(rule (if malfunctions is yes) (then select type.malfunctions))
(rule (if malfunctions is no) (then "Machine is work"))
(question is "Malfunctions is tightening of the film?")
(rule (if type.malfunctions is yes) (then "Breakage of the spring of
the clamped tweezers" ))
(rule (if type.malfunctions is no) (then select type.malfunctions ))
```

In addition to the formed array of facts, a rule for conducting a dialogue with the user was also formed to create appropriate changes in the fact base.

```
(defrule ask-question-legalvalues ""
(declare (salience 10))
(legalanswers ? $?answers)
?f1 <- (goal is ?variable)
?f2 <- (question ?variable ? ?text)
(retract ?f1)
(format t "%s " ?text)
(printout t ?answers " ")
(bind ?reply (read))
(if (member (lowcase ?reply) ?answers)
then (assert (variable ?variable ?reply))
(retract ?f2) else (assert (goal is ?variable))))
```

Obviously, in a similar way, the functional structure of all other malfunctions shown in table 2 is carried out.

5. Conclusions

The process of diagnosing technological equipment using ES allows to increase production efficiency by reducing equipment downtime in repair. To do this, the current state of the equipment is tracked by the monitoring system and compared with the reference one, and the decision on the type and timing of specific maintenance is made with the participation of the ES. By comparing the current state of the equipment with a virtual sample, it is possible to predict future malfunctions and act proactively, eliminating problems before they lead to breakage

Using a specific example of MPAM for packing paste into packs, an analysis of the reliability of its components based on annual observation was carried out, the failures and malfunctions of these components were ranked, the most likely malfunctions and processes characterizing the state of the MPAM were determined, and the necessary sensors for monitoring (temperatures in the main working areas of the machine, laminate movement force, resistance force to move the batcher piston, viscosity and paste temperature, fluctuations in the consumption of electricity and compressed air, the level of vibration and noise during operation).

An example of the formation of production rules set for diagnosing a multi-position automatic machine for paste packing and designing the functional structure of software for diagnosing typical malfunctions has been demonstrated.

References

[1] Becker T., Wagner D.: Identification of Key Machines in Complex Production Networks. Procedia CIRP 41, 2016, 69–74 [http://doi.org/10.1016/j.procir.2015.12.006].

[2] Chaoyang G., Fenli G.: Embedded fault diagnosis expert system on weapon equipment. International Journal of Advanced Network, Monitoring and Controls 1(2), 2016, 25–33 [http://doi.org/10.2991/mcei-16.2016.234].

[3] Dekker R. et al.: A review of multi-component maintenance models with economic dependence. Mathematical Methods of Operations Research 45, 1997, 411–435 [http://doi:10.1007/bf01194788].

[4] Erik L. J.: Expert system for diagnosing computer numerically controlled machines: a case-study. Computers in Industry 32(3), 1997, 233–248 [http://doi.org/10.1016/S0166-3615(96)00077-2].

[5] He Q., Li X. Q.: Management of knowledge base of expert system for fault diagnosis of rotating machinery. Applied Mechanics and Materials 44–47, 2010, 2935–2939 [http://doi.org/10.4028/www.scientific.net/AMM.44-47.2935].

[6] IEC 60300-3-1:2003, Dependability management – Part 3-1: Application guide – Analysis techniques for dependability – Guide on methodology.

[7] ISO 17359:2003(E), Condition monitoring and diagnostics of machines – General guidelines.

[8] Lee J., Bagheri B., Kao H.-A.: A Cyber-Physical Systems architecture for Industry 4.0-based manufacturing systems. Manufacturing Letters 3, 2015, 18–23 [http://doi.org/10.1016/j.mfglet.2014.12.001].

[9] Majstorovic V. D.: Expert systems for diagnosis and maintenance: The state-of-the-art. Computers in Industry 15(1–2), 1990, 43–68 [http://doi.org/10.1016/0166-3615(90)90084-3].

[10] Mobley R. K.: An Introduction to Predictive Maintenance. Elsevier Science, 2002.

[11] Mourtzis D., Vlachou E., Milas N.: Industrial Big Data as a Result of IoT Adoption in Manufacturing. Procedia CIRP 55, 2016, 290–295 [http://doi.org/10.1016/j.procir.2016.07.038].

[12] Olatunbosun A., Arulogunol O.: An expert system based equipment diagnostics. Journal of Applied Science, Engineering and Technology 5, 2005, 63–70 [http://doi.org/10.4314/jaset.v5i1.38299].

[13] Palchevskyi B., Krestyanpol L.: The Use of the "Digital Twin" Concept for Proactive Diagnosis of Technological Packaging Systems. Babichev S., Peleshko D., Vynokurova O. (eds): Data Stream Mining & Processing. Communications in Computer and Information Science 1158, Springer, Cham. 2020 [http://doi.org/10.1007/978-3-030-61656-4_29].

[14] Palchevskyi B., Krestyanpol L.: Strategy of Construction of Intellectual Production Systems. IEEE Third International Conference on Data Stream Mining & Processing (DSMP), 2020, 362–365 [http://doi.org/10.1109/DSMP47368.2020.9204190].

[15] Palchevskyi B.: Improving the efficiency of intelectual packaging systems. Technological complexes 15, 2018, 4–14.

[16] Sang G. M., Xu L., de Vrieze P.: Simplifying Big Data analytics systems with a reference architecture. Camarinha-Matos L., Afsarmanesh H., Fornasiero R. (eds): Collaboration in a Data-Rich World. PRO-VE 2017. IFIP Advances in Information and Communication Technology 506. Springer, Cham. [http://doi.org/10.1007/978-3-319-65151-4_23].

[17] Tobon-Mejiaab D. A., Medjahera K., Zerhounia N.: CNC machine tool's wear diagnostic and prognostic by using dynamic Bayesian networks. Mechanical Systems and Signal Processing 28, 2012, 167–182 [http://doi.org/10.1016/j.ymssp.2011.10.018].

[18] Van Horenbeek A., Pintelon L., Muchiri P.: Maintenance optimization models and criteria. International Journal of System Assurance Engineering and Management 1, 2010, 189–200 [http://doi:10.1007/s13198-011-0045-x].

[19] Wang H.: A survey of maintenance policies of deteriorating systems. European Journal of Operational Research.Volume 139(3), 2002, 469–489 [http://doi.org/10.1016/S0377-2217(01)00197-7].

[20] Wu W., Hu J., Zhang J.: Prognostics of Machine Health Condition Using an Improved ARIMA-Based Prediction Method. Second IEEE Conference on Industrial Electronics and Applications ICIEA, 2007, 1062–1067 [http://doi.org/10.1109/iciea.2007.4318571].

[21] Zhang Z., Li Z., Zhao C.: Research on condition monitoring and fault diagnosis of intelligent copper ball production lines based on big data. IET Collaborative Intelligent Manufacturing 4(1), 2022, 45–57 [http://doi.org/10.1049/cim2.12043].

Prof. Bogdan Palchevski
e-mail: bogdan_pal@ukr.net

Doctor of Technical Sciences, professor of the Department of Automation and Computer-integrated Technologies of the Lutsk National Technical University. Academician of the Public Organization National Academy of Sciences of Higher Education of Ukraine. Member of East European Scientific Society. Author of more than 310 scientific papers, 33 patents for 33 patents for inventions et 27 patents for utility models.
Research interests: Automation of food production and packaging processes; Control and diagnostic systems of automatic technological complexes (mechatronic technological systems).

http://orcid.org/0000-0002-4000-4992

Ph.D. Lyubov Krestyanpol
e-mail: lkrestyanpol@gmail.com

Expert of National Agency for Higher Education Quality Assurance (Ukraine).
Member of East European Scientific Society.
Associate Professor of Lesya Ukrainka Eastern European National University.
Author of more than 60 scientific papers, 4 patents for utility models.
Research interests: information and communication technology.

http://orcid.org/0000-0003-3617-7900

http://doi.org/10.35784/iapgos.3032

received: 19.07.2022 | revised: 28.08.2022 | accepted: 15.06.2022 | available online: 30.09.2022

PREDICTION MODEL OF PUBLIC HOUSES' HEATING SYSTEMS: A COMPARISON OF SUPPORT VECTOR MACHINE METHOD AND RANDOM FOREST METHOD

Andrii Perekrest[1], Vladimir Chenchevoi[2], Olga Chencheva[1], Alexandr Kovalenko[3], Mykhailo Kushch-Zhyrko[1], Aliya Kalizhanova[4,5], Yedilkhan Amirgaliyev[5]

[1]Kremenchuk Mykhailo Ostrohradskyi National University, Department of Computer Engineering and Electronics, Kremenchuk, Ukraine, [2]Kremenchuk Mykhailo Ostrohradskyi National University, Department of Systems of Automatic Control and Electric Drive, Kremenchuk, Ukraine, [3]Cherkasy State Technological University, Cherkasy, Ukraine, [4]University of Power Engineering and Telecommunications, Almaty, Kazakhstan, [5]Institute of Information and Computational Technologies MES CS RK, Almaty, Kazakhstan

Abstract. *Data analysis and predicting play an important role in managing heat-supplying systems. Applying the models of predicting the systems' parameters is possible for qualitative management, accepting appropriate decisions relating control that will be aimed at increasing energy efficiency and decreasing the amount of the consumed power source, diagnosing and defining non-typical processes in the functioning of the systems. The article deals with comparing two methods of ma-chine learning: random forest (RF) and support vector machine (SVM) for predicting the temperature of the heat-carrying agent in the heating system based on the data of electronic weather-dependent controller. The authors use the following parameters to compare the models: accuracy, source cost and the opportunity to interpret the results and non-obvious interrelations. The time spent for defining the optimal hyperparameters and conducting the SVM model training is deter-mined to exceed significantly the data of the RF parameter despite the close meanings of the root mean square error (RMSE). The change from 15-min data to once-a-minute ones is done to improve the RF model accuracy. RMSE of the RF model on the test data equals 0.41°C. The article studies the importance of the contribution of variables to the prediction accuracy.*

Keywords: building heat supply, random forest, support vector machine

MODEL PROGNOZOWANIA SYSTEMÓW GRZEWCZYCH BUDYNKÓW UŻYTECZNOŚCI PUBLICZNEJ: PORÓWNANIE METODY SUPPORT VECTOR MACHINE I RANDOM FOREST

Streszczenie. Analiza danych i prognozowanie odgrywają ważną rolę w zarządzaniu systemami zaopatrzenia w ciepło. Wykorzystanie modeli do przewidywania parametrów systemu jest możliwe do zarządzania jakością, podejmowania odpowiednich decyzji sterujących, które będą miały na celu poprawę efektywności energetycznej i zmniejszenie ilości zużywanego źródła energii elektrycznej, diagnozowania i wykrywania nietypowych procesów w funkcjonowaniu systemu. W artykule porównano dwie metody uczenia maszynowego: Random Forest (RF) i Support Vector Machine (SVM) do przewidywania temperatury czynnika grzewczego w systemie grzewczym na podstawie danych elektronicznego regulatora pogodowego. Do porównania modeli autorzy wykorzystują następujące parametry: dokładność, koszt początkowy oraz możliwość interpretacji wyników i nieoczywistych zależności. Ustalono, że czas poświęcony na wyznaczenie optymalnych hiperparametrów i wytrenowanie modelu SVM znacznie przekracza dane parametru RF, pomimo zbliżonych wartości błędu średniokwadratowego (RMSE). Zmiana z danych 15-minutowych na dane raz na minutę została dokonana w celu poprawy dokładności modelu RF. RMSE modelu RF z danych testowych wynosi 0,41°C. W pracy zbadano znaczenie wkładu zmiennych w dokładność prognozy.

Słowa kluczowe: zaopatrzenie w ciepło budynku, random forest, metoda wektorów wspierających

Introduction

Nowadays economic challenges require searching for solving the issues of energy saving and energy efficiency. The efficiency of the actions aimed at saving the energy source are usually insufficient due to the lack of the complex approach to the issues of managing energy saving and energy efficiency, insufficiency of financing. It causes a significant improvement for the existing and developing information and technical decisions in the energy management [22, 23, 28]. Most of such decisions are based on monitoring and parameterizing the system by an energy manager that allows receiving and saving significant data. The intellectual data processing is known to play more and more important role in the issues of the optimal complex system management. Thus, the predicting models of the parameters of energy consuming systems allow the energy managers at different levels accepting substantiated decisions relating energy management based on the history data about the takes decisions and the received result, analyzing the factors influencing the energy efficiency and noting non-typical values of the system parameters that can be caused by technical breaks or inefficient managerial decisions.

1. Related work

Active implementation of the decisions relating to the automated monitoring and controlling the heating system allows not only controlling the amount of the consumed energy source but also saving large amounts of information on the system functioning, the amount of the consumed source itself and decisions concerning the system management accepted by an energy manager. Various methods of machine learning are widely spread due to the dramatic development of the artificial intelligent in the tasks of managing energy consumption [22, 23, 28].

In the research [24] the authors study the opportunity to predict the energy consumption in the central heating system with the help of Elman network with the use of the genetic algorithm that allows determining the shares in the models.

The comparison of the results received when using the neural networks and the random forest method in the task of predicting the amount of the used energy source observes the higher accuracy is achieved when using the first method [3]. The research6 compares the accuracy of the models of neural nets for predicting heat supply of a range of the building of the budget field and determines that the model of NARX type gives the most accurate results with the simplest design. The authors [10] develop the method of determining energy efficiency of the building with the use of multi-parameter regression based on the data of the municipal service bills and weather websites. SVM method is becoming more common for solving the practical tasks. The article [9] shows the results of modelling and studying the efficiency of the geo-thermal system with the use of SVM method that allows simplifying the modelling process. The authors have conducted a range of researches to determine the optimal parameters for regularization and the kernel parameters. In [8] uses the same method to predict the energy consumption in several buildings in Singapore: uses the data of the external temperature, solar radiation and relative humidity as the input parameters. In the researches [2] and [1] the comparison of the SVM, RF, Extra Trees and regression trees models determines that the stated models have comparative accuracy, different learning time and can be used for predicting solar energy received from the geothermal system. Moreover, RF and Extra Trees can be additionally applied as a tool for decreasing the dimension

of the input data. The issues of managing the heat supplying systems and the implementing the received results into the work of energy man-agers are not fully covered in spite of the number of researches that use machine learning methods for solving the practical tasks in the energy field [3, 24].

The article presents the research on the following aspects:

- comparing SVM and RF methods for predicting the temperature of the heat-carrying agent in the heating system based on the data of electronic controller since a lot of researches focus on neural nets [10, 21];
- using the ensemble RF method to analyze the importance of the contribution of variables into the prediction accuracy. The conducted analysis allows understanding the data and the interrelations between the parameters better [8, 9].

2. Machine learning methods

This part presents two algorithms: RF and SVM used for predicting the temperature of the heat-carrying agent in the heating system based on the data of electronic weather-dependent controller.

The SVM (method of data analysis that is applied for the tasks of classification and regression) is chosen as one of the methods of machine learning to create a predicting model of the heat-carrying agent temperature in the heating system [26]. It is based on the SRM principle that minimizes the upper error boundary that includes the sum of the learning error and the confidence interval instead of minimizing the learning error (empirical risk minimization) [1, 2].

Let us consider that we describe the objects with n-dimensional vectors where X – space of the objects, Y – target output: $X = R^n$, $Y = R$.

SVM of the linear separated data finds the linear function that approximate the output vector Y the best, the function ε – sensitivity that does not consider deviations $a(x_i)$ from y_i less than ε as errors.

The function is the following [7, 26]:

$$a(x) = w \cdot x + b \tag{1}$$

The method is used with different kernel functions to solve the problems of linear non-separability. This is the transfer from the initial space of the feature descriptions of the objects X to a new space H with the help of some transformations $\psi : X \to H$. If the space H has a comparatively high dimensionality, one can hope the sampling to appear linearly separable.

If we consider the vectors $\psi(x_i)$ and not the vectors x_i to be the feature descriptions of the objects, the SVM development is conducted as before. The expression (1) becomes the following [6, 20]:

$$a(x) = w \cdot \psi(x) + b \tag{2}$$

Minimization (2) is equal to a task of the quadratic programming with linear limitation of the types of inequalities. The dual task depending only on the dual variables appears hereby; only the objects of control should be left in the sample; the result is expressed through the scalar product of the objects and not through objects them-selves; kernels can be used.

Let introduce additional variables ξ_i^+ and ξ_i^- which meaning equal the lose on the increased and decreased answer $a(x_i)$ according to the meaning ε.

In this case, the minimization task (2) can be rewritten into the equivalent form as a task of the quadratic programming with linear limitations-inequalities relating to variables w_i, b, ξ_i^+, ξ_i^-

$$\begin{cases} \frac{1}{2}\langle w, w\rangle + C\sum_{i=1}^{l}\left(\xi_i^+ + \xi_i^-\right) \to \min\limits_{w,b,\xi^+,\xi^-} \\ y_i - \varepsilon - \xi_i^- \le w \cdot \psi(x_i) + b \le y_i + \varepsilon + \xi_i^+, \ i = 1,\ldots,l \\ \xi_i^- \ge 0, \ \xi_i^+ \ge 0, \ i = 1,\ldots,l \end{cases} \tag{3}$$

The positive constant C is a control parameter of the method and allows finding the compromise between the minimization of the separating hyperplane and the summary error [25, 29, 30].

The Lagrangian is expressed through dual variables λ_i^+, λ_i^-, $i = 1,\ldots,l$, and the scalar products $\langle x_i, x_j\rangle$ are replaces by the kernel $K(x_i, x_j)$:

$$\begin{cases} L(\lambda^+, \lambda^-) = -\varepsilon\sum_{i=1}^{l}\left(\lambda_i^- + \lambda_i^+\right) + \sum_{i=1}^{l}\left(\lambda_i^- - \lambda_i^+\right)y_i + \\ -\frac{1}{2}\sum_{i,j=1}^{l}\left(\lambda_i^- - \lambda_i^+\right)\left(\lambda_j^- - \lambda_j^+\right)K(x_i, x_j) \to \max\limits_{\lambda^-,\lambda^+} \\ 0 \le \lambda_i^+ \le C, \ 0 \le \lambda_i^- \le C, \ i = 1,\ldots,l \\ \sum_{i=1}^{l}\left(\lambda_i^- - \lambda_i^+\right) = 0 \end{cases} \tag{4}$$

Only the range of coefficients λ_i^+, λ_i^-, $i = 1,\ldots,l$ will differ from zero, and the data relating to them are the support vectors [11, 27].

The regression equation is expressed through the dual variables:

$$a(x) = \sum_{i=1}^{l}\left(\lambda_i^- - \lambda_i^+\right)K(x_i, x_j) + b \tag{5}$$

There are several control parameters in this method: accuracy parameter ε, constant C and parameters relating to the chosen kernel type. All the parameters are interdependent. The constant C controls the smoothness and flatness of the approximation function: the bigger one C leads to the bigger error fine and makes the learning machine bulky; the smaller one C, in the contrary, leads to the excessive error "transfer" that worsens the algorithm accuracy. The parameter ε influences the smoothness and the number of control vectors [12, 13, 14].

RF is the algorithm of machine learning that lies in the use of the bagging method on the set of the decision trees with the use of the method of random subspaces and can solve the tasks of classification and regression [13].

CART (classification and regression tree) is based on decreasing the level of heterogeneity – the task of classification or the chosen error level of assessing prediction – the task of regression on each node of the tree.

The characteristics of the trees of RF lie in their development without the padding function – the usage of the full depth: since we consider the average result of the set of trees, there is no need in adjusting each of them that is a deviation from the standard CART algorithm [12, 18].

Training of separate trees in RF takes place independent of each other, on different subset which parts can be repeated due to the use of the bagging method in the algorithm.

Bagging (from bootstrap aggregation) is one of the first and the simplest types of ensembles based on the statistic bootstrap method. Leo Breiman developed it in 1994. The method lies in the equal selection of N objects from the sample with returning: an object is selected from the sample (we consider each object with probability 1/N) though every time from all output N objects. Approximately 37% of samples are out of the bootstrap sampling and are not used.

The probability of the object getting into the sample (i.e. it is taken N times):

$$\left(1-\frac{1}{N}\right)^N \approx 1-\frac{1}{e} \approx 63\% \tag{6}$$

The bagging lies in training the regressors or classifiers on the samples that are generated by the bootstrap and creating the summing regressor or classifier that average the results of all the algorithms in the regression tasks and in the case of classification – on the voting results [5, 19].

Bagging allows decreasing the dispersion of the taught classifier by decreasing the value of the error difference when training the model on different data sets or, in other words, prevents overfitting. The efficiency of bagging is achieved due to the basic algorithms being taught on different samples and having compensating errors because of the diversity; rejections and absent values can't get to a part of samples that makes the RF algorithm resistant to them.

If there are missed values of predictors for the full observation when developing the model with the RF method, the prediction for the case is based on the previous node of the corresponding tree [4, 16].

The method of random subspaces allows decreasing the level of correlation be-tween the trees and avoiding overfitting. When building each of the stated number of trees in RF while creating nodes the selection of the feature used for the basis of separation is done only from the randomly chosen features from the sets of all data features. The basis algorithms are taught on different subset of the feature description [15, 17].

It is worth noting that the absence of the need in the usage of a separate set of data for validation is an advantage of the algorithm: since a part of data does not get into the bootstrap sample (approximately 37%), the mean squared error and the percentage of the described dispersion is calculated with the help of an out-of-bag error.

3. Materials and methods

To build a prediction model, the authors gather a set of data with 15-min interval from the monitoring and control automated system (MCAS) of multi-storey building during the period of October 13, 2017 – February 12, 2018 that include 32 parameters: Date – date, Time – time, Tout – outer temperature, Tin – inner temperature, Tin_yst – setting 1 of inner temperature for mode 1, Tin_yst_max – influence on the setting of inner temperature, , Tin_yst1 – setting of the inner temperature for mode 0, Tv – temperature of the heat-carrying agent when powering the heating system, Tvmin – setting of the minimal temperature Tv, Tvmax – setting of the maximal temperature Tv, Tv_yst – setting of the heat-carrying agent temperature when powering the heating system, Tv_tg – heat-carrying agent temperature when powering the heating system on the temperature diagram, S – diagram pitch, P – diagram shift, T1_tg – heat-carrying agent temperature when powering the house on the temperature diagram, Tret – heat-carrying agent temperature in the reverse heating system piping, Tret_tg – heat-carrying agent temperature in the reverse heating system piping on the temperature diagram, Tam – the combined temperature of the outer air, Tad – smooth value of the outer temperature, etc.

The following measurements are used to assess the efficiency of the developed models on the study and test samples: root mean square error (RMSE), mean absolute error (MAE) and determination coefficient (R^2):

$$RMSE = \sqrt{\frac{\sum_{i=1}^{N}\left(y_i-\hat{y}_i\right)^2}{N}} \tag{7}$$

$$MAE = \frac{1}{N}\sum_{i=1}^{N}\left|\hat{y}_i - y_i\right| \tag{8}$$

$$R^2 = 1-\frac{\sum_{i=1}^{N}\left(y_i-\hat{y}_i\right)^2}{\sum_{i=1}^{N}\left(y_i-\bar{y}_i\right)^2} \tag{9}$$

where y_i – actual value, $\hat{y}_i$ – predicted value, N – number of values.

Root mean square error (RMSE) is used as a primary evaluation metric. Described dispersion is calculated with the help of an out-of-bag error [14].

Table 1. Value ranges of some predictors

No	Variable	Minimum, °C	Maximum, °C
1	Tout	-14.2031	15.1250
2	Tin	13.0000	19.9531
3	Tin_yst	12.0000	22.1094
4	Tin_yst_max	0.5000	0.5000
5	Tin_yst1	16.1250	20.1094
6	Tv	21.6562	67.1875
7	Tvmin	8.0000	45.0000
8	Tvmax	40.0000	80.0000
9	Tv_yst	0.0000	58.0000
10	Tv_tg	51.0000	66.0000
11	Tret	21.8437	140.0000
12	Tret_tg	46.0000	58.0000
13	Tam	-12.5781	14.7656
14	Tad	-10.6562	14.6719

4. Results and discussion

Hyperparameters of SVM model significantly influence the prediction accuracy and reliability. The number of parameters that require adjusting depend, first, on the choice of the kernel functions. Researches relating to the subject area often use the RBF (radial basis function) kernel to solve regression tasks, since it allows expressing non-linearly the sample in the high space and has a smaller number of hyperparameters for adjustment comparing to the polynomial kernel: kernel coefficient (γ), the "C" – constant of the regularization term in the Lagrange formulation (*C*), accuracy parameter (ε). The kernel coefficient equals $1/K$ as a default, where K – number of input variables. Thus, in this case γ = 1/31 = 0.032.

Since there in not a distinct method for determining the optimal adjustments of the model parameters, the adjustment of hyperparameters is the next stage. Grid search is a traditional ways of optimizing hyperparameters. It is an exhausting search through the manually determined subset of the hyperparameter space of the algorithm. The search algorithm should be guided by a metrics of efficiency that is usually measured by cross-validation in the training set. Since the hyperparameters being optimized are built in the Cartesian space and are checked in pairs when cross-validating, the algorithms suffers from the excessive dimension that leads to a significant increase of the execution time.

When cross-validating the train set of data is divided into k subsets of the same size. Each subset k is used as a set of data for checking while other subsets k-1 are used as a set of data for trainings. This research deals with the 10-times checks for choosing the optimal hyperparameters. Model parameters received after the grid search are given in Fig. 1.

```
Parameter tuning of 'svm':

- sampling method: 10-fold cross validation

- best parameters:
 epsilon cost
     0.2  128

- best performance: 1.596522
```

Fig. 1. Model parameters received after the grid search

RF method usually requires correction of the two main hyperparameters that influence maximally the adequacy and the result of the model: Number of trees (M) and minimal

number of variables used for splitting (n_{min}). Parameter M is a total number of the trees in the forest and relates to the efficiency of the calculation that creates the need in choosing such number of trees, which allows balancing the performance time and the prediction accuracy. 100 trees are chosen for our research, since the increase of the number do not result in the significant increase of the accuracy with the increase of the performance time. The typical value of the number of variables used for splitting (n_{min}) in the regression task is $p/3$, where p – number of input variables, in this research n_{min} – 10. The depth of trees is not limited in this work; the trees are developed in the full depth.

The table gives RMSE, R2 and MAE on the study and test samples for predicting Tv. The value of RMSE model of SVM is 0.95. Despite the accepted error level, time spent on the model adjustment and SVM sensitivity to the missing values, the complexity of the interpretations of the data contribution make the method too resource-consuming that, in its turn, causes the need in using more optimal method for predicting the heat-carrying agent temperature when powering the heating system.

Since random forest is used for the regression task, it is necessary to consider that the model will predict the value Tv adequately if the input values are within the range of the values of predictors (Table 1) used for the model training (train set).

The data are divided into two sets (train – 70% and test – 30%) before the model development. One set of 15-min data is used for modelling in both models.

The diagram of the comparison of the actual values of the heat-carrying agent temperature when powering the heating system and the values predicted by models with the additionally stated temperature of the outer air is given in Fig. 2.

In spite of the smaller error when using SVM method (table 2), RF algorithm is chosen for further research due to the opportunities of the result interpretation and non-obvious interrelations. The model training is decided to be conducted on every-minute data during the same period to increase the model accuracy (table 3).

Table 2. Results of prediction models performed by RF and SVM

Model	Train			Test		
	RMSE, °C	MAE, °C	R^2, %	RMSE, °C	MAE, °C	R^2, %
SVM	0.92	0.32	97.52	1.13	0.43	97.3
RF	1.1	0.39	97.49	1.19	0.42	97.13

Table 3. results of prediction model performed by RF (every-minute data)

Set	RMSE, °C	MAE, °C	R^2, %	Max. error, °C
Train	0.44	0.08	99.61	15.1
Test	0.41	0.075	99.65	14.95

There is a decrease of the RMSE value and the increase of the percentage of the describes dispersion on the approbation data. Thus, RF temperature model can be considered acceptable for the use aimed at predicting parameters of the heat-consuming system. Despite a big value of the maximal error, the authors note that the number of the predicted data on the approbation sample with the absolute value of error that higher than 5 degrees is 56 from 54,255 values.

The diagram of the comparison of the actual values of the heat-carrying agent temperature when powering the heating system and the values predicted by models with the additionally stated temperature of the outer air is given in Fig. 3.

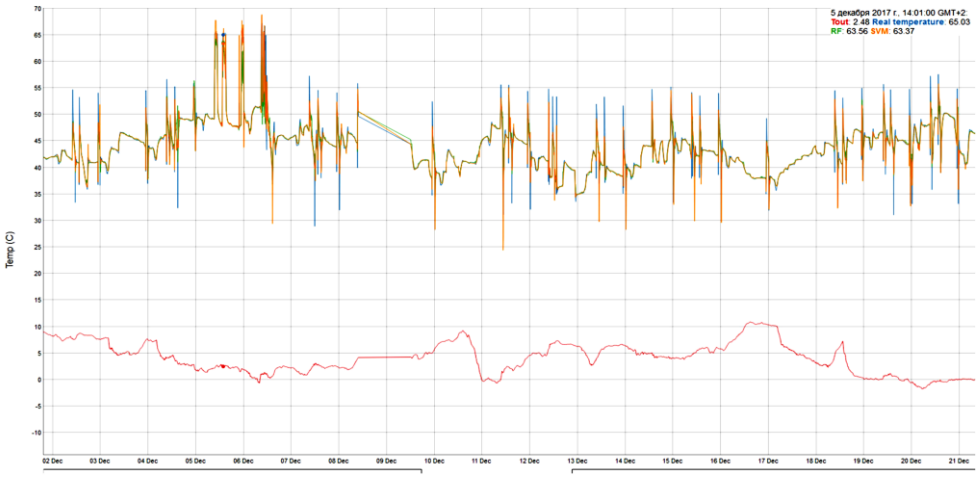

Fig. 2. The curve of the temperature estimated with the random forest and the SVM on the testing set

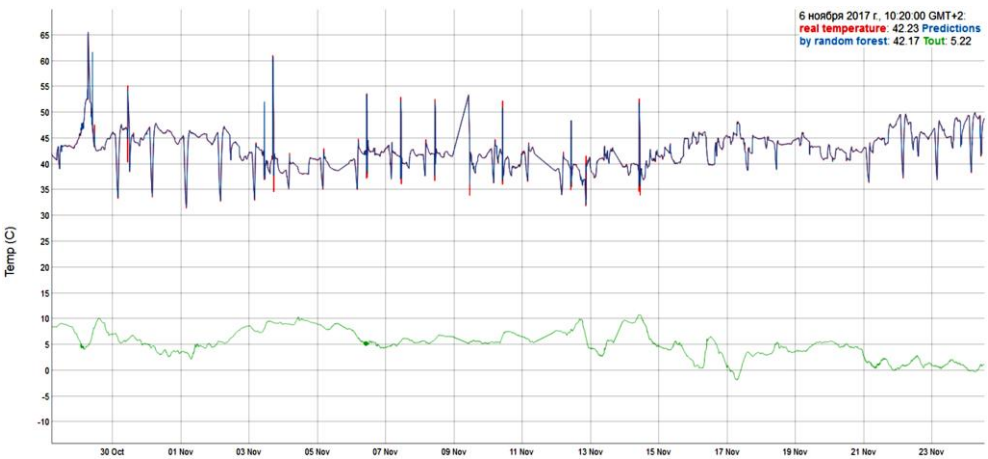

Fig. 3. The curve of the temperature estimated with the random forest on the testing set

The comparison of the result of the RF end model and the actual data is given on table 4. Mean value measuring the middle tendency in the set of data proves that the data predicted by the model are similar to the actual data. The standard deviation is the indicator of dispersing the values comparing to the values of the actual data is determined that SVM has almost similar standard deviation like actual data. The median of values received with the help of RF corresponds to the values received on the actual data. Minimal and maximal values allow dividing the data discharge. RF has a maximal value that is bigger than the actual data value. The kurtosis and skewness reflect the form of the data distribution. Skewness is a measurement of the data set symmetry. Kurtosis is the value describing the form of the distribution tail area and not the sharpness or the filling of the distribution [11, 30].

Table 4. Comparison of the statistical measures

Factor/Variable	Actual TV	RF
Mean	43.5	43.5
Median	43.8	43.8
Standard deviation	7.05	7.03
Kurtosis	3.14	3.16
Skewness	-1.26	-1.28
Range	45.56	45.14
Minimum	21.66	21.67
Maximum	67.22	66.81

The distribution of the mean minimal depth of each tree is studied to determine the importance of parameters: the depth of the node which splits on this variable and is the closest to the root of the tree (Fig. 4) and the complex measurement of the importance of variables (Fig. 5).

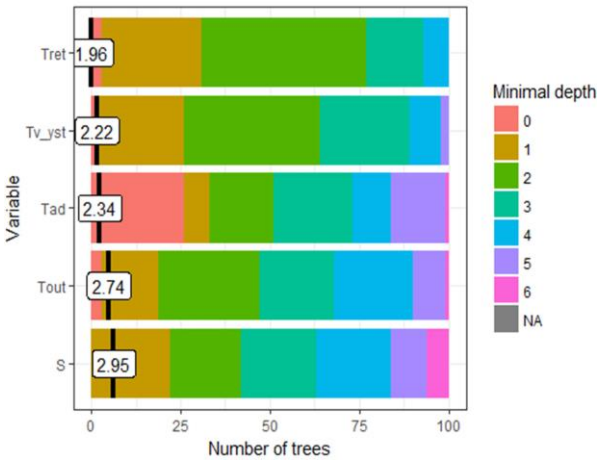

Fig. 4. The distribution of mean minimal depth

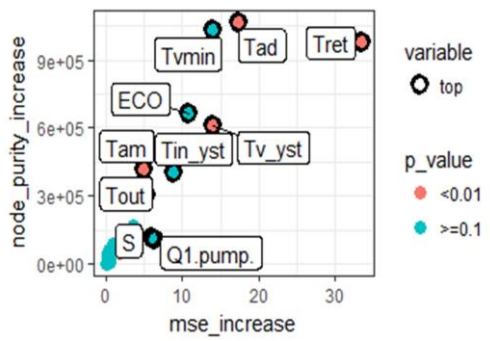

Fig. 5. The complex measurement of the importance of variables

Ordering variables on their mean minimal depth is quite accurate, thought considering the distribution of the minimal depth, the authors state that the predictor Tad should be assessed higher since it is the variable that is used more often for the first split at the root.

The values of the average increase of the mean square error [15] after the random replacement of the variable value (mse_increase) and increase of the mean node purity (node_purity_increase) which is the sum of square errors (SSE) are chosen as measurement of the complex (Fig. 5). P-values based on the binominal distribution of the node number that are split on the variable are used additionally. If the variable is important, it is used for splitting more often comparing to the random choice.

Although Tar and Tret are similar in the increase of the node purity and p-value based on the binominal distribution, the second one influences the prediction error more. It is worth noting that despite the high values of the chosen measurements on the variable Tvmin, the test based on the binominal distribution proves that the theoretical number of nodes where the variable is used for splitting exceeds the actual number, thus, the variable is seldom used for splitting and influences the prediction insignificantly.

5. Conclusions

The use of MCAS allows collecting a significant number of data relating to the system parameters and decisions accepted by the energy manager in addition to the decrease of the level of the consumed heating energy. It causes the opportunity for studying the issues of the efficient usage of energy sources with the help of the analysis of historic data and the support of the taken decisions. The article deals with comparing the methods of machine learning that allows applying the historic data instead of the complex mathematical apparatus to describe the building heat balance: RF and SVM are accuracy, source cost and the opportunity to interpret the results and non-obvious interrelations. RF algorithm is chosen for further research.

The authors develop the model of the heat-carrying agent temperature when powering the heating system based on the data on the parameters of the electronic weather-dependent controller with the help of RF algorithm. The values of the heat-carrying agent temperature in the reverse piping of the heating system and the smooth value of the outer temperature influence the value of the mean square error, besides these variables are often used to split the trees at the root that proves their significance. RMSE of the RF model on the test data equals 0.41°C. Maximal error is 14.96°C.

References

[1] Ahmad M. V. et al.: Tree-based ensemble methods for predicting PV power generation and their comparison with support vector regression. Energy 164, 2018, 465–474 [http://doi.org/10.1016/j.energy.2018.08.207].
[2] Ahmad, M. V. et al.: Predictive modelling for solar thermal energy systems: A comparison of support vector regression, random forest, extra trees and regression trees. Journal of Cleaner Production 203, 2018, 810–821 [http://doi.org/10.1016/j.jclepro.2018.08.207].
[3] Ahmad M. W. et al.: Trees vs Neurons: Comparison between random forest and ANN for high-resolution prediction of building energy consumption. Energy and Buildings 147, 2017, 77–89 [http://doi.org/10.1016/j.enbuild.2017.04.038].
[4] Azarov A. D. et al.: Class of numerical systems for pipe-line bit sequential development of multiple optoelectronic data streams. Proc. SPIE 4425, 2001, 406-409.
[5] Azarov A.D. et al.: Static and dynamic characteristics of the self-calibrating multibit ADC analog components. Proc. SPIE 8698, 2012, 86980N.
[6] Breiman L.: Out-of-bag estimation. Tech. rep. University of California, 1996 [https://www.stat.berkeley.edu/~breiman/OOBestimation.pdf].
[7] Breiman L.: Random Forests. Machine Learning 45(1), 2001, 5–32 [http://doi.org/10.1023/A:1010933404324].
[8] Dong B. et al.: Applying support vector machines to predict building energy consumption in tropical region. Energy and Buildings 37(5), 2005, 545–553 [http://doi.org/10.1016/j.enbuild.2004.09.009].
[9] Esen H. et al.: Modelling of a new solar air heater through least-squares support vector machines. Expert Systems with Applications 36(7), 2009, 10673–1068 [http://doi.org/10.1016/j.eswa.2009.02.045].
[10] Geng Y. et al.: Building energy performance diagnosis using energy bills and weather data. Energy and Buildings 172, 2018, 181–191 [http://doi.org/10.1016/j.enbuild.2018.04.047].
[11] Kaczmarek C. et al.: Measurement of pressure sensitivity of modal birefringence of birefringent optical fibers using a Sagnac interferometer. Optica Applicata 45(1), 2015, 5–14.

[12] Kukharchuk V. V. et al.: Method of magneto-elastic control of mechanic rigidity in assemblies of hydropower units. Proc. SPIE 10445, 2017, 104456A.
[13] Kukharchuk V. V. et al.: Noncontact method of temperature measurement based on the phenomenon of the luminophor temperature decreasing. Proc. SPIE 10031, 2016, 100312F.
[14] Kukharchuk V. V. et al.: Discrete wavelet transformation in spectral analysis of vibration processes at hydropower units. Przegląd Elektrotechniczny 93(5), 2017, 65–68.
[15] Kvyetnyy R. et al.: Blur recognition using second fundamental form of image surface. Proc. SPIE 9816, 2015, 98161A.
[16] Kvyetnyy R. et al.: Method of image texture seg-mentation using Laws' energy measures. Proc. SPIE 10445, 2017, 1044561.
[17] Kvyetnyy R. et al.: Modification of fractal coding algorithm by a combination of modern technologies and parallel computations. Proc. SPIE 9816, 2015, 98161R.
[18] Osadchuk A. et al.: Pressure transducer of the on the basis of reactive properties of transistor structure with negative resistance. Proc. SPIE 9816, 2015, 98161C.
[19] Osadchuk O. et al.: The Generator of Superhigh Frequencies on the Basis Silicon Germanium Heterojunction Bipolar Transistors. 13th International Conference on Modern Problems of Radio Engineering, Telecommunications and Computer Science (TCSET), 2016, 336 – 338.
[20] Paluszyska A.: Structure mining and knowledge extraction from random forest with applications to The Cancer Genome Atlas project. 2017. [https://rawgit.com/geneticsMiNIng/BlackBoxOpener/master/randomForestExplainer_Master_thesis.pdf].
[21] Parfenenko Yu. V. et al.: Prediction the heat consumption of social and public sector buildings using neural networks. Radio Electronics, Computer Science, Control 2, 2015, 41–46.
[22] Perekrest A. et al.: Key Performance Indicators Assessment Methodology Principles Adaptation for Heating Systems of Administrative and Residential Buildings. IEEE Problems of Automated Electrodrive. Theory and Practice (PAEP), 2020, 1–4.
[23] Perekrest A. et al.: Complex information and technical solutions for energy management of municipal energetics. Proc. SPIE 10445, 2017, 1044567 [http://doi.org/10.1117/12.2280962].
[24] Ruiz L. G. B. et al.: Energy consumption forecasting based on Elman neural networks with evolutive optimization. Expert Systems with Applications 92, 2018, 380–389 [http://doi.org/10.1016/j.eswa.2017.09.059].
[25] Smolarz A. et al.: Fuzzy controller for a lean premixed burner. Przegląd Elektrotechniczny 86(7), 2010, 287–289.
[26] Vapnik V., Chapelle O.: Bounds on error expectation for support vector machines. Neural Computation 12 (9), 2000, 2013–2036 [http://doi.org/10.1162/089976600300015042].
[27] Vedmitskyi Y. G. et al.: New non-system physical quantities for vibration monitoring of transient processes at hydropower facilities, integral vibratory accelerations. Przegląd Elektrotechniczny 93(3), 2017, 69–72.
[28] Wei Y. et al.: A review of data-driven approaches for prediction and classification of building energy consumption. Renewable and Sustainable Energy Reviews 82, 2018, 1027–1047 [http://doi.org/10.1016/j.rser.2017.09.108].
[29] Wójcik W. et al.: Concept of application of signals from fiber-optic system for flame monitoring to control separate pulverized coal burner. Proc. SPIE 5484, 2004, 427–431.
[30] Wójcik W. et al.: Vision based monitoring of coal flames source. Przegląd Elektrotechniczny 84(3), 2008, 241–243.

Prof. Andrii Perekrest
e-mail: pksg13@gmail.com

Doctor of Technical Sciences, Professor, Head of the Department of Computer Engineering and Electronics.
The main direction of his scientific activities is development of energy and resource saving building, automation energy efficiency

http://orcid.org/0000-0002-7728-9020

Ph.D. Vladimir Chenchevoi
e-mail: vladchen.86@gmail.com

Ph.D., Associate Professor of Department of Systems of Automatic Control and Electric Drive.
The main direction of his scientific activities is development of energy and resource saving building, automation energy efficiency

http://orcid.org/0000-0002-6478-3767

Ph.D. Olga Chencheva
e-mail: chenchevaolga@gmail.com

Ph.D., Associate Professor
The main direction of his scientific activities is development of energy and resource saving building, automation energy efficiency

http://orcid.org/0000-0002-5691-7884

Ph.D. Alexandr Kovalenko
e-mail: a.kovalenko1964@gmail.com

Ph.D., associate professor, Department of Technology and Equipment of Machine-building Industries, Faculty of Computer Technologies of Mechanical Engineering and Design, Cherkasy State Technological University.
He has 37 scientific papers. The main direction of his scientific activities is development of mathematical models of physical processes and objects, their numerical study and optimization as a part of CAE.

http://orcid.org/0000-0002-5073-3507

M.Sc. Mykhailo Kushch-Zhyrko
e-mail: k.zh.mhl@gmail.com

Ph.D. student at the Department of Computer Engineering and Electronics.
The main direction of his scientific activities is development of energy and resource saving building, automation energy efficiency

http://orcid.org/0000-0001-9622-9114

Ph.D. Aliya Kalizhanova
e-mail: kalizhanova_aliya@mail.ru

Candidate of physical and mathematical sciences, professor, University of Power Engineering and Telecommunications, the chief researcher of the Institute of Information and Computational Technologies of the Ministry of Education and Science CS of the Republic of Kazakhstan. Scientific interests of the leader: mathematical modeling of systems, models of transport systems network analysis, optimization methods, technologies for developing sensor systems for signals receive-transmit, mathematical modeling of Bragg fiber gratings.
http://orcid.org/0000-0002-5979-9756

Prof. Yedilkhan Amirgaliyev
e-mail: amir_ed@mail.ru

Doctor of technical sciences, professor, Head of the Laboratory of Mathematical and Computer Modelling of the Institute of Information and Computing Technologies of the Science Committee of RK MES. The Institute is the leading organization in the field of information technology in the country. The main directions of the research laboratory is an intelligent decision-making systems, robotics, wireless sensor technology, computer modelling of technological processes, etc.

http://orcid.org/0000-0002-6528-0619

http://doi.org/10.35784/iapgos.3030

received: 19.07.2022 | revised: 28.08.2022 | accepted: 15.09.2022 | available online: 30.09.2022

NATURAL-SIMULATION MODEL OF PHOTOVOLTAIC STATION GENERATION IN PROCESS OF ELECTRICITY BALANCING IN ELECTRICAL POWER SYSTEM

Petr Lezhniuk[1], Viacheslav Komar[1], Iryna Hunko[1], Daniyar Jarykbassov[2,3], Dinara Tussupzhanova[4], Bakhyt Yeraliyeva[5], Nazbek Katayev[6]

[1]Vinnytsia National Technical University, Vinnytsia, Ukraine, [2]Kazakh Academy of Transport & Communication, Almaty, Kazakhstan, [3]Alatau Zharyk Kompaniyasy JSC, Almaty, Kazakhstan, [4]Almaty University of Energy and Communications named after Gumarbek Daukeev, Almaty, Kazakhstan, [5]M. Kh. Dulaty Taraz Regional University, Taraz, Kazakhstan, [6]Kazakh National Women's Teacher Training University, Almaty, Kazakhstan

***Abstract**. The paper analyzes the methods of stabilizing generation schedules of photovoltaic stations (PV) in electric power systems (EPS) in the process of balancing electricity. Since PV is characterized by the instability of electricity production due to dependence on weather conditions, an automatic system for forecasting their generation schedules (ASFG) for the next day has been created to increase the energy efficiency of PV. The process of automating the prediction of the power stations as part of the balancing group of the power stations and the algorithm for adjusting the prediction of power plant generation are considered. The criterion for managing the forecasting process is the minimization of the difference between the values of forecasted and actual generation for the same period of time. Checking the performance and tuning of the ASFG PV in order to evaluate its functioning and the effectiveness of its application in the task of balancing the states of the EPS is possible only by means of simulation. It is shown that based on the nature of the process of forecasting the generation of PV using ASFG, it is advisable to use simulation modeling. Since the actual value of generation is constantly monitored during balancing using ASFG, it is possible to use these values during simulation and proceed to real-time simulation. In this case, modeling is considered as an experimental method of research, according to which it is not the object itself that is subjected to perturbations and research, but the software-implemented computer model of the object. The real-life simulation model of the operation of the PV makes it possible to more fully consider the various modes of their operation in the process of balancing the modes of the EPS as part of the balancing group and to more reasonably choose decisions regarding the participation of the PV in generation, taking into account weather conditions and the limitations of the system operators of transmission and distribution of electricity.*

Keywords: power system, photovoltaic stations, unstable generation, stabilization of generation schedules, natural-simulation modeling

NATURALNY MODEL SYMULACYJNY GENERACJI STACJI FOTOWOLTAICZNEJ W PROCESIE BILANSOWANIA ENERGII ELEKTRYCZNEJ W SYSTEMIE ELEKTROENERGETYCZNYM

***Streszczenie**. W artykule przeanalizowano metody stabilizacji harmonogramów generacji stacji fotowoltaicznych (PV) w systemach elektroenergetycznych (EPS) w procesie bilansowania energii elektrycznej. Ponieważ PV charakteryzuje się niestabilnością produkcji energii elektrycznej ze względu na zależność od warunków atmosferycznych, w celu zwiększenia efektywności energetycznej PV stworzono automatyczny system prognozowania ich harmonogramów generacji (ASFG) na dzień następny. Rozpatrywany jest proces automatycznego kojarzenia predykcji elektrowni w ramach grupy bilansującej elektrownie oraz algorytm korygowania predykcji generacji elektrowni. Kryterium zarządzania procesem prognozowania jest minimalizacja różnicy pomiędzy wartościami generacji prognozowanej i rzeczywistej dla tego samego okresu czasu. Sprawdzenie działania i dostrojenie ASFG PV w celu oceny jego funkcjonowania i skuteczności zastosowania w zadaniu bilansowania stanów EPS jest możliwe tylko za pomocą symulacji. Wykazano, że na podstawie charakteru procesu prognozowania generacji PV z wykorzystaniem ASFG, wskazane jest zastosowanie modelowania symulacyjnego. Ponieważ podczas bilansowania z wykorzystaniem ASFG stale monitorowana jest rzeczywista wartość generacji, możliwe jest wykorzystanie tych wartości podczas symulacji i przejście do symulacji w czasie rzeczywistym. W tym przypadku modelowanie traktowane jest jako eksperymentalna metoda badań, zgodnie z którą perturbacjom i badaniom poddawany jest nie sam obiekt, ale zaimplementowany programowo komputerowy model obiektu. Model symulacyjny pracy PV w warunkach rzeczywistych umożliwia pełniejsze uwzględnienie różnych trybów ich pracy w procesie bilansowania trybów pracy EPS w ramach grupy bilansującej oraz bardziej racjonalny wybór decyzji dotyczących udziału PV w wytwarzaniu, z uwzględnieniem warunków pogodowych oraz ograniczeń operatorów systemu przesyłu i dystrybucji energii elektrycznej.*

Słowa kluczowe: system elektroenergetyczny, stacje fotoelektryczne, niestabilność generowania, stabilizacja wykresów generowania, modelowanie makietowo-imitacyjne

Introduction

Despite the benefits of photovoltaic stations (PV), they have a number of problems when using them in electric power systems (EPS). One of them is their unstable generation during the day due to dependence on natural conditions. This is especially evident when their electricity generation begins to significantly affect the electricity balancing process in the EPS. This occurs when the relative part of PV in the EPS reaches a value that is commensurate with and greater than the reserves of maneuvering power in the EPS. As a rule, this happens when the capacity of renewable energy sources (RES) in the EPS reaches 20% or more [1, 8]. With the development of solar and wind power stations, in order to be able to regulate the frequency and voltage in the EPS and ensure the stability of the energy system, it is necessary to increase the reserve of maneuvering power in it or to use means to compensate for the unstable generation of the PV [2, 24]. In essence, this is also capacity reservation, but with the use of the PV itself. Since PV can work in the modes of surplus or deficit of electricity in the EPS, they must be provided with means of energy storage and its conversion into electricity if necessary. These can be, for example, electrochemical electricity storage system, hydrogen technologies, hydraulic storage stations [3, 23]. Other methods can be used to coordinate unsustainable power generation with the EPS tasks in the process of power and electricity balancing: biogas technologies, changing electricity consumption schedules by consumers in accordance with power generation schedules, etc. [9, 12].

The task of achieving the minimum difference between the actual schedule of generation by EPS stations and the declared (forecast) for a certain period of time is common to all means of reserving the instability of PV generation and methods of agreeing schedules of electricity generation and consumption in the EPS. The declared electricity generation schedule in the EPS is formed on the basis of the forecasted consumption schedule for the same time period. As a rule, in operational tasks, this period of time is the next day. Accordingly, for PV, the task is set in such a way that it is necessary to forecast their hourly generation schedule for the next day, depending on weather conditions and their technical condition [10, 17].

1. Formulation of the task for the formation of a natural-simulation model of generation of PV in the process of balancing electricity in the EPS

The EPS is considered, which includes nuclear, thermal and large hydroelectric power stations (NPS, TPS, HPS), as well as power stations that use renewable energy sources, in particular PV. To ensure stability in periods of maximum (minimum) consumption or limited throughput of the centralized power supply system, the optimization of PV modes is relevant. In order to minimize deviations from the centrally set schedule of aggregate generation of the PV under the established restrictions on primary energy resources, the task is formulated as follows [11]:

$$\int_{t_0}^{t_k} \frac{1}{2}\left(P_{PV}(t) - \sum_{i=1}^{n} P_i(t) \right)^2 dt \to \min , \qquad (1)$$

taking into account the balance limit:

$$P_{CPS}(t) + \sum_{i=1}^{n} P_i(t) - P_{load}(t) - \Delta P(t) = 0 \qquad (2)$$

where $P_{PV}(t)$ – the predicted total schedule of PV generation in the balancing group; $P_i(t)$ – actual generation of all n PV of the balancing group;P_{CPS} – centralized power supply from TPS, NPS, HPS; $P_{load}(t)$ – total load of electricity consumers; $\Delta P(t)$ – power losses in electrical grids.

Task (1), as a rule, should be considered as a whole for the EPS. Another option is when for simpler and more accurate control of generation of PV stations in the EPS, several balancing groups of PV stations are allocated. In each balancing group, an automated system of commercial electricity accounting (ASCEA) is installed for each PV and forecasting of the hourly schedule of electricity generation for the next day is carried out [13]. That is, for each i-th PV, the actual and forecasted electricity generation values for a given time period are known. Therefore, in accordance with problem (1), for each i-th PV, the problem of achieving a certain accuracy between the predicted and actual electricity generation for a certain time, for example, one hour, is formulated:

$$\delta_i = \frac{w_i^P - w_i^A}{w_i^A} \le \delta_{per} \qquad (3)$$

where w_i^P, w_i^A – predicted and actual values of electricity generation of the i-th PV for the same time; δ_i, δ_{per}– current and permissible value of errors (the margin of error is often set at 0.05).

In order to control the value of the error δ_i, it is necessary to simulate two graphs: the predicted and the actual generation of the PV. The error δ_i as the difference between these graphs should be in the permissible zone or approaching it (see Fig. 1). The following implementations of this task are possible: 1) the actual schedule is what it is, and the predicted schedule is adjusted every hour or every 15–20 minutes; 2) the predicted schedule is as it is, and the actual one is adjusted to the predicted one, more precisely, it is entered into the permissible zone. True, in the last option, electricity generation and, accordingly, profit decreases. It is decided what is better: whether to lose electricity generation, or to reduce sanctioning fines for deviations from the permissible zone? A third option is also possible, when the predicted schedule is simultaneously adjusted and the actual generation is changed to enter the permissible zone or approach it.

The goal of the article is to develop a natural-simulation model for researching the processes of short-term forecasting and operational management of the generation of PV stations in the EPS mode balancing system using SMART Grid technologies.

2. Automation of the PV forecasting process as part of the balancing group

In order to build an effective algorithm for forecasting the schedule of electricity generation by photovoltaic stations (Fig. 2) and its successful automation, it is necessary to have a suitable array of output data and software. The first step is the formation of a mathematical model of the PV itself. For this, it is necessary to have information with the characteristics of PV modules, which are written in the passport data. The determining information is: the orientation of the modules relative to the South, the angle of their inclination, the type of module, the number of elements of the photovoltaic module, the no-load voltage, the short-circuit current, etc. The configuration of the electrical circuit of the PV consists of information on the number of modules in the string, the number of strings per inverter, the number of inverters and the number of transformer substations.

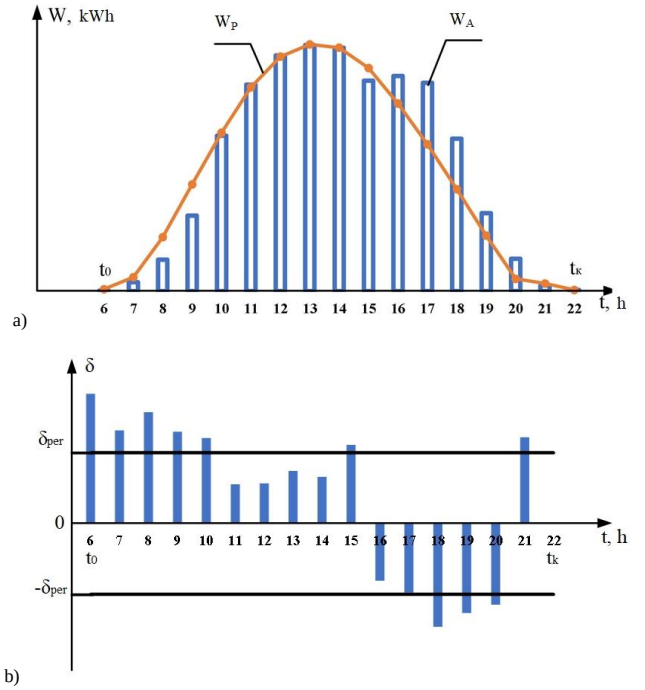

Fig. 1. Schedule of the actual and forecasted generation of PV (a) and, accordingly, forecasting errors (b)

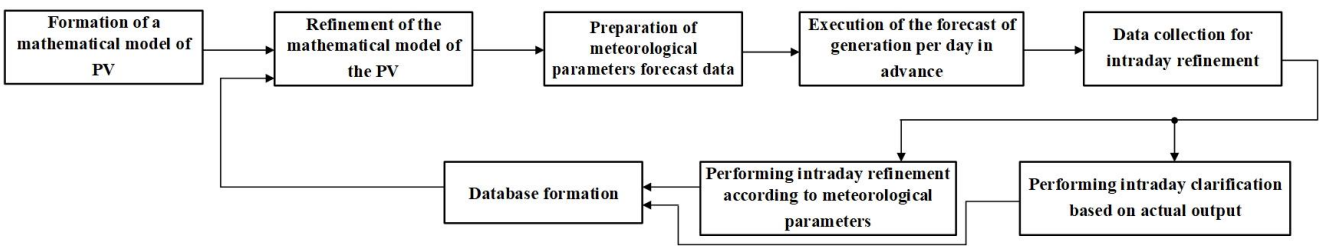

Fig. 2. Structural diagram of the automation of the PV forecasting process as part of the balancing group

Since the operating conditions of PV are constantly changing, their mathematical model is constantly refined. A parameter database (DB) is being created to automate the process of refining the PV generation prediction model. Usually, MySQL is used, so it slows down its work when it is significantly filled. The necessary meteorological parameters from various services are collected in the database. There are quite a lot of such services on the market, all of them allow you to organize API communication, which allows you to automate the data collection process, in addition, there are a significant number of libraries in C#, Python, etc., which implement such communication.

After making a forecast for one-day ahead, no company that provides such services can guarantee sufficient accuracy, so it is necessary to use the possibility of intraday correction. In different countries, the market accepts the results of this adjustment with different discreteness. As a rule, this time is from 15 minutes to 2 hours. Obviously, the smaller this interval, the better results can be obtained. Intraday adjustments can be made in two ways: recalculating the generation schedule based on refined meteorological parameters or based on the results of monitoring the current production of electric energy by the PV.

The first algorithm requires the use of weather services that adjust their forecasts during the current day. The second requires the use of telemetry, which can provide polling almost every minute, or ASCEA, which usually operates with greater discreteness.

After correction, the results are sent to the operator of the balancing group.

All data on meteorological parameters, production forecast and the actual value of the produced energy are also entered in the database for further correction of the mathematical model of the power station. Such correction is carried out during the first month of provision of forecast services and then provided as needed to take into account seasonal changes and degradation processes in the equipment of the PV.

3. Automation of the PV forecasting process as part of the balancing group

The logical scheme for calculating the adjusted value of the hourly forecast of PV generation for the next hour of the current day is as follows. Hour i is determined, from which i_b starts and ends i_e of PV electricity generation, where i is the current value of the hour number.

Further:

- $i = i_b$, the prediction error for the i-th hour is determined $\delta_i = \frac{w_i^P - w_i^A}{w_i^A}$;
- i = i+1, the prediction error for the i+1st hour is determined $\delta_{i+1} = \frac{w_{i+1}^P - w_{i+1}^A}{w_{i+1}^A}$.

If $\delta_{i+1} \succ 0$, then:

if $\delta_{i+1} \le \delta_{per}$, then k = 1 $w_{i+1}^P = k\, w_{i+1}^P$ (That is, the forecast remains the same, in the permissible area);

if $\delta_{i+1} \le \delta_i$, then we go to the beginning of the cycle i = i+1 ("Prediction" is getting closer to "fact");

if $\delta_{i+1} \succ \delta_i$ ("Forecast" differs from "fact") and $\delta_{i+1} \succ \delta_{per}$, then $k = 1 - \delta_i$ and $w_{i+1}^P = k\, w_{i+1}^P$ and go to the beginning of the cycle i = i+1.

If $\delta_{i+1} \prec 0$, then:

if $\delta_{i+1} \ge -\delta_{per}$, then k = 1 $w_{i+1}^P = k\, w_{i+1}^P$ (That is, the forecast remains the same, in the permissible area!);

if $\delta_{i+1} \succ \delta_i$, then we go to the beginning of the cycle i = i+1 ("Prediction" is getting closer to "fact");

if $\delta_{i+1} \prec \delta_i$ ("Forecast" differs from "fact") and $\delta_{i+1} \prec -\delta_{per}$, then $k = 1 - \delta_i$ and $w_{i+1}^P = k\, w_{i+1}^P$ and go to the beginning of the cycle i = i+1.

In Fig. 3 shows the algorithm of the hourly adjustment program for forecasting the electricity generation of the PV, and Fig. 4 shows an example of the result of an hourly prediction of the generation of the PV using the forecast correction program with error compensation δ_i,.

As can be seen, the forecasting error of PV electricity generation per day decreased from 15.6% to 4.7%. That is, the algorithm with compensation of hourly errors in forecasting the generation of PV gives a satisfactory result.

It can be used along with the adjustment of PV generation based on hourly refinement of daily meteorological parameters.

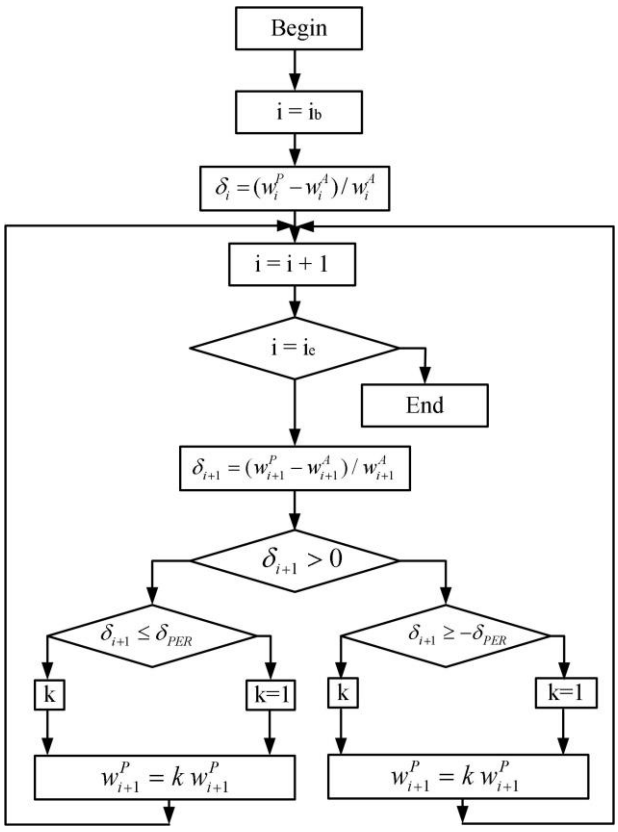

Fig. 3. Algorithm of the program for hourly adjustment of forecasting of electricity generation of PV

4. Natural-simulation modeling of PV generation in the process of balancing EPS modes

The process of automating the forecasting of the power station generation schedules and their current adjustment in accordance with changes in operating conditions, primarily weather conditions, is an important element of the successful balancing of the state of the power station.

As in all dynamic processes related to electric power systems, and in our case, a feature is the impossibility of studying them in different modes directly on the object [7, 21].

Therefore, checking the performance and setting of the automatic generation forecasting system (AGFS) of the PV in order to evaluate its functioning and the effectiveness of its application in the task of balancing the modes of the EPS is possible only by means of simulation.

Based on the nature of the AGFS process, it is advisable to use simulation modelling.

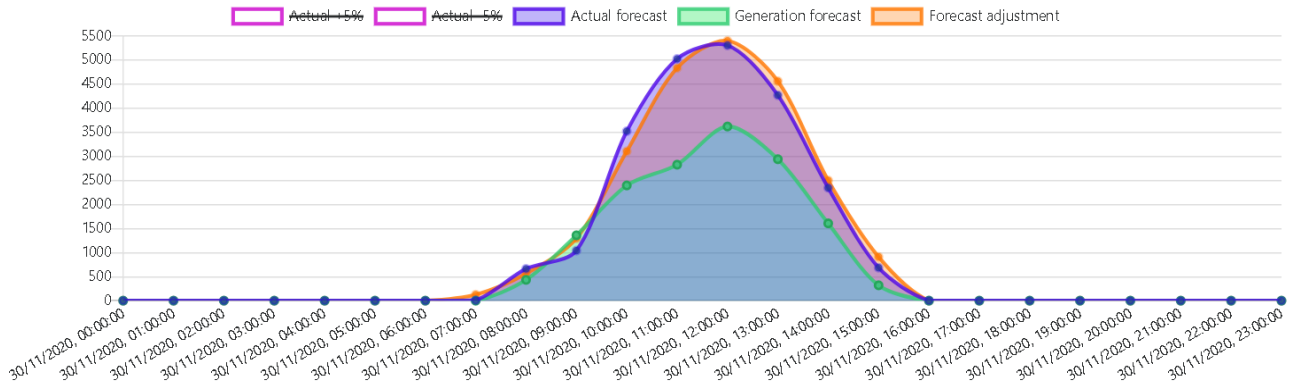

Fig. 4. Correction of PV generation forecasting based on the results of error control

Because during balancing using AGFS, the actual value of generation is constantly monitored w_i^A, then it is possible to use these values during simulation. Such a model can be classified as natural-simulation [7, 22]. The method of nature-simulation modeling is considered as an experimental method of research, according to which the object itself is subjected to disturbance and research, but the simulation model of the object implemented on a computer.

In Fig. 5 shows the structure of the nature-simulation model (NSM) of checking and adjusting the AGFS PV.

It contains a functional model of the object (FMO), which together with the AGFS PV forms a closed system. This allows for a fairly accurate modeling of the control object to achieve the maximum probability of testing the AGFS PV, since the test system can reproduce an arbitrary mode of the object in the permissible area of existence. Along with the benefits, it is necessary to note a certain complexity in the implementation of the structure, which is primarily reflected in the need for not only informational, but also physical compatibility of the model and AGFS. The assessment of the correct functioning of the AGFS in this structure is provided by comparing the outputs of the AGFS with the control data of the modes of the real object.

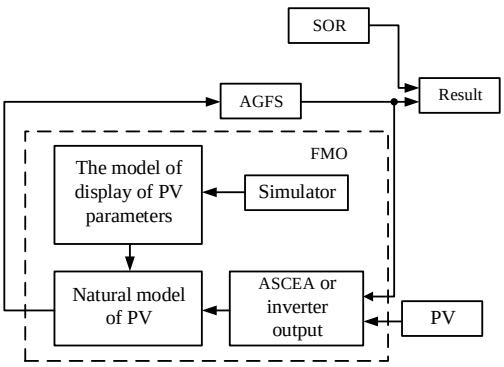

Fig. 5. The structure of the natural-simulation system of AGFS testing

The key link in the organization of the NSM test system is the construction of the simulator, which is part of the FMO.

The simulator is designed to reproduce a certain number of modes of the object. The regime of PV [14, 15] is an admissible set of its states and processes of its change. During the transition from one state to another, the current mode indicators (mode parameters) change, which occurs under the influence of external disturbances (changes in loads) or control signals to change the actual generation of the power stations.

When creating and testing a control system based on simulation, the continuous operation of the PV is replaced by a set of characteristic modes. The correct implementation of this principle ensures the necessary reliability of the process of checking control devices. Correctness in this case implies the appropriate choice of modes and their number, a set of parameters and the accuracy of their measurement by means of the automatic system of commercial electricity accounting (ASCEA). When introducing signals simulating the parameters of the PV modes into the control system, system operator restrictions (SOR) of the EPS are taken into account. First of all, this is the mode of the EPS in relation to the deficit or surplus in the electricity balance.

The mathematical formulation of the task of organizing the FMO simulator can be formulated as follows. Dependency given (function):

$$y = f(t), \tag{4}$$

where f and, accordingly, y is an n-dimensional vector in the general case, $f = [f_1, f_2, \ldots, f_n]^T$; independent variable t, which is the time specified on some finite interval $t \in [t_0, t_k]$. The process of reproducing function (4) is organized subject to certain conditions: the necessary modeling accuracy must be ensured, given, for example, in the form of a value

$$\varepsilon = \left|\max y(t) - \bar{y}(t)\right|, \quad t_0 \le t \le t_k \tag{5}$$

that is, in the form of the maximum permissible difference between the reproduced process y(t) and its machine model; the system for entering function (4) into the model should have the properties of flexible control (stop, repeat, change modes, etc.) to ensure the effectiveness of the test system as a whole; the reproduction process must be controlled to ensure the reliability and validity of the exam results.

Experiments can be carried out both according to a previously prepared plan and sequentially, the purpose of a new experiment is established based on the analysis of the results of the previous one. In the case of implementing the simulator on a computer, not only the actual simulator program is created, but also the experiment management program, which leads to the fact that: the state of the simulator does not change after conducting the next experiment and the next experiment is conducted; after each experiment, the simulator returns to the initial state common to all experiments; the results of the experiment lead to a change in the imitator, that is, the model [4].

The PV functional model has the same transforming properties as the modeled object itself. FMO PV is built with a defined set of structures and is described in the form of an equation

$$\mathbf{Y} = F(\mathbf{y}, \mathbf{x}, \mathbf{u}, t) \tag{6}$$

where $\mathbf{y}$ – n-dimensional vector of initial coordinates $y_i(t)$, $i = \overline{1, n}$; $\mathbf{x}$ – r-dimensional vector of disturbing influences $i = \overline{1, r}$; $\mathbf{u}$ – m-dimensional vector of controlling influences $u_i(t)$, $i = \overline{1, m}$; the ranges of variable values are known: $y \in Y$, $x \in X$, $u \in U$.

An important condition determining the field of application of the model is the requirement that the input and output variables of the model are natural. If there are requirements for naturalness of variables, the model is based on the following principles [5, 16]. As three main, functionally independent interdependent parts, the system contains a reference model of the reproduced object (reproduced image), fixed in the form of an information

carrier, a controlled carrier of real variables (real model) and a control system (control device). The functioning of the modeling system is organized by the control system, which provides control of the input variables of the real model in such a way that its output variables change according to the law set by the reference model, that is, the nature model monitors the behavior of the reference model.

The reference model is the carrier of the image of the modeled object. It is implemented by dependencies that record the capacity of the certified generation of the PV or the calculated generation according to the reference model is the carrier of the image of the modeled object. It is implemented by dependencies that record the capacity of the certified generation of the PV or the calculated generation according to the volt-ampere characteristics (VAC) taken during the commissioning of the PV. In all cases, the reference model is described by the given equation (6) or solves it. The variables reproduced by the reference model differ from real processes by scale factors. The time scale of the output signals is equal to one, since real control signals must be received at the input of the natural model in the simulation system.

Since the natural model must satisfy the requirements for the full-scaleness of its initial characteristics [5, 6], its internal properties must satisfy the controllability conditions. This is achieved by ASCEA or parameters transmitted directly from the output of PV inverters. In the latter case, additional equipment is required, but it is possible to control the ASCEA errors, which are introduced into the results of the actual electricity generation of the PV. If a natural model is selected, then its equation is known and has the form

$$\mathbf{Z} = \Phi(\mathbf{z},\ \mathbf{v},\ \mathbf{x},\ t) \tag{7}$$

where $\mathbf{z} \in \mathbf{Z}$ – coordinates of the mode, i.e. modeling variables of the system; $\mathbf{v} \in \mathbf{V}$ – control variables; $\mathbf{x} \in \mathbf{X}$ – natural external influences (the same variables that enter the equation of the modeled object, since the object and the model are designed to work in the same external environment).

According to the principle of replacing the object with a model, equations (6) and (7) do not coincide, i.e. $F \neq \Phi$, and, in addition, the scopes of the variables included in these equations do not coincide, and the dimensions of the vectors **y** and **z** may also not coincide. Therefore, in the general case, it is impossible to ensure a full reproduction in the model of all modes of operation of the modeled object [18, 19, 20].

The control system is built on the basis of known control principles. The choice of the method of synthesis of the control system and its structure is determined by similarity criteria [21].

Restrictions on the ratio between the simulated variables y_i coming from the reference model and the modeling variables z_i reproduced by the natural model are accepted as similarity criteria. The determining criteria of similarity are the functionals of the modeling error $\varepsilon = y - z$.

Different structures of modeling systems can be obtained depending on the type of given equations of the reference model, the adopted control method (by disturbance, by deviation, program method), type of control law. We will consider the organization of some structures of modeling systems using the example of a linear object described by a linear, in general, matrix equation of the form

$$\mathbf{Y} = \mathbf{F}\mathbf{y} + \mathbf{u} \tag{8}$$

where is the vector of initial coordinates is **y** and the vector of input influences **u**, having the same dimension n; **F** is a matrix of operators of dimension n×n .

The structure of the modeling system implementing the functional model of the object is described by the equation

$$\mathbf{Z} = \mathbf{\Phi}\mathbf{z} + \mathbf{v} \tag{9}$$

where the components **z**, **v** and **F** are analogous to the components of equation (7) and have the same dimension.

The similarity of the model and the object is ensured by the input into the modeling system of the control signal **u** with the condition

$$\mathbf{Z} = \mathbf{Y} \tag{10}$$

Since condition (10) is equivalent to equality

$$\mathbf{F}\mathbf{y} + \mathbf{u} = \mathbf{\Phi}\mathbf{z} + \mathbf{v} \tag{11}$$

and this control leads to the observation of coordinates **z** by the ratio of variables **y**.

Management is carried out using regional dispatch centers, which are coordinated by operators of the transmission and distribution system. The control criterion is the achievement of a stable balance of electricity in the system with the optimal composition of available means. One of the necessary methods of balancing is the limitation of RES generation in order to maintain the frequency and voltage within acceptable limits. In natural-simulation modeling, a complex system of balancing groups of PV can be divided into subsystems. In this case, a simulation model is developed for individual subsystems, other subsystems are not simulated and a natural experiment is carried out for them.

A subsystem can be a separate PV or a group of PV united by some feature (for example, territorially, when a group of PV is characterized by the same meteorological parameters). At the same time, appropriate AGFS with their own databases are used, which does not require any additional costs for information support of natural-simulation modeling.

5. Conclusions

The application of the developed natural-simulation model of the process of assessing the compliance of the predict and the actual generation of the PV makes it possible to assess in real time the consequences of non-fulfillment of the power balance by individual balancing groups. This is taken into account for the improvement of the existing operational and information complex of PV with means of compensation for the instability of their generation. As a result, the efficiency of the functioning of distribution electric grids increases, operational management of distributed generation operating modes based on SMART Grid principles is improved, and power quality indicators are improved.

As a result of research and consistent implementation of natural-simulation modeling to improve the automatic forecasting system of PV generation during short-term forecasting and operational management of PV generation in the EPS mode balancing system, regulation accuracy increases. This approach to reducing the error of compensating the instability of generation of power stations creates favorable conditions for their wider and effective use in the EPS. A technical possibility is provided for increasing the volume of PV generation in electric power systems in accordance with the values declared by investors and the technical conditions issued for them to connect to electric grids.

References

[1] Amrane Y. et al.: Study of Photovoltaic Power Plant Distribution Network Integration: Case of Algeria-Djanet City Distribution Network. Algerian Large Electrical Network Conference (CAGRE), 2019, 1–6 [http://doi.org/10.1109/CAGRE.2019.8713294].

[2] Chudy A.: The Review of Selected Electrical Energy Storage Techniques. Informatyka, Automatyka, Pomiary w Gospodarce i Ochronie Środowiska 9(1), 2019, 23–28 [http://doi.org/10.5604/01.3001.0013.0890].

[3] Dragoon K. et al.: Hydrogen as Part of a 100% Clean Energy System. IEEE Power & Energy Magazine 20(4), 2022, 85–95 [http://doi.org/10.1109/MPE.2022.3168947].

[4] Dubovoi V.M. et al.: Modeling and optimization of systems. TD Edelweiss, Vinnytsia 2017.

[5] Htun Htun L. et al.: Full-scale and Simulation Modeling of a Centralized Control System for Transport Robots. International Journal of Open Information Technologies 8(4), 2020.

[6] Kukharchuk V. V. et al.: Information Conversion in Measuring Channels with Optoelectronic Sensors. Sensors 22(1), 2022, 271 [http://doi.org/10.3390/s22010271].

[7] Lebedev A. N.: Modeling in scientific and technical research. Radio and Communication, Moscow 1989.

[8] Lezhniuk P. D. et al.: Relative evaluation of balancing means of electric power systems with renewable energy sources. Visnik VPI 3, 2022, 24–30 [http://doi.org/10.31649/1997-9266-2022-162-3-24-30].

[9] Lezhniuk P. et al.: Criterion modeling of the process redundancy of renewable energy sources power generation instability by electrochemical accumulators. Computational Problems of Electrical Engineering 11(2), 2021, 12–17.

[10] Lezhniuk P. et al.: Forecasting Hourly Photovoltaic Generation On Day Ahead. IEEE 6th International Conference on Energy Smart Systems (ESS), 2019, 184–187 [http://doi.org/10.1109/ESS.2019.8764245].
[11] Lezhniuk P. et al.: Optimal Integration of Photoelectric Stations in Electric Networks. LAP LAMBERT Academic Publishing, 2019.
[12] Ma Y. et al.: Multi-objective Optimal Scheduling of Power Systems Based on Complementary Characteristics of Heterogeneous Energy Sources. IEEE 4th Conference on Energy Internet and Energy System Integration (EI2), 2020, 1533–1538 [http://doi.org/10.1109/EI250167.2020.9347052].
[13] Malvoni M., Hatziargyriou N.: One-day ahead PV power forecasts using 3D Wavelet Decomposition. 2019 International Conference on Smart Energy Systems and Technologies (SEST), 2019, 1–6 [http://doi.org/10.1109/SEST.2019.8849007].
[14] Nerush V. B., Kurdega V. V.: Simulation modeling of systems and processes: Electronic educational edition. NUU "KPI", Kyiv 2012.
[15] Rudenko D. V., Vasyuchenko P. V.: Modeling of physical processes of operation of solar photovoltaic batteries. Scientific notes of TNU named after V. I. Vernadskyi 30(2), 2019, 42–47.
[16] Tomashevskyi V. M.: Modeling of systems. Publishing Group, Kyiv 2005.
[17] TOP-5 Program for Modeling Solar Power Plants. http://solargis.com
[18] Vasilevskyi O. M. et al.: Spectral method to evaluate the uncertainty of dynamic measurements. Technical Electrodynamics 4, 2017, 72–78.
[19] Vasilevskyi O. M. et al.: Vibration diagnostic system for evaluation of state interconnected electrical motors mechanical parameters. Proc. SPIE 10445, 2017, 104456C [http://doi.org/10.1117/12.2280993].
[20] Vasilevskyi O. M.: Metrological characteristics of the torque measurement of electric motors. International Journal of Metrology and Quality Engineering 8(7), 2017 [http://doi.org/10.1051/ijmqe/2017005].
[21] Venikov V. A.: Theory of similarity and modeling. Higher School, Moscow 1976.
[22] Verlan A. F., Galkin V. V.: Simulation of dynamics of energy objects in systems of testing software control tools. Naukova dumka, Kyiv 1991.
[23] Xu G. et al.: A Hierarchical Energy Scheduling Framework of Microgrids With Hybrid Energy Storage Systems. IEEE Access 6, 2018, 2472–2483.
[24] Zedak C. et al.: Photovoltaic and Battery Systems Control and Monitoring for Energy Management using IoT. 9th International Renewable and Sustainable Energy Conference (IRSEC), 2021, 1–6 [http://doi.org/10.1109/IRSEC53969.2021.9741199].

D.Sc. Eng. Petr Lezhniuk
e-mail: lezhpd@gmail.com

Professor of the Department of Electric Stations and Systems, Vinnytsia National Technical University. Research interests include application of similarity theory and modeling for optimum control of electro power systems modes. He has published 600 scientific papers, developed a number of basically new devices and software complexes for computers. The main directions of his scientific activity are mathematical modelling and optimization of electric power systems modes.

http://orcid.org/0000-0002-9366-3553

D.Sc. Eng. Viacheslav Komar
e-mail: kvo1976@ukr.net

D.Sc. (Eng), professor, Head of the Department of Electric Stations and Systems, Vinnytsia National Technical University. He has published 155 scientific papers. The main direction of his scientific activity is automation of optimal control of electric power systems modes.

http://orcid.org/0000-0003-4969-8553

Ph.D. Iryna Hunko
e-mail: iryna_hunko@ukr.net

Ph.D., associate professor, Department of Power Plants and Systems, Vinnytsia National Technical University. She has published 75 scientific papers. The main direction of his scientific activity is optimal control of electric power systems with renewable energy resources.

http://orcid.org/0000-0003-2868-4056

M.Sc. Daniyar Jarykbassov
e-mail: daniyarjarykbassov@yandex.kz

M.Sc., graduated from NJSC "Almaty University of Energy and Communications named after Gumarbek Daukeev", Faculty of Power Engineering. Works at "Alatau Zharyk Kompaniyasy JSC".
He has published 6 scientific papers. The main direction of his scientific activity is automation of optimal control of electric power systems modes.

http://orcid.org/0000-0002-0051-5560

M.Sc. Dinara Tussupzhanova
e-mail: diko__13@mail.ru

M.Sc., graduated from NJSC "Almaty University of Energy and Communications named after Gumarbek Daukeev" Faculty Labor protection. She has published 5 scientific papers.
The main direction of his scientific activity is labor protection, safety precaution, fire safety, environmental protection.

http://orcid.org/0000-0002-1316-2020

M.Sc. Bakhyt Yeraliyeva
e-mail: yeraliyevabakhyt81@gmail.com

Senior lecturer of the Information Systems Department, Faculty of Information Technology, M. Kh. Dulaty Taraz Regional University, Taraz, Kazakhstan. Research interests: Information technologies, fiber-optic technologies, microprocessor systems.

http://orcid.org/0000-0002-8680-7694

Ph.D. Nazbek Katayev
e-mail: nazbekkataev@gmail.com

Candidate of Pedagogical Sciences, Associate Professor of the Department of Computer Science and Applied Mathematics of Kazakh National Women's Teacher Training University. Author of more than 70 publications. Research area: Big data, software engineering, data processing.

http://orcid.org/0000-0003-0501-3719

http://doi.org/10.35784/iapgos.2903 received: 18.03.2022 | revised: 24.06.2022 | accepted: 08.07.2022 | available online: 30.09.2022

APPLICATION FOR VIBRATION DIAGNOSTICS

Anzhelika Stakhova
National Aviation University, Department of Computerized Electrical Systems and Technologies, Kiev, Ukraine

Abstract. *This paper considers the issue of developing an application for vibration diagnostics of bearings of functional pairs of critical structures, this application should help in monitoring and diagnosing bearings, using vibration signals, without disassembling the functional unit itself. It is known that vibration diagnostics is effective and there is a tendency to reduce the cost of its implementation. Monitoring and diagnostics based on vibration parameters can be applied at any time, even after several years of equipment operation, when the costs of preventive maintenance and repair will exceed the economically justified value. Also, in the work, the basics of the subject area for the development of mobile applications are considered, and a review of existing solutions is made. Requirements for the application for performing vibration diagnostics are formulated. The architecture is designed and the data description for the application of vibration diagnostics is carried out.*

Keywords: vibration diagnostic, application, bearing, vibration signal

APLIKACJA DO DIAGNOSTYKI WIBRACYJNEJ

Streszczenie. *W artykule poruszono problematykę opracowania aplikacji do diagnostyki wibracyjnej łożysk par funkcjonalnych konstrukcji krytycznych, która to aplikacja powinna pomóc w monitorowaniu i diagnozowaniu łożysk z wykorzystaniem sygnałów wibracyjnych, bez demontażu samego zespołu funkcjonalnego. Wiadomo, że diagnostyka wibracyjna jest skuteczna i istnieje tendencja do obniżania kosztów jej wykonania. Monitoring i diagnostyka na podstawie parametrów drgań może być stosowana w dowolnym momencie, nawet po kilku latach eksploatacji urządzeń, gdy koszty obsługi prewencyjnej i napraw przekroczą ekonomicznie uzasadnioną wartość. W pracy rozważane są również podstawy tematyki tworzenia aplikacji mobilnych oraz dokonywany jest przegląd istniejących rozwiązań. Sformułowano wymagania dla aplikacji do wykonywania diagnostyki wibracyjnej. Zaprojektowano architekturę i wykonano opis danych dla aplikacji diagnostyki wibracyjnej.*

Słowa kluczowe: diagnostyka wibracyjna, aplikacja, łożysko, sygnał wibracyjny

Introduction

At the present stage of development in production, a continuous technological process is very important, which is ensured by the trouble-free operation of the equipment. This requires a constant increase in the requirements for the accuracy of measuring control points of equipment and methods of technical control, as part of technological processes. Therefore, one of the urgent tasks is to conduct vibration control.

Increased vibration in machines can cause serious damage. Stresses caused by vibration contribute to the accumulation of damage in materials, cracks and damage. Such problems can be detected at the beginning using vibration measurement methods. Thus, there is a great need to measure, evaluate and control the vibration of industrial equipment.

Thus, improving the technical level, quality, and reliability of machines, and improving their use largely depends on the technical diagnostics used [6, 11]. Continuous diagnostics or vibration monitoring is used for critical units or expensive machines. Monitoring provides continuous monitoring of the condition of the machine and alarm in case exceeding the maximum permissible vibration level. Continuous vibration testing allows [9]:

1) To build a graph of the vibration level change depending on the operating time.
2) To predict the unit's residual operating time before scheduled repairs.
3) To avoid damage to the unit due to a sharp increase in vibration.

Periodic vibration diagnostics is used to diagnose machines that do not require continuous vibration monitoring. Periodic vibration diagnostics allows [5]:

1) To identify the causes of increased vibration, when vibration becomes perceptible, but has not yet led to a breakdown of the mechanism.
2) To assess the compliance of the vibration level with the established standards.
3) To determine the possibility of further operation or methods of modernization of "problem" units.

Diagnostic methods are based on the analysis of vibration generated in rolling bearings by frictional forces [5]. One of the methods for searching for defects that have found wide application is frequency (spectral) analysis of vibration [6], which allows it to be divided into components of different frequencies, excited by different sources of vibration forces and having different natures and different properties.

The presence of a defect in the rolling bearing during their rotation leads to the appearance of intense spectral components in the vibration signal [10], the position of which on the frequency axis depends on the location of the defect, the rotation speed, and the geometric dimensions of the diagnosed nodes. The amplitude of these spectral components determines the degree of development of a particular defect. Thus, the frequency analysis of the spectrum of the vibration signal makes it possible to determine both the defect itself and its location [3]. It should be noted that different methods for detecting defects are in varying degrees sensitive to different degrees of development of a defect in a controlled object. For example, spectral analysis, as a rule, begins well to identify defects at their middle stage of development [4].

Monitoring and diagnostics based on vibration parameters can be applied at any time, even after several years of equipment operation, when the costs of preventive maintenance and repair will exceed the economically justified value. The diagnostic program automatically, knowing the rotational speed, finds all the characteristic frequencies of the bearing elements (cage, rollers, rings), determines the amplitude of these harmonics, and stores it. After collecting the required statistical sample, it determines and calculates the standard deviation (RMS). The standard deviation is used to determine the measure of the spread of a random variable.

To increase the efficiency of diagnostics, successive refinements of the diagnostic algorithm are necessary with the accumulation of sufficient information. Thus, the work will consider the issue of developing an application for vibration diagnostics of bearings, this application should help in checking bearings without disassembling the friction unit itself.

1. Analysis of technologies of development of web applications

The development of a web application consists of many stages, the difference in the cost of the site will depend on the amount of time that a software engineer needs to spend to implement certain functionality. Today, website developers have a wide variety of choices regarding which language (or technology) to use to build a website. There are many options: Perl, PHP, ASP,

ASP.NET, JSP, Coldfiisio, etc. The most common (by a large margin from the rest) today are PHP and ASP.NET [8].

PHP (Hypertext Preprocessor) is a language for writing server-side scripts. The language interpreter is free and open-source, versions have been created for various web servers, primarily for Apache and Internet Information Services [2].

The advantages of PHP are: fast customization of a ready-made solution (for example, overlaying a new design on an existing site, which is managed by a CMS); a large number of free solutions on this platform; absolute free of charge; simplicity of language; any data in a language can implicitly be textual.

ASP.NET (Active Server Pages .Net) is a tool for developing web applications from Microsoft. Asp.net is not a programming language, it is a technology that includes many components [7].

The advantages of ASP.NET include: availability of visual programming tools – reducing development time by 2 or more times; implementation of the application object model; executable code – compiled application; Microsoft.net technology support is built into Microsoft OS; built-in support for AJAX technology – any form element can be executed in the "classic" native version or using AJAX [7].

For an experimental study of the effectiveness of development technologies, it is necessary to create a website and evaluate which technology made it possible to achieve the set goals as much as possible while spending a minimum amount of time and effort to implement the project.

Thus, after the implementation of the project, it is necessary to analyze the development process and identify by means of which technology it was possible to achieve the maximum result, and estimate the time during which this result was achieved.

Thus, after the implementation of the project, it is necessary to analyze the development process and identify using which technology it was possible to achieve the maximum result and estimate the time during which this result was achieved.

To implement this system, the following set of subsystems is required:

1) Application with a graphical interface for Windows.
2) Api – a server application for working with data written in php.
3) MySQL – a database for storing registered users and data on diagnostics of functional units, which is not desirable to replace, otherwise you will have to rewrite most of the server application.
4) Chrome, since the application is written based on a chrome application in JavaScript, and if it is replaced, you will have to rewrite almost the entire client application.

1.1. Functional requirements

In this subsection, we will define what functionality will be in the application. To do this, we will use a use case diagram.

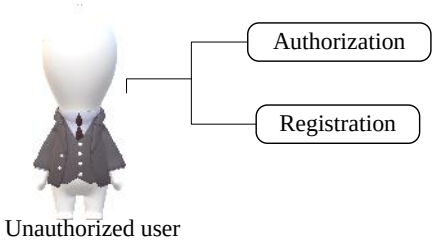

Fig. 1. Diagram of application use cases for an unauthorized user

Figure 1 shows a diagram of the application use cases for a user who has not yet been logged into the application. This diagram shows that to access any functions of the application, you must have your account in this application.

1) Authorization. The first thing a user needs to start working on the application is to log in to the system using their account. As soon as the user is logged in, the application creates a request through the server to the database and checks if this user exists with this password. If such a username and password are in the database, then an answer comes about the authorization of the user, if such a user was not found, then the answer comes that "The username or password was entered incorrectly.
2) Registration. If the user does not have an account, then his first step is to create an account before he can start working in the application. When the user clicks the registration button, the application opens the corresponding form, which he must fill out. Upon completion of this, a request will be created, and as a result of the execution of which a new account will be created in this application with the data of this user. Then he will be able to start working on this application.

Figure 2 shows a diagram of the use cases for the application. This diagram shows all the capabilities of this application from the point of view of a simple Operator and Administrator. The following main factors can be distinguished that interact with this system.

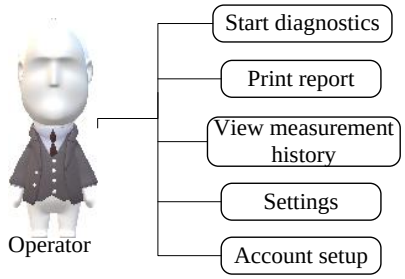

Fig. 2. Diagram of application use cases after authorization in the system

1) Operator (Administrator). An application user is an operator who performs the actual diagnostics of a functional unit or an administrator who is responsible for the system's performance, the work of operators, etc. Depending on the role, the user is assigned different access rights. So, for example, if a user has administrator rights, he can not only view the history of diagnostics of all functional units but also change or even delete any of the accounts of any of the operators.
2) To start diagnostics. After authorization, if the authorized user is the Operator, then he can start the calibration after he sets up the calibration process itself. And he can configure this in the diagnostic parameters, which can be set in advance.
3) To print the report. After completing the work, the operator can print the entire report for the entire working day. The report will indicate the number of the functional unit, the time when it was checked, which of the operators checked it, what indicators the operator received at the end of the diagnosis, and whether this functional unit is defective or not. But you can also get all this data for any period of work and any of the operators.
4) To view the history of measurements, for example, if at the end of the week you need to view the entire history of measurements and then print the necessary data for a certain period or a certain operator, then this can be done in this function. In other words, first, you view the history of all diagnostics, and then a report is generated based on this data and printed.
5) Diagnostic parameters. Before proceeding with the diagnostics, the operator must enter the appropriate parameters, which he can obtain by diagnosing the calibration pair, which is already with a defect in the bearing. Then he can proceed with the calibration of other functional pairs that need to be checked.
6) Setting up accounts. When a user is logged in and his account has administrator rights, then he has access to this function, which allows not only completely changing the account data, but also completely deleting the account. And the changeable data also includes the issuance or removal of administrator rights from any account.

When describing the architecture of the developed application, a general component diagram was designed to display the interaction of the logical parts of the application, which is shown in figure 3.

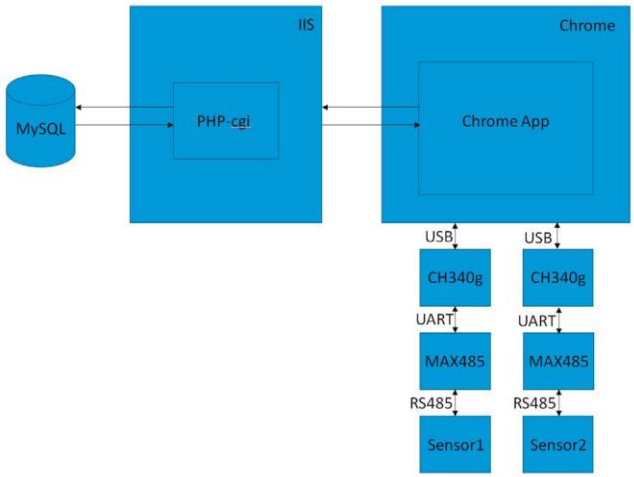

Fig. 3. Diagram of the components of the designed system

MySQL is the database that stores all measurement and account data for all operators.

PHP-cgi is an HTTP server with a back-end application on it, which processes data and requests from the client application and sends the necessary data from the database:

- add user – the function responsible for registering new accounts;
- change user – the function responsible for changing the account and for changing the account data;
- delete user – the function responsible for deleting an account;
- get measure chart – a function responsible for receiving "raw" data, that is, without processing;
- get measures –function responsible for obtaining measurement results after diagnostics;
- login – the function responsible for user authorization;
- save measure – Saving measurements obtained during diagnostics;
- user list – a list of all user accounts;
- auth is a function that is responsible for user authorization, that is, it checks the existence of a particular account.

Chrome App – A client web application that is responsible for obtaining data on the nodal pairs using two sensors that measure vibration and then receive the standard deviation, based on which you can find out whether the bearing is working or repairs are required:

- login – a function that generates a request to the server for user authorization;
- print – a function that is responsible for printing the generated report on the diagnostics of the bearings of the nodal pairs;
- start – the function responsible for the beginning of receiving data from sensors that measure vibration;
- disconnect – a function that is responsible for disconnecting an account, in other words, an exit;
- users – a function that opens a list of users who are registered in the system;
- history.cancel & history.filter – functions that are responsible for applying a specific filter in the history of all diagnostics per-formed, all functional pairs;
- save_measure – the function is responsible for saving the data that was received after diagnostics of the node pair;
- settings.cancel – the function that is responsible for canceling the settings, returning all diagnostic parameters to their default values;
- settings.start_calibration – the function responsible for starting the calibration, this is the diagnostics of the calibration functional pair, which is known in advance to be defective;
- users.add – a function that generates a request to the server to add new users, i.e. creating a new account;
- users.modal.add, users.modal.change, users.modal.delete – functions that are responsible for all operations that an operator with administrator rights can carry out, for changing account information, for deleting an account, for adding data to an account, for example, issuing administrator rights.

All data to the application is received and sent in JSON format. This format was chosen for readability and lightness, rather than, for example, XML.

1.2. Description of the database

The application has its own local database, which stores information not only about all accounts, but also about all performed calibrations, all node pairs. And all this information is stored in JSON format. List of tables and values:

Measuring table:

- ID (Integer) – identifier;
- calibration (TinyInt) – data obtained during the diagnostics of the calibration functional pair;
- wheelset_number (Integer) – number of functional pair;
- operator_id (Integer) – operator identifier;
- operator_opinion (Text) – operator's opinion, which he makes after diagnosing a functional pair;
- date (Biglnteger) – date of the diagnostics;
- sensor1 (Json) – sensor # 1;
- sensor2 (Json) – sensor # 2;
- sensor1_max_sko (Integer) – maximum RMS value from sensor # 1;
- sensor2_max_sko (Integer) – maximum RMS value from sensor # 2;
- sensor1_ max (Integer) – maximum value of raw data, without processing from the first sensor;
- sensor2_max (Integer) – maximum value of raw data, without processing from the second sensor:
- sensor1_solution (TinyInt) – shows the state of the functional pair to sensors # 1;
- sensor2_solution (TinyInt) – shows the state of the functional pair to sensors # 2.

Session key table:

- user (Integer) – data of the account of the operator who diagnosed one of the functional pairs;
- key (VarChar) – foreign keys;
- auth_date (TimeStamp) – date and time of the diagnostic session.

Users table:

- ID (Integer) – account identifier;
- login (VarChar) – account login;
- pass (VarChar) – account password;
- first_name (VarChar) – the name of the operator in the account;
- middle_name (VarChar) – middle name of the operator in the account;
- last_name (VarChar) – operator's surname in the account;
- admin (TinyInt) – the presence or absence of rights;
- deleted (TinyInt) – the account has been deleted or not.

2. Implementation of the application

The application was implemented in the Netbeans IDE, an open-source environment for software developers. The environment provides all the tools you need to create professional desktop applications, enterprise, mobile and web applications on the Java platform, as well as C / C ++, PHP, JavaScript, Groovy, and Ruby.

The client application was implemented in JavaScript (js) and the backend was implemented in PHP. PHP is a server-side programming language that runs on the server-side, while JavaScript is executed in the browser on the user side.

JavaScript – Supports object-oriented, imperative b functional styles. Plus, a large number of all kinds of frameworks have been created for it, sharpened for different tasks, and facilitating the development process.

PHP is a programming methodology based on representing a program as a collection of objects, each of which is an instance of a certain class, and the classes form an inheritance hierarchy.

Ideologically, OOP is an approach to programming to modeling information objects, which solves at a new level the main task of structured programming: structuring information from the point of view of controllability, which significantly improves the controllability of the modeling process itself, which, in turn, is especially important when implementing large projects.

After starting the application, the operator can log into his account and start his work, or find the necessary data and print it.

After going through the authorization process, the operator can immediately start diagnostics if the diagnostics settings have been preset. The operator can print a report on the diagnostics of functional pairs, absolutely for any period. The report will reflect all the information about each diagnostic process. Based on information from history, a report is formed and determined. In other words, in history, you can find out for what period the report needs to be generated for reporting.

3. Conclusion

The current state of technologies of vibration control of equipment with measurement of vibration parameters is considered and analyzed in the work. The simplest means of vibration control includes a measuring transducer, an analyzer (actually a vibrometer), as well as an external program for collecting and analyzing measurements. The issue of developing an application for vibration diagnostics of bearings is considered. All the main positions were analyzed that are associated with the design, development and commissioning of applications for vibration diagnostics of bearings of functional pairs of critical structures. The following tasks were completed:

1) The materials and experience of development in the field of creating web applications, conducting vibration diagnostics and checking bearings for wear using vibration diagnostics have been studied.
2) Analyzed technologies that will be useful in the development of this application and which will help to simplify its development.
3) Based on the data obtained, an application for vibration diagnostics of bearings of functional pairs of critical structures was developed and implemented.
4) The results were analyzed and the efficiency of the application for vibration diagnostics of bearings of functional pairs was determined.

The web application is fully implemented under the Windows operating system.

- As a result of the work done, the following conclusions can be drawn:
- the architecture of the application is built based on the chrome application;
- an application for vibration diagnostics of bearings of functional pairs of critical structures has been implemented;
- convenient search and automatic generation of reports of necessary data on diagnostics of bearings of functional pairs of critical structures is organized;
- a back-end application was developed to process the received data and interact with the database.

The work aimed at designing an application for vibration diagnostics of bearings will improve the efficiency of defect detection based on the results of vibration measurements and promptly eliminate detected bearing defects without disassembling the functional unit itself.

References

[1] Azeez N. Alex A.: Detection of rolling element bearing defects by vibration signature analysis: A review. 2014 Annual International Conference on Emerging Research Areas: Magnetics, Machines and Drives (AICERA/iCMMD), 1–5.

[2] Gilmore W.: Beginning PHP and MySQL: from novice to professional. Apress 2010.

[3] Jena D., Panigrahi S.: Precise measurement of defect width in tapered roller bearing using vibration signal. Measurement 55, 2014, 39–50.

[4] Kolobov A.: Vibrodiagnostics. Theory and Practice. Infra-Inzheneriya, Moscow 2020.

[5] Kostiukow B., Naumenko A.: Vibrodiagnostika porshnevykh kompressorov. Kompressornaya tekhnika i pnevmatika 3, 2002, 30–31.

[6] Kvasnikov V., Stakhova A.: Vibration Measurement Technologies and Systems. Safety in Aviation and Space Technologies. Springer, Cham 2022, 53–62.

[7] Mishra A.: Critical comparison of PHP and ASP .NET for web development. International Journal of Scientific & Technology Research 3(7), 2014, 331–333.

[8] Nizamutdinov M.: Defense and Attack Tactics for Web Applications. Petersburg 2017.

[9] Petrukhin S.: Osnovy vibrodiagnostiki i sredstva izmereniya vibratsii. Infra-Inzheneriya, Moscow 2010.

[10] Saucedo-Dorantes J. et al.: Multiple-fault detection methodology based on vibration and current analysis applied to bearings in induction motors and gearboxes on the kinematic chain. Shock and Vibration, 2016.

[11] Stakhova A.: Monitoring System of Vibroacoustic Parameters of a Working Zone. International Journal of Aviation Science and Technology 2(02), 2022, 64–72.

[12] Vafaei S., Rahnejat H., Aini R.: Vibration monitoring of high speed spindles using spectral analysis techniques. International Journal of Machine Tools and Manufacture 42(11), 2002, 1223–1234.

Ph.D. Eng. Anzhelika Stakhova
e-mail: sap@nau.edu.ua

Doctoral student at the National Aviation University (NAU). Associate Professor of Computerized electrical systems and technologies department NAU. Main scientific direction – systems for measuring mechanical quantities, the control and forecasting of the technical condition.

http://orcid.org/0000-0001-5171-6330

http://doi.org/10.35784/iapgos.3042

received: 31.07.2022 | revised: 24.09.2022 | accepted: 25.09.2022 | available online: 30.09.2022

DEEP NEURAL NETWORKS FOR SKIN LESIONS DIAGNOSTICS

Magdalena Michalska-Ciekańska
Lublin University of Technology, Department of Electronics and Information Technology, Lublin, Poland

Abstract. *Non-invasive diagnosis of skin cancer is extremely necessary. In recent years, deep neural networks and transfer learning have been very popular in the diagnosis of skin diseases. The article contains selected basics of deep neural networks, their interesting applications created in recent years, allowing the classification of skin lesions from available dermatoscopic images.*

Keywords: deep neural networks, transfer learning, dermatoscopic images, skin lesions diagnostics

GŁĘBOKIE SIECI NEURONOWE DLA DIAGNOSTYKI ZMIAN SKÓRNYCH

Streszczenie. *Nieinwazyjna diagnostyka nowotworów skóry jest niezwykle potrzebna. W ostatnich latach bardzo dużym zainteresowaniem w diagnostyce chorób skóry cieszą się głębokie sieci neuronowe i transfer learning. Artykuł zawiera wybrane podstawy głębokich sieci neuronowych, ich ciekawe zastosowania stworzone w ostatnich latach, pozwalające na klasyfikację zmian skórnych z dostępnych obrazów dermatoskopowych.*

Słowa kluczowe: głębokie sieci neuronowe, transfer learning, obrazy dermatoskopowe, diagnostyka zmian skórnych

Introduction

In recent years, skin cancers, and in particular melanoma, have been quite often diagnosed in the world. Malignant melanoma develops in the human body very quickly, according to statistics in 2016 in Poland over 3,600 people fell ill with it, and over 1,300 people died from it [39]. Still, too few patients report skin nevi to dermatologists, and early diagnosis in the case of cancer is crucial. Dermatoscopy comes to the aid of doctors. It allows for non-invasive high-resolution images of the skin. On its basis, doctors make a preliminary diagnosis.

With the help of doctors, diagnostic tools based on artificial intelligence were launched [5, 22]. Deep learning and other machine learning techniques have helped to increase the efficiency of medical image analysis. This is an area of machine learning in which subsequent layers of the network learn with each step better representations based on the information provided. The use of deep convolutional neural networks (DCNN) in recent years has been leading the way in the giagnostics of skin nevi. Many works have been created to effectively diagnose skin cancers [8, 21]. The use of selected segmentation and classification methods allows to achieve even better diagnostic success [12, 17, 28, 37].

Dermatoscopic image databases contain many images of a given case of the disease, which has been confirmed by histopathological examination. Properly prepared, they are input data for the process of training neural networks. The most commonly used databases with diagnosed dermatoscopic images by researchers include: ISIC [18], MED.-NODE [27], PH2 [30], PAD-UFES-20 [29], DERMOFIT [6]. Images from a given class are grouped and subjected to a process of initial preparation, regions of interest (ROI) are distinguished. The next stage is most often the segmentation of the cutaneous birthmark. The beginning of the classification of cutaneous nevi included binary classification [3, 14]. However, further development of technology has made it possible to create more classes. Currently, it is possible to make a classification for 5, 6, 7 and even 10 different skin diseases.

1. Deep neural networks basics

The use of models based on deep learning was possible thanks to the implementation of appropriate algorithms. A multi-layered network model is created and input data is provided to the model in the form of medical images. Each of the many layers of the model processes more complex elements of the input image. Many operations were performed on the images delivered to the network, which ultimately lead to the output. Diagnosis belongs to these data. Deep neural network architectures include: multilayer perceptrons, limited Boltzmann machines, deep belief networks, convolutional neural networks (CNNs), recursive neural networks. Very good effects are observed due to the emergence of new models of convolutional neural networks. Increasing the computing capabilities of computers has slowly moved to the development of new techniques for effective deep network learning. It is possible to diagnose skin cancers and benign lesions from dermatoscopic images more and more effectively.

Convolutional neural networks are the most popular tool used to classify medical images. Convolutional layers, on the other hand, learn local patterns selected from the image. Figure 1 shows typical weave network architecture. The basis of the network is the convolution base. It consists of an input layer and several convolutional layers connected to each other by pooling layers. Neurons are connected to neurons of the higher layer (pooling). Neurons in the convolution layers of the first layer are combined with pixels in the reception fields of the input image. In contrast, neurons from the second layer connect to a small area of the first layer. In the reception fields, e.g. with dimensions of 3×3 or 5×5, there are local patterns that the network finds. In each subsequent hidden layer, the network focuses on more details of a given feature. With more layers, you can analyze features with more detail. The last layer calculates forecasts, often it is a softmax layer. It is designed to estimate the probability of an image belonging to a given specific class.

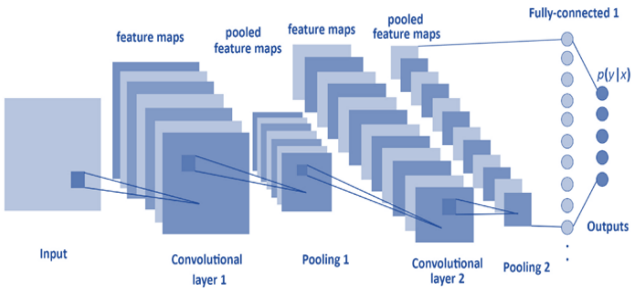

Fig. 1. Typical convolutional network architecture [34]

Linking layers are designed to sub-sample feature maps, reduce the load on algorithm calculations and the number of parameters. They do not need scales, they include the processing of input data by the aggregation function. Extraction windows process feature maps. After the convolution base, there is a classifier. The data contains its representations and the trained model determines for a given image belonging to a specific class, which is determined with a certain probability.

Transfer learning is very helpful in medical diagnostics. This is a type of machine learning that is based on learning new tasks based on previously acquired knowledge. It allows you to increase the efficiency of model learning even for a smaller amount of data. This is important in the case of dermatoscopic images, because not all available databases contain many images to fully reflect the specificity of a given skin disease in the image.

2. Used model examples

Initially, DNN was used for deep learning using the AlexNet architecture, GoogleNet. There are many network models available today. The basic ones selected for work on medical images include VGG, ResNet, MobileNet [15], DenseNet [16, 37], MobileNetV2 [33], InceptionV3. Some of the networks are created by combining the architecture of 2 or 3 other networks: NASNet, Xception, InceptionV3, InceptionRes-NetV2 and many others. The Keras library [21] is one of the most commonly used in the creation of networks for the classification of skin lesions, it uses transfer learning.

Each of the networks has characteristic elements that build it, including convolution, maxpool, soft max and fully connected layers. However, they differ in the number of layers and connections between them. One of the most frequently tested networks is VGG. This network is characterized by the smallest topological depth with a small 3×3 weave filter. Among the VGG networks, the most successful were two of them VGG16 (figure 2a) and VGG19. VGG16 is made up of 13 convolutional layers and three fully connected layers. Both networks use small 3×3 strand filters. This increases the topological depth of the network and contributes to a more effective learning process.

The ResNet network model [13] is characterized by a very deep structure, has as many as 152 layers. The problems related to the depth of the network include: difficulties in training, high training error, disappearing gradient. In this network, 3×3 filters are most often used. 1×1 convolution layers deepen the lattice and increase nonlinearity by applying the ReLU function after each 1×1 convolution layer. In this network, fully connected layers are replaced with a pooling averaging layer, which reduces the number of parameters. This structure provides the network with learning deeper representations of functions with fewer parameters. The ResNet diagram is shown in figure 2b.

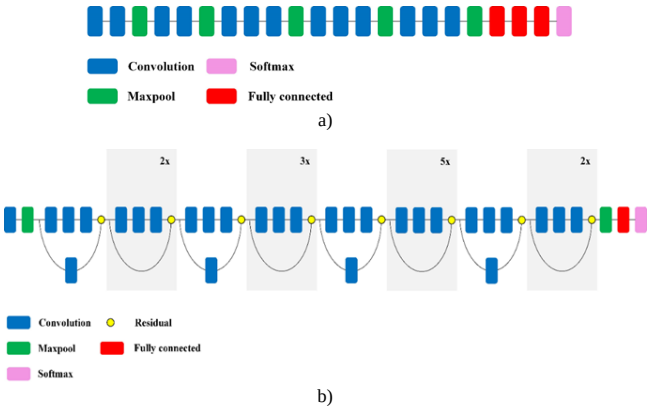

Fig. 2. Diagram of the VGG16 (a) and ResNet (b) network models [24]

3. Application examples

Deep neural networks are used to diagnose many skin diseases, mainly diagnosed cancers from dermatoscopic images are: squamous cell carcinoma, malignat melanoma, basal cell carcinoma. Among the most commonly diagnosed benign skin birthmarks should be mentioned: nevus, pigmented benign keratosis and seborrheic keratosis. Diagnostic systems based on deep neural networks allow to make binary classification, but also in high efficiency recognize simultaneously 3 [25], 5 [26], 7 [4, 36], 8 [37] and even 10 [10] different classes.

The use of machine learning tools, artificial intelligence and neural networks competes very effectively with human knowledge [10]. Figure 3 shows the entire scheme of action when selecting the segmentation of skin lesions and their classification. It takes into account the selection of the most popular databases of dermatoscopic images, the selection of the segmentation method and the selection of the network model needed for binary or multi-class classification. It assumes obtaining results based on a binary classification and two multi-class classifications (3 classes and 7 classes). Individual classes are marked with letters: include benign (B), seborrheic keratosis (SK), basal cell carcinoma (BCC), actinic keratosis (AK), dermatofibroma (DF), vascular lesion (VL) and melanoma (M).

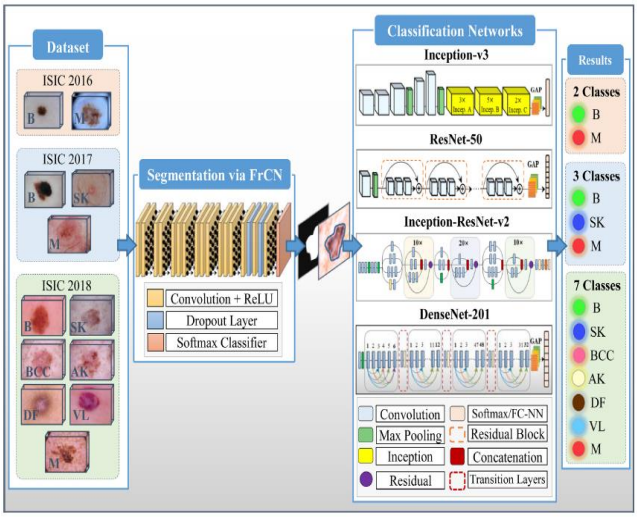

Fig. 3. An exemplary scheme of action during segmentation and classification of skin lesions [2]

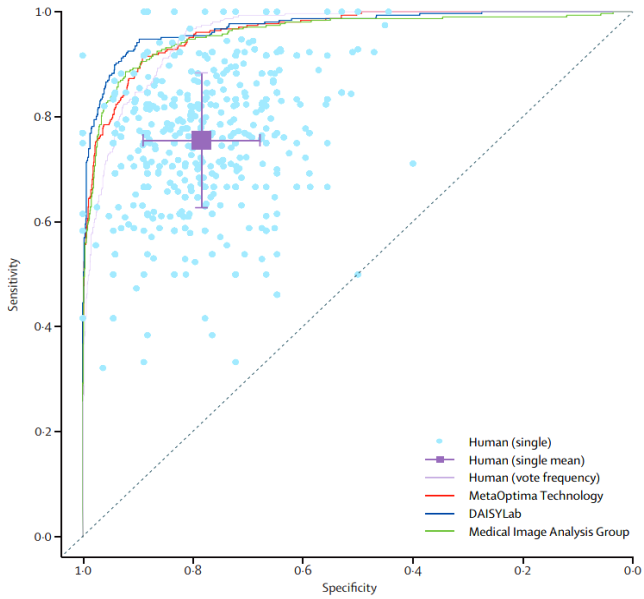

Fig. 4. ROC curves for test groups [36]

Works comparing the diagnostic capabilities of algorithms and experienced doctors are being created. In [36], the researchers undertook extensive research that aimed to compare the diagnoses of medics with randomly selected images. The results of the doctors' diagnoses were compared with more than 130 machine learning algorithms from the International Skin Imaging Collaboration 2018. Among the medics were board-certified dermatologists, dermatology residents and general practitioners. Figure 4 shows ROC curves for diagnostic efficacy to distinguish between malignant and benign skin lesions. The graph compares diagnostic capabilities single human (blue dots), vote human frequency (purple line), MetaOpima Technology (red line), DAISYLab (dark blue line) and Medical Images Analysis Group (green line). Higher diagnostic efficiency is achieved by algorithms using machine learning than human diagnostic capabilities.

Achieving high diagnostic effectiveness of algorithms based on DNN is possible due to the use of properly selected databases, selection of images for training, validation and test sets. Choosing network models and properly tuning its parameters is also not a simple task. It is also important to choose the number of epochs when training the network.

Each of the teams tries to draw knowledge and experience from the work already developed so that there is a continuous development of algorithms. Often, the achievements of several researchers are modified and combined into one work [35]. To obtain a high AUROC value, the classification layers of several models are combined into one, which ensured the competitiveness of such modified models [11, 23]. High-resolution dermatoscopic images are also used for classification to more effectively use patches-based models of skin lesion [9]. Table 1 shows the results for segmentation and classification using deep neural networks. Their accuracy ranges from over 80% to almost 98%. They also use transfer learning.

Table 1. Results for the segmentation and classification CNN's models in recent years

Authors	Used metod	Accuracy
[38]	Transfer Learning using VGG16	80.3%
[20]	Transfer Learning using ResNet50	83.5%
[32]	Transfer Learning using DenseNet201	95.9%
[1]	Stacking ensemble of fine-tuned models	97.9%
[7]	ResNet-50	95.8%
[7]	Xception	92.9%
[31]	Transfer Learning using ResNet50 GANs	95,2%
[2]	ResNet-50	81.6%

There are also works that modify known network models, models are also created that connect them with each other. In [1] the Stacking ensemble of fine-tuned models shown in figure 5 was created, it combines 4 network models: Xception, DenseNet201, DenceNet121 and Inception-ResNet-V2 and gives satisfactory results, its accuracy is 97.9%. The cumulative model was created to increase the efficiency of the best 4 network models. The use of team learning reduces variance. The presented concept assumes deep learning of stacked 4 models of pre-trained models. Stacking is a modification of the averaging unit. He is responsible for teaching the new model by combining already existing submodels.

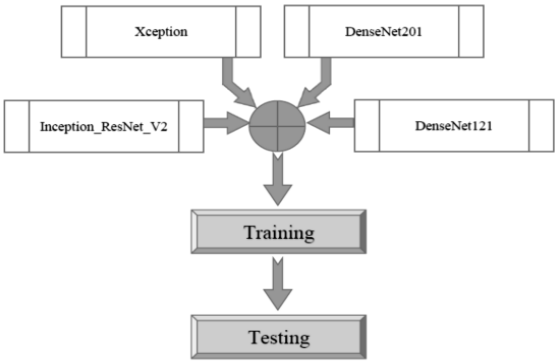

Fig. 5. Diagram of stacked ensemble model [1]

Also intriguing are deep learning techniques contraindicated on full convolutional networks (FCNs). They become effective in segment the image by using a huge amount of data during multi-level learning. Figure 6 shows the architecture of this network model.

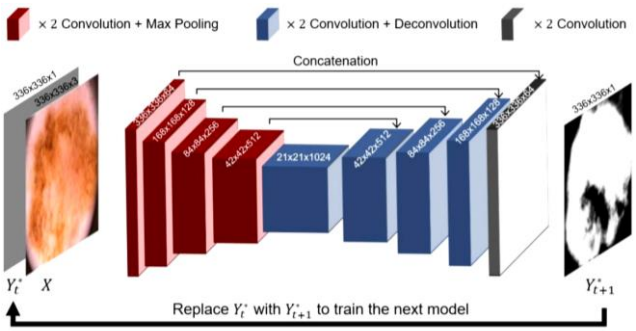

Fig. 6. Full architecture of the model from [19]

4. Discussion and conclusions

The methods proposed in the work are helpful in non-invasive diagnosis of skin lesions. They can effectively identify skin diseases based on dermatoscopic images. It is assumed that the ideal solution would be the testing of automated diagnostic systems based on deep neural networks by experienced dermatologists. This would make these 2 groups angry and help many people regain their health. In the future, automatic classifiers will work under human supervision. Further development of all methods based on deep neural networks and transfer learning will definitely increase the effectiveness of skin lesions diagnostics.

References

[1] Abunadi I., Senan E. M.: Deep learning and machine learning techniques of diagnosis dermoscopy images for early detection of skin diseases. Electronics 10, 3158, 2021 [http://doi.org/10.3390/ electronics10243158].
[2] Al-Masni M. A., Kim D. H., Kim T. S:. Multiple skin lesions diagnostics via integrated deep convolutional networks for segmentation and classification. Comput Methods Programs Biomed. 190, 105351, 2020 [http://doi.org/10.1016/j.cmpb.2020.105351].
[3] Brinker T. J. et al: Deep learning outperformed 136 of 157 dermatologists in a head-to-head der moscopic melanoma image classification task. Eur J Cancer 113, 47–54, 2019.
[4] Chaturvedi S. S., Gupta K., Prasad P. S.: Skin lesion analyser: An efficient seven-way multi-class skin cancer classification using MobileNet. Advances in Intelligent Systems and Computing 1141, Springer, Singapore, 2020 [http://doi.org/10.1007/978-981-15-3383-9_15].
[5] Codella N. C. F. et al.: Deep learning ensembles for melanoma recognition in dermoscopy images. IBM Journal of Research and Development 61(4/5), 173, 2017.
[6] DERMOFIT IMAGE LIBRARY [https://licensing.edinburghinnovations.ed.ac.uk/i/software/dermofit-imagelibrary.html?item=dermofit-image-library] (accessed 04.01.2021).
[7] Gavrilov D., Lazarenko L., Zakirov E.: AI recognition in skin pathologies detection. Proceedings of the 2019 International Conference on Artificial Intelligence: Applications and Innovations (IC-AIAI), 554–542, Belgrade 2019.
[8] Ge Y. et al.: Melanoma segmentation and classification in clinical images using deep learning. 10th International Conference on Machine Learning and Computing ICMLC, 2018, 252–256.
[9] Gessert N. et al.: Skin lesion classification using CNNs with patch-based attention and diagnosis-guided loss weighting. IEEE Trans. Biomed. Eng. 67, 495–503, 2020.
[10] Haenssle H. A. et al: Man against machine reloaded: performance of a market-approved convolutional neural network in classifying a broad spectrum of skin lesions in comparison with 96 dermato-logists working under less artificial conditions. Ann Oncol 31, 137–143, 2020.
[11] Harangi B.: Skin lesion classification with ensembles of deep convolutional neural networks. J. Biomed. Inform. 86, 25–32, 2018 [http://doi.org/10.1016/j.jbi.2018.08.006].
[12] Hasan M. M., Elahi M., Alam M. A.: DermoExpert: Skin lesion classification using a hybrid convolutional neural network through segmentation, transfer learning and augmentation. medRxiv 2021.02.02.21251038 [http://doi.org/10.1101/2021.02.02.21251038].
[13] He K. et al.: Deep residual learning for image recognition. IEEE Conference on Computer Vision and Pattern Recognition (CVPR) 2016, 770–778.
[14] Hekler A. et al.: Deep learning outperformed 11 pathologists in the classification of histopathological melanoma images, Eur J Cancer 118, 91–96, 2019.
[15] Howard A. G. et al.: MobileNets: Efficient convolutional neural networks for mobile vision applications. Computer Science, Computer Vision and Pattern Recognition, arXiv:1704.04861v1 [http://doi.org/10.48550/arXiv.1704.04861].
[16] Huang G. et al.: Densely Connected Convolutional Networks. Computer Vision and Pattern Recognition arXiv:1608.06993v5 [http://doi.org/10.48550/arXiv.1608.06993].
[17] Iqbal I. et al.: Automated multi-class classification of skin lesions through deep convolutional neural network with dermoscopic images. Computerized Medical Imaging and Graphics 88, 101843, 2021 [http://doi.org/10.1016/j.compmedimag.2020.101843].
[18] ISIC Archive [https://www.isic-archive.com/#!/topWithHeader/onlyHeaderTop/gallery] (accessed 23.03.2022).
[19] Kareem O., Mohsin Abdulazeez A., Zeebaree D.: Skin Lesions Classification Using Deep Learning Techniques: Review. Asian Journal of Research in Computer Science 9(1), 1–22, 2021 [http://doi.org/10.9734/AJRCOS/2021/v9i130210].
[20] Lee S. et al.: Augmented decision-making for acrallentiginous melanoma detection using deep convolutional neural networks. J. Eur. Acad. Dermatol. Venereol. 34, 1842–1850, 2020.
[21] Lopez A. R. et al.: Skin lesion classification from dermatoscopic images using deep learning techniques. 13th International Conference on Biomedical Engineering (BioMed) IASTED, 2017, 49–54 [http://doi.org/10.2316/P.2017.852-053].

[22] Maglogiannis I., Doukas C. N.: Overview of advanced computer vision systems for skin lesions characterization, IEEE transactions on information technology in biomedicine 13(5), 721–733, 2009.
[23] Mahbod A. et al.: Fusing finetuned deep features for skin lesion classification, Comput. Med. Imaging Graph. 71, 19–29, 2019 [http://doi.org/10.1016/j.compmedimag.2018.10.007].
[24] Mahdianpari M. et al.: Very deep convolutional neural networks for complex land cover mapping using multispectral remote sensing imagery. Remote Sens. 10(7), 2018.
[25] Marchetti M. A. et al.: Computer algorithms show potential for improving dermatologists' accuracy to diagnose cutaneous melanoma: results of the international skin imaging collaboration 2017. J Am Acad Dermatol 82, 622–627, 2020.
[26] Maron R. C. et al.: Systematic outperformance of 112 dermato-logists in multiclass skin cancer image classification by convo-lutional neural networks, Eur J Cancer 119, 57–65, 2019.
[27] MED-NODE Dataset [http://www.cs.rug.nl/~imaging/databases/melanoma_naevi/] (accessed 23.03.2022).
[28] Nida N. et al.: Melanoma lesion detection and segmentation using deep region based convolutional neural network and fuzzy C-means clustering, International Journal of Medical Informatics 124, 37–48, 2019.
[29] PAD-UFES-20 Dataset [https://data.mendeley.com/datasets/zr7vgbcyr2/1] (accessed: 23.03.2022).
[30] PH2 Dataset [https://www.fc.up.pt/addi/ph2%20database.html] (accessed 23.03.2022).
[31] Qin Z. et al.: A GAN-based image synthesis method for skin lesion classification. Computer Methods and Programs in Biomedicine, 105568, 2020.
[32] Raza R. et al.: Melanoma Classification from dermoscopy images using ensemble of convolutional neural networks. Mathematics 10, 26, 2022 [http://doi.org/10.3390/math10010026].
[33] Sandler M. et al.: MobileNetV2: Inverted Residuals and Linear Bottlenecks. IEEE Conference on Computer Vision and Pattern Recognition (CVPR), 2018, 4510–4520.
[34] Simonyan K., Zisserman A.: Very deep convolutional networks for large-scale image recognition. International Conference on Learning Representations ICLR, 2015.
[35] Szegedy C. et al.: Inception-v4, Inception-ResNet and the impact of residual connections on learning. AAAI, 4278–4284, 2017 [http://doi.org/arXiv:1602.07261].
[36] Tschandl P. et al.: Comparison of the accuracy of human readers versus machine-learning algorithms for pigmented skin lesion classification: an open, webbased, international, diagnostic study. Lancet Oncol 2019b(20), 938–947, 2019.
[37] Villa-Pulgarin J. et al.: Optimized convolutional neural network models for skin lesion classification, Computers, Materials & Continua Tech Science Press, CMC 70(2), 2022
[38] Yu C. et al.: Acral melanoma detection using a convolutional neural network for dermoscopy images. PLoS ONE 2018, 13, e0193321, 2018.
[39] Zakład Epidemiologii i Prewencji Nowotworów Centrum Onkologii – Instytut w Warszawie. Krajowy Rejestr Nowotworów (KRN) [http://onkologia.org.pl/] (accessed 02.08.2019).

M.Sc. Magdalena Michalska-Ciekańska
e-mail: magdalena.michalska@pollub.edu.pl

Ph.D. student at Department of Electronics and Information Technology, Lublin University of Technology. Recent graduate Warsaw University of Technology The Faculty Electronics and Information Technology. Her research interests include medical image processing, optoelectronics, spectrophotometry.

http://orcid.org/0000-0002-0874-3285

http://doi.org/10.35784/iapgos.3049

received: 12.08.2022 | revised: 31.08.2022 | accepted: 15.09.2022 | available online: 30.09.2022

DYNAMIC AND MATHEMATICAL MODELS OF THE HYDROIMPULSIVE VIBRO-CUTTING DEVICE WITH A PRESSURE PULSE GENERATOR BULT INTO THE RING SPRING

Roman Obertyukh[1], Andrii Slabkyi[1], Leonid Polishchuk[1], Oleksandr Povstianoi[2], Saule Kumargazhanova[3], Maxatbek Satymbekov[4]

[1]Vinnytsia National Technical University, Vinnytsia, Ukraine, [2]Lutsk National Technical University, Lutsk, Ukraine, [3]D. Serikbayev East Kazakhstan Technical University, Ust-Kamenogorsk, Kazakhstan, [4]Al-Farabi Kazakh National University, Almaty, Kazachstan

Abstract. *Structural calculation scheme of the hydropulse device for vibration cutting with built-in ring with pressure pulse generator (PPG) is considered. On the basis of the structural scheme and cyclogram of the working cycle of the device, its dynamic and mathematical models were developed, in which the hydraulic link is represented by a visco-elastic model of the working fluid (energy carrier) composed of the inertial elastic and dissipative elements (Kelvin-Foyga's body).*

Keywords: mathematical model, dynamic model, hydropulse device, ring spring, frequency, amplitude

MODELE DYNAMICZNE I MATEMATYCZNE HYDRAULICZNEGO URZĄDZENIA IMPULSOWEGO DO CIĘCIA WIBRACYJNEGO Z GENERATOREM IMPULSÓW WBUDOWANYM W SPRĘŻYNĘ PIERŚCIENIOWĄ

Streszczenie. *Rozważa się schemat konstrukcyjny i projektowy hydraulicznego urządzenia impulsowego do cięcia wibracyjnego z wbudowanym generatorem impulsów ciśnieniowych ze sprężyną pierścieniową (PPG). Na podstawie schematu strukturalnego i cyklu pracy urządzenia opracowano jego modele dynamiczne i matematyczne, w których ogniwo hydrauliczne reprezentowane jest przez lepkosprężysty model cieczy roboczej (nośnika energii), złożony z bezwładnych elementów sprężystych i dyssypacyjnych (ciał Kelvina-Foiga).*

Słowa kluczowe: model matematyczny, model dynamiczny, hydrauliczne urządzenie impulsowe, sprężyna pierścieniowa, częstotliwość, amplituda

Introduction

Vibration cutting and vibration turning in particular, in comparison with conventional turning, have a number of known technological advantages, especially when processing viscous materials such as stainless steels and titanium alloys [6]. The massive introduction of vibration cutting processes is constrained by the practical absence of compact, with a wide range of vibration loading parameters, devices. The authors of the work proposed a number of designs for devices for vibration cutting on the basis of a hydropulse drive using elastic elements of high rigidity such as slit, plate and ring springs [16]. The novelty of the developed designs is confirmed by dozens of patents for utility models of Ukraine.

The purpose of conducting theoretical studies of dynamic processes, which reflect their course in the studied devices, as well as their experimental verification, which establishes the adequacy of the mathematical model to real physical processes, is the development of a scientifically based methodology for the design calculation of the created structure, which allows optimization of its design parameters [5, 6, 7].

1. Analysis of research methods

Research of oscillating systems by theoretical methods [5, 7, 9] is in most cases carried out by researching mathematical models, in particular hydraulic impulse machines – by researching the mathematical model of the executive links in the form of differential equations of motion and equations of the consumption of the energy carrier flowing through the pressure pulse generator (PPG) during the working cycle. In the case of applying the macromodeling method to simplify the original mathematical model, only those variables that influence, in the researcher's opinion, the most, are taken into account in the initial space of variables. Other unaccounted for effects can be taken into account in a parametric form by changing the coefficients near the considered variables for the case of multiplicative effects or by introducing free terms in the equations for the case of additive effects. This approach is quite often used to simplify the mathematical models of the hydraulic impulse drive, in particular, the PPG operation is considered to be instantaneous ("relay"). With this approach, it is not possible to adequately describe the dynamics of this issue, and it creates significant discrepancies between the results of theoretical and experimental research.

In our opinion, studies of simplified models that describe the cycle of the hydraulic impulse vibration drive as a single-act process [2, 10] significantly reduce the correctness of the results of theoretical studies of the processes taking place in the vibration drive and the machine as a whole.

Modern software tools for mathematical modeling of physical processes make it possible to study the dynamics of processes occurring in oscillating systems without simplifying mathematical models. Taking into account all stages of the work cycle of the drive elements ensures the possibility of creating correct methods for the design calculation of the design of the machine or device.

The mathematical models of the hydropulse drive, built on the basis of a detailed step-by-step analysis of the driving cycle of the drive [9, 12], are more correct, and the engineering calculation methods developed on the basis of these models allow to determine the design, power and power parameters of the PPG and the drive, which more precisely with the experimentally established ones under the same conditions initially set during simulation [11, 15].

An important aspect of mathematical models and methods of calculating the hydropulse drives is the choice of model of energy. Known mathematical models of the drive are based in the simplest forms on the "rigid" [10, 13] model of the energy carrier, which does not take into account the elastic and viscous characteristics of the energy carrier, and in more precise forms an „elastic" energy carrier model is used that takes into account the elastic properties of the fluid [3, 8, 14].

2. Theoretical studies

The structural scheme of the hydropulse device for vibration cutting with a built-in ring spring (further RS1) by a pulse pressure generator in a constructive form is shown in Fig. 1.

The device consists of two hydraulically connected units – the PPG and the hydraulic cylinder of the drive in a vibratory movement, for example a turning cutter for radial vibration. The PPG contains a locking element in the form of a valve-spool of 1 mass m_{k9}, the right-hand side (according to the drawing) which is a supporting ring of a ring-spring PPG (RS1) with

rigidity k_1 and mass m_{k1}, consisting of a set of outer 2 and inner 3 rings that interact with each other by the mediation of internal and external conical surfaces. The pre-deformation y_{01} of the PPG ring spring is controlled by means of a screw 4 that moves the pressure plunger 5, the left end (which is illustrated) is designed as the second bearing ring RS1. The plunger 5 is sealed with a rubber ring of 6 round sections. The body of the PPG and the device in general is not conventionally shown in Fig. 1

With the block of the hydraulic cylinder actuator (located in the unit body, like the PPG), the PPG is combined through a common pressure cavity *A* (hole diameter d_1). The hydraulic cylinder consists of a plunger of 7 with a mass m_{pl} compacted by a rubber ring 8. On the right (in the drawing) of the end of the plunger 7, a protrusion is formed which is the support and guide surface of the bearing ring 9 of the ring spring, the hydraulic cylinder (RS2). the stiffness k_2 and the mass m_{k2}.

RS2 consists of external 10 and internal 11 rings and two identical in shape and sizes of support rings 9 and 12. The rings RS2 are in contact with each other through the inner and outer conical surfaces. The pre-deformation y_{02} of the RS2 is controlled by means of a collar nut 13 that is screwed onto the threaded projection 14 of the device casing conventionally shown by an icon „x". The nut 13 clicks on the step cap 15 in the inner dull groove which places and regulates the left (as shown in the drawing) bearing ring 12 RS2. The nut 13 is locked with a spline nut 16.

In the rectangular aperture of the step cap 13, a cutter 17 is provided, equipped with a cylindrical rod 18 with a buccal ledge. The right part of the rod 18 (behind the buckling protrusion) enters the landing gear in the central hole of the plunger 7, and a spring 19 is installed on the left part of the rod 18 (in front of the hill), with one end resisting the bust of the rod, and the other to the cover 13. The spring 19 is installed during the assembly of the hydraulic cylinder with the estimated pre-deformation and carries the axial pre-fixing of the cutter 17.

In order to provide a stable mode of landing the valve-spool 1 at the end of its reverse, a throttle 20 is provided. The function of the throttle 20 can be provided by the gap in the conjugation of the valve-spool 1 by the diameter d_2 of the mortar in the body (or the sleeve in the real construction) of the device or by the experimentally selected folding length $l_L \geq h_d$ (here h_d – a positive overlap of the spool valve part-spool 1) connects intermediate *B* and drain *C* device cavity. The placement cavity RS1 is connected to the drainage cavity with radial openings „*a*" in the direct part of the valve-spool 1.

Power supply of the working fluid (energy carrier) is carried out from a compact hydro pump station, which connects to the device with two flexible hoses of high pressure. The energy supply sleeve joins the pressure cavity *A*, and the sleeve of the drainage *C* connects the latter with the hydraulic tank of the station.

Given the radial stretching of the outer rings 2 and 10 RS1 and RS2 during their working deformation, the cylindrical surfaces of the outer rings 2 and 10, which RS1 and RS2 are guided in the holes of the device body, are tied to the surfaces of the holes of the hull under running landings not exceeding 9-10 qualifications. Since, in abso-lute value, the radial deformations of the rings are small, the gaps that provide the named qualities are guaranteed to exclude the possible stitching of the rings [1, 4, 17].

The „opening" pressure of the PPG is determined by the known dependence [3, 14, 16]

$$p_1 \geq k_1 \cdot y_{01} / A_1 = 4k_1 \cdot y_{01} / (\pi d_1^2) = 0,785 k_1 \cdot y_{01} / d_1^2, \qquad (1)$$

where $A_1 = \pi d_1^2 / 4 = 0,785 d_1^2$ – the area of the cross-section along the facet of the valve-spool 1 for its small diameter d_1 (the first degree of sealing of the sealing element of the PPG – valve-spool 1), provided that the sealing is carried out on a facet of small width, which can be calculated according to the formulas given in the work [17].

The movement of the plunger 7 of the hydraulic cylinder of the drive of the cutter 17 in the vibrational movement will begin after the increase in the pressure of the energy carrier in the pressure cavity *A* to the level (without taking into account frictional forces between the plunger 7 and its guiding surface)

$$p_c \geq k_2 y_{02} / A_3 = 4k_2 y_{02} / \left(\pi d_3^2\right) = 0,785 k_2 y_{02} / d_3^2, \qquad (2)$$

where p_c – stationary pressure of the energy carrier, at which the plunger 7 movement begins 7; $A_3 = \pi d_3^2 / 4 = 0,785 d_3^2$ – square cross-section of the plunger 7.

The maximum possible displacement of the plunger 7 and the cutter 17, because due to the force of the spring 19, it is located with a plunger 7 in a rigid contact, can be estimated from the equation of dynamic equilibrium:

The maximum possible displacement $h_{F\max}$ of the plunger 7 and the cutter 17, because due to the force of the spring 19, it is located with a plunger 7 in a rigid contact, can be estimated from the equation of dynamic equilibrium:

$$p_1 \cdot A_3 = k_2 \left(y_{02} + h_{F\max}\right) \qquad (3)$$

where

$$h_{F\max} = p_1 A_3 / k_2 - y_{02\max} \approx 0,785 p_1 d_3^2 k_2^{-1}. \qquad (4)$$

The displacement h_F of the plunger 7 is essentially the amplitude of the vibration oscillations of the cutter 17 and, as can be seen from dependence (4), can be regulated by changing the energy pressure p_1 and previous deformation y_{02} of the RS2.

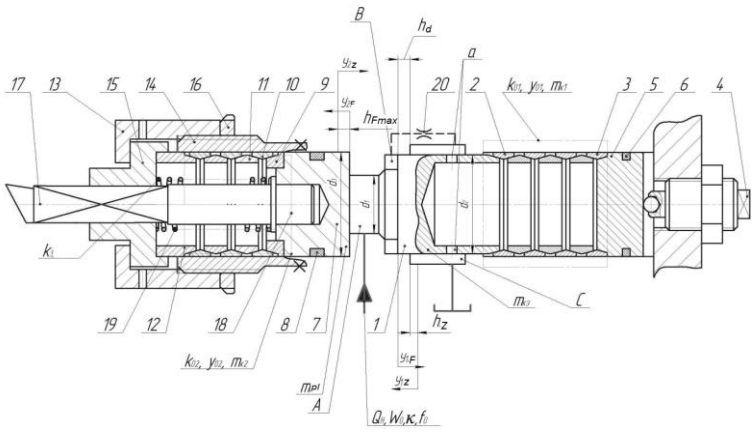

Fig. 1. Structural diagram of the hydropulse device for vibratory turning device with a pressure pulse generator built into the ring spring PPG

3. Results

Taking into account the given structure of assumptions and the oriented cyclogram of the working cycle [11, 12, 15], the dynamical models of the direct (Fig. 2a) and reverse (Fig. 2b) moves of the valve-spool 1 and plunger 7 (cutter 17) (see Fig. 1) they consist of two lumped masses m_1 and m_2 interact with *HL*, in the form of connected parallel elastic k_{or} and dissipative c_o elements, due to the transfer ratios $U_{01(02)}$ and U_{03}. *HL* during the operating cycle of the device deforms with variable speed $\dot{x}_{or}$ in directions x_{or}.

Moving masses m_1 and m_2 during their direct (y_{1F} and y_{2F}) and reverse (y_{1Z} and y_{2Z}) moves counteract the positional forces of elastic resistance, which are characterized by stiffness k_1, k_2 and k_3 viscous resistance, the level of which is determined by the coefficients c_1 and c_2 and velocities $\dot{y}_{1F}$, $\dot{y}_{2П}$, $\dot{y}_{1Z}$ and $\dot{y}_{23}$ by the force of dry friction *R* and the force of cutting F_y, which supposed to act only during direct mass m_2 movement.

An important point in the use of RS1 and RS2 as power elastic elements of the PPG and the hydraulic cylinder of the drive cutter 17 in the vibratory motion is to determine their rigidity and deformation (deposition) under the action of the maximum axial forces acting on RS1 $F_{a1\max}$ and RS2 $F_{a2\max}$

$$F_{a2\max} = p_{1\max} \cdot A_3, \tag{5}$$

$$F_{a1\max} = p_{1\max} \cdot A_2; \tag{6}$$

where $p_{1\max}$ – the maximum possible pressure „opening" the PPG.

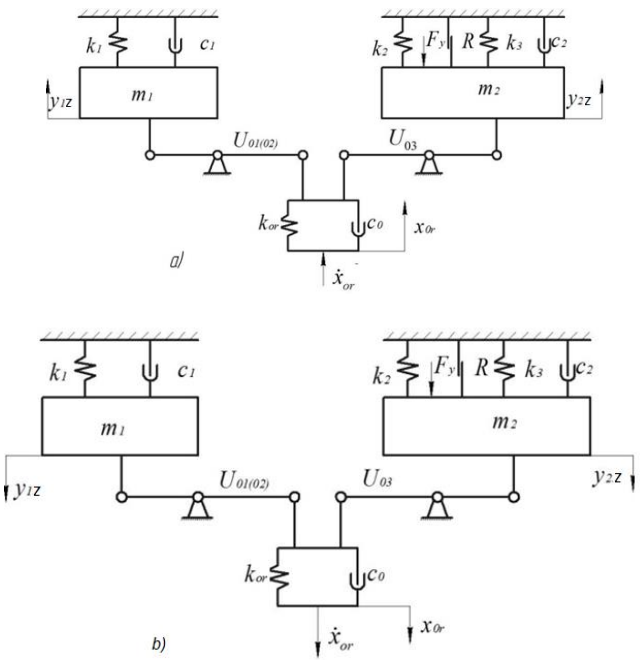

Fig. 2. Dynamic models of direct a) and reverse b) mass movements m_1 and m_2

The determination of the rigid and structural parameters of RS1 and RS2 can be made on the basis of known works [4, 17] in the calculation and design of ring springs.

To construct a mathematical model of the device for vibration cutting, the initial dynamic models of direct and reverse moves of the model of direct and reverse mass movements m_1 and m_2 expediently to simplify the principle of dismemberment [15] by bringing the *HL* to mass m_1 and m_2.

As a result of this reduction, we obtain four simple dynamic models of direct (Fig. 3a, b) and reverse (Fig. 3c, d) of mass m_1 and m_2.

On the basis of the principle of D'Alembert, we compile with the help of the given dynamic models the differential equations of the movement of the valve-spool 1 (mass m_1) and the executive link of the device of the plunger 7 (cutter 17) (mass m_2, see Fig. 1) during the moves:

direct $(x_{01} \geq x_{0r} \geq x_{02})$:–

$$\begin{cases} m_1\ddot{y}_{1П} = U_{01(02)} \cdot k_{or}(x_{A1(2)} - y_{1П}) - k_1(y_{1П} + y_{01}) - c_1\dot{y}_{1П} - U_{01(02)}^{0,25} \cdot c_0(\dot{x}_{A1(2)} - \dot{y}_{1П}); \\ m_2\ddot{y}_{2П} = U_{03} \cdot k_{or}(x_{A3} - y_{2П}) - k_2(y_{2П} + y_{02}) - k_3(y_{2П} + y_{03}) - U_{03}^{0,25} \times \\ \times c_0(\dot{x}_{A3} - \dot{y}_{2П}) - R - F_y - c_2\dot{y}_{2П}; \end{cases} \tag{7}$$

reverse $(x_{02} \geq x_{0r} \geq 0)$:

$$\begin{cases} m_1\ddot{y}_{13} = k_1(y_{01} + h_k + y_{13}) - U_{01(02)} \cdot k_{or}\left[x_{A1(2)} - (h_k - y_{13})\right] - U_{01(02)}^{0,25} \cdot c_0(\dot{x}_{A2(1)} - \dot{y}_{13}) - c_1\dot{y}_{13}; \\ m_2\ddot{y}_{23} = k_2(y_{02} + h_{П\max} - y_{23}) + k_3(y_{03} + h_{П\max} - y_{23}) - U_{03} \cdot k_{or}\left[x_{A3} - (h_{П\max} - y_{23})\right] - \\ U_{03}k_{0r}\left[x_{A3} - (h_{П\max} - y_{23})\right] - R - c_2\dot{y}_{23}, \end{cases} \tag{8}$$

where

$$x_{01} = p_1 A_0 \cdot k_{or}^{-1}; \tag{9}$$

$$x_{02} = p_2 A_0 \cdot k_{or}^{-1} = x_{01} \cdot U_{21}^{0,5} + k_1 h_k U_{02}^{-0,5} \tag{10}$$

the boundary deformations of *HL*; $U_{21} = A_1^2 \cdot A_2^{-2}$ for $0 < y_{1F} \leq h_k$ and $0 \leq y_{1Z} \leq h_k$; $x_{A1(2)} = x_{or} \cdot U_{01(02)}$; $\dot{x}_{A1(2)} = \dot{x}_{or} \cdot U_{01(02)}$; ($x_{A1(2)}$ and $\dot{x}_{A1(2)}$ are determined by changes $U_{01(02)}$ on the interval $0 < y_{1F} \leq h_k$); $x_{A1(2)} = x_{or} \cdot U_{01(02)}$; $\dot{x}_{A1(2)} = \dot{x}_{or} \cdot U_{01(02)}$; ($x_{A1(2)}$ and $\dot{x}_{A1(2)}$ are determined by changes $U_{01(02)}$ on the interval $0 \leq y_{1F} \leq h_k$); $x_{A2(1)} = x_{or} \cdot U_{01(02)}$; $\dot{x}_{A2(1)} = \dot{x}_{or} \cdot U_{01(02)}$; ($x_{A2(1)}$ and $\dot{x}_{A2(1)}$ are determined by changes $U_{01(02)}$ on the interval $0 \leq y_{1F} \leq h_k$); $x_{A3} = x_{or} \cdot U_{03}$; $\dot{x}_{A3} = \dot{x}_{or} \cdot U_{03}$; y_{1F}, y_{2F}, y_{1Z}, y_{2Z}, $\dot{y}_{1F}$, $\dot{y}_{2F}$, $\dot{y}_{1Z}$, $\dot{y}_2$ – respectively, the current coordinates and velocities of the masses m_1 and m_2 during the direct and the return of their moves; y_{03} – predeformation of the spring 19 (see Fig. 1).

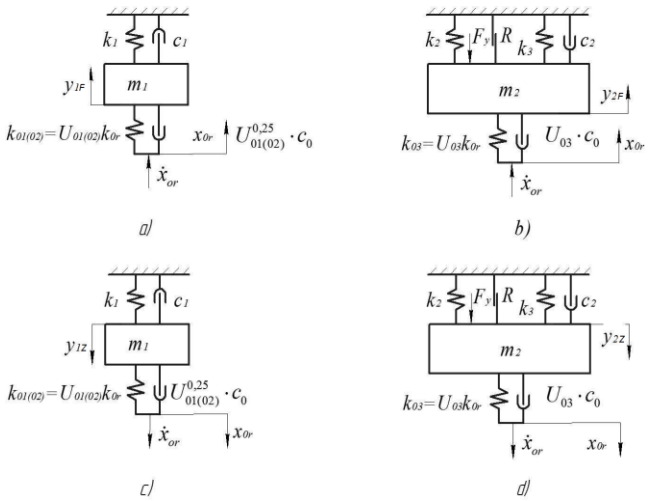

Fig. 3. Simplified dynamic models of direct (a, b) and inverse (c, d) mass movements m_1 and m_2

Differential equations of systems (7) and (8), in order to exclude free members, replace variables y_{1F}, y_{2F}, y_{1Z} and y_{2Z} variables:

$$z_{1F} = y_{1F} + \omega_{\Sigma 1}^{-2}\omega_{01}^{2}y_{01};$$
$$z_{2} = y_{2F} + \omega_{\Sigma 1}^{-2}\left[\omega_{02}^{2}y_{02} + \omega_{03}^{2}y_{03} + (R+F_y)m_{\Sigma}^{-1}\right];$$
$$z_{1Z} = y_{1Z} - \omega_{\Sigma 1}^{-2}\left[\omega_{01}^{2}(y_{01}+h_k) + \omega_{p1}^{2}U_{02}h_k\right]; \quad (11)$$
$$z_{2Z} = y_{2Z} - \omega_{\Sigma 2}^{2}\left[\omega_{02}^{2}(y_{02}+h_{F\max}) + \omega_{p2}^{2}U_{03}h_{F\max} + (R+F_y)m_{2}^{-1}\right],$$

where:

$$\omega_{\Sigma 1} = \sqrt{\omega_{p1}^{2}U_{01(02)} + \omega_{01}^{2}};$$
$$\omega_{p1} = \sqrt{k_{0r}m_1^{-1}};$$
$$\omega_{01} = \sqrt{k_1 \cdot m_1^{-1}};$$
$$\omega_{\Sigma 2} = \alpha\omega_{\Sigma 1};$$
$$\omega_{p2} = \gamma^{-1}\omega_{p1};$$
$$\omega_{02} = \gamma^{-1}\cdot\delta\omega_{01};$$

$\omega_{03} = \gamma^{-1}\delta_1\omega_{01}$ – own frequencies (circular) of the drive system, determined relative to the mass m_1 – respectively, the valve-spool system 1 – HL, HL solidified to the masses m_1, valve-spool system 1, system of plunger 7 (cutter 17) – HL, reduced to mass m_2, HL solidified to the masses m_2; plunger 7 (cutter 17), loaded with a spring 19; $\alpha = \left\{U_{HD}\left[1+\omega_{01}^{2}\omega_{\Sigma 1}^{-2}(\gamma^{-1}\delta U_{HD}^{-1}-1)\right]\right\}^{0,5}$; $\gamma = m_1/m_2$; $\delta = k_1/k_2$; $\delta_1 = k_1/k_3$; $U_{HD} = U_{03}/U_{01(02)}$ – the internal gear ratio between the hydraulic cylinder of the drive of the plunger 7 (cutter 17) and the PPG), which do not change the nature of the mass motion m_1 and m_2, after corresponding algebraic transformations, can be brought into the form, respectively, for the direct and reverse mass movements m_1 and m_2 which, in form and content, describes the forced oscillations of these masses under the influence of variable oscillations of the amplitude of linear deformation x_{or} *HL*:

$$\begin{cases} \ddot{z}_{1F} + 2\beta_{1F}\dot{z}_{1F} + \omega_{\Sigma 1}^{2}z_{1F} = \omega_{p1}^{2}U_{01(02)}^{0,5}\cdot x_{or}; \\ \ddot{z}_{2F} + 2\beta_{2F}\dot{z}_{2F} + \alpha\omega_{\Sigma 1}^{2}z_{2F} = \gamma^{-1}\omega_{p1}^{2}U_{03}^{0,5}\cdot x_{or}; \\ \ddot{z}_{1Z} + 2\beta_{1Z}\dot{z}_{1Z} + \omega_{\Sigma 1}^{2}z_{1Z} = -\omega_{p1}^{2}U_{01(02)}^{0,5}\cdot x_{or}; \\ \ddot{z}_{2Z} + 2\beta_{2Z}\dot{z}_{2F} + \alpha\omega_{\Sigma 1}^{2}z_{2Z} = -\gamma^{-1}\omega_{p1}^{2}U_{03}^{0,5}\cdot x_{or}; \end{cases} \quad (12)$$

where

$$\beta_{1F} = 0,5m_1^{-1}\left[c_1 + U_{01(02)}^{0,25}\cdot c_0(\dot{x}_{A1(2)}\dot{y}_{1II} - 1)\right];$$
$$\beta_{1Z} = 0,5m_1^{-1}\left[c_1 + U_{01(02)}^{0,25}\cdot c_0(\dot{x}_{A2(1)}\dot{y}_{13} - 1)\right];$$
$$\beta_{2F} = 0,5m_2^{-1}\left[c_2 + U_{03}^{0,25}\cdot c_0(\dot{x}_{AZ}\dot{y}_{2F} - 1)\right];$$

$\beta_{2F} = 0,5m_2^{-1}\left[c_2 + U_{03}^{0,25}\cdot c_0(\dot{x}_{AZ}\dot{y}_{2Z} - 1)\right]$ – variable coefficients of damping during mass motion m_1 and m_2. In order to complete the mathematical model of the hydropulse device for vibration cutting, the equation of energy-transport equation for the displacement of the valve-spool 1, plunger 7 (cutter 17) and the flow of energy into the tank through the open of the PPG must be added to the system of differential equations (36), and the uniqueness conditions that describe the displacement of the PPGs and the hydraulic cylinder of the drive of the cutter 17 (see Fig. 1) at the characteristic intervals of time in the corresponding sections of the movement of the device links.

4. Conclusions

Comprehensive analysis and research of the proposed models of a hydropulse device for vibrating cutting with a pulse pressure generator built into the ring spring with subsequent experimental verification of the degree of adequacy of these models to the actual system of the device, will allow to create scientifically grounded method of design calculation of similar designs of devices with a hydropulse drive.

References

[1] Abramov E. I. et al.: Elements of the hydraulic drive: reference book. Technics, Kiev 1977.

[2] Berezyuk O. V.: Mathematical modeling of the hydraulic drive dynamics of the working bodies of the container reversal during the loading of solid household waste in the garbage truck. Bulletin of Khmelnytsky National University 5, 2013.

[3] Bocharov Yu. A.: Fundamentals of the general theory of hydraulic forge-stamping machines. Machinery and technology of metal processing by pressure. Collection of scientific works MVTU 330, 1980, 12–40.

[4] Chuprakov Yu. I.: Hydraulic actuator and means of hydraulics. Engineering 1979.

[5] Cieplok G.: Estimation of the resonance amplitude in machines with inertia vibrator in the coast-down phase. Mechanics & Industry 19(102), 2018.

[6] Danilchik S. S.: Vibration turning of structural steels. BNTU, Minsk 2018.

[7] Gursky V. et al.: Dynamic Analysis of an Enhanced Multi-Frequency Inertial Exciter for Industrial Vibrating Machines. Machines 10(130), 2022 [http://doi.org/10.3390/machines10020130].

[8] Iskovich-Lototskiy R. D. et al.: Pressure pulse generators for controlling the hydropulse drives of vibratory and vibration damping technological machines. UNIVERSUM, Vinnitsya 2008.

[9] Iskovich-Lototskiy R. D. et al.: Vibration and vibro-shock machines. Technics, Kiev 1982.

[10] Khmara L. A. et al.: Algorithm to calculate work tools of machines for performance in extreme working conditions. Mechatronic Systems I. Applicationsin Transport, Logistics, Diagnostics and Control. Taylor & Francis Group – CRC Press, New York 2021, 29–38.

[11] Kozlov L. et al.: Optimization of design parameters of a counterbalance valve for a hydraulic drive invariant to reversal loads. Mechatronic Systems I. Applications in Transport, Logistics, Diagnostics and Control. Taylor & Francis Group –CRC Press, New York 2021, 137–148.

[12] Kozlov L. G. et al.: Experimental research characteristics of counterbalance valve for hydraulic drive control system of mobile machine. Przegląd Elektrotechniczny 95(4), 2019, 104–109.

[13] Obertyukh R. et al.: Mathematical Modeling of the Device for Radial Vibroturning. Advanced Manufacturing Processes II. Inter Partner, Springer, Cham. 2020 [http://doi.org/10.1007/978-3-030-68014-5_55].

[14] Obertyukh R. et al.: Method of design calculation of a hydropulse device for strain hardening of materials. Przegląd Elektrotechniczny 4, 2019, 65–73.

[15] Obertyukh R. R. et al.: Dynamic and mathematical models of the hydraulic-pulse device for deformation strengthening of materials. Proc. 10808, 2018.

[16] Obertyukh R. R. et al.: Pat No 76517 Ukraine, IPC (2013, 01) B23B 1/00. Hydropulse vibrationshock device for radial and axial vibration turning with integrated pulse generator type pressure valve. Applicant and owner of the Vinnytsia National Technical University. 10.01.2013. Bull No. 1.

[17] Polishchuk L. et al.: Mechatronic Systems II. Applications in Material Handling Processes and Robotics. Taylor & Francis Group – CRC Press, Boca Raton, London, New York, Leiden 2021.

[18] Ponomarev S. D., Andreeva L. E.: Calculation of elastic elements of machines and instruments. Machine-building, Moscow 1980.

[19] Roganov L. L., Karnaukh S. G.: Calculation of springs and elastic shock absorbers. DSEA, Kramatorsk 2000.

[20] Song T.: Rapid Calculation and Optimization of Vibration and Noise of Permanent-Magnet Synchronous Motors for EVs Based on Equivalent Structural Network. Machines 10(4), 2022, 281 [http://doi.org/10.3390/machines10040281].

[21] Wójcik W. et al.: Mechatronic Systems I. Applications in Transport, Logistics, Diagnostics and Control. Taylor & Francis Group –CRC Press, London, New York 2021 [http://doi.org/10.1201/9781003224136].

Ph.D. Roman Obertyukh
e-mail: obertyuh557@gmail.com

Ph.D., Associate Professor, Professor of department of industrial engineering Vinnytsia National Technical University, Research Interests: research and improvement of vibration technology.

http://orcid.org/0000-0003-2939-6582

Ph.D. Andrii Slabkyi
e-mail: slabkiyandrey@gmail.com

Ph.D., Associate Professor, Associate Professor of department of industrial engineering Vinnytsia National Technical University.
Research Interests: development and research of new technology samples, in particular for vibration cutting and surface deformation strengthening of machine parts.

http://orcid.org/0000-0001-9284-2296

D.Sc. Leonid Polishchuk
e-mail: leo.polishchuk@gmail.com

Doctor of Technical Sciences, professor, academician at the Ukraine Academy of Hoisting-and-Transport Sciences. Vinnytsia National Technical University.
Head of the Department of Industrial Engineering at Vinnytsia National Technical University.
The scientific focus is the dynamics of drive systems with devices and control systems with variable operating modes and diagnostics of metal structures of hoisting-and-transport and technological machines.

http://orcid.org/0000-0002-5916-2413

D.Sc. Oleksandr Povstianoi
e-mail: povstjanoj@ukr.net

Doctor of science, Professor of the Department of applied mechanics and mechatronics Lutsk National Technical University.
Research Interests: application and development of computer and information technologies in modern materials science

http://orcid.org/0000-0002-1416-225X

Ph.D. Saule Kumargazhanova
e-mail: SKumargazhanova@gmail.com

She is currently the dean of the Department of Information Technologies and Intelligent Systems of D. Serikbayev East Kazakhstan Technical University. She is a co-author over 50 papers in journals and conference proceedings.
Her professional interests are software engineering, data processing and analysis.

http://orcid.org/0000-0002-6744-4023

Ph.D. Maxatbek Satymbekov
e-mail: m.n.satymbekov@gmail.com

Assistant Professor of the Department of Computer Science of Al-Farabi Kazakh National University. Author of more than 25 scientific works published in leading journals of Kazakhstan Republic and the far abroad.
Research area: High performance computing, intelligent systems of control, software engineering, artificial intelligence, soft computing.

http://orcid.org/0000-0002-4621-6646

http://doi.org/10.35784/iapgos.3037

received: 21.07.2022 | revised: 24.08.2022 | accepted: 15.09.2022 | available online: 30.09.2022

EXPERT FUZZY SYSTEMS FOR EVALUATION OF INTENSITY OF REACTIVE EDEMA OF SOFT TISSUES IN PATIENTS WITH DIABETES

Liudmyla Shkilniak[1], Waldemar Wójcik[2], Sergii Pavlov[3], Oleg Vlasenko[1], Tetiana Kanishyna[1], Irina Khomyuk[3], Oleh Bezverkhyi[4], Sofia Dembitska[3], Orken Mamyrbayev[5], Aigul Iskakova[6]

[1]National Pirogov Memorial Medical University, Vinnytsya, Ukraine, [2]Lublin University of Technology, Lublin, Poland, [3]Vinnytsia National Technical University, Vinnytsia, Ukraine, [4]Vinnitsa State Pedagogical University named after M. Kotsiubynskyi, Vinnytsia, Ukraine, [5]Al Farabi Kazakh National University, Institute of Information and Computer Technologies, Almaty, Kazakhstan, [6]Kazakh National Research Technical University, Almaty, Kazakhstan

Abstract. *The paper analyzes the main areas of application of mathematical methods in medical diagnostics, formulates principles of diagnostics based on fuzzy logic; developed mathematical models and algorithms that formalize the process of making diagnostic decisions based on fuzzy logic with quantitative and qualitative parameters of the patient's condition; developed mathematical models of membership function. Mathematical models and algorithms have been developed that formalize the process of making diagnostic decisions based on fuzzy logic with quantitative and qualitative parameters of the patient's condition; developed mathematical models of membership functions, formalizing the representation of quantitative and qualitative parameters of the patient's condition in the form of fuzzy sets, used in models and algorithms for diagnosis and finding a diagnosis of assessing the intensity of reactive postoperative edema in patients of all study groups. An expert system was implemented for solving the problems of medical diagnosis based on fuzzy logic when assessing the intensity of reactive swelling of soft tissues, which develops in the postoperative period in patients of all study groups against the background of diabetes. The paper analyzes the main areas of application of mathematical methods in medical diagnostics, formulates the principles of diagnostics based on fuzzy logic.*

Key words: information expert system, control, method of fuzzy sets, medical diagnostics, diabetes, dentistry

EKSPERCKIE SYSTEMY ROZMYTE DO OCENY INTENSYWNOŚCI REAKTYWNEGO OBRZĘKU TKANEK MIĘKKICH U PACJENTÓW Z CUKRZYCĄ

Streszczenie*. W pracy analizowane są główne kierunki zastosowania metod matematycznych w diagnostyce medycznej, formułowane są zasady diagnostyki opartej na logice rozmytej; opracowywane są modele matematyczne i algorytmy formalizujące proces podejmowania decyzji diagnostycznych w oparciu o logikę rozmytą z ilościowymi i jakościowymi parametrami stanu pacjenta; opracowywane są modele matematyczne funkcji przynależności. Opracowano modele matematyczne i algorytmy formalizujące proces podejmowania decyzji diagnostycznych w oparciu o logikę rozmytą z ilościowymi i jakościowymi parametrami stanu pacjenta; opracowano modele matematyczne funkcji przynależności formalizujące reprezentację ilościowych i jakościowych parametrów stanu pacjenta w postaci zbiorów rozmytych wykorzystywanych w modelach i algorytmach diagnozowania i znajdowania rozpoznania nasilenia reaktywnego obrzęku pooperacyjnego u pacjentów wszystkich grup badawczych. Wdrożono system ekspercki do rozwiązywania problemów diagnostyki medycznej oparty na logice rozmytej w ocenie nasilenia reaktywnego obrzęku tkanek miękkich, który rozwija się w okresie pooperacyjnym u pacjentów wszystkich grup badawczych z cukrzycą. W artykule przeanalizowano cechy zastosowania metod matematycznych w diagnostyce medycznej, sformułowano zasady diagnostyki opartej na logice rozmytej.*

Słowa kluczowe: informacyjny system ekspercki, sterowanie, metoda zbiorów rozmytych, diagnostyka medyczna, cukrzyca, stomatologia

Introduction

The development of methods and strategies for the implementation of diagnostic functions in expert systems is becoming more and more important nowadays. Structurally, it contains a number of subsystems: language processor (interface subsystem), information-reference, information-diagnostic (machine for drawing conclusions), information-analytical subsystems, and the actual information base – a database and knowledge base. The interface subsystem provides topic-oriented communication with the system of its users, who can belong to one of two main groups: the actual users (patients) and the owner (owner) of the system, who can act both in the role of an expert (source of knowledge) and in the role of an administrator information resources [6, 13].

However, it is often impossible to strictly adhere to such requirements in practice – due to both objective and subjective circumstances: the real world transfers our vision of things to the so-called fuzzy information environment. Today, it can be confidently asserted that the intelligence embedded in modern information technologies is largely based on the theory of fuzzy mathematics and the results of its numerous applications, mostly for the creation of so-called fuzzy software systems. However, the reorientation of components of intelligent systems to fuzzy mathematical support is a difficult problem from both a theoretical and a technological point of view. In the first case, the focus is on fuzzy output methods, in the second, on fuzzy database and knowledge structures, control methods, and fuzzy interfaces.

The problems of fuzzy expert systems are now intensively researched by specialists all over the world, almost half of them concern the class of fuzzy systems, in particular, a significant part of them is devoted to the problems of creating diagnostic technologies [6, 13, 14].

1. Statement of the problem

World and domestic dentistry has unique fundamental information about the physiology of the dental pulp and hardware tools for painless lifelong monitoring of the state of both the intact pulp and its various pathological conditions. However, despite the digital methods of medical diagnostics, the dentist often does not have the opportunity to establish an accurate diagnosis of the state of the dental pulp, since all existing basic and additional diagnostic methods are relative and have a number of disadvantages [5, 13, 14]. The need to develop new methods is dictated by the inconsistency of the results obtained from clinical data using various diagnostic methods and tooth plaster [5, 11, 14].

To date, the world uses the ICD-10 classification (1997) to systematize pulp diseases. In the section "Diseases of the dental pulp" K04.00 Initial pulpitis, K04.01 Acute pulpitis, K04.02 Purulent pulpitis, K04.02 – K04.05 Chronic forms of pulpitis are distinguished. When making a diagnosis, the dentist mainly focuses on his own interpretation of clinical data, based on complaints, the patient's pain history and clinical examination indicators. Thus, without objective data on the condition of the tooth pulp, the choice of treatment method is usually determined empirically. The analysis of numerous subjective and objective data during the clinical examination allows the doctor to establish a diagnosis [12].

In order to objectify information about the state of the dental pulp, specialists from around the world have developed and improved special diagnostic methods, such as reodontography, photoplethysmography, ultrasound Doppler, laser Doppler flowmetry, etc. [4, 11, 12]. For the first time, F. Liebman and F. Cosenza (1962) [11] applied to the study of the pulp by the rheography method. The developed method made

it possible to study some issues of the physiology of the blood circulation of the tooth pulp, however, this method turned out to be unsuitable in practice, since it was hindered by the high electrical resistance of the hard tissues of the tooth.

In this work, we propose to expand the range of indicators for assessing the intensity of edema in patients of all groups of the study in patients with diabetes. The results are presented regarding the further development of the method based on fuzzy sets and an automated expert system for solving problems of medical diagnostics based on fuzzy logic. This method is an interconnected set of mathematical models, algorithms and software for evaluating the intensity of edema in patients with diabetes at given values of the parameters of his condition.

2. The purpose and objectives of the research

The purpose of the study is to implement an expert system for solving medical diagnostic problems based on fuzzy logic in assessing the intensity of reactive edema of soft tissues, which develops in the postoperative period in patients of all study groups against the background of diabetes [2, 7].

The paper analyzes the main areas of application of mathematical methods in medical diagnostics, formulates principles of diagnostics based on fuzzy logic; developed mathematical models and algorithms that formalize the process of making diagnostic decisions based on fuzzy logic with quantitative and qualitative parameters of the patient's condition; developed mathematical models of membership functions, formalizing the representation of quantitative parameters of the patient's condition in the form of fuzzy sets, used in models and algorithms for diagnosis and assessment of the intensity of reactive postoperative edema in patients of all study groups.

3. Using a mathematical apparatus of fuzzy logic for processing diagnostic information

Taking into account the fact that during clinical research it is quite often necessary to use not only clear digital criteria, but also certain linguistic characteristics of changes in indicators (terms), we analyzed some of them using a mathematical apparatus of fuzzy logic. Thus, using the principles of fuzzy logic, we will present the ranges of change of each of the indicators of face size presented in the table in qualitative fuzzy terms, which consist of the levels: L – low, LA – lower that average, A – average, HA – higher than average, H – (table 2).

Each of the specified terms represents a fuzzy set, which is described by membership functions defined on the interval [0;1].

Each of the specified terms is a fuzzy set, which is specified using special membership functions and can be represented by a certain interval, which has its digital degrees from 0 to 1. Absolute non-belonging to the set is indicated by 0, and absolute membership is indicated by 1.

The application of the mathematical apparatus of fuzzy logic can be important in cases where it is necessary to determine the probability of the relationship of pathological conditions that have different clinical characteristics [6, 13, 14].

In our case, the fuzzy logic apparatus is used to assess the intensity of reactive postoperative edema in patients of all study groups.

4. Research methodology

90 patients took part in the clinical study, who were divided into three groups: 1st group (comparison, 30 patients) – patients without diabetes, who underwent tooth extraction and the postoperative wound healed independently. The 2nd group (experimental, 30 patients) – patients suffering from diabetes, who underwent tooth extraction without the use of additional local treatment, the 3rd group (experimental, 30 patients) – patients suffering from diabetes, who underwent tooth extraction, photon therapy was used and Platelet-Rich Fibrin (PRF) was injected into the socket of the extracted tooth.

Patients were examined before surgery and on the 1st, 3rd, 5th, and 7th days after surgery, and the amount of tissue swelling in the area of the postoperative wound was determined using the method of determining the average size of the face by G. Arakeri (2013).

The patient was seated in a chair with his mouth closed and 5 segments were marked. The first – from the lateral corner of the eye to the corner of the jaw; the second – from the wing of the nose to the corner of the jaw; the third – from the corner of the mouth to the corner of the jaw; the fourth – from the chin to the corner of the jaw; the fifth – from the wing of the nose to the bridge of the ear.

With the help of a flexible centimeter tape, which could repeat the contour of the face, the length of each segment was measured, the sum of the lengths is considered the face size (FS). Using the formula:

$$(FS_{\text{after surgery}} - FS_{\text{before surgery}}) / FS_{\text{before surgery}} \times 100\%$$

where FS is the size of the face, the change in the size of the face was calculated as a percentage, which characterized the amount of edema.

On the first day after surgery, the size of the face increased in patients of all three groups. However, in the patients of the 1st group, the increase was insignificant (up to 57.28±0.87) and amounted to 0.06±0.01 cm. While in the patients of the 2nd and 3rd groups, a distinct increase in the average size of the face was observed (up to 62.45±0.99 cm and 61.92±1.17 cm, respectively), which was statistically significant compared to the preoperative level.

The absolute and relative increase in indicators in the 1st group on the first day after surgery were 0.06±0.01 cm and 0.10±0.09%, which is significantly less than the absolute – 4.67±0.09 cm and 3.91±0.60 cm and a relative 8.08±0.11% and 6.74±0.73% increase in average face sizes in the 2nd and 3rd groups, respectively.

A similar situation was observed on the third day after the operation. Thus, in the patients of the 1st group, the increase in the size of the face remained insignificant (up to 57.25±0.90) and amounted to 0.03±0.01 cm. In the patients of the 3rd group, the size of the face decreased slightly compared to the 1st day and approached its preoperative level (> 0.05). In the 2nd group, the absolute increase in the average face size was 4.8±0.17 cm, and the relative increase was 8.31±0.18%, which was statistically significant compared to the preoperative level.

On the first and third day after the operation, the dimensions of the face of the patients of the 1st group differed significantly from the dimensions of the 2nd and 3rd studied groups ($p < 0.001$). The indicators of the 2nd and 3rd studied groups during this period did not differ from each other ($p > 0.05$).

On the seventh day after the operation, the average facial dimensions of the patients of the first, second and third groups approached their preoperative level and were 57.21±0.88 cm, 59.21±0.85 cm and 58.83±0.97 cm, respectively.

The average facial sizes of patients in the three studied groups on the seventh day after surgery did not differ. However, when comparing the indicators of absolute and relative increase in facial sizes in pairs, group No. 1 – group No. 3 and group No. 2 – group No. 3, a significant difference was established between them ($p < 0.001$). While the difference between the indicators of groups No. 1 and No. 2 was not statistically significant ($p > 0.05$).

During the period from the 3rd to the 10th day after the operation, the average size of the face decreased only in patients of the third group (from 63.45±1.23 to 60.05±1.21 cm, ($p < 0.001$).

5. Formation of databases for the implementation of an expert decision-making system

Table 1 shows the database of studies evaluating the intensity of edema in patients of all study groups in patients with diabetes.

Table 1. Indicators of intensity of reactive swelling of soft tissues in patients with diabetes

	M±m, (sm)			The significance of the difference between indicators (p)		
Indicators face size	1 group (n = 30)	2 group (n = 30)	3 group (n = 30)	1–2 groups	1–3 groups	2–3 groups
Before the surgery	57.22± 0.91	57.78± 0.91	58.01± 1.09	> 0.05	> 0.05	> 0.05
1st day	57.28± 0.87	62.45± 0.99***	61.92± 1.17*	< 0.001	< 0.01	> 0.05
3rd day	57.25± 0.90	62.58± 0.81***	60.15± 1.01	< 0.001	< 0.05	> 0.05
7th day	57.21± 0.88	59.21± 0.85•††	58.83± 0.97•	> 0.05	> 0.05	> 0.05
Growth indicators	1 group (n = 30)	2 group (n = 30)	3 group (n = 30)	1–2 groups	1–3 groups	2–3 groups
Δ 1st day	0.06± 0.01	4.67± 0.09	3.91± 0.60	< 0.001	< 0.001	> 0.05
% 1st day	0.10± 0.09	8.08± 0.11	6.74± 0.73	< 0.001	< 0.001	> 0.05
Δ 3rd day	0.03± 0.01‡	4.8± 0.17	2.14± 0.54‡	< 0.001	< 0.001	< 0.001
% 3rd day	0.05± 0.03‡	8.31± 0.18	3.69± 0.69‡	< 0.001	< 0.001	< 0.001
Δ 7th day	-0.01± 0.01‡‡‡	1.43± 0.12‡‡‡	0.82± 0.11‡‡‡	< 0.001	< 0.001	< 0.001
% 7th day	-0.02± 0.01‡‡‡	2.47± 0.12‡‡‡	1.41± 0.24‡‡‡	< 0.001	< 0.001	< 0.001

Notes:
1. The significance of the difference between the indicators before the operation and on the 1st/3rd/7th day after the operation: * -p < 0.05, ** -p < 0.01, *** -p < 0.001.
2. Significance of the difference between indicators on the 1st and 3rd/7th day after surgery: • -p < 0.05, •• -p < 0.01, ••• -p < 0.001.
3. Significance of the difference between indicators on the 3rd and 7th day after surgery: † -p < 0.05, †† -p < 0.01, ††† -p < 0.001.
4. Significance of the difference between growth indicators on the 1st/3rd/7th day after surgery: ‡ -p < 0.05, ‡‡ -p < 0.01, ‡‡‡ -p < 0.001.

Based on Table 1, a database based on fuzzy terms is formed to assess the intensity of edema in patients by study group by group (table 2).

Table 2. A database for evaluating the intensity of edema in patients

Diagnosis	Before the surgery (X_1)	1st day (X_2)	3rd day (X_3)	7th day (X_4)
I group (d_{1a})	L	L	L	L
	L	LA	L	LA
	LA	L	LA	L
II group (d_{2a})	L	HA	H	LA
	LA	H	H	LA
	LA	H	H	A
III group (d_{3a})	L	HA	A	LA
	LA	H	A	LA
	LA	H	A	A

Corresponding membership functions are determined for each indicator from the databases in order to formalize the indicators.

Therefore, mathematical models for assessing the intensity of edema in patients with diabetes have the following form (1-3):

$$\mu^{d1}(X_1,X_2,X_3,X_4)=\mu^L(X_1)\cdot\mu^L(X_2)\cdot\mu^L(X_3)\cdot\mu^L(X_4)\cdot\cup \mu^L(X_1)\cdot\mu^{LA}(X_2)\cdot\mu^L(X_3)\cdot\mu^{LA}(X_4) \cup\mu^{LA}(X_1)\cdot\mu^L(X_2)\cdot\mu^{LA}(X_3)\cdot\mu^L(X_4); \quad (1)$$

$$\mu^{d2}(X_1,X_2,X_3,X_4)=\mu^L(X_1)\cdot\mu^{HA}(X_2)\cdot\mu^H(X_3)\cdot\mu^{LA}(X_4)\cdot \cup\mu^{LA}(X_1)\cdot\mu^H(X_2)\cdot\mu^H(X_3)\cdot\mu^{LA}(X_4)\cup \mu^{LA}(X_1)\cdot\mu^H(X_2)\cdot\mu^H(X_3)\cdot\mu^A(X_4); \quad (2)$$

$$\mu^{d3}(X_1,X_2,X_3,X_4)=\mu^L(X_1)\cdot\mu^{HA}(X_2)\cdot\mu^A(X_3)\cdot\mu^{LA}(X_4)\cdot \cup\mu^{LA}(X_1)\cdot\mu^H(X_2)\cdot\mu^A(X_3)\cdot\mu^{LA}(X_4)\cup \mu^{LA}(X_1)\cdot\mu^H(X_2)\cdot\mu^A(X_3)\cdot\mu^A(X_4); \quad (3)$$

Graphic form of the membership functions is shown in Fig. 1. The selection of the similar curves is stipulated by the fact that they are piecewise linear approximations of the expert membership functions $\mu^j(x_i)$, obtained for the factors $x_1 \div x_4$ by the method of paired comparisons [3, 9, 10].

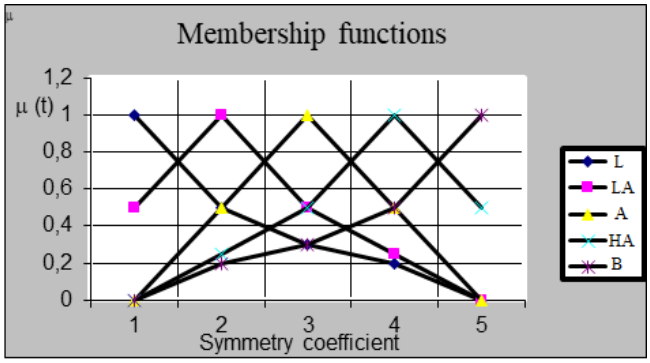

Fig. 1. Membership functions of fuzzy terms

Transition from $\tilde{\mu}^j(u)$ function to the required functions $\mu^j(x_i)$ is realized in the following way:

$$u_i = 4\frac{x_n - \underline{x}_n}{\overline{x}_n - \underline{x}_n}, \mu^j(u_n)=\mu^j(x_n) \quad (4)$$

Analytical expressions of the functions $\mu^j(x_1 \div x_4)$:

$$\tilde{\mu}^L(X_1 \div X_4)=\begin{cases}16.82-0.28x, x_1\in[56.31;58.09]\\ 5.93-0.09x, x_1\in[58.09;63.44]\end{cases}$$

$$\tilde{\mu}^{LA}(X_1 \div X_4)=\begin{cases}0.28x-15.31, x_1\in[56.31;58.09]\\ 17.31-0.28x, x_1\in[58.09;59.87]\\ 8.89-0.14x, x_1\in[59.87;63.44]\end{cases}$$

$$\tilde{\mu}^{A}(X_1 \div X_4)=\begin{cases}0.28x-15.82, x_1\in[56.31;59.87]\\ 17.77-0.28x, x_1\in[59.87;63.44]\end{cases}$$

$$\tilde{\mu}^{HA}(X_1 \div X_4)=\begin{cases}0.14x-7.91, x_1\in[56.31;59.87]\\ 0.28x-16.31, x_1\in[59.87;61.65]\\ 18.22-0.28x, x_1\in[61.65;63.44]\end{cases}$$

$$\tilde{\mu}^{H}(X_1 \div X_4)=\begin{cases}0.09x-5.21, x_1\in[56.31;61.65]\\ 0.28x-16.72, x_1\in[61.65;63.44]\end{cases}$$

Decision-making in assessing the intensity of edema in patients with diabetes can be done by making a decision (5)

$$\mu^{d_0}(x_1,x_2,...x_n)=\max[\mu^{d_n}(x_1,x_2,...x_n)] \quad (5)$$

This solution will correspond to the necessary range, which indicates the intensity group of reactive swelling of soft tissues in patients with diabetes.

6. Practical implementation of the information medical expert system for assessing the intensity of edema in patients with diabetes

The principles of obtaining a reliable diagnosis based on fuzzy sets were used to implement the operation of the tuning blocks, storage of membership functions and fuzzy processing and derivation of the expert system [1, 8].

The basic ideology of the information medical expert system for assessing the intensity of reactive postoperative edema in patients of all study groups in patients with diabetes based on the introduction of fuzzy logic blocks is shown in Fig. 2.

As a result of the implementation of these blocks, a software shell has been developed, while the user is asked to enter the values of the upper and lower scale of values that are in the database for a certain pathology after starting the program, in our case, we enter the values that are basic in the determination [1, 6].

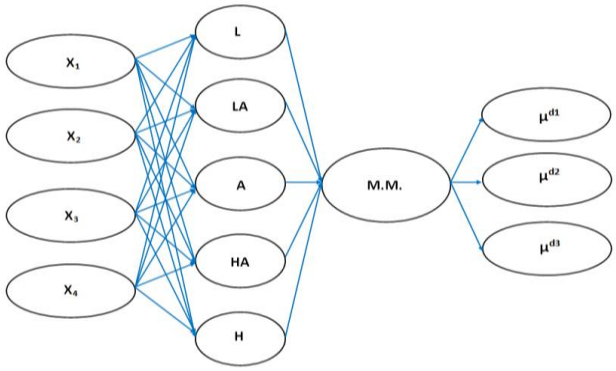

Fig. 2. Medical expert system for evaluating the intensity of reactive postoperative edema in patients with diabetes

The result of the implementation of these blocks was a software shell that works as follows.

1) After starting the program, the user is asked to enter the values of the upper and lower scale of values that are in the database on a certain basis based on the face size indicators, in our case we enter the values that are the main ones when determining
2) To continue working with the program, after filling in all the fields, click "save", to restore previous data that was entered earlier, the user needs to click "retire".

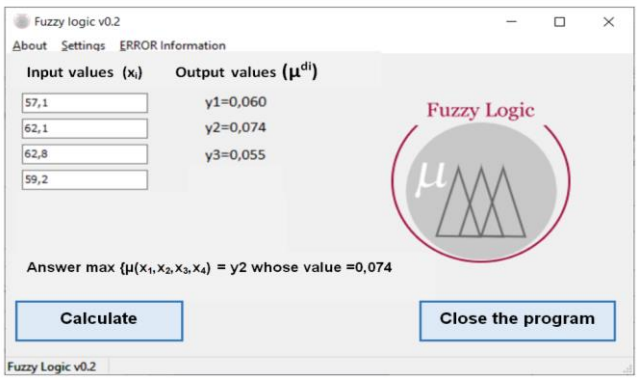

Fig. 3. An example of a dialog window of a program for evaluating the intensity of a reactive postoperative edema in patients with diabetes

Based on the data, a program was developed for assessing the intensity of reactive postoperative edema in patients with diabetes. An example of a dialog box is shown in Fig. 3.

7. Conclusions

The method of using fuzzy sets in the implementation of an information expert system for solving the problems of medical diagnostics, in particular, in assessing the intensity of reactive edema of soft tissues, which develops in the postoperative period in patients of all groups of the study against the background of diabetes, has gained further development.

The paper analyzes the main areas of application of mathematical methods in medical diagnostics, formulates the principles of diagnostics based on fuzzy logic.

Main scientific results: mathematical models and algorithms were developed that formalize the process of making diagnostic decisions based on fuzzy logic with quantitative and qualitative parameters of the patient's condition; developed mathematical models of membership functions, formalizing the representation of quantitative and qualitative parameters of the patient's condition in the form of fuzzy sets, used in models and algorithms for estimating the intensity of edema in patients with diabetes

The developed models and algorithms of medical diagnostics are based on the ideas and principles of artificial intelligence and knowledge engineering, the theory of experiment planning, the theory of fuzzy sets and linguistic variables. The expert system was validated on real data.

The practical value of the work lies in the possibility of using an automated expert system to solve the problems of medical diagnosis based on fuzzy logic when assessing the intensity of reactive swelling of soft tissues, which develops in the postoperative period in patients of all study groups against the background of diabetes.

References

[1] Abdikerimova G. B. et al.: The analysis of textural images on the basis of orthogonal transformations. Journal of Theoretical and Applied Information Technologythis link is disabled 97(1), 2019, 15–22.
[2] Arakeri G. et al.: A randomized clinical trial to compare the efficacy of submucosal Aprotinin injection and intravenous Dexamethasone in reducing pain and swelling after third molar surgery: A prospective study. Journal of Maxillofacial and Oral Surgery 12(1), 2013, 71–75.
[3] Azarova A., Zhytkevych O.: Mathematical methods of identification of ukrainian enterprises competitiveness level by fuzzy logic using. Economic Annals-XXI 9–10(2), 2013, 59–62.
[4] Clinical guidelines for the management of pulpal diseases, approved by Decree 15 of the Council of Public Association "Russian Dental Association". Dated August 2, 2018.
[5] Nizhynska-Astapenko Z. et al.: Information medical fuzzy-expert system for the assessment of the diabetic ketoacidosis severity on the base of the blood gases indices. Proc. SPIE 12126, 2021, 1212626.
[6] Rotshtein A.: Design and Tuning of Fussy IF – THEN Vuly for Medical Didicol Diagnosis. Fuzzy and Neuro-Fuzzy Systems in Medicine. CRC-Press, 1998, 235–295.
[7] Serkova V. K. et al.: Medical expert system for assessment of coronary heart disease destabilization based on the analysis of the level of soluble vascular adhesion molecules. Proc. SPIE 10445, 2017, 104453O.
[8] Taubayev G. et al.: Machine learning algorithms and classification of textures. Journal of Theoretical and Applied Information Technologythis 98(23), 2020, 3854–3866.
[9] Vasilevskyi O. et al.: Method of evaluating the level of confidence based on metrological risks for determining the coverage factor in the concept of uncertainty. Proc. SPIE 10808, 2018, 108082C.
[10] Vassilenko V. et al.: Automated features analysis of patients with spinal diseases using medical thermal images. Proc. SPIE 11456, 2020, 114560L.
[11] Vavilova T. P. et al.: Dental pulp responsiveness. Moscow State University of Medicine and Dentistry, 2017.
[12] Volgin M. A. et al.: Comparative analysis of IL-1. COX-2 and type II collagenase gene expression profile in acute inflammed pulps. Endodontics today 4, 2016, 16–20.
[13] Wójcik W. et al.: Information Technology in Medical Diagnostics II. Taylor & Francis Group. CRC Press, Balkema Book. London 2019.
[14] Wójcik W. et al.: Information Technology in Medical Diagnostics. CRC Press. 2017.

Ph.D. Liudmyla Shkilniak
e-mail: lusinkalusja@gmail.com

Ph.D., National Pirogov Memorial Medical University, Vinnytsya.
Scientific direction: medical diagnostics, diabetes, dentistry, therapeutic effect, regeneration.

http://orcid.org/0000-0002-4925-7734

Prof. Waldemar Wójcik
e-mail: waldemar.wojcik@pollub.pl

He is profesor of the Department of Electronics and Information Technology, former long-time dean of the Faculty of Electrical Engineering and Computer Science at Lublin University of Technology. Doctor Honoris Causa of five universities in Ukraine and Kazakhstan.
In his research he mainly deals with process control, optoelectronics, digital data analysis and also heat processes or solid state physics. In total, he has published 56 books, over 400 papers, and authored several patents

http://orcid.org/0000-0002-6473-9627

Prof. Sergii Pavlov
e-mail: psv@vntu.edu.ua

Academician of International Applied Radioelectronic Science Academy, Professor of Biomedical Engineering and Optic-Electronic Systems Department, Vinnytsia National Technical University. Scientific direction – biomedical information optoelectronic and laser technologies for diagnostics and physiotherapy influence.
Deals with issues of improving the distribution of optical radiation theory in biological objects, particularly through the use of electro-optical systems, and the development of intelligent biomedical optoelectronic diagnostic systems and standardized methods for reliably determining the main hemodynamic cardiovascular system of comprehensive into account scattering effects.

http://orcid.org/0000-0002-0051-5560

D.Sc. Oleg Vlasenko
e-mail: vlasenko@vnmu.edu.ua

Doctor of Medical Sciences, Professor, Vice-rector of for Scientific Work of National Pirogov Memorial University of Vinnytsia, professor at the Department of Human Physiology.
Scientific direction – neural circuits that are responsible for voluntary control of movements, interaction between autonomic and somatic divisions of CNS during operant movements, detection of stress by dynamical position of body center mass and physiological parameters.

http://orcid.org/0000-0001-8759-630X

M.Sc. Tetiana Kanishyna
e-mail: kanyshyna@gmail.com

Postgraduate student, National Pirogov Memorial Medical University, Vinnytsya.
Scientific direction: medical diagnostics, diabetes, dentistry, therapeutic effect, regeneration.

http://orcid.org/0000-0001-9922-5960

D.Sc. Irina Khomyuk
e-mail: vikiraivh@gmail.com

Doctor of Science (Ped.), Professor of the Department of Higher Mathematics the Vinnytsia National Technical University.
Author of more than 190 publications, including 3 monographs, 3 collective monographs, 15 textbooks, more than 100 scientific articles in peer-reviewed journals.
Scientific direction: mathematical modeling of systems, optimization methods, theory and methods of professional education.

http://orcid.org/0000-0002-2516-2968

Ph.D. Oleh Bezverkhyi
e-mail: bezoleg2016@gmail.com

Ph.D., senior lector, Vinnitsa State Pedagogical University named after M. Kotsiubynskyi. Scientific direction: information technologies in medicine, family psychology, modern learning technologies.

http://orcid.org/0000-0001-9322-2646

D.Sc. Sofia Dembitska
e-mail: sofiyadem13@gmail.com

Doctor of Science, docent, Vinnytsia National Technical University, Vinnitsa.
Scientific direction: formation of labor protection culture of future information technology specialist mathematical modeling of systems, optimization methods, theory and methods of professional education.

http://orcid.org/0000-0002-2005-6744

Ph.D. Orken Mamyrbayev
e-mail: morkenj@mail.ru

Deputy Deputy General Director in science and Head of the Laboratory of computer engineering of intelligent systems at the Institute of Information and Computational Technologies of the Kazakh National Technical University named after K. I. Satbayev and associate professor in 2019 at the Institute of Information and Computational Technologies.
Main research field: machine learning, deep learning, and speech technologies.

http://orcid.org/0000-0001-8318-3794

M.Sc. Eng. Aigul Iskakova
e-mail: Iskakova1979@mail.ru

Lecturer of the Kazakh National Research Technical University named after K. I. Satpayev.
Total number of scientific and methodological developments and articles – 45.

http://orcid.org/0000-0001-8043-819X

http://doi.org/10.35784/iapgos.3033

received: 19.06.2022 | revised: 03.09.2022 | accepted: 15.09.2022 | available online: 30.09.2022

SIMULATION OF INFORMATION SECURITY RISKS OF AVAILABILITY OF PROJECT DOCUMENTS BASED ON FUZZY LOGIC

Oleksii M. Shushura[1], Liudmyla A. Asieieva[2], Oleksiy L. Nedashkivskiy[1], Yevhen V. Havrylko[1], Yevheniia O. Moroz[3], Saule S. Smailova[4], Magzhan Sarsembayev[5]

[1]National Technical University of Ukraine "Igor Sikorsky Kyiv Polytechnic Institute", Department of Design Automation for Energy Processes and Systems, Kyiv, Ukraine, [2]State University of Telecommunications, Kyiv, Ukraine, [3]Taras Shevchenko National University of Kyiv, Kyiv, Ukraine, [4]D.Serikbayev East Kazakhstan State Technical University, Ust-Kamenogorsk, Kazakhstan, [5]Al-Farabi Kazakh National University, Almaty, Kazakhstan

Abstract. *The widespread use of computer technology, its rapid development and use in almost all areas of human activity requires constant updating of information security issues. The activities of many enterprises in the field of IT, construction, and other areas are of a project nature and therefore further research on information security management of projects is relevant. Appearance of changes and the current state of the project results at certain points of time describe the documents that accompany it. In this paper, the information structure of the project is considered as a set of specific documents. During the life cycle of each project document, which includes the creation, transfer, preservation and transformation, there are generally threats to its confidentiality, integrity, accessibility and authenticity. This paper develops a method for assessing the risks of violation of the availability of project documents in solving information security problems. A formal description of many project documents in the form of a generalized hierarchical structure is presented, the connection of documents with the operations performed on them and information systems used during these operations is formalized. Given the incompleteness and dimension of the data, the based on fuzzy logic model was developed to assess the risk of document accessibility. Approaches to the assessment of the damage from the violation of the availability of the project document and the method of calculating the overall assessment of the risk of violation of the documents availability are proposed. The results presented in this paper can be used in decision-making processes regarding information security of projects in organizations that have project activities. The approaches proposed in this paper can serve as a basis for the creation of specialized information technologies to automate the calculation of project risk assessments.*

Keywords: information security of the project, cybersecurity risk assessment, fuzzy logic, risk of accessibility breach

SYMULACJA ZAGROŻEŃ BEZPIECZEŃSTWA INFORMACJI W ZAKRESIE DOSTĘPNOŚCI DOKUMENTÓW PROJEKTOWYCH W OPARCIU O LOGIKĘ ROZMYTĄ

Streszczenie. *Powszechne stosowanie techniki komputerowej, jej szybki rozwój i wykorzystanie niemal we wszystkich dziedzinach działalności człowieka wymaga ciągłej aktualizacji zagadnień związanych z bezpieczeństwem informacji. Działalność wielu przedsiębiorstw w zakresie informatyki, budownictwa i innych dziedzin ma charakter projektowy, dlatego istotne są dalsze badania nad zarządzaniem bezpieczeństwem informacji w projektach. Pojawienie się zmian i aktualny stan wyników projektu w określonych momentach czasu opisują towarzyszące mu dokumenty. W niniejszej pracy struktura informacyjna projektu jest rozpatrywana jako zbiór określonych dokumentów. W cyklu życia każdego dokumentu projektu, który obejmuje tworzenie, przekazywanie, przechowywanie i przekształcanie, występują na ogół zagrożenia dla jego poufności, integralności, dostępności i autentyczności. W pracy opracowano metodę oceny ryzyka naruszenia dostępności dokumentów projektowych w rozwiązywaniu problemów bezpieczeństwa informacji. Przedstawiono formalny opis wielu dokumentów projektowych w postaci uogólnionej struktury hierarchicznej, sformalizowano związek dokumentów z wykonywanymi na nich operacjami oraz systemami informatycznymi wykorzystywanymi podczas tych operacji. Biorąc pod uwagę niekompletność i wymiar danych, opracowano oparty na logice rozmytej model oceny ryzyka dostępności dokumentów. Zaproponowano podejście do oceny szkody z tytułu naruszenia dostępności dokumentu projektu oraz metodę obliczania ogólnej oceny ryzyka naruszenia dostępności dokumentów. Wyniki przedstawione w pracy mogą być wykorzystane w procesach decyzyjnych dotyczących bezpieczeństwa informacyjnego projektów w organizacjach prowadzących działalność projektową. Zaproponowane w pracy podejścia mogą stanowić podstawę do tworzenia specjalistycznych technologii informatycznych automatyzujących obliczanie oceny ryzyka projektu.*

Słowa kluczowe: bezpieczeństwo informacji projektu, ocena ryzyka cyberbezpieczeństwa, logika rozmyta, ryzyko naruszenia dostępności

Introduction

The widespread use of computer technology, its rapid development and use in almost all areas of human activity requires constant updating of information security issues. The use of information technology vulnerabilities by both cybercriminals and certain organizations and states makes it necessary to systematically apply cybersecurity methods and tools both at the national level and at individual enterprises. This is especially important for critical infrastructure companies and their business partners, including construction companies. The introduction of info-communication technologies in the construction industry has raised the question of improving existing and developing new means of cybersecurity to take into account its specifics [1, 7, 9, 21]. The issue of cybersecurity of information systems should be considered not only from the angle of protection of classified or important data, but also in terms of ensuring the functional stability of these systems [6].

Decisions regarding the management of information security of the enterprise should be based on the assessment of its risks, which requires sufficiently accurate quantitative methods and tools. However, in the current environment of increasing risks and costs in the field of information security, the measurement of cybersecurity still remains an underdeveloped topic that requires further research [11].

In the field of information technology for modeling uncertainty, the methods and means of fuzzy logic proposed by L. Zadeh [24] have become widespread. The use of this mathematical apparatus allows in many cases to obtain better results than other approaches, for example, in determining the state of a computer system [8]. The characteristics of information security components often contain incomplete and blur ed information, so fuzzy logic has been widely used in risk assessment models. In particular, fuzzy logic is involved in the system administrator warning system in cybersecurity management of critical infrastructure enterprises [4], in the risk mitigation model based on its effective assessment and human behavioral intervention [3], for generalized risk assessment based on vulnerability, threat, probability and impact [2], when modeling information security risks of enterprise management systems [15]. It is known that the most secure information networks are optical networks, and especially the passive optical networks (PON), the study and modeling of which is devoted many works [16–18]. And even their effective use does not completely solve the problem of information security. However, it should be noted that the activities of many enterprises are project-based and therefore information security management should also be implemented within each project, which requires further research in this area.

In a general sense, a project is seen as a set of operations to achieve goals with limited time and resources. Appearance of changes and the current state of the project results at certain points in time describe the documents that accompany it. For example, for a construction company, the document accompanying

the project is the main information asset of the project. Consider the information structure of the project as a set of specific documents. During the life cycle of each project document, which includes the creation, transfer, preservation and transformation, there are threats to its confidentiality, integrity, accessibility and authenticity.

1. Formulation of the problem

The purpose of this work is to develop a model for assessing the risks of information security violations of the availability of project documents based on fuzzy logic. To achieve this goal in this paper formalized the information structure of the project as a set of certain documents, identified input and output linguistic variables, proposed a generalized structure of submodels for calculations.

2. Theoretical research

To formalize the information structure of the project, we denote in the general case the document as $d_{lk}^{i} \in D$, where D – is the set of project documents; i – document number; l – document form, $l \in \{0, 1, 2, 3\}$: 0 – electronic copy, 1 – signed paper original, 2 – paper copy, 3 – electronic document with electronic-digital signature; k – the number of document copy.

All replicas of the i-th document of l document form will be denoted as d_{l}^{i}, and determined by the formula:

$$d_{l}^{i} = \bigcup_{k} d_{lk}^{i} \tag{1}$$

All replicas of the i-th document of all document form will be denoted as (generalized document), and determined by the formula:

$$d^{i} = \bigcup_{l} d_{l}^{i} \tag{2}$$

The set of documents D of the project will be divided into their types:

$$D = \bigcup_{m=1}^{n} D_m, D_j \bigcap D_m = \varnothing, j \neq m \tag{3}$$

where D_m – type of document.

During the life cycle of a document, many different operations can be performed with it, including creation, editing, approval, use, disposal, archiving, and so on. Denote the set of operations on the document d^{i} as P_i. Each operation $p_{ij} \in P_i$ involves the use of certain software and hardware, the work of certain personnel with different levels of access, and so on. Denote as ISP_{ij} the set of information systems used during the operation $p_{ij} \in P_i$ on the document.

An employee of the enterprise and an employee of the contractor or customer (owner) may be involved in the operation $p_{ij} \in P_i$. The set of operations P_i on the document d^{i} can be represented in the form of a network graph showing the technological scheme of document processing. Thus different copies of documents in various forms $d_{lk}^{i} \in D$ can be created, that is to each operation $p_{ij} \in P_i$ in the general case some set of copies of documents is matched.

Violation of the accessibility of the document will be considered the creation of such conditions or the implementation of actions that make it impossible or difficult to access it. Access is blocked or, if possible, for a time that will not ensure the achievement of certain goals or business processes. The threat to the availability of a document is understood as its blocking or destruction, which is associated with user actions, internal failures of the information system, failures of the infrastructure that supports the information system. For example, inability to work with the required document due to lack of appropriate training (lack of general computer education, inability to interpret incoming or outgoing messages, ignorance of the necessary techniques, inability to work with documentation).

The level of risk of violation of the availability RAv^{i} of the document will defined as:

$$RAv^{i} = PAv^{i} \cdot UAv^{i} \tag{4}$$

where PAv^{i} – assessment of the possibility of endangering the availability of the document d^{i}; UAv^{i} – assessment of damage from the threat of violation of the availability of the document d^{i}.

The calculation of the assessment of the possibility of endangering the availability of the document d^{i} is carried out as:

$$PAv^{i} = \min_{l,k} \{ \max_{p_{ij} \in P_i^{lk}} PAv_{j}^{i} \} \tag{5}$$

where PAv_{j}^{i} – the possibility of the threat of violation of the availability of the document d^{i} during the operation, where P_i^{lk} – the set of operations in which the document $d_{lk}^{i} \in D$ is used in l-form and k-replica.

We apply a linguistic approach to the description of risk factors of information security of the project. This will ensure the creation of quantitative estimates for the elements of the model in terms of unclear information about the importance of the level of risk, damage from the threat, the possibility of certain threats, levels of vulnerability to vulnerabilities [15].

To calculate the possibility PAv_{j}^{i} of violation of the availability of the document d^{i} during the operation $p_{ij} \in P_i^{lk}$, a fuzzy model is proposed, the generalized structure of which is shown in figure 1.

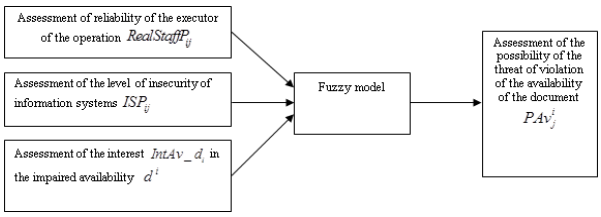

Fig. 1. Fuzzy model for assessing the possibility of endangering the availability of the document

As can be seen in figure 1, in the fuzzy model, the inputs are linguistic variables:

- the level of reliability of the executor of the operation $RealStaffP_{ij}$;
- assessment of the level of insecurity of information systems ISP_{ij};
- assessment of the interest $IntAv\_d_i$ of third-party actors in the impaired availability of the document d^{i}.

For simplicity, we assume that there is only one executor in the operation $p_{ij} \in P_i$. This can be easily achieved, given this assumption when forming a set of operations on the document. An appropriate model based on fuzzy logic can be used to assess the level of reliability of the executor. In this case, a hierarchical fuzzy inference should be used to perform the calculations.

To assess the reliability $RealStaffP_{ij}$ of the executor of the operation $p_{ij} \in P_i$, a fuzzy model is proposed, the structure of which is shown in figure 2.

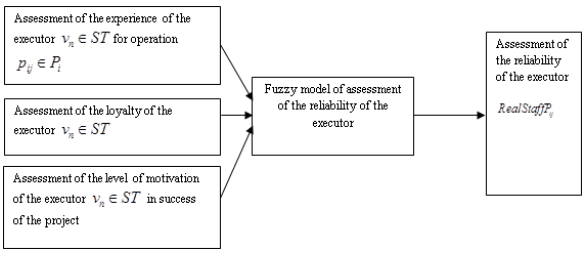

Fig. 2. Fuzzy model for assessing the reliability of the executor

In the fuzzy model of estimating the reliability of the executor, the following linguistic variables with the corresponding characteristics are included:

- experience of the executor $ExpStaffP$;
- assessment of the loyalty of the executor $SatStaffP$;
- level of motivation of the executor in success of the project $MotStaffP$.

The description of the above linguistic variables is shown in tables 1–3 in accordance with the methodology of infographic modeling of fuzzy control problems [19].

Table1. Characteristics of the linguistic variable of the executor's work experience CatStaffP

Experience of the executor *ExpStaffP* .	
Type	Input
Block of variables	
Experience	The set of valid values {0...55 years}
Block of terms	
Experience unavailable	Linear z-shaped membership function $\mu(x, 0.5, 1)$
Beginner	Triangular membership function $\mu(x, 0.5, 2, 3)$
Experienced	Linear s-shaped membership function $\mu(x, 1.5, 3)$
Description of the procedure for forming new terms - not specified	
Description of the procedure for forming the membership functions of terms - not specified	

Table 2. Characteristics of the linguistic variable of the executor's work experience CatStaffP

Loyalty of the executor *SatStaffP*	
Type	Input
Block of variables	
Loyalty level	The set of valid values {0…10}
Block of terms	
Disloyal	Linear z-shaped membership function $\mu(x, 0.5, 1)$
Neutral	Triangular membership function $\mu(x, 0.5, 2, 3)$
Loyal	Linear s-shaped membership function $\mu(x, 2, 3)$
Description of the procedure for forming new terms - not specified	
Description of the procedure for forming the membership functions of terms - not specified	

Table 3. Characteristics of the linguistic variable loyalty of the executor MotStaffP

Level of motivation of the executor in the success of the project *MotStaffP*	
Type	Input
Block of variables	
Level of motivation	The set of valid values {0…10}
Block of terms	
Low	Linear z-shaped membership function $\mu(x, 0.5, 2)$
Neutral	Triangular membership function $\mu(x, 0.5, 2, 3)$
High	Linear s-shaped membership function $\mu(x, 2, 3)$
Description of the procedure for forming new terms - not specified	
Description of the procedure for forming the membership functions of terms - not specified	

The description of the initial linguistic variable reliability of the executor *StaffP* is shown in table 4.

Table 4. Characteristics of linguistic variable reliability of the executor StaffP

Reliability of the executor *StaffP*	
Type	Input
Block of variables	
Level of reliability of the executor	The set of valid values {0…10}
Block of terms	
Unreliable	Linear z-shaped membership function $\mu(x, 2, 5)$
Questionable	Triangular membership function $\mu(x, 2, 5, 8)$
Reliable	Linear s-shaped membership function $\mu(x, 5, 8)$
Description of the procedure for forming new terms of the use of quantifiers is very reliable, more or less reliable, very unreliable, unquestionable	
Description of the procedure for forming the membership functions of terms - very reliable $(\mu(x, 5, 8))^2$; more or less reliable $\sqrt{\mu(x, 5, 8)}$; very unreliable $(\mu(x, 2, 5))^2$; unquestionable $1-\mu(x, 2, 5)$	

To assess the level of insecurity of information systems, it is proposed to use the CVSS standard [10] and calculate the vulnerability of information systems of the operation. Based on this indicator, a linguistic variable is proposed, the description of which in accordance with the methodology of infographic modeling [19] is given in table 5.

Table 5. Description of the linguistic variable of the level of insecurity of information systems

Level of insecurity of information systems *LevelISP* **using CVSS vulnerability estimates**	
Type	Input
Block of variables	
Level of insecurity using CVSS	The set of valid values {1…10}
Block of terms	
None	Linear z-shaped membership function $\mu(x, 0, 0.1)$
Low	Triangular membership function $\mu(x, 0.1, 3.9, 4)$
Medium	Trapezoidal membership function $\mu(x, 3.9, 4.0, 6.9, 7)$
High	Trapezoidal membership function $\mu(x, 6.9, 7.0, 8.9, 9)$
Critical	Triangular membership function $\mu(x, 8.9, 9, 10)$
Description of the procedure for forming new terms - not specified	
Description of the procedure for forming the membership functions of terms - not specified	

To form the membership functions of the terms of the linguistic variable, the processing of expert estimates based on the method of analysis of Saaty hierarchies was used [5, 20].

In order to assess the level of interest in impaired accessibility of the document, it is proposed to use the method of hierarchy analysis, based on expert assessments according to the three-level hierarchy of threat actors and types of documents shown in figure 8. In other cases, when this assumption cannot be applied, this assessment is established by an expert [12–14].

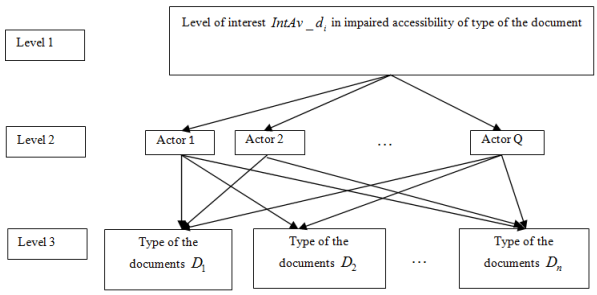

Fig. 8. Tree of criteria for assessing the level of interest in violating the availability of the document

The description of the linguistic variable of the possibility of violation of the accessibility of the document is shown in table 6.

Table 6. Description of the linguistic variable possibility of violation of document accessibility

Level of the possibility of violation of the accessibility PAv of the document	
Type	Output
Block of variables	
The name of an ordinary variable	The set of valid values [0,1]
Block of terms	
Low	Linear z-shaped membership function $\mu(x,0,0.5)$
Medium	Triangular membership function $\mu(x,0,0.5,1)$
High	Linear s-shaped membership function $\mu(x,0.5,1)$
Description of the procedure for forming new terms - not specified	
Description of the procedure for forming the membership functions of terms - not specified	

On the basis of the offered linguistic variables and their terms the fuzzy production rules for performance of calculations on models are constructed [23, 24].

In a simplified form, the set of rules for fuzzy products is as follows:

$$\text{Rule } R\text{: <IF> } \bigcap_{i=1}^{N} A_i \text{ <THEN> } \bigcap_{j=1}^{M} C_j$$

where N – the number of subconditions included in the rule R; M – the number of subconclusions included in the rule R; A_i – is a subcondition that is part of the R rule and is a fuzzy statement consisting of an input linguistic variable and a corresponding term; C_j – is a subconclusion that is part of the rule R and is a fuzzy statement consisting of the original linguistic variable and the corresponding term.

Using one of the algorithms of fuzzy inference, for example, the Mamdani method, based on the rules of the fuzzy model to assess the possibility of violation of the availability of the document calculates the possibility PAv^i of violation of the availability of the document d^i during the operation $p_{ij} \in P_i^{lk}$. Next, using formula (5), a general assessment PAv^i of the possibility of a threat of violation of the availability of the document d^i is calculated.

To calculate the quantitative assessment of the risk of violation of the availability of the document in accordance with formula (4), it is necessary to calculate the assessment UAv^i of the damage from the threat of violation of the availability of the document d^i.

The calculation of the damage assessment UAv^i from the threat of violation of the availability of the document d^i requires the creation of a set of partial indicators that form the damage or loss. A generalized list of these partial indicators is presented in table 1. The indicators are divided into three groups: external loss or damage to the enterprise, internal loss or damage to the enterprise, financial losses of the enterprise. It is proposed to calculate the value of UAv^i by using the method of hierarchy analysis, the tree of criteria which consists of the levels of partial indicators of damage, types of project documents and documents distributed by type. Damage from accessibility is assessed in monetary terms or in points that can be used to make decisions about information security.

Table 7. List of partial damage/loss indicators

No	Title of the indicator	Group of indicators
1	Damage to the authority of the organization	External damage/loss
2	Damage to the authority of the state in the international arena	
3	Legal costs	
4	Negative reaction at the government level	
5	Publication of negative materials in the press	
6	The possibility of committing terrorist acts	
7	The possibility of man-made disasters	
8	Dismissal of specialists of the organization	Internal damage/loss
9	Reducing the level of information security	
10	Loss or destruction of the organization's assets	
11	Influence on the decisions made by the staff of the organization in business processes	
12	The need to verify and restore the integrity of the asset	
13	Deterioration of the emotional climate in the team	
14	Disorganization of activities	
15	The need for manual work	
16	Reducing the competitiveness of the organization	Financial loss
17	Loss of benefits when concluding contracts	
18	Decrease in liquidity and share price	
19	Inability of the organization to fulfill its obligations to customers and suppliers	
20	The need for additional research	
21	Ability to steal assets and conduct unaccounted transactions	
22	Decrease in prices for products, sales	
23	Loss of patenting, sale of licenses	
24	Anticipation of competitors bringing similar products to market	
25	Abandonment of strategic decisions that have become ineffective	
26	Deterioration of credit conditions	
27	Falling profitability	
28	Reducing the level of cooperation with business partners	
29	Mass theft, fraud	

3. Conclusions

1) The paper develops a method for assessing the risks of violation of the availability of project documents in solving information security problems. A formal description of many project documents in the form of a generalized hierarchical structure is presented, the connection of documents with the operations performed on them and information systems used during these operations is formalized. Given the incompleteness and dimension of the data, based on fuzzy logic, a model was developed to assess the risk of document accessibility. Approaches to the assessment of the damage from the violation of the availability of the project document and the method of calculating the overall assessment of the risk of violation of the availability of documents are proposed.
2) These results can be used in decision-making processes regarding information security of projects in organizations that have project activities, including IT companies, construction companies, critical infrastructure companies and others. The approaches proposed in this paper can serve as a basis for the creation of specialized information technologies to automate the calculation of project risk assessments.

References

[1] Abid H. et al.: Structuration Model of Construction Management Professionals, Use of Mobile Devices. Journal of Management in Engineering 37(4), 2021 [http://doi.org/10.1061/(ASCE)ME.1943-5479.0000930].

[2] Al-Ali M. et al.: Improving risk assessment model of cyber security using fuzzy logic inference system. Computers & Security 74, 2018, 323–339 [http://doi.org/doi:10.1016/j.cose.2017.09.011].

[3] Al-Ali M., Al Mogren A.: Fuzzy logic methodology for cyber security risk mitigation approach. Journal of Networking Technology 8(3), 2017.

[4] Alam J. et al.: Advance Cyber Security System using fuzzy logic. Journal of Management & IT ACME 10, 2014, 17–29.

[5] Azarova A.: Information Technologies and Neural Network Means for Building the Complex Goal Program Improving the Management of Intellectual Capital. Lecture Notes on Data Engineering and Communications Technologies 77, 2022, 534–547.

[6] Barabash O. et al.: Application of Petri Networks for Support of Functional Stability of Information Systems. IEEE First International Conference on System Analysis & Intelligent Computing (SAIC), Kyiv 2018, 36–39.
[7] Bharadwaj R. K., de Sotob B. G.: Cyber security challenges and vulnerability assessment in the construction industry. Conference Creative Construction, Budapest 2019, 30–37 [http://doi.org/10.3311/CCC2019-005].
[8] Gavrylenko S. et al.: Development of a method for identifying the state of a computer system using fuzzy cluster analysis. Advanced Information Systems 4(2), 2020, 8–11 [http://doi.org/10.20998/2522-9052.2020.2.02].
[9] https://www.construction-institute.org/events/education/free-webinar-cybersecurity-for-construction (available 09.02.2022).
[10] https://www.first.org/cvss/v3.1/user-guide (available 16.02.2022).
[11] https://www.nist.gov/cybersecurity/measurements-information-security (available 09.02.2022).
[12] Kvyetnyy R. et al.: Blur recognition using second fundamental form of image surface. Proc. SPIE 9816, 2015, 98161A.
[13] Kvyetnyy R. et al.: Method of image texture segmentation using Laws' energy measures. Proc. SPIE 10445, 2017, 1044561.
[14] Kvyetnyy R. et al.: Modification of fractal coding algorithm by a combination of modern technologies and parallel computations. Proc. SPIE 9816, 2015, 98161R.
[15] Mishchenko A. V. et al.: A vague model for assessing the security of information security and the level of security of ERP systems. Telecommunications and Information Technologies 66, 2020, 142–151 [http://doi.org/10.31673/2412-4338.2020.011451].
[16] Nedashkivskiy O. et al.: Mathematical support for automated design systems for passive optical networks based on the β-parametric approximation formula. International Journal of Advanced Trends in Computer Science and Engineering 9(5), 2020, 8207–8212 [http://doi.org/10.30534/ijatcse/2020/186952020].
[17] Nedashkivskiy O.: Precise method of balancing passive optical networks with irregular splitter with two or more outputs. 2nd International Conference on Advanced Information and Communication Technologies (AICT), 2017, 228–231 [http://doi.org/10.1109/AIACT.2017.8020107].
[18] Nedashkivskyy O. L. et al.: Methods of creating passive optical networks with the distributing bus topology. Control, Navigation and Communication Systems 2(42), 2017, 206–217.
[19] Shushura O. M.: Infological modeling of information systems subject industries in solving of fuzzy control tasks. Link 2, 2018, 53–56.
[20] Shyian A. A. et al.: Modeling communication between the public and the authorities while implementing innovative projects in the context of e-democracy and public administration. Science and Innovation 16(6), 2021, 18–27.
[21] Sonkor M., de Sotob B. G.: Operational Technology on Construction Sites: A Review from the Cybersecurity Perspective. Journal of Construction Engineering and Management 147(12), 2021 [http://doi.org/10.1061/(ASCE)CO.1943-7862.0002193].
[22] Trishch R. et al.: Methodology for multi-criteria assessment of working conditions as an object of qualimetry. Engineering Management in Production and Services 13(2), 2021, 107–1141.
[23] Trishch R. et al.: Qualimetric method of assessing risks of low quality products. MM Science Journal 2021, 4769–4774.
[24] Zadeh L.A.: Fuzzy sets. Information and Control 8, 1965, 338–353.

D.Sc. Oleksii M. Shushura
e-mail: leshu@i.ua

Doctor of Technical Sciences, Associate Professor, Professor of the Department of Automation of Designing of Energy Processes and Systems, National Technical University of Ukraine "Igor Sikorsky Kyiv Polytechnic Institute", Kyiv, Ukraine. Author of over 101 publications, including 1 monographs, 4 textbooks, more than 47 scientific articles in professional journals, of which 1 are in the scientometric databases Scopus and Web of Science.

http://orcid.org/0000-0003-3200-720X

M.Sc. Liudmyla A. Asieieva
e-mail: aseewal@i.ua

Postgraduate student, State University of Telecommunications, Kyiv, Ukraine. Author of 4 publications in professional journals.

http://orcid.org/0000-0001-5954-4211

D.Sc. Oleksiy L. Nedashkivskiy
e-mail: al_1@ua.fm

Doctor of Technical Sciences, Associate Professor, Professor of the Department of Automation of Designing of Energy Processes and Systems, National Technical University of Ukraine "Igor Sikorsky Kyiv Polytechnic Institute", Kyiv, Ukraine. Author of more than 40 publications, including 1 monographs, 5 textbooks, more than 25 scientific articles in professional journals, of which 4 are in scientometric databases Scopus and Web of Science.

http://orcid.org/0000-0002-1788-4434

D.Sc. Yevhen V. Havrylko
e-mail: gev.1964@ukr.net

Doctor of Engineering Sciences, Professor, Department of design automation for energy processes and systems National Technical University of Ukraine "Igor Sikorsky Kyiv Polytechnic Institute", Kyiv, Ukraine. Author of more than 33 publications, including 2 textbooks, 3 patents for inventions and more than 20 scientific articles in professional journals, of which 5 are in scientometric databases Scopus and Web of Science.

http://orcid.org/0000-0001-9437-3964

Ph.D. Yevheniia O. Moroz
e-mail: morozeo@knu.ua

Associate professor, Ph.D. Department of Theory and History of Sociology, Taras Shevchenko National University of Kyiv. Scientific interests: history of sociology, modern sociological theories, theories of cultural capital, post-structuralist approach, urban studies, data analysis.

http://orcid.org/0000-0002-2618-3541

Ph.D. Saule Smailova
e-mail: Saule_Smailova@mail.ru

Saule Smailova is currently a lecturer at the Department of Information Technology. She is a co-author over 60 papers in journals, book chapters, and conference proceedings. Member of Expert Group in the Computer Science specialization of IQAA. Her professional interests are teaching, artificial intelligence, software engineering, data processing.

http://orcid.org/0000-0002-8411-3584

Ph.D. Magzhan Sarsembayev
e-mail: magatrone@mail.ru

Senior lecturer of the Department of Computer Science of Al-Farabi Kazakh National University. Author of more than 10 scientific works published in leading journals of Kazakhstan Republic and the far abroad. Research area: High performance computing, intelligent systems of control, software engineering, 3d modeling and design.

http://orcid.org/0000-0003-2139-2456

http://doi.org/10.35784/iapgos.3031

received: 19.06.2022 | revised: 24.08.2022 | accepted: 15.09.2022 | available online: 30.09.2022

MANAGEMENT OF THE WORKPLACES BY THE FACILITIES OF OPERATIONS RESEARCH

Nataliia Geseleva[1], Ganna Proniuk[2], Olexander Romanyuk[3], Olga Akimova[4], Tetiana Troianovska-Korobeynikova[3], Liudmyla Savytska[3], Saule Rakhmetullina[5], Nurbapa Mekebayev[6]

[1]State University of Trade and Economics, Department of Digital Economy and System Analysis, Kyiv, Ukraine, [2]Kharkiv National University of Radio Electronics, Department of Occupational Safety, Kharkiv, Ukraine, [3]Vinnytsia National Technical University, Vinnytsia, Ukraine, [4]Vinnytsia National Technical University, Department of Pedagogy and Vocational Education, Vinnytsia, Ukraine, [5]D. Serikbayev East Kazakhstan Technical University, Ust-Kamenogorsk, Kazachstan, 6 Kazakh National Women's Pedagogical University, Almaty, Kazachstan

Abstract. *The optimal location of workplaces plays an important role in the structure of occupational safety. The design of the workspace should ensure the optimal distribution of functions between person and machine in order to create safe working conditions, reduce the severity of work and the level of production injuries. Most often, workplace planning is carried out manually, by simple calculation, and then the rationality of workplace planning is evaluated, based on statistics of industrial accidents and occupational diseases, as well as indicators of labor productivity, for example, the ratio of compliance with norms. To solve the problem of optimal placement in the work mathematical models are built that can take into account various regulatory restrictions and are simple for further software implementation. It is proposed to choose the theory of φ-functions as a basis, which can be characterized as measures of proximity of objects. Thus, the set task of optimal placement of workplaces is reduced to the task of mathematical programming. The objective function determines the criterion of optimality – the minimization of the area or perimeter that will be occupied by the objects. This formulation of the problem is relevant because the use of the smallest production area, taking into account safety requirements, is an economic condition for effective production management. The constraint on the relative location of workplaces is set using φ-functions, which defines the decision domain. That, when formalizing restrictions, you can take into account all regulatory safety distances between workplaces, equipment, walls, etc. Thus, the work explores an approach that will allow automatic planning of the placement of a large number of technological objects, workplaces in accordance with occupational safety standards. Use of the software application, which can be implemented on the basis of the φ-functions apparatus, will significantly reduce the time of workplaces planning and increase its efficiency.*

Keywords: occupational safety, working place, φ-functions, occupational ergonomics, operations research

ZARZĄDZANIE MIEJSCEM PRACY ZA POMOCĄ BADAŃ OPERACYJNYCH

Streszczenie. *W strukturze ochrony pracy ważną rolę odgrywa optymalna organizacja miejsc pracy. Projektowanie przestrzeni roboczej powinno zapewnić optymalny podział funkcji pomiędzy człowieka i maszynę w celu stworzenia bezpiecznych warunków pracy, zmniejszenia uciążliwości pracy i poziomu urazów odniesionych w pracy. Najczęściej planowanie miejsca pracy odbywa się ręcznie, poprzez proste obliczenia, a następnie ocenia się racjonalność planowania miejsca pracy na podstawie statystyk urazów i chorób zawodowych, a także wskaźników wydajności pracy, na przykład współczynnika zgodności z normami. Do rozwiązania problemu optymalnego rozmieszczenia budowane są modele matematyczne, które mogą uwzględniać różne ograniczenia normatywne i są proste do dalszej implementacji programowej. Proponuje się wybór teorii funkcji φ, którą można scharakteryzować jako miarę bliskości obiektów. W ten sposób problem optymalnego rozmieszczenia miejsc pracy sprowadza się do problemu programowania matematycznego. Funkcja celu określa kryterium optymalności – minimalizację obszaru lub obwodu, który ma być zajęty przez obiekty. Takie postawienie problemu jest istotne, ponieważ wykorzystanie najmniejszej powierzchni produkcyjnej, z uwzględnieniem wymogów bezpieczeństwa, jest ekonomicznym warunkiem efektywnego zarządzania produkcją. Ograniczenia wzajemnej lokalizacji miejsc pracy ustalane są za pomocą funkcji φ, co określa domenę decyzyjną. Tak więc przy formalizowaniu ograniczeń można uwzględnić wszystkie normatywne odległości bezpieczeństwa między miejscami pracy, urządzeniami, ścianami itp. W związku z tym w artykule badane jest podejście, które będzie automatycznie planować rozmieszczenie dużej liczby obiektów technologicznych, miejsc pracy odpowiednio do standardów bezpieczeństwa pracy. Zastosowanie oprogramowania, które może być realizowane na bazie funkcji φ, znacznie skróci czas planowania miejsc roboczych i zwiększy jego efektywność.*

Słowa kluczowe: ochrona pracy, miejsce pracy, funkcja φ, ergonomia miejsc pracy, badania operacyjne

Introduction

The issues of workplace ergonomics in safety play an important role. Equipment and organization of the workplace must ensure that all its elements and the mutual position of all workplaces according with ergonomic requirements, taking into account the nature and characteristics of work. Production equipment should be installed, located and used in the way to reduce risks for operators and other workers (sufficient space between moving and stationary parts of equipment or moving parts around it, safe supply and disposal of all energy and substances used or produced). Workers must have safe access to all areas intended for operation, regulation and maintenance, as well as the ability to safely stay in them and safely leave these areas.

At the same time, occupational safety and environmental protection requirements are basic, and are present in every sphere of human activity. Many of them boil down to the fact that objects should be placed in a limited area, as close (further) as possible to each other or to some fixed objects, with restrictions on the pairwise minimum (maximum) distance, the presence of prohibition zones, etc. Forbidden areas may be residential buildings, reserves, sanitary zones, landscape elements and other areas. Objects can be, for example, hazardous production, waste disposal, noise and vibration generators, or simply workplaces of PC users and light sources [7].

Under the workplace is understood as a place equipped with means of displaying information, management and auxiliary equipment, where the work of a specialist is carried out. The organization of the workplace is called a system of measures to equip the workplace with tools and objects of labor and their placement in a certain order to optimize the working conditions, security, maximum efficiency and reliability of human.

The standard approach in the occupational safety system to the placement of workplaces is as follows: specialists study all the requirements for the size of workplaces, their mutual placement and manually draw up a layout. However, often there are problems of planning a large number of workplaces in a limited space. This paper proposes a formalized approach to the organization of workplaces, which can be used when planning the placement of objects of various purposes and shapes. There are several ways to solve this problem, in this paper it is proposed to use the mathematical apparatus of operations research, namely, the construction of φ-functions, which can be characterized as a measure of the proximity of an object.

The tasks of optimal placement of objects – one of the most important classes of problems in the operations research. Their applications arise in various fields of science and technology, and take of great practical importance. When placing technological equipment, enterprises and other objects of the real world, as a rule, it is required to locate them on a smaller area, not chaotically, but with observance of a certain order, taking into account the many restrictions dictated by state regulations.

The purpose of this work is to apply the formal apparatus of operations research, namely φ-functions, to solving the problem of workplaces placing, taking into account all occupational safety requirements. The proposed model can be easily implemented programmatically using any modern applications and languages, which will allow you to automatically receive a layout of production facilities in the shortest possible time, which takes into account various safety requirements and will be cost-effective, as it allows to reduce production resources, which is certainly interesting from a practical point of view.

1. Formulation of the problem

The correct organization of the workplace should ensure, firstly, the safety of work, and secondly, high labor productivity. When designing a workplace, it is necessary to proceed from the analysis of a specific labor process performed by a person on this equipment, take into account the anthropometric data of a person, sanitary and hygienic working conditions.

The main role among ergonomic indicators belongs to anthropometric parameters, which determine the conformity of the equipment to the size and shape of the human body, the distribution of his mass. The design of the workplace should provide such physical loads for the worker, in which the energy consumption of the human body during the working day would not exceed 1046.7 kJ/h [5].

At the same time, the equipment should be able to support the work process that eliminate the monotony of job by limiting the frequency of simple repetition processes and the duration of continuous monitoring. Production equipment has to provide the necessary space to operator for any of its positions.

The rational layout of the workplace provides a comfortable working posture, the possibility of using advanced techniques and methods of work, minimal trajectories of movements of the worker, objects of labor, which prevents premature fatigue and a decrease in labor productivity. At the same time, the placement of workplaces and equipment on it must comply with the norms and requirements for occupational safety. In modern conditions at enterprises this issue is solved by a safety specialist, based on theoretical calculations in each specific case (taking into account the production tasks performed, the technologies used, etc.). This approach takes a lot of time, especially when planning large industrial premises, and does not exclude the appearance of calculation errors.

Subsequent estimation and rationalization of the layout of the workplace are carried out on the basis, for example, of the occupancy rate of the production area or during the certification of the workplace (on average once every 5 years). The occupancy rate of the production area is calculated as the sum of the ratios of the norms of the area occupied by the equipment element to the area of the workplace according to its layout (should be in the range of 0.4–0.65).

Thus, the task of the study is to apply the mathematical apparatus of operations research to the problem of workplace placement, which allows you to automatically obtain the optimal placement in accordance with the specifics of production, taking into account the requirements of regulatory documents on safety.

The use of the proposed mathematical apparatus will speed up the planning of workplaces, help save enterprise resources and guarantee a safe organization of the workplace and high work productivity.

2. Theoretical research

Placement problems, as the most important class of optimization geometric design tasks, determine the optimal position of a finite set of geometric objects of arbitrary spatial shape in given areas of placement in the presence of various restrictions and quality criteria and related to geometric information processing. The beginning of the development of approaches to modeling and solving problems of optimal placement, especially the problems of cutting and packaging, was laid by the works of L.V. Kantarovich, B.A. Zalgaller, Yu.G. Stoyan, P. Gilmore and others.

Development of geometric design, thanks to the works of the scientific school Yu.G. Stoyan and O.O Yemets, contributed to the creation in the 1990s of Euclidean combinatorial optimization, which allowed the optimal placement of objects using analytical [4] and algorithmic [13] optimization methods on combinatorial sets.

The creation of the theory of optimization geometric design, which is based on the construction and study of various types of mappings of geometric information, allowed to build a mathematical apparatus for modeling such important applied problems as the problem of optimal cutting of industrial materials [5, 6], development of master plans of industrial enterprises, waste management, design and management of complex technical systems, including taking into account physical fields of various nature [3], if the carriers of these fields have an arbitrary spatial shape.

One of the most important stages in the construction and study of mathematical models of such problems is analytical modeling of constraints (geometric constraints, taking into account the spatial shape of objects and areas of location, and constraints due to the peculiarities of this problem, such as constraints on the characteristics of the resulting physical fields, technological constraints, etc.), which highlight the area of acceptable solutions to the optimization problem. Therefore, to solve the problems of these classes it is necessary to develop tools for modeling the basic geometric constraints, namely, the conditions of mutual non-intersection of objects and their affiliation to the location, based on the apparatus of φ-functions [10].

The objects to be placed are divided into many simplest geometric objects, such as a rectangle, a polygon and a circle. Using the theory of φ-functions, a decision tree is constructed, the leaves of which are independent linear programming tasks. Each such subtask consists of an objective function and a system of linear constraints, operating with a measure of the proximity of objects and implementing the constraints of the model. Introduce the some definitions.

An object T_i, translated on a vector u_i is denoted as

$$T_i(u_i) = \{X \in R^n \mid X = u_i + Y, Y \in T_i\}, \tag{1}$$

where $u_i \in R^n, n = 2, 3$ is the vector of parameters of object placement T_i, $i = 1,2$.

A continuous and everywhere defined function

$$\varphi : R^{2n} \to R^1, n = 2, 3, \tag{2}$$

is called φ-function of objects $T_1(u_1)$ and $T_2(u_2)$ if it satisfies the following characteristic properties [17]:

- $\varphi(u_1, u_2) > 0$, if $cl\,T_1(u_1) \cap cl\,T_2(u_2) = \varnothing$,
- $\varphi(u_1, u_2) = 0$, if $\operatorname{int} T_1(u_1) \cap \operatorname{int} T_2(u_2) = \varnothing$ and $fr\,T_1(u_1) \cap fr\,T_2(u_2) \neq \varnothing$,
- $\varphi(u_1, u_2) < 0$, if $\operatorname{int} T_1(u_1) \cap \operatorname{int} T_2(u_2) \neq \varnothing$.

Due to the fact that it is of interest to locate workplaces (for example tables), i.e. objects of rectangular shape, then we give an example of constructing a φ-function for two rectangles. The task of optimal placement of workplaces is reduced to the problem of mathematical programming. The objective function determines the optimality criterion – minimizing the area or perimeter occupied by objects. Restrictions on the mutual arrangement of tables are set with the help of φ-functions, and describe the scope of the solutions search.

Let the rectangles $R_1(u_1)$ and $R_2(u_2)$ be given by the length $2a_1$, $2a_2$ and width $2b_1$, $2b_2$ and respectively. Construct a curve γ_{12} – a set of points at which $\varphi_{12}(u_1, u_2)=0$ (as was shown in Fig. 1), so

$$\gamma_{12} = fr\{R_1(0) + (-1)R_2(0)\}. \tag{3}$$

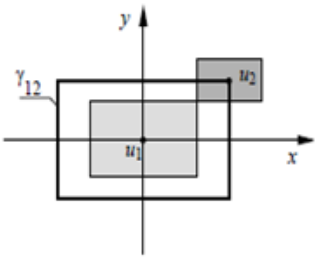

Fig. 1. The curve γ_{12} for rectangles

Consider the equations of four lines that limit γ_{12}:

$$\chi_1(x, y) = x - A, \qquad \chi_2(x, y) = y - B,$$
$$\chi_3(x, y) = -x - A, \qquad \chi_4(x, y) = -y - B, \tag{4}$$

where $A = a_1 + a_2$, $B = b_1 + b_2$.

Thus $T_{12} = \{(x, y) \in R^2: \chi_i(x, y) \le 0,\ i=1,\dots,4\}$, and therefore:

$$\gamma_{12} = \left\{(x, y) \in R^2 : \chi(x, y) = \max_{i=1,\dots,4} \chi_i(x, y) = 0\right\} \tag{5}$$

The corresponding orientation $\chi(x, y)=0$ is set so that the φ-function of the rectangles takes the form:

$$\varphi_{12}(u_1, u_2) = \chi(x_2 - x_1, y_2 - y_1). \tag{6}$$

It should also be noted that φ_{12} is not normalized [9] since the values of $\varphi_{12}(u_1, u_2)$ are not equal to the distances between the rectangles $R_1(u_1)$ and $R_2(u_2)$ in the general case, namely: in cases when (dx, dy) with $dx = x_2 - x_1$ and $dy = y_2 - y_1$ satisfy one of the following systems:

$$\begin{cases}\chi_1(dx, dy) > 0\\ \chi_2(dx, dy) > 0\end{cases} \quad \begin{cases}\chi_2(dx, dy) > 0\\ \chi_3(dx, dy) > 0\end{cases}$$
$$\begin{cases}\chi_3(dx, dy) > 0\\ \chi_4(dx, dy) > 0\end{cases} \quad \begin{cases}\chi_4(dx, dy) > 0\\ \chi_1(dx, dy) > 0\end{cases} \tag{7}$$

For construct a normalized φ-function of two rectangles $R_1(u_1)$ and $R_2(u_2)$ it is necessary to introduce some additional functions:

$$\tilde{\chi}_1(x, y) = x+y-s, \qquad \tilde{\chi}_2(x, y) = -x+y-s, \tag{8}$$

$$\tilde{\chi}_3(x, y) = -x-y-s, \qquad \tilde{\chi}_4(x, y) = x-y-s, \qquad s = A+B, \tag{9}$$

$$\varphi_1(x, y) = \sqrt{(x-A)^2 + (y-B)^2},$$
$$\varphi_2(x, y) = \sqrt{(x+A)^2 + (y-B)^2}, \tag{10}$$
$$\varphi_3(x, y) = \sqrt{(x+A)^2 + (y+B)^2},$$
$$\varphi_4(x, y) = \sqrt{(x-A)^2 + (y+B)^2}. \tag{11}$$

Then we have

$$\varphi_{12}(0, 0, x, y) = \omega(x, y) =$$
$$= \max\left\{\max_{i=1,2,3,4} \chi_i(x, y),\ \max_{i=1,2,3,4} \min\{\varphi_i(x, y), \chi_i(x, y)\}\right\} \tag{12}$$

Normalized φ-function $R_1(u_1)$ and $R_2(u_2)$ takes the form

$$\varphi_{12}(u_1, u_2) = \omega(x_2 - x_1, y_2 - x_1). \tag{13}$$

Thus, the optimization problem was formulated, and constraints were chosen to model the optimal placement of workplaces (rectangular tables) in the minimum area.

3. Experimental research

It is proposed to solve the obtained system of linear equations (8–12) with the help of a simplex-method, which provides a fast working time for tasks of small and medium dimension. In the future, the solution of the obtained system of linear equations will give the opportunity to correctly locate workplaces in the minimum area in compliance with all the rules and regulations.

The proposed solution to the task of optimal placing of workplaces can have several interpretations. It depends on the choice of the optimization function and the specifics of the setting requirements. For example, you need to minimize the space between a few geometrical objects. In this case, with known geometric dimensions of the given rectangle, this model has the solution shown in the figure 2.

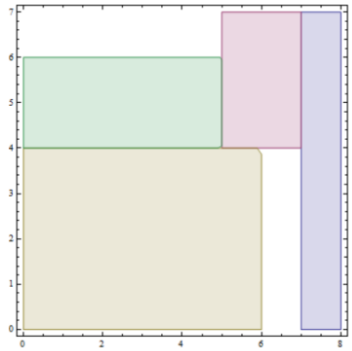

Fig. 2. Example of model realization

Above, we considered the simplest case of placing workplaces (for example, tables). However, this mathematical apparatus is applicable to all the simplest mathematical objects. Consider a situation where the optimization of placement is necessary for the workplace and some equipment [2].

Let the object $R_1^*(u_1)$ and the rectangle $R_2(u_2)$ be known, while R_1^* is characterized by $2a_1$ and $2b_1$. The length $2a_2$ and width $2b_2$ of rectangle R_2 are such that $a_1 \ge a_2$ and $b_1 \ge b_2$. In this case

$$\gamma_{12} = \mathrm{fr}T_{12} = \mathrm{fr}\{R_1^*(0)+(-1)R_2(0)\}, \tag{14}$$

where $T_{12} = \mathrm{cl}(R^2 \setminus \{(x, y) \in R^2: -A \le x \le A, -B \le y \le B\})$, $A = a_1 - a_2$, $B = b_1 - b_2$.

Setting,

$$\chi_1(x, y) = A-x,\ \chi_2(x, y) = B-y,$$
$$\chi_3(x, y) = A+x,\ \chi_4(x, y) = B+y, \tag{15}$$

we have

$$D_0 = \mathrm{cl}(R^2 \setminus T_{12}) = \{(x, y) \in R^2: \chi_i(x, y) \ge 0,\ i = 1,\dots, 4\} \tag{16}$$

and therefore

$$\gamma_{12} = \mathrm{fr}D_0 = \mathrm{fr}T_{12} = \{(x,y) \in R^2: \chi(x,y) = 0\}, \tag{17}$$

where $\chi(x, y) = \min\{\chi_1(x, y), \chi_2(x, y), \chi_3(x, y), \chi_4(x, y)\}$.

Thus, the normalized φ-function of the object $R_1^*(u_1)$ and the rectangle $R_2(u_2)$ takes the form

$$\varphi_{12}(u_1, u_2) = \chi(x_2 - x_1, y_2 - y_1). \tag{18}$$

Suppose that we need to place two round objects $C_1(u_1)$ and $C_2(u_2)$. Let C_1 and C_2 be circles of radiuses r_1 and r_2 respectively (Fig. 3). In this case

$$T_{12} = C_1(0) + (-1)C_2(0) =$$
$$= \{(x, y): \chi(x, y) = x^2 + y^2 - (r_1+r_2)^2 \le 0\}. \tag{19}$$

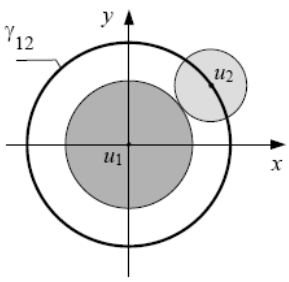

Fig. 3. The curve γ_{12} for objects $C_1(u_1)$ and $C_2(u_2)$

Therefore, the curve $\chi_{12} = \mathrm{fr}T_{12}$ can be described by the equation $\chi(x, y) = 0$, i.e. the set of positions of the circle C_2 relative to C_1 is such that the circles are touching [2]. The equation $\chi(x, y) = 0$ according to [10]. Therefore, in order to determine the φ-function, in this case it is sufficient to set the corresponding orientation of the equation $\chi(x, y) = 0$.

Then,

$$\varphi_{12}(0, 0, x_2, y_2) = x_2^2 + y_2^2 - (r_1 + r_2)^2,$$
$$\varphi_{12}(u_1, u_2) = (x_2 - x_1)^2 + (y_2 - y_1)^2 - (r_1 + r_2)^2, \tag{20}$$

where $u_i = (x_i, y_i)$, $i = 1, 2$ – circle broadcast vector C_1 and C_2 .

Next, we consider the mutual placement of some object $C_1^*(u_1)$ and the circle $C_2(u_2)$. Let C_1 and C_2 be circles of radiuses r_1 and r_2, and let $r_1 \ge r_2$ (Fig. 4).

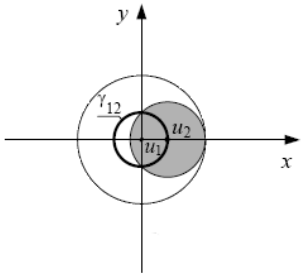

Fig. 4. The curve χ_{12} for object $C_1^*(u_1)$ and circle $C_2(u_2)$

Then,

$$T_{12} = C_1^*(0) + (-1)C_2(0) = \\ = \{(x, y): \chi(x, y) = (r_1 - r_2)^2 - (x^2 + y^2) \le 0\}. \quad (21)$$

Therefore, the curve χ_{12} can be determined by the equation $\chi(x, y) = 0$. Then,

$$\varphi_{12}(0, 0, x_2, y_2) = \chi(x_2, y_2) = (r_1 - r_2)^2 - x_2^2 - y_2^2, \\ \varphi_{12}(u_1, u_2) = -(x_2 - x_1)^2 - (y_2 - y_1)^2 + (r_2 - r_1)^2. \quad (22)$$

To construct a normalized φ-function of the objects $C_1^*(u_1)$ and $C_2(u_2)$, instead of the function χ, use the function

$$\tilde{\chi}(x, y) = (r_1 - r_2) - \sqrt{x^2 + y^2} \quad (23)$$

then

$$\tilde{\Phi}_{12}(u_1, u_2) = (r_1 - r_2) - \sqrt{(x_2 - x_1)^2 + (y_2 - y_1)^2}. \quad (24)$$

The theory of φ-functions for 3-dimension space is called a φ-polytope [1, 8]. Other objects can be approximated by polygons and polytops, which is a common practice [15, 17, 18].

In the future, the solution of this system of linear equations will give the opportunity to correctly locate workplaces on a minimum area in compliance with all rules and regulations. Further study and application of this mathematical apparatus can help improve the efficiency of production planning [12, 14, 16].

4. Conclusions

Proper placement and layout of workplaces that satisfy the requirements of ergonomics and occupational safety ensure the most productive workflow and reduce employee fatigue. Insufficient organization of workplaces leads to professional burnout, even injuries. The optimal placement of workplaces, which contributes to high labor productivity and the preservation of the health of workers, occupies an important place in occupational safety.

This work is devoted to modeling and solving the general problem of optimizing the workplaces placement, taking into account safety standards. The apparatus of φ-functions was used to solve the stated problem. The optimization problem of workplaces placing according to the criterion of the minimum area of premises is formulated, which is important for ensuring the minimum cost per unit of production (rental cost, energy costs, etc.). To describe the full class of φ-functions required to represent all technological units in the workplace, it is necessary to study each pair of such objects. All elements of the workplace can be conditionally represented as objects of elementary geometric shapes. An interesting problem is the placement of objects of an arbitrary multidimensional shape, which would make it possible to carry out 3D modeling of workplaces for rooms of various configurations. Notice, the considered algorithm is transformed to the problem of packing n-dimensional parallelepipeds. If we consider n-dimensional polygons, then this problem already belongs to the class of NP-hard problems and requires additional study, maybe to involve quasi φ-functions. This approach is currently being studied and may be applied in the future.

Analytical representation of constraints in the presented optimization problem using φ-functions allows you to set any constraints on the relative position of objects, i.e. take into account all safety requirements when organizing workplaces. For example, according to Normative legal acts on occupational safety of Ukraine No. 0.00-7.15-18 "Requirements on the safety and health of person working with screen devices", workplaces with computers are located at a distance of at least 1 meter from the walls with windows; the distance between the side surfaces of monitors should be at least 1.2 meter; the passage between the rows of tables with PC should be at least 1 meter. All these restrictions are easily added to the mathematical model or removed in the shortest possible time.

This method is easily applicable for software implementation, for example, using the Mathematica environment. In a few seconds, such a program can produce solutions in the form of a layout of the placement of geometric objects. The constructed constraints contain an insignificant number of variables for modern computing systems. In this regard, it is considered that the solution time of the constructed mathematical model is insignificant. Undoubtedly, the effective application of this approach to workplace planning is impossible without a specialist who can correctly formally describe the restrictions, taking into account all the requirements of regulatory documents in the field of occupational safety. Thus, the professional training of an employee has a significant impact on the effectiveness of this technique, in turn, this drawback can be eliminated in software implementation by creating active functionality.

References

[1] Bennell J. A., Oliveira J. F.: The geometry of nesting problems: A tutorial. Europ. J. Operational Research 184, 2008, 397–415.
[2] Chernov N. et al.: Mathematical model and efficient algorithms for object packing problem. Comput. Geometry: Theory & Appl. 43, 2010, 535–553.
[3] Chub I. A., Novozhilova M. V.: Solution of the extreme problem of resource allocation as a problem of placing rectangles with variable metric characteristics. Informatics and System Science. ISS–2011: science–pract. Conf. Poltava, 2011, 331–334.
[4] Emets O. A., Roskladka A. A.: On estimates of minima of criterion functions in optimization on combinations. Ukrainian Mathematical Journal 51(8), 1999, 1262–1265.
[5] Karwowski W, Marras W. S.: Occupational Ergonomics: Principles of Work Design. CRC Press, 2003.
[6] Romanova I. E. et al.: Mathematical model and method for solving the problem of optimization of packing of arbitrary two-dimensional objects in rectangular areas. Reports of the National Academy of Sciences of Ukraine 1, 2009, 48–53.
[7] Stack T. et al.: Occupational Ergonomics: A Practical Approach, Wiley 2016.
[8] Stoyan Y. et al.: Packing of convex polytopes into a parallelepiped. Optimization 54, 2005, 215–235.
[9] Stoyan Y. et al.: φ-function for complex 2D-objects, 4OR: Quarterly J. Belgian, French and Italian Operations Research Soc. 2, 2004, 69–84.
[10] Stoyan Yu. Et al.: Phi-function for primary 2D-objects, Studia Informatica Universalis 2, 2001, 1–32.
[11] Verkhoturov M.A.: The problem of irregular cutting of flat geometric objects: modeling and calculation of rational cutting. Information Technologies 5, 2000, 37–42.
[12] Wójcik W., Pavlov S., Kalimoldayev M.: Information Technology in Medical Diagnostics II. London: Taylor & Francis Group, CRC Press, Balkema book, 2019 [http://doi.org/10.1201/9780429057618].
[13] Yemets O.A., Roskladka A.A.: Algorithmic solution of two parametric optimization problems on a set of complete combinations. Cybernetics and Systems Analysis 35(6), 1999, 981–986.
[14] Vyatkin S. et al.: A GPU-based multi-volume rendering for medicine. Proc. SPIE 11045, 2019, 1104513.
[15] Vyatkin S. et al.: A function-based approach to real-time visualization using graphics processing units. Proc. SPIE 11581, 2020, 115810E.
[16] Vyatkin S. et al.: Offsetting and blending with perturbation functions. Proc. SPIE 10808, 2018, 108082Y.
[17] Vyatkin S. et al.: Offsetting and blending with perturbation functions. Proc. SPIE 11045, 2019, 110450W.
[18] Vyatkin S. et al.: Transformation of polygonal description of objects into functional specification based on three-dimensional patches of free forms. Proc. SPIE 11176, 2019, 1117622.

Ph.D. Nataliia Geseleva
e-mail: gesnata@ukr.net

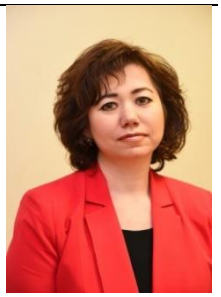

Ph.D., Associate Professor of Department of Digital Economy and System Analysis, State University of Trade and Economics. Research Interests: system analysis and modeling of processes of economic and technological development, synergistic models of the economy, management of innovative activities.

http://orcid.org/0000-0001-9188-9738

Ph.D. Ganna Proniuk
e-mail: ganna.proniuk@nure.ua

Ph.D., Associate Professor of Department of Occupational Safety and Department of Infocommunication Engineering V.V. Popovsky, Kharkiv National University of Radio Electronics. Research Interests: synergetic approach to the management of working conditions, risk management; modeling of data flows in telecommunication networks. Author of more than 100 publications, including 4 collective monographs, 1 textbook.

http://orcid.org/0000-0001-7648-0360

Prof. Olexander Romanyuk
e-mail: rom8591@gmail.com

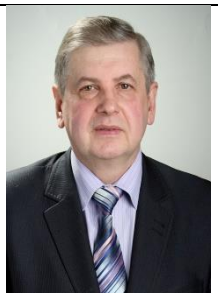

Doctor of Science, Professor of the Department of Software Vinnytsia National Technical University. Research Interests: development of highly efficient interpolation methods and tools for machine graphics systems, highly effective rendering methods and tools, methods and structures for parallelization of the computational process in computer graphics.

http://orcid.org/0000-0002-2245-3364

Prof. Olga Akimova
e-mail: sopogov@ukr.net

Doctor of science, Professor, Head of the of the Department of Pedagogy and Vocational Education, Vinnitsa State Pedagogical University. Author of more than 86 publications, including 3 textbooks, 33 patents for inventions and more than 51 scientific articles in professional journals, of which 9 are in scientometric databases Scopus and Web of Science.

http://orcid.org/0000-0001-6988-6258

Ph.D. Tetiana Troianovska-Korobeynikova
e-mail: luydik0304@gmail.com

Ph.D., Associate Professor of the Department of Computer Engineering, Vinnytsia National Technical University.
Research Interests: development of highly efficient interpolation methods and tools for machine graphics systems, highly effective rendering methods and tools, methods and structures for parallelization of the computational process in computer graphics.

http://orcid.org/0000-0003-2487-8742

Ph.D. Liudmyla Savytska
e-mail: luydik0304@gmail.com

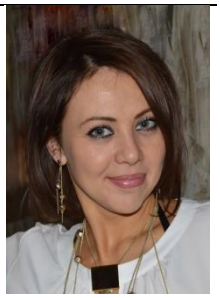

Ph.D., Associate Professor of the Department of Computer Engineering, Vinnytsia National Technical University. Research interests: Information technologies.

http://orcid.org/0000-0003-1130-2621

Ph.D. Saule Rakhmetullina
e-mail: Rakhmetullinas@mail.ru

She is currently a Chairman of the Board-rector of the D. Serikbayev East Kazakhstan Technical University. She is a co-author over 40 papers in journals, book chapters, and conference proceedings and has 3 copyright certificates for software products. She is a Republican expert on reforming higher education. Her professional interests are mathematical and computer modeling of complex processes.

http://orcid.org/0000-0002-3142-0249

Ph.D. Nurbapa Mekebayev
e-mail: nurbapa@gmail.com

Associate professor of the Kazakh National Women's Pedagogical University, Head of the Department of Mathematics. About 60 of scientific articles have been published in various foreign and domestic journals. Research area: machine learning, deep learning, artificial intelligence, speech technologies.

http://orcid.org/0000-0002-9117-4369

http://doi.org/10.35784/iapgos.3040

received: 24.07.2022 | revised: 16.09.2022 | accepted: 19.09.2022 | available online: 30.09.2022

MODELING OF LABOR POTENTIAL OF UKRAINE: FORMATION OF KNOWLEDGE BASE

Ivan V. Zayukov, Iryna M. Kobylianska, Oleksandr V. Kobylianskyi, Sofia V. Dembitska
Vinnytsia National Technical University, Faculty of Information Technologies and Computer Engineering, Vinnytsia, Ukraine

Abstract. *The adaptation of the Ukrainian economy to the requirements of the European Union requires increasing the effectiveness of the system of making public management decisions regarding the development and assessment of the labor potential of our country. Currently, a unified system of evaluation indicators of the labor potential of Ukraine has not yet been developed. The authors substantiated and systematized the groups of medico-demographic, socio-economic and educational factors that affect the health of the employed population, and suggested the use of the "preserving the health of the employed population" indicator for assessing the labor potential. Accordingly, a mathematical model for evaluating the health of the employed population at the macro level is proposed, which is based on the theory of fuzzy logic. The application of the proposed model will make it possible to increase the efficiency of the system of public management decision-making in the process of developing concepts, strategies, and practical measures for the implementation of policies for the preservation of the health of the employed population, as well as to make timely adjustments during implementation, which should positively reflect on the steady growth of the index human development (HDI).*

Keywords: labor potential, knowledge base, evaluation terms, factors, modeling, fuzzy logic

MODELOWANIE POTENCJAŁU SIŁY ROBOCZEJ UKRAINY: BUDOWANIE BAZY WIEDZY

Streszczenie. *Dostosowanie gospodarki ukraińskiej do wymogów Unii Europejskiej wymaga zwiększenia efektywności systemu podejmowania decyzji z zakresu zarządzania publicznego dotyczących rozwoju i oceny potencjału pracy kraju. Obecnie nie został jeszcze opracowany jednolity system wskaźników oceny potencjału pracy Ukrainy. Autorzy uzasadnili i usystematyzowali grupy medyczno-demograficznych, społeczno-ekonomicznych i edukacyjnych czynników, które wpływają na zdrowie populacji zatrudnionych, i zaproponowali wykorzystanie wskaźnika "zachowanie zdrowia populacji zatrudnionych" do oceny potencjału pracy. W związku z tym zaproponowano model matematyczny oceny stanu zdrowia populacji zatrudnionych na poziomie makro, który opiera się na teorii logiki rozmytej. Zastosowanie proponowanego modelu umożliwi zwiększenie efektywności systemu podejmowania decyzji w zarządzaniu publicznym w procesie opracowywania koncepcji, strategii i praktycznych środków realizacji polityki zachowania zdrowia populacji zatrudnionych, a także dokonywania terminowych korekt w trakcie realizacji, co powinno pozytywnie wpłynąć na stały wzrost wskaźnika rozwoju społecznego (HDI).*

Słowa kluczowe: potencjał pracy, baza wiedzy, warunki oceny, czynniki, modelowanie, logika rozmyta

Introduction

Despite the significant amount of research, a single system of evaluation indicators of labor potential of Ukraine has not yet been developed. labor potential should be understood as a set of quantitative and qualitative characteristics of the productive forces of the country, which are formed and developed in the social environment. Domestic scientists [1, 2, 10–17, 20, 21, 23, 24, 26] and many others consider the qualitative and quantitative characteristics of the economically active population to be labor potential.

Considering the structure of labor potential, domestic scientists identify the following main components, namely, professional, moral, demographic, educational, creative, social, intellectual, qualification, organizational, psychophysiological, natural-biological, organizational, communicative, personal, competence and others. Thus, in [1, 2, 10–17, 20, 21, 23, 24, 26] the structure of labor potential consists of the following interconnected subsystems: socio-economic, demographic and socio-psychological. In addition, the structure of labor potential has been thoroughly studied in scientific work [1, 2, 10–17, 20, 21, 23, 24, 26].

Comparative analysis and generalization of the existing methodological approaches to the assessment of labor potential of Ukraine convinces that both theoretically and methodologically it is necessary to conduct a deep meaningful assessment. Thus, the main components of labor potential were studied in [1, 12, 14, 23], and methodological aspects of labor potential assessment using qualitative and quantitative characteristics, in particular, applying the methods of mathematical modeling, attention were paid attention in [3–7].

The first step in creating such an assessment methodology should be the provision of clear understanding what elements, components, phenomena of labor potential development are subject to assessment, to create the notion regarding its real state in both functional and territorial terms. Numerous approaches are used in in the methodology and evaluation. But the most reliable, in our opinion, is the rating assessment. The essential component of the introduction of rating assessment in various areas is the calculation of the integrated indices as a basis for ranking. Integral assessment itself is becoming more common in measuring labor potential [3–7].

1. Formulation of the problem

Since the specific values of any index are usually not assessed in comparison with standards or other samples, such assessments do not actually measure the real situation, but its differentiation between regions and countries. As a result of calculations of integrated indices it is possible to estimate regional differences, but in itself such index is pointless. Without discarding the scientific and analytical value of such research, we will try to evaluate the tools of rating assessment [6, 7, 27].

Since only the information that allows the authorities and economic entities to make effective decisions is useful, ratings (as a tool for decision-making) should be part of certain information-analytical systems. In the absence of regulatory application of ratings, their only value lies in the reliability of the information they contain for potential investors, the government, including managers of budget funds. However, the situation changes if ratings determine the conditions under which budget funds can be allocated, benefits, investments, etc. are provided (in particular, credit ratings determine the conditions under which an investor can buy securities, obtain loans, etc.).

Assessing the adequacy of the level of development of labor potential should involve solving a number of theoretical and methodological issues:

- analysis of labor potential, carried out on the basis of opinion polls, which characterize the state of its development;
- assessment of compliance of actual indicators with current standards;
- comparison with sample indicies, which can be considered standards recommended by experts of international organizations (ILO, WHO, IBRD, UN projects, etc.) and adopted in the most developed socially oriented economies of the world. Conformity assessment of developed

countries can be done by comparing economic indicies such as employment growth, reducing unemployment, improving public health [8, 9, 25].

Therefore, it is necessary to build a new concept of labor potential assessment. We propose to make such an assessment based on the use of mathematical modeling methods, namely the theory of fuzzy sets. When assessing the rating of labor potential, a number of parameters are not available for accurate quantitative measurement, so a subjective component is introduced, which is expressed by fuzzy estimates such as "high", "low", "medium", etc. What appears in science is defined as a linguistic description and is set by the so-called membership functions of a fuzzy set factor.

2. Theoretical research

In order to create an expert modeling system for multifactor analysis of labor potential assessment (R), we used a mathematical apparatus based on the theory of fuzzy logic, which was studied by well-known scientists [3, 22].

The generalized algorithm for estimating R Ukraine is the follows:

- construction of a logical conclusion tree, which will determine the sequence of further calculations;
- fuzzification of the Input variables. A term set is defined to evaluate each variable and the membership functions of each term are built on a discrete universal set. Using these functions and forming knowledge bases, we obtain analytical models of membership functions of terms and setting fuzzy knowledge bases for the corresponding relations, as well as the values of all input variables;
- calculation of values of membership functions of terms – estimates for all variables, and, according to the constructed logical equations, values of membership functions for all nonterminal vertices;
- calculation of the values of membership functions for the terms of a complex indicator of labor potential assessment and by defuzzification of the fuzzy set of determining the rank of labor potential.

Linguistic statements should correspond to the obtained fuzzy logical equations at the appropriate hierarchical level: system (R) and the proposed factors that bound the membership functions of input and output variables, due to the use in their construction operations "max" and "min". That is, the logical operations "I" (∧) and "OR" (∨). Over the membership functions are replaced by the operations "max" and "min" [18, 19]:

$$\mu_{(a)} \wedge \mu_{(b)} = \min[\mu_{(a)}, \mu_{(b)}];$$
$$\mu_{(a)} \vee \mu_{(b)} = \max[\mu_{(a)}, \mu_{(b)}].$$

The considered algorithm uses the idea of identification of a linguistic term by the maximum of the membership function and generalizes this idea to the whole matrix of knowledge. Using membership functions and corresponding formulas, we find analytical models of membership functions of estimates of the input variables for all the terms. Since there are cases when the maximum membership functions are the same for two adjacent terms and this complicates the ranking of projects, for greater clarity it is proposed to consider the interval of changes of the input parameter R as continuous and rank projects on a given scale [D^1: D_2]. To obtain a clear number that corresponds to the rank of the project, in this interval you need to use the operation of the defuzzification, i.e. the operation of converting fuzzy information into clear or quantitative.

The calculation of the fuzzy logical set D^* is given in [18]. According to the principle of the center of gravity, defuzzification of the fuzzy set gives a quantitative estimate of D^* – the rank of the complex estimate R for given input factors (1).

$$D^* = (R^*) = \sum \left[D_2 + (i-1)\frac{D^1 - D_2}{m-1} \right] \mu^{u_i}(D) \Big/ \sum_{i=1}^{m} \mu^{u_i}(D) \quad (1)$$

where m is the number of terms of the variable D;
D^1, D_2 − lower and upper limits of the range of variable D;
$\mu^{ui}(D)$ is a function of belonging of variable D to fuzzy term u_i.

3. Experimental research

The source of knowledge base, which models the relationship between integrated and individual indicies of labor potential rating (R), are the opinions of experts, specializing in this field. The peculiarity of expressions such as "if – then, otherwise", which are formulated in natural language, is that their adequacy, unlike the quantitative models, does not change with slight fluctuations in input estimates in one direction or another. The set of such statements is a set of points in the space "individual criteria – an integral criterion". The integral criterion is evaluated by fixed linguistic estimates of individual criteria R.

Expert evaluation is formalized in the form of answers to the questions of the expert questionnaire and provides the following options for the final expert opinion (we give the example of evaluation R): d1 (or the value falls in the interval [15, 16, 21]) − labor potential is quite low; d2 (value of the interval [16, 20]) − the level of labor potential can be assessed as average; d3 (the value lies in the interval [20, 24]) − labor potential is used effectively and there are prospects for its further growth. We will consider in more detail the specific parameters of the proposed model and give the composition of factors that should be determined when estimating R, that depends, in our opinion, on the following factors:

$$R = f_r = (X, Y, Z) \quad (2)$$

where: X − medical and demographic factors; Y – socio-economic factors of influence; Z − educational factors.

Medico-demographic factors can be presented as follows:

$$X = f_x(x_1, x_2, x_3, x_4, x_5, x_6) \quad (3)$$

where: x_1 − the share of persons in epy working age, %;
x_2 − the level of occupational injuries per 100 thousand employees;
x_3 − the level of occupational injuries with a fatal outcome per 100 thousand workers, %;
x_4 − the level of occupational disease per 100 thousand employees;
x_5 − the share of employees who work in conditions that do not meet sanitary and hygienic standards, in the average number of registered personnel (ANRP), %;
x_6 − the proportion of employees who were absent from work due to illness in ANRP, %.

Socio-economic factors of impact can be written as:

$$Y = f_y(y_1, y_2, y_3, y_4, y_5, y_6, y_7, y_8) \quad (4)$$

where:
y_1 is the level of employment (population aged 16–59 years, %);
y_2 − the level of registered unemployment, %;
y_3 − turnover ratio in connection with the release, %;
y_4 − workload per vacancy, %;
y_5 − average duration of unemployment, months;
y_6 − the share of funds of the Social Insurance Fund in case of unemployment, which are directed to the active employment policy, %;
y_7 − level of forced under employment, %;
y_8 − loss of working time, %.

Educational factors of influence are written in the form:

$$Z = f_z(z_1, z_2) \quad (5)$$

where z_1 is the share of persons who have improved their skills (in % to ANRP); z_2 − share of employees with higher education in% to ANRP.

Estimates of the values of linguistic variables given in relations (2–5) are performed using a system of qualitative terms, the number of which for each individual variable may be different, for example, for variable x_1 – „*Specific weight of people of working age*" (with universal set from 15–75% − the

terms for evaluation are: „Low" (L), „Below average" (BA), „Medium" (M).

The tree of the logical conclusion of the hierarchical connections of the factors that allow to assess R is shown in Fig. 1, where the root of the tree is R, and the leaves, respectively, are the factors influencing this rating: medical-demographic, socio-economic and educational factors.

To compile fuzzy logical equations, knowledge bases are set (table 1−4) in the form of expert statements about the connections of fuzzy terms of input and output linguistic variables in the ratios (2−5).

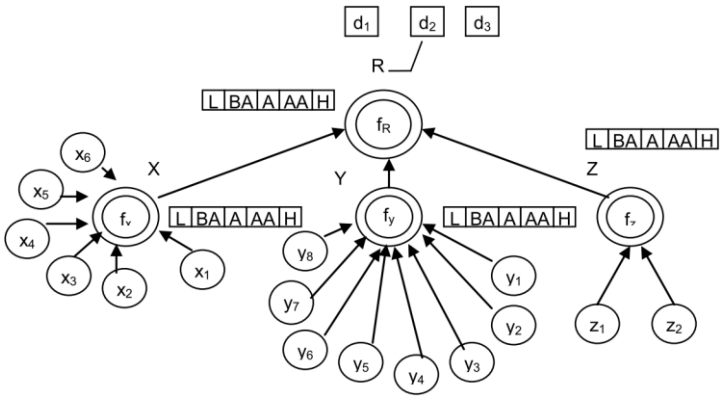

Fig. 1. Tree of logical conclusion of hierarchical connections of the factors, where L, BA, A, AA, H − terms for assessment (respectively: L – "low level", BA – "below average level", A – "average level", AA – "above average level", H – "high level")

Table 1. Knowledge bases and systems of fuzzy logical equations for the dependence 2

IF			THEN
Medico-demographic factors of influence (X)	Socio-economic factors of influence (Y)	Educational factors of influence (Z)	Rating of labor potential of Ukraine (R)
Low (L)	Low (L)	Low (L)	Low (L)
Low (L)	Low (L)	Lower average (LA)	
Low (L)	Lower average (LA)	Lower average (LA)	
Lower average (LA)	Lower average (LA)	Lower average (LA)	Lower average (LA)
Lower average (LA)	Lower average (LA)	Lower average (LA)	
Lower average (LA)	Lower average (LA)	Average (A)	
Lower average (LA)	Average (A)	Average (A)	Average (A)
Average (A)	Average (A)	Average (A)	
Average (A)	Above average (AA)	Above average (AA)	
Average (A)	Above average (AA)	Above average (AA)	Above average (AA)
Average (A)	Above average (AA)	Above average (AA)	
Above average (AA)	Above average (AA)	Above average (AA)	
Above average (AA)	Above average (AA)	Above average (AA)	High (H)
Above average (AA)	High (H)	High (H)	
High (H)	High (H)	High (H)	

Source: author's calculations.

System of fuzzy logical equations based on knowledge base (table 1):

$\mu_L(R) = \mu_{Lx} \wedge \mu_{Ly} \wedge \mu_{Lz} \vee \mu_{Lx} \wedge \mu_{Ly} \wedge \mu_{Baz} \vee \mu_{Lx} \wedge \mu_{Bay} \wedge \mu_{Baz};$

$\mu_{BA}(R) = \mu_{BAx} \wedge \mu_{Bay} \wedge \mu_{Baz} \vee \mu_{BAx} \wedge \mu_{Bay} \wedge \mu_{Baz} \vee \mu_{BAx} \wedge \mu_{Bay} \wedge \mu_{Az};$

$\mu_A(R) = \mu_{BAx} \wedge \mu_{Ay} \wedge \mu_{Az} \vee \mu_{Ax} \wedge \mu_{Ay} \wedge \mu_{Az} \vee \mu_{Ax} \wedge \mu_{AAy} \wedge \mu_{AAz};$

$\mu_{AA}(R) = \mu_{Ax} \wedge \mu_{AAy} \wedge \mu_{AAz} \vee \mu_{Ax} \wedge \mu_{AAy} \wedge \mu_{AAz} \vee \mu_{AAx} \wedge \mu_{AAy} \wedge \mu_{AAz};$

$\mu_H(R) = \mu_{AAx} \wedge \mu_{AAy} \wedge \mu_{AAz} \vee \mu_{AAx} \wedge \mu_{Hy} \wedge \mu_{Hz} \vee \mu_{Hx} \wedge \mu_{Hy} \wedge \mu_{Hz}.$

Table 2. Knowledge bases and systems of fuzzy logical equations for the dependence 3

IF						THEN
Specific weight of working age persons, %, (x1)	The level of occupational injuries per 100 thousand employees, % (x2)	The level of occupational injuries with fatal consequences per 100 thousand employees, (x3)	The level of occupational disease per 100 thousand employees, % (x4)	The share of employees working in conditions that do not meet sanitary and hygienic standards in the average number of employees, %, (x5)	Proportion of employees who were absent from work due to illness in ANRP %, (x6)	Medical and demographic factors of influence, (X)
Low (L)	Above average (AA)	High (H)	High (H)	High (H)	High (H)	Low (L)
Low (L)	Above average (AA)	High (H)	High (H)	High (H)	High (H)	
Lower average (LA)	Above average (AA)	High (H)	High (H)	High (H)	High (H)	
Lower average (LA)	Above average (AA)	High (H)	High (H)	High (H)	High (H)	Lower average (LA)
Lower average (LA)	Above average (AA)	High (H)	High (H)	High (H)	High (H)	
Average (A)	Above average (AA	High (H)	High (H)	High (H)	High (H)	
Average(A)	Average (A)	High (H)	High (H)	High (H)	High (H)	Average (A)
Average (A)	Average (A)	Average (A)	Average (A)	High (H)	High (H)	
Above average (AA)	Average (A)	Average (A)	Average (A)	Average(A)	Average (A)	
Above average (AA)	Lower average (LA)	Average (A)	Low (L)	Average (A)	Low (L)	Above average (AA)
Above average (AA)	Lower average (LA)	Low (L)	Low (L)	Average (A)	Low (L)	
High (H)	Lower average (LA)	Low (L)	Low (L)	Low (L)	Low (L)	
High (H)	Low (L)	Low (L)	Low (L)	Low (L)	Low (L)	High(H)
High (H)	Low (L)	Low (L)	Low (L)	Low (L)	Low (L)	
High (H)	Low (L)	Low (L)	Low (L)	Low (L)	Low (L)	

Source: author's calculations.

System of fuzzy logical equations based on knowledge base (table 2):

$\mu_L(X) = \mu_{L(x1)} \wedge \mu_{AA(x2)} \wedge \mu_{H(x3)} \wedge \mu_{H(x4)} \wedge \mu_{H(x5)} \wedge \mu_{H(x6)} \vee \mu_{L(x1)} \wedge \mu_{AA(x2)} \wedge \mu_{H(x3)} \wedge \mu_{H(x4)} \wedge \mu_{H(x5)} \wedge \mu_{H(x6)} \vee$
$\mu_{BA(x1)} \wedge \mu_{AA(x2)} \wedge \mu_{H\,(x3)} \wedge \mu_{H(x4)} \wedge \mu_{H(x5)} \wedge \mu_{H(x6)};$
$\mu_{BA}(X) = \mu_{BA(x1)} \wedge \mu_{AA(x2)} \wedge \mu_{H(x3)} \wedge \mu_{H(x4)} \wedge \mu_{H(x5)} \wedge \mu_{H(x6)} \vee \mu_{BA(x1)} \wedge \mu_{AA(x2)} \wedge \mu_{H(x3)} \wedge \mu_{H(x4)} \wedge \mu_{H(x5)} \wedge \mu_{H(x6)} \vee$
$\mu_{A(x1)} \wedge \mu_{AA(x2)} \wedge \mu_{H(x3)} \wedge \mu_{H(x4)} \wedge \mu_{H(x5)} \wedge \mu_{H(x6)};$
$\mu_A(X) = \mu_{A(x1)} \wedge \mu_{A(x2)} \wedge \mu_{H(x3)} \wedge \mu_{H(x4)} \wedge \mu_{H(x5)} \wedge \mu_{H(x6)} \vee \mu_{A(x1)} \wedge \mu_{A(x2)} \wedge \mu_{A(x3)} \wedge \mu_{A(x4)} \wedge \mu_{H(x5)} \wedge \mu_{H(x6)} \vee$
$\mu_{AA(x1)} \wedge \mu_{A(x2)} \wedge \mu_{A(x3)} \wedge \mu_{A(x4)} \wedge \mu_{A(x5)} \wedge \mu_{A(x6)};$
$\mu_{AA}(X) = \mu_{AA(x1)} \wedge \mu_{BA(x2)} \wedge \mu_{A(x3)} \wedge \mu_{L(x4)} \wedge \mu_{A(x5)} \wedge \mu_{L(x6)} \vee \mu_{AA(x1)} \wedge \mu_{BA(x2)} \wedge \mu_{L(x3)} \wedge \mu_{L(x4)} \wedge \mu_{A(x5)} \wedge \mu_{L(x6)} \vee$
$\mu_{H(x1)} \wedge \mu_{BA(x2)} \wedge \mu_{L(x3)} \wedge \mu_{L(x4)} \wedge \mu_{L(x5)} \wedge \mu_{L(x6)};$
$\mu_H(X) = \mu_{H(x1)} \wedge \mu_{L(x2)} \wedge \mu_{L(x3)} \wedge \mu_{L(x4)} \wedge \mu_{L(x5)} \wedge \mu_{L(x6)} \vee \mu_{H(x1)} \wedge \mu_{L(x2)} \wedge \mu_{L(x3)} \wedge \mu_{L(x4)} \wedge \mu_{L(x5)} \wedge \mu_{L(x6)} \vee$
$\mu_{H(x1)} \wedge \mu_{L(x2)} \wedge \mu_{L(x3)} \wedge \mu_{L(x4)} \wedge \mu_{L(x5)} \wedge \mu_{L(x6)}.$

Table 3. Knowledge bases and systems of fuzzy logical equations for the dependence 4

IF								THEN
Employment rate (% of the population aged 16−59),%, (y1)	Registered unemployment rate, %, (y2)	Turnover ratio, %, (y3)	Load per vacancy (vacancy), % (y4)	Average duration of unemployment, months, (y5)	Share of the Fund's funds in case of unemployment for active employment policy, %, (y6)	Level of forced underemployment, %, (y7)	Loss of working time, %, (y8)	Socio-economic factors
Low (L)	High (H)	High (H)	High (H)	Above average (AA)	Low (L)	High (H)	High (H)	Low (L)
Low (L)	High (H)	Above average (AA)	High (H)	Above average (AA)	Low (L)	High (H)	High (H)	
Low (L)	Above average (AA)	Above average (AA)	High (H)	Above average (AA)	Low (L)	High (H)	High (H)	
Low (L)	Above average (AA)	Above average (AA)	Above average (AA)	Above average (AA)	Low (L)	High (H)	High (H)	Lower average (LA)
Lower average (LA)	Above average (AA)	Above average (AA)	Above average (AA)	Above average (AA)	Average (A)	High (H)	Average (A)	
Lower average (LA)	Above average (AA)	Average(A)	Above average (AA)	Above average (AA)	Average (A)	High (H)	Average (A)	
Lower average (LA)	Average (A)	Average (A)	Average (A)	Above average (AA)	Average (A)	High (H)	Average (A)	Average (A)
Average (A)	Average(A)	Average (A)	Average (A)	Average(A)	Average (A)	Average (A)	Average (A)	
Average (A)	Lower average (LA)	Lower average (LA)	Average (A)	Average (A)	Average (A)	Average (A)	Average (A)	
Average (A)	Lower average (LA)	Lower average (LA)	Average(A)	Average (A)	Average (A)	Average (A)	Average (A)	Above average (AA)
Average (A)	Lower average (LA)	Lower average (LA)	Lower average (LA)	Lower average (LA)	Average (A)	Low (L)	Low (L)	
Above average (AA)	Lower average (LA)	Lower average (LA)	Lower average (LA)	Lower average (LA)	High (H)	Low (L)	Low (L)	
Above average (AA)	Lower average (LA)	Lower average (LA)	Lower average (LA)	Low (L)	High (H)	Low (L)	Low (L)	High (H)
Above average (AA)	Low (L)	Low (L)	Low (L)	Low (L)	High (H)	Low (L)	Low (L)	
High (H)	Low (L)	Low (L)	Low (L)	Low (L)	High (H)	Low (L)	Low (L)	

Source: author's calculations.

System of fuzzy logical equations based on knowledge base (table 3):

$\mu_L(У) = \mu_{L(y1)} \wedge \mu_{H(y2)} \wedge \mu_{H(y3)} \wedge \mu_{H(y4)} \wedge \mu_{AA(y5)} \wedge \mu_{L(y6)} \wedge \mu_{L(y7)} \wedge \mu_{H(y8)} \vee$
$\mu_{L\,(y1)} \wedge \mu_{H(y2)} \wedge \mu_{AA(y3)} \wedge \mu_{H(y4)} \wedge \mu_{AA(y5)} \wedge \mu_{L(y6)} \wedge \mu_{H(y7)} \wedge \mu_{H(y8)} \vee \mu_{L(y1)} \wedge \mu_{AA(y2)} \wedge \mu_{AA(y3)} \wedge \mu_{H(y4)} \wedge \mu_{AA(y5)} \wedge \mu_{L(y6)} \wedge \mu_{H(y7)} \wedge \mu_{H(y8)};$
$\mu_{BA}(У) = \mu_{L(y1)} \wedge \mu_{AA(y2)} \wedge \mu_{AA(y3)} \wedge \mu_{AA(y4)} \wedge \mu_{AA(y5)} \wedge \mu_{L(y6)} \wedge \mu_{H(y7)} \wedge \mu_{H(y8)} \vee$
$\mu_{BA(y1)} \wedge \mu_{AA(y2)} \wedge \mu_{AA(y3)} \wedge \mu_{AA(y4)} \wedge \mu_{AA(y5)} \wedge \mu_{A(y6)} \wedge \mu_{H(y7)} \wedge \mu_{A(y8)} \vee \mu_{BA(y1)} \wedge \mu_{AA(y2)} \wedge \mu_{A(y3)} \wedge \mu_{AA(y4)} \wedge \mu_{AA(y5)} \wedge \mu_{A(y6)} \wedge \mu_{H(y7)} \wedge \mu_{A(y8)};$
$\mu_A(У) = \mu_{BA(y1)} \wedge \mu_{A(y2)} \wedge \mu_{A(y3)} \wedge \mu_{A(y4)} \wedge \mu_{AA(y5)} \wedge \mu_{A(y6)} \wedge \mu_{H(y7)} \wedge \mu_{A(y)} \vee$
$\mu_{A(y1)} \wedge \mu_{A(y2)} \wedge \mu_{A(y3)} \wedge \mu_{A(y4)} \wedge \mu_{A(y5)} \wedge \mu_{A(y6)} \wedge \mu_{A(y7)} \wedge \mu_{A(y8)} \vee \mu_{A(y1)} \wedge \mu_{BA(y2)} \wedge \mu_{BA(y3)} \wedge \mu_{A(y4)} \wedge \mu_{A(y5)} \wedge \mu_{A(y6)} \wedge \mu_{A(y7)} \wedge \mu_{A(y8)};$
$\mu_{AA}(У) = \mu_{A(y1)} \wedge \mu_{BA(y2)} \wedge \mu_{BA(y3)} \wedge \mu_{A(y4)} \wedge \mu_{A(y5)} \wedge \mu_{A(y6)} \wedge \mu_{A(y7)} \wedge \mu_{A(y8)} \vee$
$\mu_{A(y1)} \wedge \mu_{BA(y2)} \wedge \mu_{BA(y3)} \wedge \mu_{BA(y4)} \wedge \mu_{BA(y5)} \wedge \mu_{A(y6)} \wedge \mu_{L(y7)} \wedge \mu_{L(y8)} \vee \mu_{AA(y1)} \wedge \mu_{BA(y)} \wedge \mu_{BA(y3)} \wedge \mu_{BA(y4)} \wedge \mu_{BA(y5)} \wedge \mu_{H(y6)} \wedge \mu_{L(y7)} \wedge \mu_{L(y8)};$
$\mu_H(У) = \mu_{AA(y1)} \wedge \mu_{BA(y2)} \wedge \mu_{BA(y3)} \wedge \mu_{BA(y4)} \wedge \mu_{L(y5)} \wedge \mu_{H(y6)} \wedge \mu_{L(y7)} \wedge \mu_{L(y8)} \vee$
$\mu_{AA(y1)} \wedge \mu_{L(y2)} \wedge \mu_{L(y3)} \wedge \mu_{L(y4)} \wedge \mu_{L(y5)} \wedge \mu_{H(y6)} \wedge \mu_{L(y7)} \wedge \mu_{L(y8)} \vee \mu_{H(y1)} \wedge \mu_{L(y2)} \wedge \mu_{L(y3)} \wedge \mu_{L(y4)} \wedge \mu_{L(y5)} \wedge \mu_{H(y6)} \wedge \mu_{L(y7)} \wedge \mu_{L(y8)}.$

Table 4. Knowledge bases and systems of fuzzy logical equations for the dependence 5

IF		THEN
Proportion of % who improved their skills (in % to ANRP), (z1)	Share of employees with higher education (in % to ANRP), (z2)	Educational factors
Low (L)	Low (L)	Low (L)
Low (L)	Low (L)	
Low (L)	Low (L)	
Low (L)	Low (L)	Lower average (LA)
Average (A)	Low (L)	
Average (A)	Low (L)	
Average (A)	Average (A)	Average (A)
Average (A)	High (H)	
Average (A)	High (H)	
Average (A)	High (H)	Above average (AA)
High (H)	High (H)	
High (H)	High (H)	
High (H)	High (H)	High (H)
High (H)	High (H)	
High (H)	High (H)	

Source: author's calculations.

System of fuzzy logical equations based on knowledge base (table 4):

$\mu_L(Z) = \mu_{L(z1)} \wedge \mu_{L(z2)} \vee \mu_{L(z1)} \wedge \mu_{L(z2)} \vee \mu_{L(z1)} \wedge \mu_{L(z2)}$;

$\mu_{BA}(Z) = \mu_{L(z1)} \wedge \mu_{L(z2)} \vee \mu_{A(z1)} \wedge \mu_{L(z2)} \vee \mu_{A(z1)} \wedge \mu_{L(z2)}$;

$\mu_A(Z) = \mu_{A(z1)} \wedge \mu_{L(z2)} \vee \mu_{A(z1)} \wedge \mu_{A(z2)} \vee \mu_{A(z1)} \wedge \mu_{H(z2)}$;

$\mu_{AA}(Z) = \mu_{A(z1)} \wedge \mu_{H(z2)} \vee \mu_{H(z1)} \wedge \mu_{H(z2)} \vee \mu_{H(z1)} \wedge \mu_{H(z2)}$;

$\mu_H(Z) = \mu_{H(z1)} \wedge \mu_{H(z2)} \vee \mu_{H(z1)} \wedge \mu_{H(z2)} \vee \mu_{H(z1)} \wedge \mu_{H(z2)}$.

4. Conclusion

The analysis of scientific works on the definition of the structure and main components of the labor potential and the methodology of its assessment using the use of qualitative and quantitative characteristics and the application of mathematical modeling methods was carried out. Based on the results of research, the groups of demographic, socio-economic and educational factors that have the main influence on the health of the employed population have been substantiated and systematized. The need for the application of mathematical modeling is argued and a mathematical multifactorial model is built for the analysis and evaluation of indicators of health preservation of the employed population at the macro level using a mathematical apparatus based on the theory of fuzzy sets. This creates opportunities for increasing the effectiveness of the system of making public management decisions in the process of developing concepts, strategies, and practical measures to ensure opportunities for the employed population to live a long and healthy life, in particular working, to acquire, expand and update knowledge throughout life in the system of professional education and have access to decent working conditions and wages; and also to make timely adjustments during their implementation, which should be positively reflected in the steady growth of the human development index (HDI): increase in life expectancy, improvement in the quality of education, growth in real GDP per capita.

References

[1] Chukhrai N. I., Kulynyak I. Ya., Glyantseva O. I.: Assessment of the labor potential of the enterprise. Actual problems of the economy 10(160), 2014, 338–347.

[2] Koshkalda I. et al.: Motivation mechanism for stimulating labor potential. Research in World Economy 11(4), 2020, 53–61.

[3] Kozlovsky S. V. et al.: Ensuring sustainable economic development of the agro-industrial complex of the region: monograph. Mercury Podillya, Vinnytsia 2016.

[4] Kozlovsky S. V., Kireeva E. A.: Management of regional security on the basis of modern modeling methods. Economy of Ukraine 8, 2015, 57–73.

[5] Kozlovsky S. V., Kozlovsky A. V., Zhurakivsky E. S.: Modeling and forecasting the level of economic security of the agricultural sector of Vinnytsia region by means of the theory of fuzzy logic. Economic space: collection, science, 2016, 112–125.

[6] Kozlovsky S. V., Mazur G. F.: Modeling and forecasting the level of state incentives for agro-industrial production in Ukraine based on the theory of fuzzy logic. Economy and state 9, 2017, 8–15.

[7] Kozlovsky S. V.: Ensuring the stability and development of modern economic systems: monograph. Nilan Ltd., Vinnytsia 2017.

[8] Krak Y. V. et al.: Text entry system for alternative speech communications. Journal of Automation and Information Sciences 49 (1), 2017, 65–75.

[9] Kryvonos Iu. G. et al.: Predictive text typing system for the Ukrainian language. Cybernetics and systems analysis 53 (4), 2017, 495–502.

[10] Ladunka I. S., Burkova M. S.: Improving the efficiency of using the labor potential of the enterprise. Economy and existence – Economy and society 14, 2018, 421–425.

[11] Lapshin I. M.: Labor potential of the population: the dominant factor in the development of demographic and economic processes. Priazovsky economic bulletin – Priazovsky economic bulletin 2 (13), 2019, 241–245.

[12] Leonenko N. A.: The role of labor potential in the formation of the economic potential of the region. Global and national problems of the economy 23, 2018, 366–372.

[13] Lincaru C. et al.: Low-Low (LL) high human capital clusters in public administration employmentpredictor for digital infrastructure public investment priority – Romania case study. Entrepreneurship and Sustainability Issues 6(2), 2018, 729–753.

[14] Mazur-Vezhbitskaya E.: Human resources as a fundamental element that determines the development of innovation. Marketing and Innovation Management 1, 2019, 335–356 [http://doi.org/10.21272/mmi.2019.1-28].

[15] Migai N. B.: Monitoring the effectiveness of using the labor potential of the region. Young Scientist 44(4), 2017, 77–81.

[16] Navolska N. V.: Factors influencing the formation and use of labor potential of the enterprise. Global and national problems of the economy: electronic professional publication 43(7), 2015, 426.

[17] Raikovskaya I.: Determination of the essence of the components of labor potential to improve the efficiency of business management. Scientific Bulletin of the National Academy of Statistics, Accounting and Auditing 3, 2019, 87–95.

[18] Rothstein A. P.: Intelligent identification technologies: fuzzy logic, genetic algorithms, neural networks. UNIVERSUM-Vinnytsia, Vinnytsia 1999.

[19] Rotshtein A., Shtovba S.: Modeling of the human operator reliability with the aid of the sugeno fuzzy knowledge base. Automation and Remote Control 70(1), 2009, 163–169.

[20] Rusan V. N., Zhurakovska L. A.: Reproducing labor potential in the agricultural sector of Ukraine: current state and problems. Scientific Papers of the Legislation Institute of the Verkhovna Rada of Ukraine 4, 2019, 78–88.

[21] Shostak L. V., Petrini V. A.: Labor potential as a driving force of effective enterprise development. Global and national problems of the economy: electronic professional publication 21, 2018, 450–454.

[22] Timchenko L. et al.: Precision measurement of coordinates of power center of extended laser path images. Proc. SPIE 10808, 2018, 1080810.

[23] Utkina Yu. M., Solomnikov I. V.: Labor potential of the enterprise: essence, structure, approaches to formation. Bulletin of the Economics of Transport and Industry 41, 2013, 223–227.

[24] Valinkevich N. V., Korbut K. E.: The current state and development trends of the labor potential of the Zhytomyr region. European Journal of Management Problems 26(1–2), 2018, 55–63 [http://doi.org/10.15421/191807].

[25] Vassilenko S. et al.: Energy harvesting: an interesting topic for education programs in engineering specialties. Proc. of Internet, Education, Science IES-2016, 2016, 149–156.

[26] Wei L.: Features of management of labor potential in educational sphere. Ekonomika ta derzhava 6, 59–63, 2019.

[27] Wójcik W., Smolarz A.: Information Technology in Medical. CRC Press, London 2017 [http://doi.org/10.1201/9781315098050].

D.Sc. Ivan V. Zayukov
e-mail: Zivan@i.ua

Doctor of Science (Economics), Associate Professor of Department of Life Safety and Safety Pedagogy, Vinnytsia National Technical University. Research Interests: preserving the health of the employed population, current problems of human development, economic and social aspects of life safety and occupational health and safety.

http://orcid.org/0000−0002−7225−2827

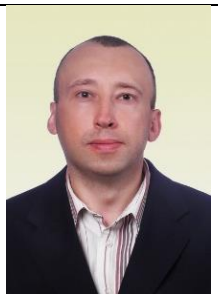

Ph.D. Iryna M. Kobylianska
e-mail: irishakobilanska@gmail.com

Candidate of Sciences (Pedagogy), Associate Professor of Department of Life Safety and Safety Pedagogy, Vinnytsia National Technical University.
Research Interests: professional pedagogy, formation of information and communication competence, professional education in the field of digital technologies, life safety, occupational health and safety.

http://orcid.org/0000-0002-3430-5879

Prof. Oleksandr V. Kobylianskyi
e-mail: akobilanskiy@gmail.com

Doctor of Science (Pedagogy), Professor of Department of Life Safety and Safety Pedagogy, Vinnytsia National Technical University.
Research Interests: professional pedagogy, formation of information and communication competence, professional education in the field of digital technologies, life safety, occupational health and safety.

http://orcid.org/0000-0002−9724-1470

Prof. Sofia V. Dembitska
e-mail: sofiyadem13@gmail.com

Doctor of Science (Pedagogy), Professor of Department of Life Safety and Safety Pedagogy, Vinnytsia National Technical University.
Research Interests: professional pedagogy, formation of information and communication competence, professional education in the field of digital technologies, life safety, occupational health and safety.

http://orcid.org/0000-0002-2005-6744